TGF-β2 at the crossroads between tumor acidosis, lipid metabolism and epithelial-to-mesenchymal transition

João Pedro Santiago de Jesus

Supervisor: Prof. Olivier Feron

Co-supervisor: Dr. Cyril Corbet

2020

ABSTRACT

Cancer progression is strongly influenced by the physico-chemical properties of the tumor microenvironment. In particular, tumor cells must adapt to survive and proliferate not only under low pO_2 (hypoxia) but also low pH (acidosis). Indeed, extracellular pH in tumors is about 10-fold more acidic than in healthy tissues, with mean values ranging from 6.2 to 6.8.

While tumor acidosis has been already reported to promote cancer cell invasion, evasion to immune system, drug resistance and metastatic dissemination, little is known about its influence on the metabolic preferences in cancer cells. Here, we demonstrate that cancer cells chronically exposed to acidosis (pH 6.5) exhibit a dysregulated fatty acid (FA) metabolism with the concomitance of mitochondrial FA oxidation (FAO) and cytosolic glutamine-fueled FA synthesis (FAS). This is enabled due to a downregulation of acetyl-CoA carboxylase ACC2 making mitochondrial fatty acyl-CoA degradation compatible with cytosolic lipogenesis. Perturbations of these regulatory processes lead to tumor growth inhibitory effects further identifying FA metabolism as a critical determinant of tumor cell proliferation under acidosis.

We also report that TGF-β2 is at the interface between these metabolic alterations and progression of tumor disease. We document that acidic pH promotes autocrine TGF-β2 signaling which in turn favors the formation of lipid droplets (LD) that represent energy stores readily available to support anoikis resistance and cancer cell invasiveness. Acidosis-induced TGF-β2 activation promotes both partial epithelial-to-mesenchymal transition (EMT) and fatty acid metabolism. We have shown that upon TGF-β2 stimulation, PKC-zeta-mediated translocation of CD36 facilitates the uptake of fatty acids that are either stored as

triglycerides in LD through DGAT1 activity or oxidized to generate ATP to fulfill immediate cellular needs. We also document how, by preventing fatty acid mobilization from LD, distant metastatic spreading can be inhibited.

Finally, we provide experimental evidence documenting how TGF-β2 is activated in acidosis-adapted cancer cells. We identify an upregulation of thrombospondin 1 (TSP-1), under chronic acidosis, that can bind to latent TGF-β2 and convert it to its biologically active form, through a non-proteolytic mechanism. Moreover, TGF-β2-dependent translocation of CD36, a fatty acid transporter, works as an "anchor" for TSP-1 at the cell membrane. Indeed, we show that CD36 is expressed in lipid rafts at the surface of acidosis-adapted cancer cells, where it co-localizes with TGF-β receptors. This leads to a local effect of TGF-β-signaling that promotes RhoA degradation and consequent cytoskeleton remodeling needed for lamellipodia formation and cell migration.

In conclusion, the work presented in this PhD thesis, points out fatty acid metabolism and TGF-β2 signaling as key drivers of the aggressiveness of cancer cells exposed to chronic acidosis. Our results also open new therapeutic perspectives with the validation of strategies interfering with these processes to prevent metastatic dissemination in mouse models.

ACKNOWLEDGEMENTS

Everyone knows the saying: “It is not the destination is the journey”. It is true if you understand that the journey is made of moments and people. And I would like to give thanks for that.

In the last four years I was very lucky to have been working in such a wonderful laboratory with great colleagues and friends. I know I could not have found a better PhD supervisor, so my enormous thanks goes to **Pr. Olivier Feron**. It is rare to find a supervisor that cares about you not only on a professional level but also in a personal one. You wanted me to grow as a scientist and a person. You not only made sure I was listening and improving when I was doing something wrong, but you also let me know when you saw something positive or I demonstrated my qualities. I appreciated your support and guidance, the way you consider my ideas, your advice and in general the time you spent with me. I am also very grateful to my co-promoter **PhD. Cyril Corbet**. From my perspective, for your first time supervising someone, it was a very good experience. I hope I did not give you too much trouble, but I appreciated it when you were there for me. I enjoyed the way you guide me through the scientific problems, the corrections that you made until the very last detail. The way that you try to resolve everyone’s conflicts helps to create a good group atmosphere in the laboratory. I wish you a stroke of great luck in this new journey of having your own research group, I do not know a better-prepared person to do that.

I would like to express my gratitude to all the members of my PhD committee (**Pr. Jean-Pascal Machiels, Pr. Luc Bertrand, Pr. Nathalie Delzenne**): our meetings were very enjoyable and contributed to the completion of this book. I

want to thank Pr. **Stine Pedersen** and Pr. **Nor-Eddine Sounni** for agreeing to review my work as external members.

I also want to acknowledge and thank the funds that have allowed me to pursue this work: the **FNRS** for the grant Televie-FNRS and **UCLouvain** for the bourse du patrimoine.

I must thank all the members of the O. Team for their support. To **Celine, Laurenne** and **Alizée** I want to thank you for your help and availability. **Natalia, Adan, Estelle, Ruben, Caroline, Florence, Merel** and **Valentin** I want to thank you for our conversations and the help with my project.

To my very special O. PhD team **Bastien, Emeline** and **Catherine**. We had so much fun together and I appreciated every single moment spent with you (a bit less when I was the center of the french-speaking jokes). I am going to miss all the CVLs, Emeline saying djodjo and our Belgium beer after work. Bastien, you have been there since the start of this journey, and sometimes you drove me nuts with your will to know everything we did (fouine)! However, it would not be the same without you. All the jokes, the activities that we did together and the time that we had each other's backs.

Thanks to all the other members of FATH whom I shared great moments inside and outside the lab. Especially for **Loic, Joanna, Vincent, Valery, Laurent, Thomas** and of course **Thibaut**. Thank you for the board game nights, paddle tournaments or the usual talks. I would like to take this opportunity to just remind Thibaut about the Euro2016 final.

I have great friends outside of the lab, who support me as well, and that has to be also recognized. To the Portuguese community invading Belgium, you guys are too many to put your names here but I just want to give a special thanks

to **David, Ana, Filipa, Miguel** and **Saroco. Pombo**, for our conversations and special moments. To **Nuno**, thank you for every little thing, to keep me here when I was homesick, for the great weekends together, for the great conversations and travels we had. To **Viktor, Ana Lima, Sara** and **Inês** for the way we support each other in a new country. **Ana** and **João Carlos** we do not talk as much but you will always be important. And finally, the malha-vacas group (**Tadeu, Zé, Lhó, o outro Nuno, Ruben and Gonçalo**) thank you I guess.

To **Camille's family**, for being my adoptive family in Belgium, thank you all for the support and the good moments. To my very special **Fado**. My company through the writing process, telling me that sometimes you have to take a break and go for a walk.

To my **lovely sisters (Ana e Diana)**, that I miss every single day. It was hard to see you grow up like that and not be there to be part of that. I want you to know that I am so proud of you two and the way you are living. Amo-vos!

To my parents, **Mãe e Pai**, muito obrigado por tudo o que me deram. Motivaram me a ser sempre melhor. Nunca me deram tudo o que queria mas sim o que precisava. Este ultimo passo foi meu mas foram vocês que meteram la a escada. Um grande obrigado, amo-vos.

To my very special **Camille Selvais**. No words can express what you are and what you have done for me. You have been looking out for me since the day that you found my university card, and you never stopped. The energy, the words, the charisma, the "trambolhice", everything that makes you wonderful and I love you for that.

Table of Contents

LIST OF ABBREVIATIONS

A

acetyl-CoA..... *Acetyl-coenzyme A*

AE ..... *Anion exchanger*

ATF3..... *Activating transcription factor 3*

C

CA .....*Carbonic anhydrase*

CAFs ..... *Cancer-associated fibroblasts*

CDKi .....*Cyclin-dependent kinase inhibitors*

Co-Smads.....*Common partner Smads*

CSCs .....*Cancer stem cells*

CTCs ..... *Circulating tumor cells*

D

DC .....*Dendritic cells*

E

ECM .....*Extracellular matrix*

EMP ..... *Epithelial–mesenchymal plasticity*

EMT.....*Epithelial to mesenchymal transition*

EPO ..... *Erythropoietin*

ETC.....*Electron transport chain*

F

FA .....*Fatty acids*

FAO ..... *Fatty acid oxidation*

FAS .....*Fatty acid synthesis*

FASN..... *Fatty acid synthase*

FFA .....*Free Fatty Acids*

G

GLUT1 ..... *Glucose transporter 1*

GPCR ..... *G-protein coupled receptors*

H

H^+ ..... *Proton*

HIF.....*Hypoxia-inducible factor*

I

IFN-γ.....*Interferon-γ*

IL .....*Interleukin*

I-Smads ..... *Inhibitory Smads*

K

KG .....*Ketoglutarate*

L

LAP ..... *Latency-associated protein*

LD ..... *Lipid droplets*

LDH ..... *Lactate dehydrogenase*

LOH ..... *Loss of heterozygosity*

M

MAPK ..... *Mitogen-activated protein kinases*

MCT ..... *Monocarboxylate–H+ efflux cotransporters*

MDSC ..... *myeloid-derived suppressor cells*

MET ..... *Mesenchymal to epithelial transition*

MMP *Matrix metalloproteases, Mitochondrial membrane potential*

MMR ..... *Mutation mismatch repair system*

MRTF. *Myocardin-related transcription factor*

MSI ..... *Microsatellite instability*

N

NBC ..... *Na+/HCO3− co-transporter*

NHE ..... *Na+/H+ exchanger*

NK ..... *Natural killer*

NL ..... *Neutral lipids*

N-TAD .... *N-Terminal Transactivation Domain*

O

OCR ..... *Oxygen consumption rate*

OGR1 ..... *Ovarian cancer G-protein-coupled receptor 1*

OxLDL ..... *Oxidized low-density lipoprotein*

OXPHOS ..... *Oxidative phosphorylation*

P

PAR6 ..... *Partitioning defective 6*

PDH ..... *Pyruvate dehydrogenase*

PDK1 ..... *Pyruvate dehydrogenase kinase 1*

PHD ..... *Prolyl hydroxylase domain*

pHe ..... *Extracellular pH*

pHi ..... *Intracellular pH*

pHLIP ..... *pH-low insertion peptides*

PI3K ..... *Phosphoinositide 3' kinase*

PL ..... *Phospholipids*

R

Rb ..... *Retinoblastoma protein*

RC ..... *Reductive carboxylation*

R-Smads ..... *Receptor-regulated Smads*

T

TCA ..... *Tricarboxylic acid*

TDAG8 ..... *T cell death-associated gene 8*

TGFβR ..... *TGF-β receptor*

TME ..... *Tumor microenvironment*

TRAF6 ..... *TNF receptor-associated factor 6*

TSP-1 ..... *Thrombospondin-1*

V

VEGF .....*Vascular endothelial growth factor*

VHL .....*Von Hippel-Lindau*

INTRODUCTION

1. Cancer biology in a nutshell

The oldest medical record known to describe cancer goes back to ancient Egypt (2500 B.C) where they were able to distinguish benign from malignant tumors and blamed the gods when unfortunate people suffer from this disease [2]. Nowadays cancer is not described as a single disease, but rather as an agglomerate of more than 100 different diseases [3], and the scientific community keeps adding medical records and scientific reports to an already complex problem. The American Cancer Society defines cancer as "a group of diseases characterized by uncontrollable growth and spread of abnormal cells. If the spread is not controlled, it can result in death". This is still a simplification of cancer biology that has nothing to do with faith but directly from the Darwinian evolutionary dynamics according to which (tumor) cells aim to adapt, under selective pressure conditions, in order to first survive and then proliferate.

This is achieved through self-adaptation, done by a succession of genetic changes, each conferring growth advantage, leading to the progressive conversion of a normal human cell into a cancer cell [4]. Most of the genetic changes (mutations) that give rise to cancer are not inherited but are instead a consequence of damages to DNA. The changes observed include:

- Point mutations that cause amino acid substitutions;
- Frame-shift mutations that either truncate the protein product or scramble its sequence;
- Chromosomal instability that results in amplification or inappropriate expression of a particular gene;
- Loss of a gene or its fusion with another gene, as a result of chromosomal breakage and rearrangement that produces a chimeric protein with altered function;
- Epigenetic DNA modifications, among which the most important one is the methylation of cytosine bases in CpG islands leading to gene silencing.

From these different genetic alterations, a cell converging to cancer can have two basic outcomes. First, mutations converting proto-oncogenes into oncogenes can increase the activity of proteins that are involved in the regulation of cell growth or apoptosis. Second, mutations can lead to inactivation of a tumor suppressor gene. These changes must perpetuate from cell to cell in order to form a tumor. Alterations in the DNA are normally edited through various mechanisms of DNA repair. A malignant cell has therefore to evade this system to allow gene modifications to be inherited by the daughter cells.

Genome instability and mutation acquisition belong to the hallmarks presented by Douglas Hanahan and Robert A. Weinberg in the well-known review called “The hallmarks of cancer” [5]. In their review, they describe the process of self-adaptation needed for a cell to surpass its regulatory circuits and become cancerous [5]. Figure 1, adapted from the review, is by now extensively used and recognized in the scientific community. Most of these hallmarks deal either with

the role of intrinsic genetic dysregulations that support cancer progression or with the role of non-cancer cells present in the tumors (*e.g*. endothelial cells, immune cells, fibroblasts). One hallmark actually stands out: the so-called *deregulating cellular energetics*. This thesis work is about tumor metabolism and, in the next pages, I will thus describe some aspects of the current understanding of the cancer bioenergetic and biosynthetic needs. Instead of a systematic description of the major metabolic pathways observed in tumors, I chose to tackle this theme through the prism of an underestimated part of the cancer hallmarks' scheme by Hanahan and Weinberg, namely the center of the circle that represents cancer cells in their complex microenvironment.

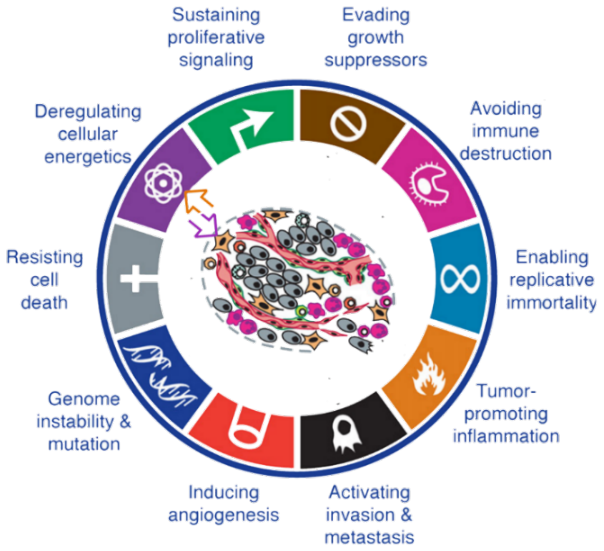

Figure 1 – The hallmarks of Cancer

Representation of a tumor and the tumor microenvironment surrounded by ten different modifications in cell physiology observed in cancer cells. The arrows represent the interconnection found between the microenvironment and the metabolism of cancer cells. Adapted from [5].

2. Tumor microenvironment

Cancer cells are indeed developing within an extracellular matrix (ECM) where they live side by side with non-cancer cells [6], but also face various gradients of physico-chemical parameters (pO_2, pH, heat, …) and are exposed to a variety of diffusible molecules (nutrients, growth factors, waste products). Altogether, this represents the so-called tumor microenvironment (TME). Along the years, the complexity added by TME was such that the scientific community was forced to stop considering a tumor just like a mass of malignant cells but instead as a complex organ (Figure 2). Tumors are thus a dynamic interaction arena where cancer cells interact with the ECM, resident and recruited host cells and soluble factors. The interplay between the genetically altered malignant cells and the TME is critical to understand cancer pathogenesis and importantly to identify new therapeutic targets.

Here below, I will first briefly summarize the current knowledge on tumor hypoxia, the most well studied component of the TME, and then expand in the next chapter on a partially related peculiarity of TME that is central for this thesis work, namely acidosis.

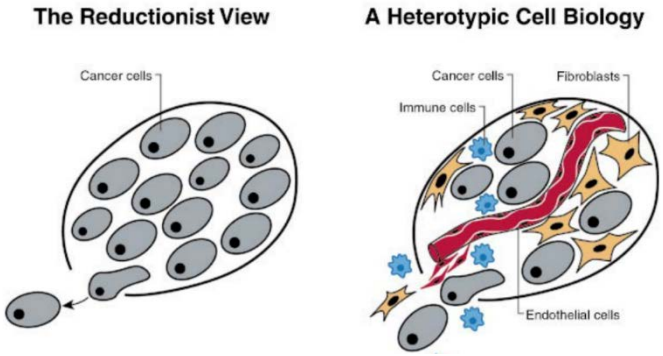

Figure 2 – Difference between the agglomerate of cancer cells and a tumor microenvironment.

The image at the left is a representation of a reductionist way of looking at a tumor as an agglomerate of cancer cells. At the right, we have a more faithful image of what a tumor looks like: cancer cells surrounded by a microenvironment that influences them. Adapted from [5].

As mentioned before, abrupt cell proliferation is a pre-requisite for cancer development and progression. Cancer cells alter expression and/or activity of cell cycle-related proteins and promote growth factors in order to multiply faster. However, this hastening in proliferation leads tumor cells to their own demise. The high-rate proliferation creates abnormal tumor vasculature resulting in different tumor areas with distinct perfusion characteristics. The location of some cells at distance from the blood vessels induces a deficiency in oxygen and nutrients. Although this should ultimately favor cell death, cancer cells in hypoxic zones can actually adapt to survive in these hostile conditions.

In hypoxia, one of the major mechanisms of response is the activation of hypoxia-inducible factor (HIF), a transcription factor that consists of HIF-1α and HIF-1β subunits [7]. The discovery of this oxygen sensor in cells was done by Gregg Semenza, the co-winner of the 2019 Nobel Prize in Physiology and Medicine. This actually started from observations of another gene, the erythropoietin (EPO) gene. *EPO* was already known to be highly expressed in situations of low oxygen, in particular in the kidney [8, 9] and the liver [8] of anemic patients. Semenza, when analyzing the *EPO* gene, found a promoter enhancer that he named hypoxia responsive element (HRE) and was further proven to interact with hypoxia-inducible factors [10]. HIF protein is a heterodimer, the activity of which is mainly regulated by the HIF-1α subunit availability, which is itself regulated by oxygen levels [11, 12]. Under normoxic conditions, HIF-1α is first hydroxylated by prolyl hydroxylase domain (PHD) proteins and then ubiquinated *via* the E3 ubiquitin ligase/von Hippel-Lindau (VHL) complex, thereby leading to proteasomal degradation [13] (Figure 3). Of note, HIF-1α affinity for VHL can be increased upon acetylation on lysine 532 [14, 15]. Under hypoxia, the activities of PHDs and other proteins are inhibited due to the lack of O_2. Therefore, HIF-1α is stabilized and can interact with the β subunit. Upon binding to HREs, both subunits then mediate the

transcription of a large number of genes to support a variety of cellular processes including angiogenesis to promote the delivery of O_2 (*e.g.* upregulation of vascular endothelial growth factor (VEGF)) [16, 17] but also metabolic adaptations to help cells to survive despite the lack of O_2 [18].

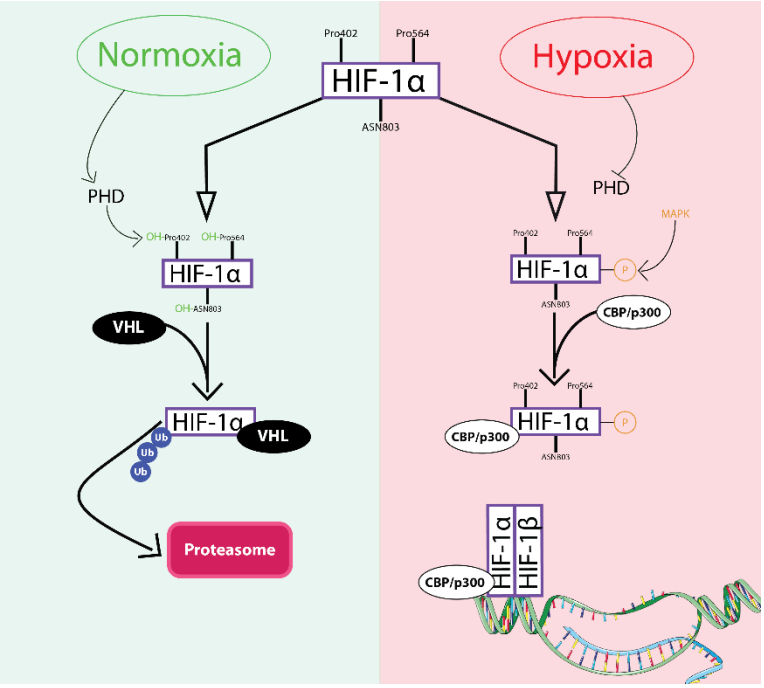

Figure 3 – Mechanism of regulation of HIF-1α subunit.

HIF-1α has different fates under normoxia and hypoxia. Under normoxia, it is hydroxylated by PHD in PRO^{402} PRO^{564} and ASN^{803}. After hydroxylated VHL can then bind to hydroxylated HIF-1α and further mediate ubiquitin-mediated protein degradation. Under hypoxia, HIF-1α is not hydroxylated because PHD is inhibited. The MAPK pathway phosphorylates HIF-1α which helps with its nuclear accumulation. When connected with HIF-1β, HIF-1α can link to the DNA and transcript a large number of genes. Image adapted from [14].

Accordingly, HIF-1 activates the expression of multiple genes in favor of a non-oxygen-dependent metabolism including glucose transporter 1 (GLUT-1) to uptake more glucose to support glycolysis and pyruvate dehydrogenase kinase

(PDK) that prevents the fueling of the tricarboxylic acid (TCA) cycle and thereby reduces the risk to generate ROS in the mitochondrial electron transfer chain. PDK is indeed responsible for phosphorylating and inactivating pyruvate dehydrogenase (PDH), thereby blocking the conversion of pyruvate to acetyl-coenzyme A (acetyl-CoA), required for pyruvate to enter the TCA cycle [19]. During glycolysis, nicotinamide adenine dinucleotide (NAD^+) is reduced to NADH via the enzymatic reaction catalyzed by glyceraldehyde phosphate dehydrogenase (GAPDH). In order to maintain glycolytic flux, NAD^+ needs to be regenerated. Therefore, under the control of HIF-1, there is also an increase in expression of lactate dehydrogenase A (LDHA) [20] which converts pyruvate to lactate coupled with the oxidation of NADH to NAD^+ and H^+.

The reductive glutamine metabolism was also shown to be supported by HIF-1α stabilization [21]. When captured by cancer cells, glutamine can actually be converted into glutamate, and then to αKG to be directed to the TCA cycle through the canonical path or instead can directly lead to citrate via reductive carboxylation (RC). The latter path is promoted under hypoxic conditions as proven by the constitutive activation of HIF in VHL-deficient cells that is associated with a strict reliance on glutamine RC [22, 23]. Glutamine RC allows hypoxic cancer cells to generate new lipids [22, 24]; this lipogenesis is critical since when RC is prevented, exogenous lipids or citrate is required to promote hypoxic cell survival *in vitro* [25]. Hypoxia-induced autophagy will also indirectly impact on cancer cell metabolism. For instance, HIF-1-induced BNIP3 expression was reported to trigger selective mitochondrial autophagy, thereby impacting on major oxidative metabolic paths [26].

Although specific pathways such as glutamine RC or mitophagy may help some hypoxic cancer cells to survive and maintain anabolic pathways, the common

denominator for cells exposed to a deficit in O_2 remains an increase in the glycolytic flux to generate ATP as well as biosynthetic intermediates including reductive equivalents through the pentose phosphate pathway. If the high glycolytic rate compensates for a lower efficiency in extracting energy from glucose molecules (when compared to TCA cycle/OXPHOS), this comes with a great price to pay, namely the progressive acidification of the extracellular medium (See section 3).

3. Tumor acidosis

The regulation of cellular pH is fundamental to life. Cells have to achieve a pH equilibrium to avoid affecting basic biological principles such as energy balance, cell proliferation and migration. It is nowadays reported that values of extracellular pH (pHe) can range between 5.7 to 7.0 in solid benign and malignant tumors [1, 27-30]. Here below I will focus on mechanisms of acid-extrusion by cancer cells and the significance of extracellular acidosis for tumor biology.

3.1 pH dysregulation in tumors

The acidic zone can be seen (in a very simplistic way) as a combination of excess protons release merged with an inadequate blood supply. I will elaborate on this concept after briefly describing how acid extruders manage to regulate intracellular pH at a cost of extracellular acidification.

3.1.1 Actors of intracellular pH regulation

Normal adult cells have an intracellular pH (pHi) around 7.2 which is lower than the pHe value of 7.4. Cancer cells invert this pH balance with a pHe usually measured below 7.0 and a pHi higher than 7.4 [31-33]. It is worth mentioning that cancer cells placed acutely at pH 6.5 exhibit a rapid and prolonged decrease in pHi. By contrast, cancer cells adapted to long-term acidic conditions have a higher capacity to recover from the initial pH fall to a neutral and even slightly alkaline pHi when transferred back from a medium at pH 7.4 to pH 6.5. [34]. Cancer cells have

implemented specific mechanisms to regulate pH changes, by altering the expression or activity of several plasma membrane molecules such as pumps and transporters that facilitate proton (H^+) efflux and maintain the alkaline pHi. Four different groups of proteins are important in this process: acid extruders, carbonic anhydrases (CAs), $Na^+/HCO3^-$ co-transporters (NBCs) and anion exchangers (AE1 and AE2). Acid-exposed cells that lack pH-regulating capabilities offered by these proteins may enter in apoptosis or growth arrest due to cytosolic H^+ accumulation [35, 36]. Although all the above pH-regulating proteins participate in the maintenance of an intracellular pH compatible with cancer cell survival and growth, they achieve it in different ways (Figure 4).

Acid extruders

Acid extruders can remove the excess intracellular H^+ ions from inside the cells in a direct way.

The Na^+/H^+ exchanger (NHE1) takes advantage of the Na^+ gradient to force protons out. It achieves it by mediating an 1:1 exchange between extracellular sodium and intracellular protons. NHE1 activation is both mediated through signaling hormones and growth factors or through cellular stresses promoted by intracellular acidification, cell shrinkage or hypoxia [37]. However, when acidosis is established within tumors, it is thought that NHE1 activity is reduced because it faces an unfavorable H^+ gradient. The role of NHE1 is directly related to different biological features associated with acidosis including protease activity [31, 38, 39], invadosome formation [40-42], migration [40, 41] and invasion [39, 41].

H^+-ATPase is probably the most essential proton transporter in non-malignant and malignant cells alike. Internal organelles such as vacuoles, lysosomes, synaptic vesicles, endosomes, secretory granules, and the Golgi apparatus have specific internal pH requirements that are controlled by H^+-ATPases

[43] [44]. H^+-ATPases are composed of two multi-subunit domains, namely V0 and V1, and exploit energy in the form of ATP in order to help extract protons. This need for ATP is associated with the presence on the surface of tumor cells of ATP synthase [44-46], an enzyme which in healthy cells is mostly present intracellularly in the inner mitochondrial membrane.

Finally, the monocarboxylate-H^+ cotransporters (MCT1 and MCT4) are bidirectional transporters that facilitate the movement of monocarboxylates such as lactate across the plasma membrane. While the primary role of MCT is to regulate monocarboxylate fluxes, they also indirectly participate to the regulation of pHi since protons are used as counter-anions in this process. There are currently nine identified MCT isoforms but MCT1 and MCT4 are the most frequently expressed in cancer cells, especially in highly proliferative tumors. MCT1 and MCT4 combination offers the possibility of a symbiotic metabolism between oxygenated cancer cells that import and consume lactate produced and released by hypoxic cells that have in turn a larger access to glucose (section 3.2.5). This is only possible due to the different affinity of MCT1 and MCT4 for lactate (Km ~3.5–10 mmol/L and ~22–28 mmol/L for MCT1 and MCT4, respectively) [47]. MCT1 has been associated with lactate export in T cells (see section 3.2.3.) and invasion [48].

Carbonic anhydrases

Carbonic anhydrases are metallo-enzymes widespread in cancer cells. There are 9 active forms of CA with different subcellular localization: CAs I, II, III, VII and XIII are cytosolic enzymes while CAs IV, IX, XII, XIV are located at the cell membrane [49]. CAII, IX and XII are the ones with a bigger significance in tumor formation. The CAs IX and XII accelerate the hydration of carbon dioxide (CO_2) to bicarbonate and proton ($CO_2 + H_2O \rightarrow HCO_3^- + H^+$). Inside the cell CA II supports the inverse reaction, transforming HCO_3^- to water and CO_2 and thus consuming a

proton (HCO_3^- + H^+ → CO_2 + H_2O); resulting CO_2 can then passively diffuse through the cell membrane.

CA IX has been shown to play essential roles in growth, survival, migration and invasion of tumor cells [50, 51]. Hypoxia, through HIF-1α induction, promotes a strong overexpression of CA IX [52], making this protein so critical for excess H^+ handling in several tumors [50] that its knockdown may dramatically inhibit tumor growth [53].

Sodium bicarbonate cotransporters (NBCs) and Anion exchangers (AEs)

NBCs are a group of proteins described to be responsible for the transport of bicarbonate from the extracellular space to the intracellular compartment together with sodium. As elaborated above, HCO_3^- can accept protons and produce CO_2, a process that balances the excess of intracellular H^+. Of note, when given orally, HCO_3^- has been shown to reduce extracellular acidity in tumors and even inhibit metastatic progression [54]. Within the NBC family, NBCn1 is upregulated in human tumors in response to ErbB2 signaling through various pathways including Akt, ERK and Src [42, 54]. Other modes of regulation also involve transcription factors Sp1 and KLF4, which represses and activate NBCn1, respectively [42]. Inhibition of NBCn1 affects tumor growth in breast cancer cells [55].

The anion exchangers 1 and 2 (also called SLC4A 1 and 2) exchange HCO_3^- for Cl^- in an electroneutral manner. Both AE1 and AE2 were shown to be upregulated in gastric and colorectal cancers and associated with tumor progression [54, 56]. Surprisingly, both proteins have also been found in the cytosol sequestering the tumor suppressor p16 [54, 56, 57].

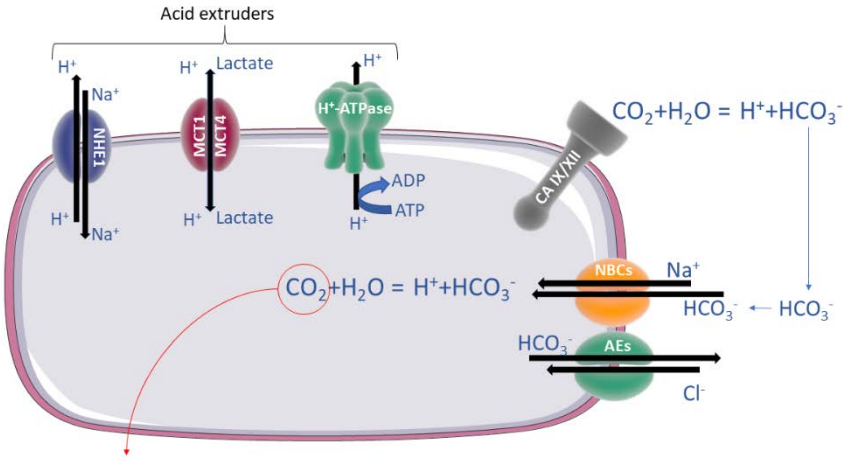

Figure 4 – Membrane transporters responsible for pH regulation in cancer cells.

The proteins NHE1, MCT1 and 4 and H^+-ATPase are classified as acid extruders because of their capacity to export protons to the extracellular space.

CA IX and XII accelerate the hydration of CO_2 to form bicarbonate.

NBCs internalize the bicarbonate which allows for the production of CO_2 at the cost of protons. The CO_2 is then passively extracted out of the cell.

AE1 and 2 promote Cl^- influx in exchange with bicarbonate.

3.1.2 Origins of tumor acidosis

Acidosis may develop for various reasons in healthy tissues [1, 32, 58], but in tumors, it is the consequence of altered metabolism leading to the release of protons but also CO_2 together with inefficient blood perfusion. The most obvious source therefore results from the low oxygen availability at distance from blood vessels and the associated stimulation of glycolysis as a major metabolic path to support cell survival and growth. Hypoxia therefore creates a continuous gradient of protons from the most hypoxic/necrotic areas within a tumor to the surrounding blood vessels (Figure 5). This has however to be nuanced by the capacity of cancer

cells to also favor the glycolytic metabolism and associated stimulated H^+ release under aerobic conditions (the so-called Warburg effect) (Figure 5). The trigger for the Warburg effect has been associated with different causes over the years. It started with Warburg himself who proposed a mitochondrial dysfunction in cancer cells as the main cause for preferential use of glucose towards the glycolytic pathway, even under aerobic conditions [59]. Later, Efraim Racker assumed that imbalances in intracellular pH and defects in ATPase activity could be the main trigger for aerobic glycolysis [60]. Nowadays, we know that oncogenes lead to aberrant regulation of growth factor signaling that may be associated with an increase in glycolysis [61]. The need to generate biosynthetic intermediates and reductive equivalents from the glycolysis is proposed to account for this preference. As observed under hypoxic conditions, pyruvate is thus converted into lactate, thereby regenerating NAD^+ to further maintain the elevated glycolytic flux. Lactate is consecutively exported out of the cell together with one proton through MCT transporters [1]. The capacity for a tumor to remove theses protons released by non-hypoxic cells will also depend on the distance from the neighbor blood vessels.

In oxygenated tumor areas, a small part of glucose but also other substrates including lactate (see below), glutamine and fatty acids fuel the TCA cycle and OXPHOS, leading to the generation of CO_2 that easily diffuses through the membrane. This CO_2 represents another important source of extracellular protons in tumors upon hydration ($CO_2 + H_2O \rightarrow HCO_3^- + H^+$) and dependent on the capacity of the tumor to get rid of this pool of CO_2/H^+. In particular, tumor compartments experiencing moderate hypoxia (*ie*, still sufficient to allow oxidative metabolism) will also contribute to acidosis, extending the zone of acidic pH beyond the hypoxic/glycolytic areas (Figure 5).

Non-cancer cells can also contribute to the microenvironment acidification. For instance, cancer-associated fibroblasts (CAFs) as well as immune cells, including activated T cells, macrophages and dendritic cells can shift their metabolic preferences towards glycolysis and lactate production, thereby participating to H^+ accumulation within TME [62].

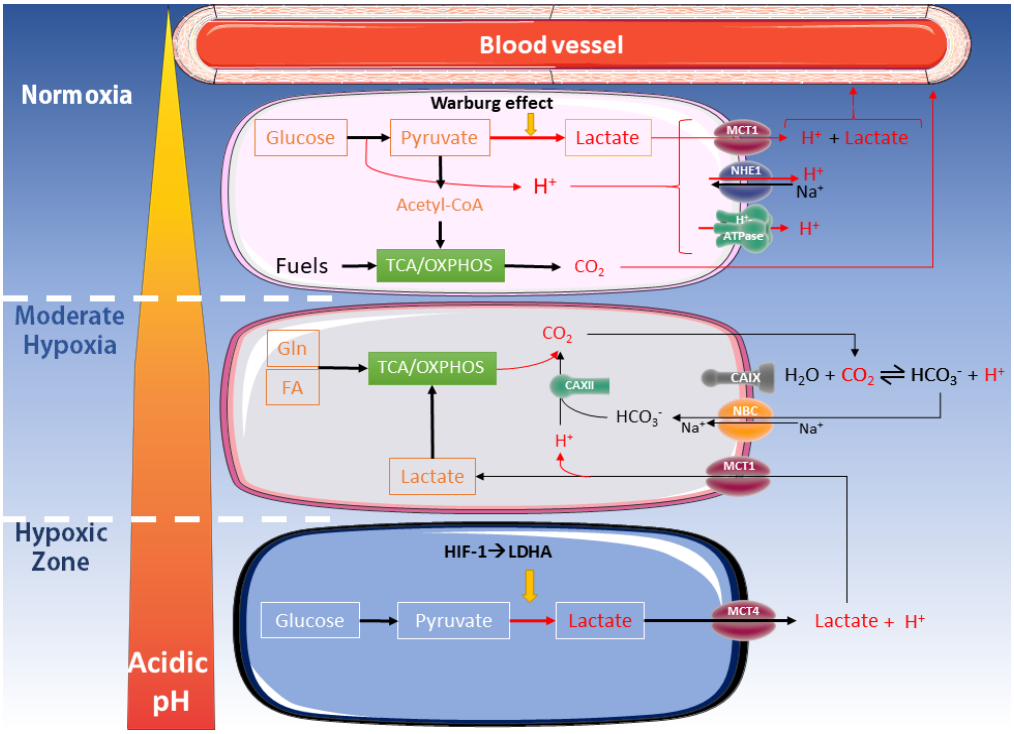

Figure 5 – Metabolism of cancer cells exposed to different levels of hypoxia.

Oxygen levels (blue color) are lower the further way it is from the blood vessel while acidity rises. Cells, divided in three zones, have a different metabolism according to O_2 and pH levels.

Normoxic cells have the physiological conditions to perform glycolysis and mitochondrial respiration. The glycolysis under the Warburg effect leads to the production of lactate and H^+. These metabolites are exported out by MCT1, NHE and H^+-ATPase. At the same time TCA/OXPHOS is occurring and producing CO_2. CO_2 can effortlessly pass through the cell membrane. All the metabolites are easily wash out due to blood vessels in proximity.

In the **hypoxic** zone, where the O_2 level is the lowest, this limits the capacity of cells to perform OXPHOS. HIF-1 activates the expression of multiple genes in favor of the highly glycolytic flux. This includes LDHA, a protein that favors the pyruvate reduction to lactate, producing high quantities of lactate and protons. Lactate and H^+ are transported by MCT4 and NHE1, respectively, to extracellular space.

Between the last two zones establishes the **moderate hypoxia.** O_2 levels are higher here than the hypoxic zone but the acidic pH does not have a significant increase. Cells present in this area are exposed to one of the lowest extracellular pH due to the consequences of the metabolic scenario of normoxic and hypoxic cells and the poor perforation that allows the accumulation of the metabolites. Therefore, cells adapt to this situation by maintaining the production of H^+ to a minimum (no glycolysis) and use the nutrients available to them (lactate). MCT1 facilitates the entry of lactate and H^+ in the cells, lactate is then transformed in pyruvate and enters the TCA cycle while CA II adds HCO_3^- to the proton to form CO_2. At the cell membrane CA IX rehydrates CO_2 to reproduce HCO_3^- that will reenter the cell through NBC. Adapted from [1].

3.1.3 Biological pH sensors

Metabolic and non-metabolic changes under acidosis still lack a major regulator, a protein (or a group of proteins) that senses an augmentation of internal pH or a diminution of extracellular pH and activates inducible factors as a response. There is a high probability that this protein might exist in acidosis-exposed cells and might function as HIF-1α does for hypoxia. Although a global and consensus transcriptional proton sensor was not yet identified, there are some proteins that were documented to drive adaptive responses to acidosis.

HIF-2α

A very common response to acidosis is the upregulation of HIF-2α [34, 63, 64], nonetheless, the mechanism of activation is still debatable. It has been proposed that a similar mechanism to oxygen-dependent control of VHL might occur in a pH-dependent manner. Acidosis causes confinement of VHL in the nucleus, stopping its ability to degrade HIF until neutral pH conditions are restored [63]. However, other reports claimed that HIF-2α could be upregulated through acidosis in a VHL-independent manner. For instance, in gliomas exposed to the synergistic influence of hypoxia and acidosis, the stress-induced chaperone HSP90 is thought to account for HIF-2α upregulation [64]. Another mechanism is based on Sirt-1 activity, a NAD^+-dependent deacetylase activated during acidosis. By promoting deacetylation of both HIF-1α and HIF-2α, Sirt-1 has actually opposite effects on the two HIF proteins. Deacetylation in HIF-1α prevents p300 recruitment and represses its activity, while deacetylation of HIF-2α lysine residues increases its activity [34]. HIF-1α and HIF-2α may regulate the expression of specific genes because of a distinct N-Terminal Transactivation Domain (N-TAD) [65] so that HIF-2α activation and HIF-1α inhibition may lead to specific metabolic changes

associated with acidosis. For example, HIF-1α, as discussed before, promotes glycolysis and fermentation, through GLUT-1 and LDHA respectively. By contrast, HIF-2α is known to promote the expression of the glutamine transporter ASCT2 and GLS1, allowing glutamine to enter the cell and through cytosolic GLS to support FAS [34]. The differences between the two isoforms is also noticeable in their interplay with the oncogene c-Myc. Indeed, while HIF-2α promotes c-Myc transcriptional activity and thereby stimulates cell proliferation, HIF-1α inhibits cell-cycle progression by opposing c-Myc [65]. Altogether, the above sets of data support the idea that during acidosis HIF-1α is downregulated whereas HIF-2α activity increases. However, this cannot explain all the significant metabolic, morphologic and physiological changes occurring in cancer cells exposed to acidosis. On top of that, the role of HIF-2α is known to vary according to the tumor type [1, 64, 65].

ASICs and GPCRs

Extracellular acidification can be sensed by specific acid-sensing ion channels (ASICs) and proton-sensing G-protein coupled receptors (GPCRs) [66]. These can be important molecules to make the transition between extracellular acidosis and intracellular signals that induce cellular adaptative mechanisms.

ASICs belong to the subfamily of degenerin/epithelial Na^+ (DEG/ENaC) channels, that are well represented in the peripheral nervous system but have been found expressed in various cancers, not only glioma but also breast [67], colorectal, cervical and stomach cancer cells [68]. By promoting local membrane depolarization, ASICs can also mediate a glutamate-independent Ca^{2+} entry. Although ASIC-triggered pathways driving cell adaptation to acidosis are still largely unknown, ASIC1 was documented to support acidosis-associated increase in tumor growth and metastases [67].

Proton-sensing GPCR expression varies from tissue to tissue but main family members include GPR4, OGR1 (GPR68) and TDAG8 (GPR65) [66]. The GPCR GRP4 has been described to be fully activated in presence of acidic extracellular pH and to have a weaker activation level at physiological pH. This proton-sensing receptor has been reported to be overexpressed in inflammatory diseases and various types of malignant cancers (most frequently in kidney, colon and ovarian tumors) [69]. Moreover, GPR4-deficient mice exhibited a significantly reduced tumor growth [70]. GRP4 responds to the extracellular acidic pH through different cascades. While the canonical pathway leads to cyclic AMP (cAMP) accumulation, a second pathway increases the activity of the enzyme p115RhoGEF (through G_{12} or G_{13} activation) that supports the formation of actin stress fibers [71]. Also, PLC activation (through Gq) leads to an increase in intracellular calcium concentration (as reported for GPR4). Nuclear factor-κB (NF-κB) activation in acidosis-exposed breast and prostate cancer cells is also proposed to result from this Gq/PLC signaling pathway [72].

Ovarian cancer G-protein-coupled receptor 1 (OGR1) is considered as a proton sensing receptor (inactive at alkaline pH and fully activated at pH 6.8) that gets activated through the protonation of histidine residues [71] and was documented to play crucial roles in cell growth, migration and differentiation.

T cell death-associated gene 8 (*TDAG8*) is a G-protein-coupled receptor mainly expressed in lymphoid organs and cancer tissues [69]. There are obvious similarities between TDAG8 signaling and GRP4 canonical pathway. When the pH values are lower than 7.2 [73], TDAG8 stimulates adenylyl cyclase which promotes the accumulation of cAMP and Rho activation. Overexpressed TDAG8 at the cell membrane has a protective effect on tumor cells in response to extracellular acidosis and can accelerate tumor development [66].

Protons

Finally, it should be stressed that the inverted pH gradient between the inside and the outside of cells can itself be a regulator of cell response. The presence of some charged residues (i.e. histidine and arginine) at the surface of membrane proteins makes them sensitive to pH changes. Therefore, changes in pH has the potential to modulate the functions of a myriad of proteins/enzymes [1]. The exact contribution of these changes in protein ionization (vs. the other bona fide pH-sensigng ASIC and GPCR) to the adaptation of cancer cells to an acidic environment is however still largely unknown.

3.2 Consequences of tumor acidosis

Acidosis provides a strong evolutionary selection. It is nowadays well accepted that the acidic pressure put on cancer cells leads to the emergence of more resistant and aggressive phenotypes. Here below I will dissect some of the features gained by cells when exposed to acidosis.

3.2.1 Lysosomes and autophagy

In cell biology, the link between pH and lysosomes is quite obvious. Lysosomes contain hydrolytic enzymes that can break down many kinds of biomolecules at an optimal pH < 5. A very common response to acidosis is an increase in the formation and trafficking of lysosomes, from a perinuclear location to the plasma membrane [38, 74, 75]. The transport of lysosomes towards the cell surface appears to be promoted by microtubule-based motors of both kinesin [38] and dynein type [74]. Once they have fused with the membrane, lysosomes can

then release proteases (see section 3.4.4) and H^+ to the surrounding microenvironment. Expansion in the volume of lysosomes is also a hallmark of acidosis-exposed cells, and these larger lysosomal vesicles are actually associated with higher metastatic capacity in breast cancer cells [75]. NHE1 seems to also have a role in the acidic pHe-induced lysosome trafficking since when it is inhibited the lysosomal trafficking is reduced as well [38]. Robert A. Gatenby and Robert J. Gillies showed that, under acidosis, the lysosomal protein LAMP2 is redistributed to the plasma membrane both *in vitro* and *in vivo* [76]. LAMP2 is a protein that protects lysosomal membranes from acid proteolysis and that is also associated with chaperone-mediated autophagy, a process that acidosis-exposed cells exploit at high-rate [76].

With the help of lysosomes, autophagy keeps the cellular homeostasis by removing dispensable or damaged intracellular structures. Under certain circumstances, autophagy can promote tumor growth and/or support cancer cell survival, providing protective responses to various stresses. Accordingly, autophagy markers are often detected in response to extracellular acidosis. For instance, in acid-exposed breast cancer cells, the LC3 protein is present in large extent in the filopodia [77] and the early autophagosome regulator ATG5 is upregulated [77]. BNIP3-induced autophagy is also described as a survival mechanism in cells exposed to either hypoxia or acidosis [78]. Interestingly, inhibiting autophagy by either ATG5 knockdown, by affecting BNIP3 stability or by exposure to 3-methyladenine promotes acidic stress-induced cell death [79] and it appears to have the same effect in acidosis [77, 79]. Altogether, these data support a critical role of autophagy in supporting the survival of cancer cells exposed to the hostile acidic tumor microenvironment.

3.2.2 Invasion and metastases

The process of invasion results from an assembly of different features, that when combined offer cancer cells a unique capacity to penetrate neighboring tissues.

Extracellular proteolysis

The acidic microenvironment promotes the expression of proteases - a group of enzymes with the ability to hydrolyze peptide bonds [80]. As a consequence, acidic cancer cells can take advantage of the degradation of the surrounding extracellular matrix that facilitates their migration.

The redistribution of lysosomes to the cell periphery directly participates to the secretion of proteases, in particular cathepsin B, a cysteine proteinase that can act as carboxy dipeptidase at an acidic pH and an endopeptidase at a neutral pH [81]. Remarkably, an increase in cathepsin B is already observed with a slight acidification of the extracellular environment [82]. Interestingly, cathepsin B may also be activated in response to the extracellular acidification resulting from NHE1 phosphorylation, itself being triggered by the interaction between hyaluronan receptor CD44 and NHE1 in lipid rafts of breast tumor cells [39, 83]. Also, staining of the vesicles containing cathepsin B identifies them in the perinuclear area of stationary cells but on the rear region of migrating cells [84], confirming the role of the protease in the detachment of cancer cells in a polarized fashion.

Another acidosis-driven event is the formation of invadosome microdomains. Invadosomes are highly invasive cell structures that are part of a dynamic group that includes lamellipodia, focal adhesions and podosomes. Those are actin-rich protrusion structures produced by a matrix remodeling process, the

formation, maturation, and function of which have been connected to both hypoxic and acidic conditions [75, 80]. These structures are rich in three classes of proteases: matrix metalloproteases (MMPs), serine proteases and cysteine proteases that were shown to co-localize with NHE1 within plasma membrane microdomains. MMPs are calcium-dependent zinc-containing endopeptidases capable of degrading all sorts of extracellular matrix proteins. They are not optimally active at low pHe, but the conversion of the latent MMP pro-form to the active form is dependent on the proteolytic activities that are activated at low pHe [85]. Of note, MMP 3 activity has an acidic catalytic optimum which is dependent on His^{224} [86] and MMP 9 is upregulated in *in vitro* acidic conditions due to activation of ERK1/2, p38 and NF-kB [87].

Cytoskeleton transformation

Acidosis has been also documented to impact cell rearrangement. The acidosis-promoted changes in the actin filaments can alter the cancer cell polarization. Cdc42, an important protein in cell polarity, has been demonstrated to be regulated by the H^+ efflux mediated by NHE1 [40]. Cofilin [88] and profilin [89] are actin-remodeling proteins that play central role in cytoskeleton modifications under acidosis. Invading cells need to remodel not only their actin filaments but also cell-to-cell adhesions. Talin, a cytosolic protein that is found in high concentrations in focal adhesions, decreases its binding capacity to actin filaments when the pHi>7.2 [90], thereby facilitating cell migration.

Epithelial to mesenchymal transition

Epithelial to mesenchymal transition (EMT) is one of the most studied processes in the scientific community working on the determinants of cancer cell invasiveness. EMT will be extensively analyzed in section 4.3.4 but we will here mention some key points in relation with acidosis. In a nutshell, EMT is the

transition of a cell, from a state where there is a strong cell cohesion and apical-basal polarity - **epithelial state**, to a state characterized by a front-rear cell polarity, cytoskeleton rearrangement and cell elongation - **mesenchymal state**. This transition can be consecutively inversed in a process that is called mesenchymal to epithelial transition (MET). EMT is mostly activated by external triggers such as cytokines (e.g. TGF-β) or hypoxia [91-93]. Association with acidosis has also been claimed but the mechanistic explanation remains unclear. For instance, it is known that acute acidosis (less than 24h) promotes the appearance of EMT markers in certain cell types [94, 95]. Riemann et al. [95] showed that acidosis can increase N-cadherin and Vimentin in solid tumors; acidosis was however induced in mice by housing them in a low pO_2 atmosphere, an experimental condition that may lead to various interpretations. In conclusion, there are indications of a connection between EMT and acidosis but is unclear how and at what degree is acidosis promoting EMT.

In general, tumor areas where the extracellular pH is the lowest are the ones where the tumor invasion is the most prominent. Acid extruders like MCT1/4 [48] and NHE1 [39] have been associated with invasive capacity. This is further proven in mathematical models [96, 97] where it is possible to observe that acidosis affects many of the features needed for invasion to occur, including changes in cytoskeletal dynamics and increase in proteolytic activity. Hence, pharmacological ways to increase the tumor pH have been proven to inhibit spontaneous metastases. For example, administration of sodium bicarbonate can increase the extracellular pH and significantly reduce the formation of metastases in certain cancer types [98].

Table 1. Mechanisms of acidosis-promoted cancer cell invasion.

System	Effector	Function	Ref.
Proteolytic	Cathepsin B	Degradation of *cell-matrix and cell-cell interactions*	[84]
	MMP 3	Extracellular protein degradation	[86]
	MMP 9	Extracellular protein degradation	[87]
Cytoskeleton transformation	Cdc42	Redistribution of cell polarity	[40]
	Profilin	Actin-remodeling	[88]
	Cofilin	Actin-remodeling	[89]
	Talin	Destruction of cell-to-cell/cell-substract adhesions	[90]
EMT	N-Cadherin	Disruption of cell–cell interactions	[95]

3.2.3 Immune evasion

In the past few years, there has been a breakthrough in the understanding of how to make the immune system capable to recognize and kill cancer cells, and thus to overcome the immunosuppressive tumor environment. Among the many processes that participate in the resistance of tumors to the immune attack is the ambient acidosis and associated increased extracellular lactate concentration, the way this impacts on major immune cell types will be briefly summarized here.

H^+ and lactate exposure was shown to decrease the capacity of T cells to produce interleukin-2 (IL-2), interferon-γ (IFNγ), granzyme B and perforin and that of monocytes to release tumour necrosis factor (TNF) [99-101]. In these studies, lactate and H^+ had a synergistic effect leading to the inhibition of proliferation. Excess pools of H^+ and/or lactate in the extracellular compartment were proposed to alter the glycolytic flux (*ie*, the needed efflux of the en-product lactate) in immune cells by preventing lactate efflux. Mechanistically, the resulting accumulation of protons and lactate inside T cells but also natural killer (NK) and dendritic cells was shown to inhibit the capacity of the transcription factor nuclear

factor of activated T cells (NFAT) to promote IFNγ production and thereby to dramatically reduce the immune response [102] [103] [104]. Of note, $CD4^+$ Treg cells, that rely on FAO for fuel [105], do not appear to be affected by the acidic tumor microenvironment as T-cells are [106].

Preventing TME acidification was also documented to improve antitumour responses to immunotherapy. For instance, the reduction in tumor acidosis using the PPI esomeprazole was documented to reverse the acidic pH-induced T cell anergy, as documented by the restored expression of IL-2Ra (CD25) and T-cell receptors (TCR) [107]. Also, treatment with bicarbonate in lymphoma-developing mice, enhances IFN-γ expression, together with an increase in the NK-cell numbers [103], thereby leading to a significant effect on tumor growth [103].

Table 2. Effects of low pH and lactate in immune cells.

Immune target	Effector	Effect	Ref.
T-cell	Low pH	Blockage of IL-2 dependent T-cell proliferation	[99]
	Low pH/Lactic acid	NFAT repression	[102]
	Lactate	Glycolysis obstruction	[102]
	Low pH	Reduction in expression of IL-2Ra and TCR and low STAT activity	[107]
Myeloid cells	Lactate	Increase in MDSC	[102]
NK cells	Low pH	Decrease in the production of perforin and granzyme B	[83]
	Low pH	Decrease in IFN-γ production	[103]
Dendritic cells	Lactate/Low pH	Decrease in antigen-presenting capacity	[104]
	Low pH	Decrease in IL-12 secretion	

3.2.4 Drug resistance

We have previously stated that acidosis exposed cancer cells have a higher pHi than normal cancer cells. This alkaline pH gives them an advantage when it comes to drug resistance. Cells with higher pHi have been shown to have higher doxorubicin [108] and cisplatin-resistance [109]. In the latter, the information was further completed with an analysis of the DNA-binding activity of cisplatin. In this study, it was observed that in accentuated acidic conditions (pH 6.8) there was more DNA-cisplatin adduct formation (important to notice that the results were obtained with non-human DNA). The study further demonstrates that V-ATPase is up-regulated in the cisplatin-resistant cells [109].

Ion trapping phenomenon

One of the biggest challenges for most cancer drugs targeting acidic exposed cells is the "Ion trapping" phenomenon. Doxorubicin, daunomycin and other drugs [110, 111] are constructed to be weak bases, this facilitates the passage across the lipid bilayer of cells. However, when exposed to acidic solutions, these weak bases are easily ionized and become positively charged protonated species, which drastically reduces cell permeability. These species are neutralized and inactivated and then trapped outside of the cells or in intracellular compartments such as acidic vesicles and endosomes. Specific inhibitors of the vacuolar H^+-ATPase and agents such as protonophores, block the acidification of these vacuoles allowing for the release of these drugs in the cytosol and nucleus [112].

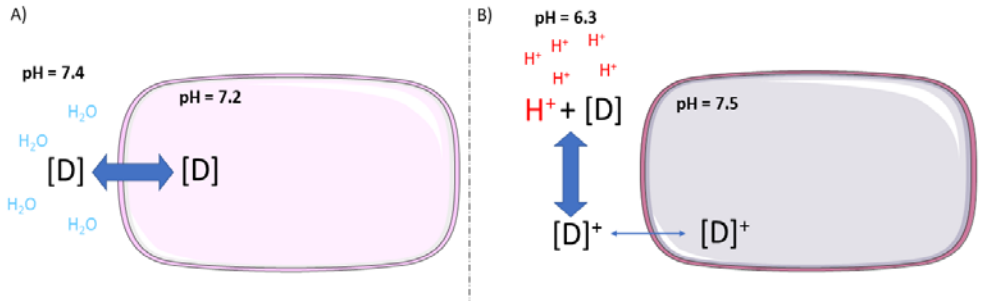

Figure 6 – The "Ion trapping" phenomenon.

The weak base drug (D) has no problem in entering cells when present in a physiological pH (a). However, it tends to be excluded when exposed to an acidic pH (b). This happens because the weak base will be protonated by the free protons present in the extracellular space, giving the drug a positive charge that will impeach it of passing the cell membrane. Adapted from [111].

3.2.5 Metabolic dysregulation of acidic cells

When the acidity of the tumor microenvironment achieves a certain threshold, cancer cells need to profoundly rewire their metabolic preferences in order to maintain intracellular pH in a viable range. In a way, acidosis induces a strong evolutionary pressure that selects for the cells the most capable to survive and thus somehow the most aggressive.

It is axiomatic that in order to survive, cells surrounded by an already inflated acidic microenvironment have to restrain the further generation and release of protons. Hence, one of the first metabolic changes is the reduction in glucose uptake and glucose fermentation. Investigators in our laboratory, for instance, documented a net reduction in the expression of GLUT-1 and MCT4 that are transporters involved in glucose uptake and lactate release, respectively [34]. This culminates in a less fermentative cell that produces fewer protons and lactate. To replace glucose, in particular for cancer cells located away from blood vessels, in a zone where nutrients can be scarce, lactate generated by the hypoxic cancer

cells may represent an alternative fuel. Interestingly, although MCT4 is downregulated, MCT1 is still present in cells exposed to acidosis [34]. MCT1 and MCT4 are both proteins that allow the release of lactate together with protons, but the Km of MCT1 for lactate makes this transporter particularly suited to also promote the entry of lactate inside of the cell when the gradient is favorable. Lactate, when present in the cytosol, can be oxidized to pyruvate via the lactate dehydrogenase (LDH) and thus give rise to acetyl CoA that can enter into the TCA cycle. This process allows for the cooperation between two cell populations: cells present in deep hypoxic zones, obliged to produce and release lactate and cells present in the acidic (moderately hypoxic) environment, exposed to high levels of lactate. Still, this mechanism is not neutral since in order to use lactate, acidic cells will face the entry of a proton (through MCT1). In the model presented in Figure 5, it is proposed that acid-exposed cells use CO_2 (resulting from OXPHOS) and carbonic anhydrase CA II and CA IX located inside and outside the cells, respectively, to deal with protons taking advantage of the interconversion between HCO_3^- and H^+; NBC being also part of the loop for HCO_3^- handling [113].

Acidosis-adapted cancer cells were also shown to use glutamine [34]. Glutamine is an abundant nutrient (the highest concentration among circulating amino acids) and it participates in different pathways: energy formation, redox homeostasis, macromolecular synthesis, and signaling in cancer cells. Besides its anaplerotic role to fuel TCA cycle through successive conversion into glutamate and then α-ketoglutarate (αKG), glutamine can also support lipogenesis via the reductive carboxylation pathway. Reductive carboxylation of glutamine can occur in both cytosol and mitochondria (Figure 7). It starts with the carboxylation of glutamine-derived αKG to produce isocitrate (with consumption of NADPH and CO_2). This reaction can be catalyzed by isocitrate dehydrogenase (IDH) 1 or 2 isoforms depending on the location of the reaction (either in the cytosol or in the

mitochondria, respectively) [24]. IDH3 is only located in the mitochondria and it is responsible for the inverse reaction [114]. Newly formed isocitrate can then be converted to citrate (which can be exported from the mitochondria via SLC25A1 protein). Mitochondrial citrate can fuel the TCA cycle (blue section in Figure 7), while citrate produced in the cytosol can contribute to the synthesis of fatty acids (yellow section in Figure 7) [24] or form oxaloacetate (OAA) to support aspartate-malate shuttle (green section in Figure 7).

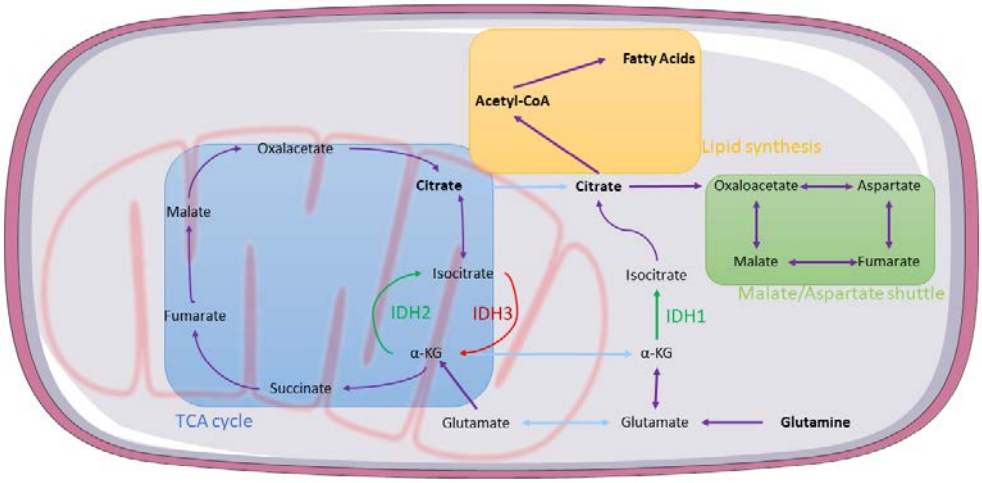

Figure 7 – Reductive carboxylation of glutamine

Reductive carboxylation of glutamine can occur both in cytosolic and mitochondrial compartments. Glutamine-derived αKG can contribute to either TCA cycle fueling in blue, lipid synthesis (in yellow) or to the malate/aspartate shuttle (in green). IDH1 and IDH2 transform αKG into isocitrate, while IDH3 performs the opposite reaction. Blue arrows demonstrate which substrates can pass through the mitochondrial membrane.

4. TGF-β signaling

As it will appear in the main experimental part of this thesis work, we identified TGF-β2 at the interface between tumor acidosis and the metabolism-supported pro-invasive phenotype of cancer cells. In this last part of the introduction, I will briefly survey the current understanding of TGF-β signaling and biology in the specific context of cancer.

TGF-β signaling regulates diverse cellular processes, including cell proliferation, differentiation, epithelial-to-mesenchymal transition, apoptosis, cell plasticity, angiogenesis and migration. Genetic alterations (*eg*. gene mutations and deletions) in numerous components of the TGF-β signaling pathway are frequently observed in human cancers. Here I will first review the role of TGF-β as a tumor suppressor and secondly how mutations drive the high tumorigenic effects of TGF-β in a variety of cancer cell models.

4.1 TGF-β signaling pathways

4.1.1 TGF-β cytokines and receptors

There are three different TGF-β cytokines expressed in mammalian cells: TGF-β1, TGF-β2, and TGF-β3. TGF-β cytokines belong to the TGF-β superfamily that includes a large group of 33 structurally-related regulatory proteins, among which activins and inhibins, bone morphogenetic proteins (BMPs), and growth differentiation factors (GDFs) [115]. Each isoform is encoded by a unique gene and expressed with tissue specificity [116]. TGF-β cytokines are produced and released by the cells in their latent form and only become active after being separated from

their latency-associated protein (LAP). The activation step is poorly understood, but the mechanism is likely to involve proteolytic processing and release of the TGF-β ligand [117-119].

TGF-β ligands regulate a variety of cellular processes by signaling through a heteromeric complex of high-affinity cell surface receptors: the type I TGF-β receptor (TGFβRI) and type II TGF-β receptor (TGFβRII) which are mostly considered as the signal propagator and activator, respectively. Seven forms of type I TGF-β receptors and five forms of type II receptors can be present in human cells [115, 120]. TGF-β can also connect with a type III TGF-β receptor (also referred to as β-glycan) which presents TGF-β to TGFβRII. However, β-glycan is not expressed in all cell types [121].

The localization of TGF-β receptors is essential for the type of message that will be sent. TGF-β receptors can be internalized *via* clathrin-dependent or caveolae-dependent endocytic pathways. The internalization of these receptors will determine the activity and termination of events (Figure 8) [122, 123]. When present in clathrin-dependent endosomes, TGF-β receptors can activate both Smad- and non-Smad-dependent signaling pathways (explored in sections 4.1.2 and 4.1.3, respectively) and, depending on the endosome, they can be recycled back to the cell surface or be degraded. This process is regulated by several proteins, but Rab5 seems to be a crucial regulator for the recycling of TGF-β receptors [122]. Whilst the formation of a ternary complex of EPS15, STAM and HRS leads the vesicles to a multivesicular endosome, which leads to receptor degradation through multiubiquitylation [123]. However, when present in *caveolae* microdomains, TGF-β receptors induce only some of the non-canonical signaling pathways (*eg*. MAPK-dependent pathways) and proceed for ubiquitination and subsequent degradation [124, 125].

Upon TGF-β binding on its receptors, there is a conformational change on TGFβRI where its dormant catalytic center is activated. TGFβRI and TGFβRII intracellular domains, that contain serine/threonine protein kinases, become phosphorylated initiating downstream cascades. Signaling continues as the complex enters the cell through the endosomes[121], promoting intracellular signaling pathways.

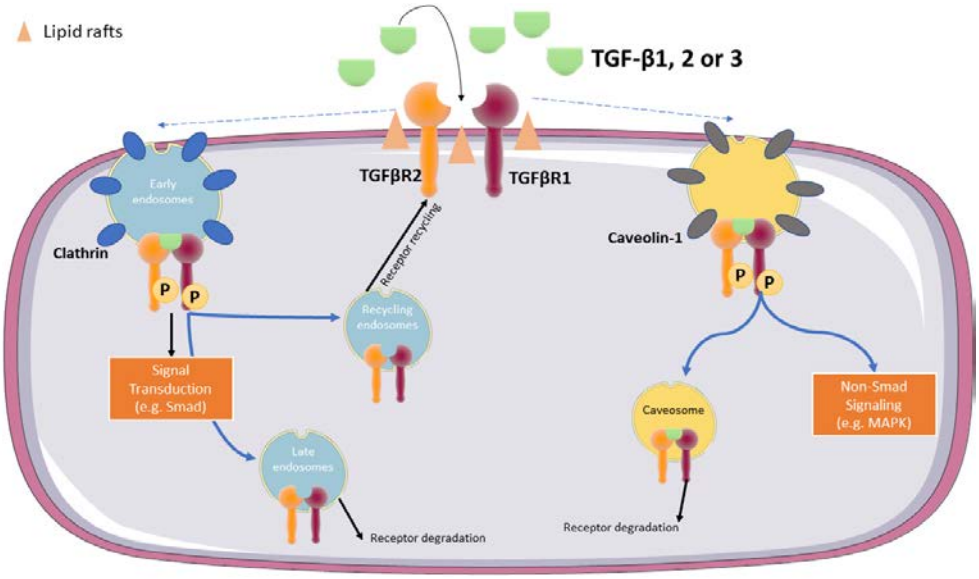

Figure 8– The fate of TGF-β receptors according to their localization (clathrin- and caveolin-expressing endosomes)

TGF-β receptors present in clathrin-expressing endosomes can transduce signals through both Smad and non-Smad pathways, before being degraded or recycled by membrane trafficking. When present in caveolin1-expressing endosomes, they can propagate some non-Smad signals before being degraded. Adapted from [123].

4.1.2 Canonical TGF-β/SMAD signaling

Smads belong to a small family of structurally related proteins, with two globular domains MH1 and MH2, connected *via* an intermediate linker (Figure 9) [126]. The MH1 domain participates in nuclear localization and DNA-binding, while most of protein-to-protein interactions occur through the MH2 domain. The linker has regulatory sites that can be phosphorylated by several kinases, including mitogen-activated protein kinases (MAPKs) [121, 126].

There are three distinct subtypes of Smads: receptor-regulated Smads (R-Smads), common partner Smads (Co-Smads), and inhibitory Smads (I-Smads) that differ between the TGF-β superfamily members. More specifically, for TGF-β cytokines, R-Smads are Smad2 and Smad3 [127]. Smad4 is a Co-Smad that binds to all R-Smads, while Smad6 and Smad7 are considered as I-Smads.

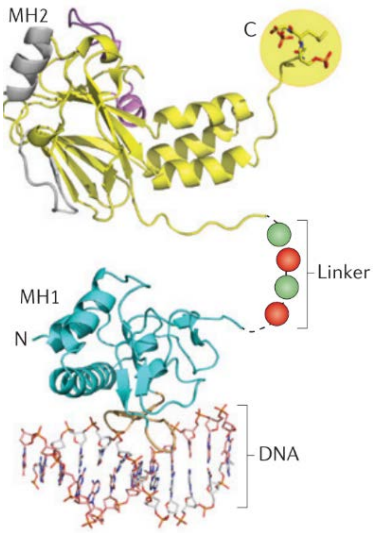

Figure 9– Structure of Smad 3.

R-smads proteins have two globular domains (named MH1 and MH2) connected through a linker region. The carboxy-terminal sequence (represented in yellow with a C) can form a bond with Smad4. The linker region (red and green circles) can be phosphorylated by cyclin-dependent kinases (CDKs), mitogen-activated protein kinases (MAPKs) and glycogen synthase kinase 3 (GSK3). This will create docking sites for positive and negative regulators of Smads. The MH1 domain can connect with the DNA directly and proceed to the expression of a series of genes. Adapted from [120].

In the canonical pathway, activated TGF-β receptors internalize through clathrin-dependent early endosomes [128, 129]. It is inside the cytosol that R-Smads are recruited and activated upon the TGFβRI-dependent phosphorylation of

their carboxy-terminal tail [115, 127, 130-133]. Once phosphorylated, they form a complex with Smad4 and translocate into the nucleus where the trimeric complex Smad 2/3/4 binds directly to DNA [121], DNA-binding transcription factors [134] or interacts with chromatin [126, 135]. This Smad complex can induce or repress up to 500 genes in mammalian cells [121]. There is a constant shuttle in and out of the nucleus for R-Smads, but the formation of the receptor-activated R-Smad/Co-Smad complex favors their nuclear accumulation [136]. The R-Smads are linked to the transcriptional machinery through interaction with CBP/p300, which is vital for their transcriptional activation [137, 138].

As seen before, clathrin-dependent endosomes activate the canonical pathway. However, in the presence of cholesterol and caveolin, TGF-β receptors degradation is promoted [124, 125], and followed by an initiation of the inhibitory activity of Smad6 and Smad7 (see figure 10). Smad7 inhibits the downstream effect of TGF-β signaling in three different ways: 1) it blocks the interaction between R-Smads and TGF-β receptors by competing with R-Smads for TGF-βRI phosphorylation, thereby preventing their activation [139], 2) binds to the DNA hence preventing the formation of a functional R-Smad-DNA complex [139] and 3) recruits E3 ubiquitin ligase that proceeds to ubiquitination and subsequent proteasomal degradation of TGF-β receptors [140, 141]. Smad6 also interferes with TGF-β signaling by preventing the formation of the Smad2/Smad4 complex [142].

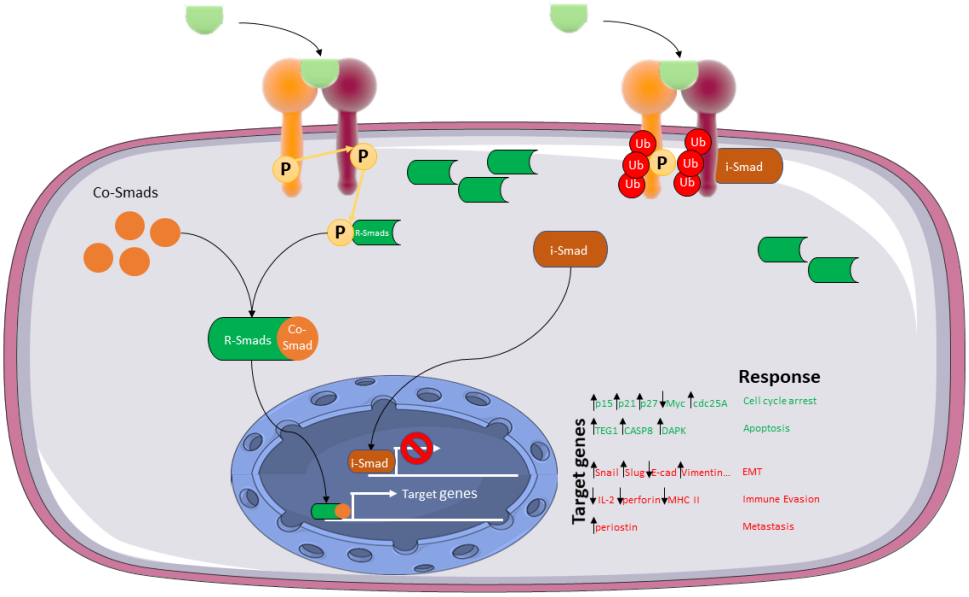

Figure 10– The Smad pathway

On the left the Smad pathway is activated. Phosphorylation of R-Smads allows them to be activated and to form a complex with co-Smads. This complex enters in the nucleus and transcribes target genes that either promote tumor suppression (in green) or are tumorigenic (in red).

On the right the Smad pathway is inhibited. The production of i-Smads leads to ubiquitination of the receptors, inhibition of the phosphorylation of R-Smads and on top of that they can repress the

4.1.3 TGF-β/Non-canonical signaling

Besides the canonical Smad-dependent signaling pathways, TGF-β proteins can also activate non-Smad proteins, including MAPKs, phosphoinositide 3' kinase (PI3K) and small GTPases. The signal transduction emanates directly from type I and II TGF-β receptors. These are signals that try to complement and sometimes regulate the Smad pathway. For example, cells can undergo EMT due to activation of Smad cascade, but TGF-β receptor II can transform even further the cell by directly phosphorylating partitioning defective 6 (PAR6). It will then recruit SMURF1 to target RhoA GTPase at tight junctions, thereby causing dissolution of the

junctions and polarized migration that help EMT process which is promoted by Smad [143-146]. Smad- and non-Smad-dependent pathways will be examined in reference to their ability to induce a tumor-suppressive effect (section 4.2) or a tumor-promoting effect (4.3). Figure 11 summarizes some of the non-Smad pathways activated by TGF-β, which include: Rho promotion and PAR6 phosphorylation done by TGFβRII and p38, JNK, ERK Pi3K and MAPK pathways promoted by TGFβRI.

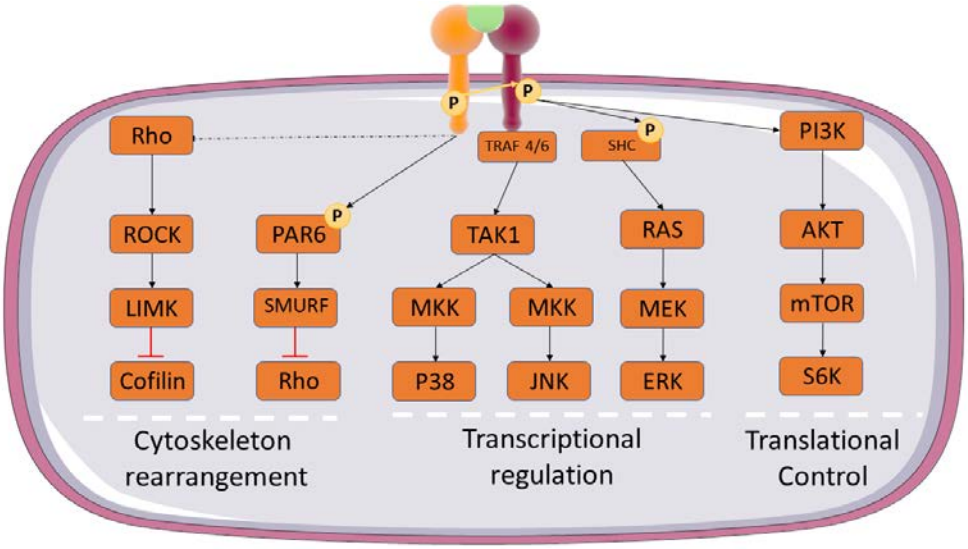

Figure 11– TGF-β-induced non-Smad signaling pathways

TGF-β can also lead to non-Smad protein activation. These have different functions and start or complement pathways connected to Smad. Adapted from [131].

4.2 TGF-β as a tumor suppressor

In a pre-malignant stage, TGF-β is secreted by tumor and/or stromal cells and can induce cell cycle arrest, promote apoptosis, and thereby play a tumor-suppressive role. These pro-apoptotic mechanisms offset the cancer-associated hyperproliferative signals.

4.2.1 TGF-β-induced antiproliferative effects

The most described contribution of TGF-β as a tumor suppressor comes from its ability to inhibit the growth of the epithelial and lymphoid cells, from which most human cancers may arise. However, TGF-β, when purified for the first time, was identified for its ability to stimulate proliferation rather than inhibit it [147]. Nowadays we know that TGF-β can prevent cell cycle progression, although the extent of growth inhibitory response differs from cell to cell and the experimental model system used.

Cyclin-dependent kinase inhibitors

TGF-β-induced cell cycle arrest is mostly supported through expression and/or stabilization of cyclin-dependent kinase inhibitors (CDKi) p15, p21 and p27 and the elimination of proliferation drivers. CDKis prevent the cyclin/CDK-mediated phosphorylation of the retinoblastoma protein (Rb), and hence allows for the sequestration/inactivation of the E2F transcription factor (responsible for cell cycle progression) and the cell cycle arrest in early G1 phase. As said before, Smad and non-Smad complement and reinforce other signals. This is especially clear in the case of CDKi since the major effectors of this signal seems to be promoted by Smad proteins like $p15^{INK4b}$ [148, 149], $p21^{CIP1}$ [150, 151] and $p27^{KIP1}$ [152]. Yet some actors of the non-Smad cascade also induce similar effects (*e.g.* ERK signaling pathway increasing $p15^{INK4b}$ levels [153] or MEK is essential for TGF-β-dependent stimulation of $p21^{WAF1/CIP1}$ which occurs in a p53-independent manner [154]). Smad proteins are known to promote the transcription of CDKis (representative scheme in figure 12). For example, the complex Smad 2/3/4 can bind to a GC-rich region of the $p15^{INK4b}$ gene promoter and activate its expression [149]. In the case of $p21^{Cip1}$, p63 and p73, which act as enhancer elements of this gene, are stabilized by direct interaction with Smads improving the expression of the $p21^{Cip1}$ gene [155], but Smad3 and

Smad2 can also produce $p21^{Cip1}$ by binding directly to the gene [156]. The already referred $p15^{INK4b}$ and $p21^{Cip1}$ are important CDKi in epithelial cells but not in hematopoietic cells. In these cells, TGF-β induces the transcription of $p57^{Kip2}$, whose role is similar to the $p21^{Cip1}$ [157]. Smad proteins can also directly affect components of the cell cycle machinery. p53 binds to specific sequences of untranslated region of the CDK4 mRNA in a Smad-promoted/instructed way, although the mechanism is not yet well clarified [158, 159].

Proliferative drivers

The major proliferative drivers affected by TGF-β are c-Myc and cdc25A. TGF-β-induced c-Myc gene repression, which in turn prevents the transcription of p21 and p15 while promoting cdc25A expression, is believed to occur dependently [160] and independently [161] of Smad proteins. The Smad-dependent process is accomplished by a nuclear phosphorylated Smad3 together with Smad4 promoting a transcriptional inhibitory element on the c-Myc promoter [160]. The Smad-independent mechanism is not clarified and only demonstrated by the fact that, in a subset of ovarian cancers rich in Ski and SnoN (Smad2 and 3 corepressors), the TGF-β inhibitory effect on c-Myc expression was still observed [161]. Finally, TGF-β inhibition of the tyrosine phosphatase cdc25A causes inactivation of Cdk4 and Cdk6 and cell cycle arrest in the G1 phase [162].

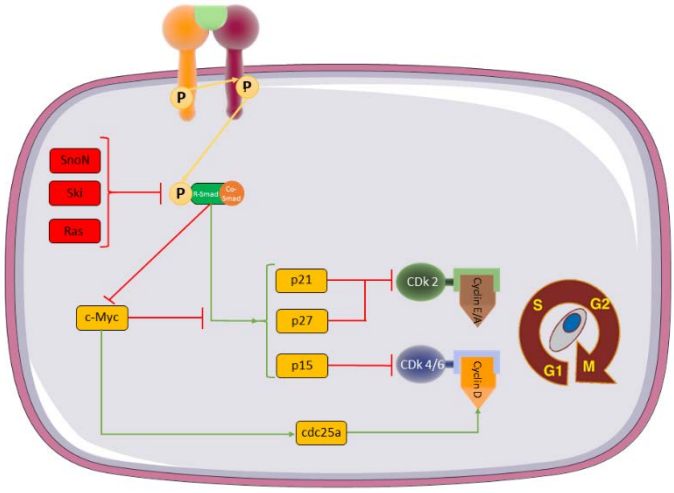

Figure 12– Molecular mechanisms supporting the TGFβ-induced antiproliferative effects.

Complexed R-Smads and Co-Smads can influence CDKis and proliferative drivers alike. Adapted from [121].

4.2.2 TGF-β-induced pro-apoptotic mechanisms

The ability to induce apoptosis in a cell type-specific manner is another tumor-suppressive feature of TGF-β. In a pre-malignant state, when cells start to face oncogenic mutations, TGF-β-mediated suppressive effects become more dramatic, as it is in this context that TGF-β triggers apoptosis. The exact mechanisms underlying the TGF-β-induced apoptosis in pre-malignant cells is not clear, but in some tumor types, the TGF-β apoptotic pressure is so strong that tumor selection creates clones with mutations that eliminate TGF-β signaling entirely [163]. Even in non-malignant cells, cell culture and *in vivo* studies can point to a pivotal role of TGF-β-mediated apoptosis in the liver, prostate, digestive, nervous, immune and reproductive cells [164]. Interestingly, TGF-β has also been reported to promote cell survival under certain conditions as well. For example, *via* Akt signaling, TGF-β stops serum starvation-induced apoptosis [165]. Smad proteins

regulate the expression of a vast number of genes connected to the apoptotic machinery. These signals are again supplemented by non-Smad cascade. Some of the Smad and non-Smad activated genes related to pro-apoptotic activities are:

- TEG1 is a transcription factor responsible for the regulation of other pro-apoptotic genes [166];
- GADD45β is a signaling protein that activates p38 MAPK through the mitogen-activated protein kinase kinase 4 (MKK4), thereby leading to caspase-8 activation which promotes the release of cytochrome C and downstream caspase-dependent pathways (caspases 9 and 3) [167, 168];
- DAPK modulates the mitochondrial membrane potential and, through a still unknown mechanism, promotes cytochrome C release and caspase activation [169];
- TAK1, a non-Smad protein activated upon direct phosphorylation of TGF-β receptor 1, can also activate caspases by the same mechanism than GADD45β [170];
- SHIP promotes changes in the intracellular pool of phospholipids which inhibits the activation of the pro-survival Akt/PKB kinase, which leads to the induction of apoptosis in hematopoietic cells [171];

4.3 Tumorigenic Effects of TGF-β

As previously said, cancer is a multistep process resulting in the evolution of a cell population that has escaped from the control of regulatory mechanisms. Inactivation of tumor suppressors like TGF-β is a way to escape regulatory systems. However, TGF-β is not a simple tumor suppressor, since it has been proven to act

also as a tumor promoter. This is further supported by the widely overexpressed levels of TGF-β in many human cancers. Because it can work as a tumor suppressor or have oncogenic roles, the TGF-β pathway does not appear to be fully active or completely off. Instead, it shows to be regulated by a rather complex dosage effect. Here I will analyze how alterations in the expression levels of different components of the TGF-β signaling pathway allow for tumor development and can be used as a metastatic factor.

4.3.1 Points of Disruption in the TGF-β Pathway in Cancer

TGF-β-mediated signaling pathways are very complex, with crosstalks between non-Smad/Smad proteins and other signaling pathways, thereby opening a great number of doors for disruption. Alterations of some components in TGF-β pathways have been observed in diverse human tumors. These include gene deletions or mutations, downregulation of components, magnification or overexpression of pathway inhibitors, and overexpression or overactivation of signaling molecules. Here I will divide TGF-β signaling modifications into three distinct parts: TGF-β receptor alterations, Smad protein alterations and modulation of TGF-β signaling by oncogenes. TGF-β overproduction or overactivation will be discussed in section 4.3.2 - Sources of TGF-β in Tumors.

TGF-β receptor alterations

The *TGFBR2* gene is modified in some tumors, a change associated with microsatellite instability (MSI) [172]. This predisposition to mutation arises from the inactivation of the mutation mismatch repair system (MMR), causing base pair mismatches during DNA replication. This leads to the accumulation of replication errors at 'microsatellite-like'' repeats. Genes containing these errors are observed

to be mutated. Such mutation, called the BAT-RII mutation, has been observed in *TGFBR2* gene. It consists of the introduction of a non-sense mutation through insertion or deletion of one or two adenines resulting in the expression of a truncated protein that lacks both the transmembrane and the intracellular serine-threonine kinase domains [173]. This alteration has been observed in tumors associated with a MSI-like phenotype, including colon [172, 173], gastric [172], lung [174] and glioma [175] cancers. Other non-MSI-associated *TGFBR2* mutations have been described, and studies report that 25% of ovarian cancers, 21% of HNSCC and 12% of breast tumors have a mutated *TGFBR2* gene while this genetic feature is very rare in pancreatic cancers [176]. Contrary to the *TGFBR2* gene, *TGFBR1* lacks a repetitive nucleotide sequence, hence reducing genomic instability, and so far there is no association with MSI mutations described in the literature. However, *TGFBR1* gene mutations have been observed in ovarian [177], metastatic breast [178], pancreatic [179] cancers and T-cell lymphomas [180]. Both *TGFBR1* and *TGFBR2* can suffer from hypermethylation of CpG islands in the gene promoters [181].

Smad protein alterations

Inactivation of tumor suppressor genes is characterized by inhibition of both alleles of a chromosome. This is commonly achieved by mutation of one allele followed by the loss of a chromosomal region containing the other one, a process known as loss of heterozygosity (LOH). Smads can suffer from this mutation, particularly *SMAD4* and *SMAD7* which can have mutations that impact tumor development. LOH in *SMAD4* can be found in up to 50% of pancreatic cancers [182], 12% of breast cancers and 7% of lung cancers [183]. The mutations are most frequent in the MH2 domain of the protein, which is the part that allows the oligomerization with the R-Smads [183]. Although the gene that encodes Smad2 is closely located to Smad4, the mutation of this gene occurs at very low frequency in

tumors [184, 185]. Contrary to Smad2 and 4, there was no mutation found in *SMAD3* gene in human cancers. However, it may be silenced *via* epigenetic inactivation since the loss of Smad3 has been identified in some gastric cancers [186], and re-introduction (knock-in) of Smad3 into human gastric tumors restored TGF-β responsiveness. This epigenetic silencing might be crucial for the loss of TGF-β-dependent tumor suppression capacity given that Smad $3^{-/-}$ mice developed aggressive colon carcinoma metastasis [187]. The gene encoding for Smad 7 is frequently mutated in tumors (Smad 7 is a I-Smad). This gene suffers from mutations leading to under-expression or, more commonly, overexpression [188]. In general, Smad mutations lead to inactivation or disruption of the Smad cascade, which allows tumors to surpass the initial tumor-suppressive status of TGF-β.

Modulation of TGF-β signaling by oncogenes

There is a particularly complicated interrelationship between the TGF-β signaling and oncogenic pathways in tumorigenesis. Oncogenes like *MAPK1*, *KRAS*, *SKI* and *SNON* are able to modulate TGF-β signaling in different ways. RAS pathways play an important role in sequestering TGF-β towards a pro-oncogenic outcome. Oncogenic RAS molecules Erk1 and 2 can phosphorylate specific serine residues in the linker domain of Smad2 and Smad3. The linker phosphorylation traps Smads in the cytoplasm, consequently blocking their physiological nuclear function [189]. The MAPK pathway can, instead, phosphorylate the C-terminal tail of Smad2, leading to hyperactivation of Smad signaling [190]. These TGF-β and activated MAPK and RAS interconnections guide cells to an aggressive metastatic state. For example kidney epithelial cells under these conditions avoid apoptosis and enhance invasive effects [191].

SKI and SNON can be deleted or amplified in human tumors. They interact with Smad2, Smad3, and Smad4, and compete with Smads for binding to CBP and

p300 [192]. When bound to the nuclear Smad, the two proteins recruit co-repressors of the N-CoR family and histone deacetylases blocking the effect of Smads [193, 194]. In the analysis, a set of well-established oncogenic mechanisms manipulate TGF-β signaling in order to convert it from a tumor suppressor to a tumor promoter.

4.3.2 Sources of TGF-β in Tumors

An excellent question asked for several years was: why do tumors generally oversecrete TGF-β, when this cytokine acts as a growth inhibitor? In fact, unstressed tissues sustain a basal release of TGF-β by local sources to maintain homeostasis. However, tumor cells show an abnormal increased expression of TGF-β mRNA, most commonly TGF-β1, when compared with the normal surrounding tissue. In fact, cancer cells take advantage of a common mechanism that occurs during tissue injury. Indeed, during this process, TGF-β is abundantly released by platelets, immune and surrounding cells to prevent uncontrollable regenerative cell proliferation and inflammation, thereby allowing TGF-β to be frequently available in the tumor microenvironment. Initially, it develops some tumor-suppressive signals, but eventually, malignant cells disrupt TGF-β signaling and use it to their own advantage. Nowadays, there are substantial pieces of evidence supporting how increased TGF-β levels promote tumor progression by enhancing migration [195, 196], invasion [116, 133, 197-199] and overall cell survival [200-203]. An explanatory scheme of alterations in TGF-β leading to poor prognosis can be found in figure 13.

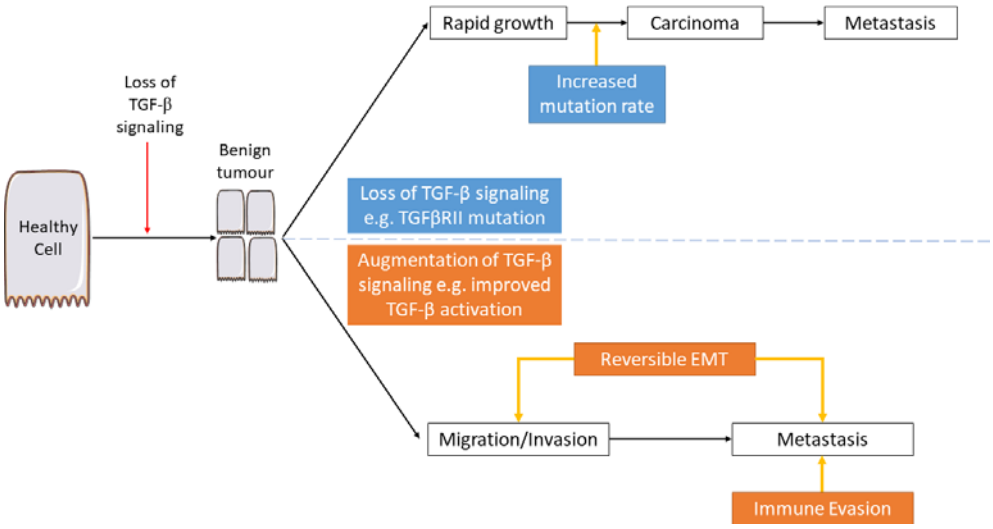

Figure 13 – The delicate balance of TGF-β levels.

Disruption of TGF-β, either by suppression or augmentation of its signal leads to higher tumorigenic levels. Adapted from [132].

Sources and activity of TGF-β vary from tumor to tumor and, even inside the same tumor, it changes according to microenvironmental conditions [204, 205]. As discussed before, the microenvironment includes: (a) cancer cells, and many overproduce TGF-β mRNA, such as cervix, renal, kidney, bladder, head and neck, lung, bone and prostate cancer, and glioblastoma, melanoma, rhabdomyosarcoma [206]; (b) various cells of the tumor stroma, including cancer-associated fibroblasts, leukocytes, macrophages, and bone marrow-derived endothelial, mesenchymal, and myeloid precursor cells that release TGF-β with the particularity that each source leads to a context-dependent functional consequence [133]. The high levels of TGF-β are associated with poor prognosis [207], as demonstrated by the specific localization of secreted TGF-β at the advancing tumor edges [208].

Activation of TGF-β is a fine-tuned molecular process, proven by the fact that tissues routinely present large amounts of latent TGF-β, but activation of only a small fraction of it is enough to generate maximal cellular response [117].

Activation of the latent form of TGF-β is a multicomplex process involving various enzymatic and nonenzymatic activities different for each type of TGF-β (1,2 and 3) and for each tumor. *In vitro* however, all three isoforms can be activated by extreme pH values (pH 2 and pH 8), high temperatures (100 °C) and substances like SDS and urea [209, 210]. *In vivo,* the situation is more complex, the three isoforms are activated by both proteolytic events (*e.g.* cathepsin D, matrix metalloprotease-9, and calpain) [211] and non-enzymatic processes (*e.g.* TSP-1/CD36) [212]. In addition, from the three major mechanisms of TGF-β-activation (i.e. plasminogen proteolytic system, integrins and thrombospondin-1), only TGF-β1 and TGF-β3 are activated by integrins, while thrombospondin-1 and the plasminogen proteolytic system can activate all isoforms in specific tumor situations [117-119, 210]. Plasmin activates TGF-β through disruption of the tertiary structure of LAP-TGF-β [213]. Integrin family αvβ6 and thrombospondin-1 cause a conformational change in LAP-TGF-β by binding to its RGD and LSKL sequences, respectively, thereby leading to release of active TGF-β [211]. To have higher levels of TGF-β signaling, cancer cells must be able to activate large amounts of latent-TGF-β and in order to do just that, they have to express the TGF-β activators previously mentioned. For example, plasmin generation by tumor cells enhances activation of TGF-β, migration and invasion [214], a good example to explain the correlation between TGF-β activation and tumor aggressiveness.

4.3.3 TGF-β signaling and immune evasion

Cancer cells express tumor-specific antigens which are normally recognized by the immune system and guide cancer cells to their death. However, cancer cells can, through multiple mechanisms, acquire the ability to escape this immuno-

surveillance. One of these mechanisms is the cell-mediated secretion of TGF-β. TGF-β is a known inhibitor of proliferation and differentiation of B and T lymphocytes. In addition, TGF-β inactivates scavenging macrophages which develops and protects the tumor from immune surveillance [215]. For those reasons, TGF-β is considered as one of the most potent natural immunosuppressors in the human body.

T-cells

One of the first evidence of TGF-β acting as an inhibitor of CD8+ cytotoxic T lymphocytes came from the fact that cells transfected with TGF-β1 did not stimulate primary $CD8^+$ T cell responses *in vitro* and *in vivo,* meaning that TGF-β1 allows immunogenic cells to escape immunosurveillance [216]. The creation of transgenic mouse models where TGFβR2 is impaired (by dominant-negative mutation) in T-lymphocytes, led to one of the most convincing evidence of the important role of TGF-β in T cells [217]. The engineered TGFβR2-deficient T cells prevented the growth of melanoma or thymoma in mice. TGF-β abrogation permitted T cells to differentiate into effector T cells granting a proper and enhanced immune response against experimental tumors implanted into the mice [217]. The above experiment illustrates how T-lymphocytes can be a potent and effective therapy against cancer when the endogenous TGF-β pathway is inactivated. With a similar methodological approach, other investigators obtained the same results in colon cancer and reported additional evidence for the contribution of a TGF-β2/interleukin 6(IL-6)-dependent activation of STAT-3 in the induction of an efficient immune response [218]. TGF-β can also block the production of interleukin 2 (IL-2), responsible for T cell proliferation [219]. A transcriptome study (followed by some validation assays) also puts TGF-β signaling as an inhibitor of perforin, granzyme A and B, Fas ligand and interferon-γ [203], all

of them described to be noxious to $CD8^+$ T cells; the inhibition of the Smad pathway seems to reverse the effect.

Other immune cells

Besides inhibitory effects on T cell activity, TGF-β can also affect antigen-presenting cells (APCs). Macrophages, for instance, can be inactivated in the presence of high TGF-β levels [220]. In dendritic cells, a study points out that TGF-β promotes their growth and differentiation by promoting the viability of DC precursors and not by inhibiting their proliferative response, the latter effect being only accomplished when TNF-α is present [221]. Smad3 can interfere with the initiation of immune responses by inhibiting the expression of MHC II molecules on several different cells [222]. Natural killer cells [223] and neutrophils [224] are other supplementary targets of TGF-β in the immune system.

In conclusion, TGF-β is produced by cancer cells and immune cells alike. At the beginning, it is set for the protection of DC growth and differentiation, but dysregulation of its levels causes an escape from proper immunological control as described in numerous human cancers.

4.3.4 TGF-β-driven regulation of the epithelial-mesenchymal transition

In a previous section, we analyzed EMT in a nutshell. Here we will break the shell and analyzed the nut (EMT) more thoroughly at the light of the TGF-β effects in this process. EMT is important in embryonic stages, for developmental programs involved in generating new tissues. Cancer cells exploit EMT to their benefit because it provides directly or indirectly metastatic advantages. In order to understand EMT one needs first to comprehend that EMT is a gradual process. In

fact, the term transition was preferred to the word 'transformation' that was initially used [225], to illustrate that the process does not occur in one step. Even further, it does not need to go until the end of the mesenchymal spectrum to EMT to be considered as significant. This is the reason why some research groups now propose to call the process epithelial–mesenchymal plasticity (EMP) [226]. The plasticity of EMT has been quantified in different cancers according to a ranking gradient from -1.0 to +1.0 [227]. The scoring system is based on the expression of some important genes for epithelial and mesenchymal cells including specific transcription factors (e.g Snail, Zeb, Twist, …), miRNAs and epigenetic regulators.

EMT starts with the repression of epithelial genes which allows the disassembly of epithelial cell-cell contacts; this translates in the removal of tight junctions, adherent junctions and gap junctions. The disassembly happens at the same time as the cell starts to lose its basal-apical polarity while developing a front-rear polarity. Cell elongation and expression of mesenchymal markers happen meshed with the previous processes [228-231]. The multiple effects promoted by EMT lead to increased migration and invasion capacities. The plasticity of EMT allows it to be reversed – mesenchymal to epithelial transition (MET). This is the final step of these cells in order to metastasize, it will cease migration and reestablish a proliferative and anchoring capacity – if the process succeeds a second tumor is formed. Circulating tumor cells (CTCs) express both epithelial and mesenchymal markers alike, further raising the possibility that EMT is causing the dissemination of cells (e.g breast CTC exhibit a range of EMT phenotypes [232]).

The critical role of EMT in tumor metastasis and its recurrence compelled scientists to link EMT with the properties of cancer stem cells (CSCs) [233-236]. Cancer stem cells have the capacity to self-renew, differentiate, promote drug resistance and anchor independently. These are cellular features needed to initiate

a tumor and support long-term growth and self-renewal capacity. This is the reason why CSC are thought to be involved in establishing metastases at distal sites [233]. The phenotypic resemblance between cancer cell populations with EMT-like features and stem-like properties led to the idea that EMT was promoting cancer cell stemness. Accordingly, mammary epithelial cells contained a subpopulation of stem cells (i.e., $CD44^{high}/CD24^{low}$ cells) that displayed a mesenchymal morphology and expressed typical mesenchymal markers (when compared with $CD44^{low}/CD24^{high}$ cells). Furthermore, these mesenchymal cells are capable of forming mammospheres, a well-known hallmark of mammary stem cells [237]. Also, EMT and CSC have been both correlated with TGF-β signaling. Breast cancer with CSC-like properties have higher levels of TGF-β1 and TGFβRII expression than differentiated cells, and inhibition of TGF-β signaling in CSCs leads to MET (i.e., re-establishes an epithelial phenotype) [238]. However, and despite all these shreds of evidence, new studies have shown that EMT and CSC development are happening in parallel rather than at the same time and through the same pathway.

Smad pathway

TGF-β has been one of the most reported drivers of EMT. Several TGF-β-mediated signaling pathways have been implicated in EMT, including Smad and non-Smad pathways. TGF-β is associated to EMT in pre-natal [239, 240] and non-carcinoma diseases (e.g. fibrosis [241]). In 1994, Oft et al. reported one of the first pieces of evidence for a TGF-β-induced EMT and tumor cell invasiveness in carcinomas (mammary tumor cells) [242]. TGF-β promotes reversible EMT through transcription factors leading to a decreased expression of the epithelial markers like E-cadherin, ZO-1, and desmoplakin I and II; this is further associated with an increased expression of mesenchymal transcription factors (e.g. AP1, ATF3,…) and markers such as fibronectin and vimentin (Figure 14), together with the inhibition of cell growth [243]. This process, like many other TGF-β features, is promoted by

Smads and complemented by non-Smads pathway. Smad pathway is essential, since inhibition of the Smad4 for instance lowers by 75% the frequency of bone metastases from circulating MDA-MB-231 cells in nude mice [244]. Still, partial depletion of Smad4 in HaCaT keratinocytes and colon carcinoma cells did not stop TGF-β-induced EMT suggesting that low levels of Smad4 are sufficient for EMT to occur. In fact, other reports have reached the same conclusion for Smad3 [245, 246], only complete Smad3 inactivation through dominant negative can entirely block TGFβ-induced EMT [246]. On the other hand, Smad2 does not appear to be required for EMT and some reports claim that it might even be prejudicial [247]. Smad complexes not only activate the expression of EMT transcription factors but additionally, they also improve their activity. Snail1 is induced in a Smad3-dependent way [247], while Snail2 is induced indirectly by Smad3-mediated myocardin-related transcription factor (MRTF) [248]. Both zinc-finger transcription factors (Snail 1 and 2) can repress E-cadherin, an epithelial protein responsible for cell–cell adhesion. Smad3 can also activate ZEB1, ZEB2 and TWIST (through activation of transcription factor 3 (ATF3)) [249, 250].

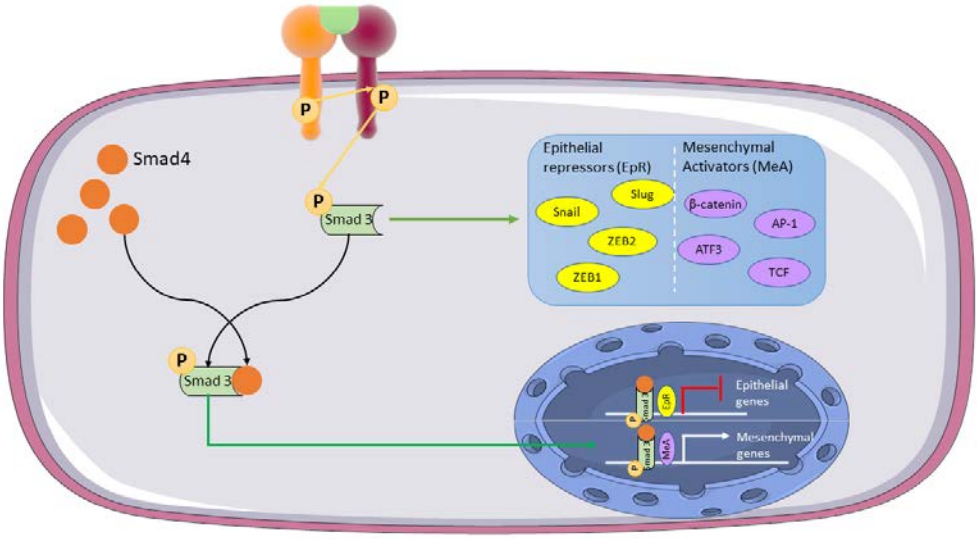

Figure 14– The TGF-β/Smad cascade contribution to the EMT phenotype.

TGFβ-induced Smad3/Smad4 signaling can directly promote EMT when conjugated with Smad4 by activating the transcription of mesenchymal-related genes (e.g. *CDH2, VIME,* …) while repressing epithelial genes (e.g. CDH1, TJP1, …). It can also indirectly promote EMT through transcription factors that englobe epithelial repressors and mesenchymal activators. Adapted from [245].

Non-Smad pathway

In order to complement the effects dependent on Smad3/Smad4 signaling, TGF-β also induces the non-Smad pathway, involving PAR-6, Rho-like GTPases, PI3K and MAPK pathway effectors. Activation of Rho GTPases, Rac, Cdc42 and phosphorylation of PAR-6 drives actin reorganization (see section 4.3.5).

TGF-β can also activate Akt through PI3K pathway, this leads to activation of mammalian TOR complex 1 (mTORC1) and mTORC2. The two mTOR complexes promote important processes for EMT: mTORC1 contributes to the increased cell size, motility and invasion [251]; mTORC2 is necessary for the loss of epithelial markers in a process still largely unknown, but its inhibition obstructs metastasis formation [252]. PI3K–Akt pathway appears to be essential in the upregulation of mTOR [252, 253]. TNF receptor-associated factor 6 (TRAF6) is a direct effector of

TGF-β receptors, that can activate TAK1, a kinase upstream of p38 MAPK. Depletion of TRAF6 does not affect the Smad cascade but prevents TGF-β from activating p38 MAPK, which is associated with a failure to stimulate EMT [170, 254]. Twist1, a potent inducer of EMT (it upregulates N-cadherin [255] while it downregulates E-cadherin [256]) can be stabilized by p38 MAPK through phosphorylation of the Ser^{68} residue that potentiates its ability to induce EMT [257]. Snail is also directly upregulated by p38 which causes the repression of E-cadherin [258]. Erk 1/2 are other MAPK effectors of TGFβ-induced transcription, boosting the delocalization of E-cadherin and ZO-1 from the plasma membrane [258, 259].

We can conclude that in carcinomas, increased expression and activation of TGF-β promotes EMT. *In vitro* and *in vivo* models of TGF-β-induced EMT have been tested over the years. In fact, a 24h treatment with TGF-β1 is enough for the *in vitro* morphological conversion of keratinocytes to the mesenchymal phenotype [260]. *In vivo,* squamous carcinoma cells expressing a dominant-negative TGFβRII could not go through EMT in response to TGF-β [260, 261]. In general, dominant-negative forms of TGFβRII or TGFβRI or pharmacological inhibition of the receptors lead to a blockade of TGF-β-induced EMT [260-262]. Metformin, a clinically used agent to lower blood glucose concentration in patients with type 2 diabetes and metabolic syndrome, has been recently described as a suppressor for TGF-β [263, 264]. Metformin transcriptionally represses Zeb1, Twist1 and Snail that are key drivers of the TGF-β-induced EMT [265]. Furthermore, metformin in MCF-7 breast cancer, stopped TGF-β repression of epithelial marker E-cadherin, and vimentin induction in MDCK cells [265].

4.3.5 TGF-β signaling and cytoskeleton rearrangement

Cells undergoing EMT reorganize their actin cytoskeleton to enable dynamic cell elongation and directional motility. In parallel, there is a formation of cell projections which include sheet-like membrane protrusions called lamellipodia and spike-like extensions called filopodia (often located at lamellipodia edge). Lamellipodia are flat, sheet-like protrusions and main responsible elements for cell locomotion. In contrast, filopodia are rod-like extensions consisting of tightly bundled actin fibers that seep into the surrounding environment. These structures are enriched with proteases (already discussed in 3.2.4) which, together with EMT, help with the migration and invasion capacity of cells.

TGF-β has been reported to facilitate a dramatic reorganization of the actin cytoskeleton in different cell types through different non-Smad pathways [266-268]. TGF-β can globally activate RhoA, Rac and Cdc42 that are the main drivers of actin reorganization and lamellipodia and filopodia formation (Figure 15) [269, 270]. Rac and CDC42 functions range from stimulating actin polymerization at the leading edge of cells to regulating invadopodia turnover and stability. They are able to activate the LIM kinase which promotes cell spreading and actin polymerization at the cell periphery [270], and the cofilin protein, responsible for the first step in actin polymerization and later steps to recycle actin filaments [271, 272].

TGF-β can also favor RhoA activation, a protein responsible for the stress fibers formation, cytokinesis and cell migration [273, 274]. RhoA modulates the level of phosphorylation of the myosin light chain, impacting the actin dynamics by either promoting polymerization or stimulating depolymerization and disruption of existing F-actin filaments [275] to develop cortex tension and rear end leading [276].

To be able to leave the primary tumor, cells must break down cell-cell and cell-matrix junctions. EMT is part of the process but RhoA degradation is also necessary. In the early EMT process, PAR6 is directly or indirectly phosphorylated by TGF-β receptor II at tight junctions [143, 144, 146]. The phosphorylated PAR6 activates E3 ubiquitin ligase Smurf1 which locally mediates RhoA ubiquitylation and degradation as the tight junctions dissolve. RhoA degradation also shows a great importance in filopodia and lamellipodia formation and turn-over [143, 145, 277].

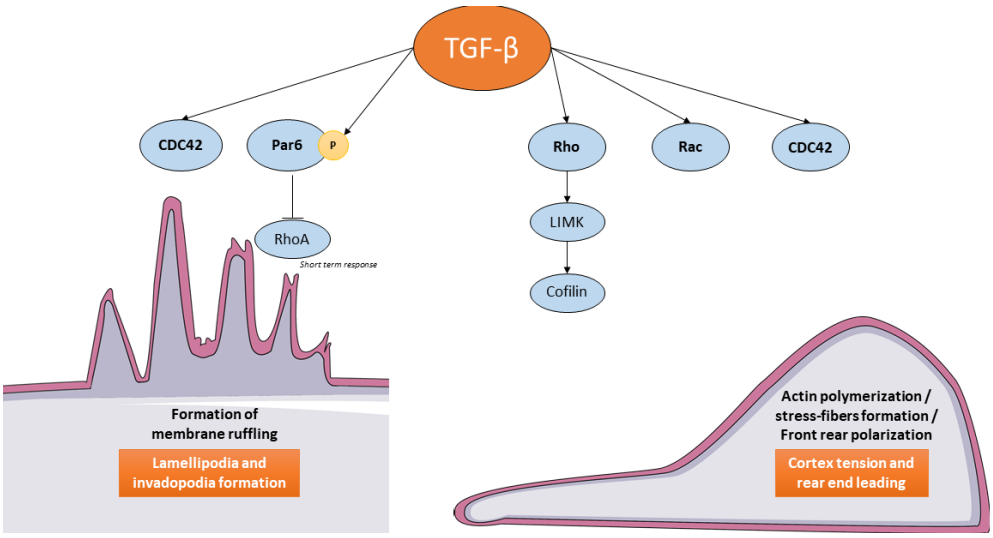

Figure 15 – Illustration of TGF-β signaling in the cytoskeleton rearrangement.

TGF-β signaling is important for formation of cortex tension, rear-end polarization and invasive structures like lamelipodias. In order to form the leading edge TGF-β activates RhoA, CDC42 and RAC. RhoA degradation is important for the turnover in membrane ruffling (important for migration) and CDC42 is crucial in formation of invasive structures.

4.3.6 TGF-β signaling and metastasis formation

Metastases are initiated by cancer cells that have the ability to disseminate and re-create a full-grown tumor in unwelcoming tissues [278]. The metastatic process requires tumor cells to first acquire migratory and invasive capabilities. TGF-β, through EMT and cytoskeleton rearrangement, already contributes largely to these two processes. Nevertheless, in addition to this local invasion role, TGF-β is also involved in the promotion of distal metastasis. It is currently accepted that the dissemination of tumor cells is a frequent event, but that the success rate of the process termed metastatic colonization (initiation of metastatic growth) is very low [279]. Many cancer cell types are inefficient in accomplishing this colonization, so that only a small minority of cancer cells that reach distant sites will give rise to metastases. In 1989, Stephen Paget, after autopsies of breast cancer patients, suggested that disseminated cancer cells, that he called "seeds", would only colonize specific organ microenvironments, or "soils," that were favorable and compatible to their growth [280, 281]. The idea of "preparation of soils for the seed" goes towards recent discoveries done with TGF-β model, where local production of TGF-β can profoundly affect the growth of secondary tumors since high levels of this cytokine provides support for CTC. For example, in a mammary chimera model, expression analyses in lung-colonizing cancer cells identified TGF-β as instrumental for the creation of a metastatic niche [282]. In the same paper, the use of genetic knock-down of TGF-β signaling led to the conclusion that low doses of ionizing radiation delivered on the homing tissue before cancer cell transplantation greatly accelerated the development of aggressive tumors in a TGF-β dependent way. Furthermore, breast cancer stem cells have been shown to produce TGF-β2 and TGF-β3 in order to stimulate stromal fibroblasts to generate periostin [279], a binding partner of tenascin C responsible for the recruitment of

Wnt factors (that are required to maintain the stemness of cancer stem cells); blocking periostin function actually prevents metastasis. Another study describes how TGF-β signaling in stromal cells increases the efficiency of organ colonization. Without TGF-β, aggressive colorectal cancer cells fail the process of colonization and mice treated with a pharmacological inhibitor of TGFBR1 develop significantly less metastatic lesions [283]. This was proposed to result from a lack of a TGF-β responsive signature containing several mediators of intravasation including IL11, ANGPTL4 and PTHLH [283]. The same result is obtained by overexpressing Smad7 and/or a dominant-negative form of the TGF-β receptor in melanoma [284] and renal carcinoma cell line xenografts [285]. These studies support the idea that TGF-β is critical at early time points of the metastatic process to facilitate the colonization of healthy tissues by disseminated cancer cells.

4.3.7 TGF-β-promoted metabolic reprogramming

Mutations or abnormal expression of oncogenes or tumor suppressors have been associated with metabolic alterations in cancer cells [286]. TGF-β signaling, that can be either considered as an oncogene or a tumor suppressor, is thus also associated with metabolic changes in tumors. It is however difficult to discriminate the metabolic effects directly driven by TGF-β from those resulting from TGF-β-dependent alterations in cell biology. For example, different reports have associated TGF-β metabolic reprogramming to TGF-β-dependent EMT. There are actually evidences that metabolic changes and EMT reinforce each other [287]. TGF-β-dependent activation of Snail in MCF-7 cells can promote the glycolytic metabolism while reducing mitochondrial respiration [288]. The latter was accomplished through suppression of cytochrome c oxidase (complex IV), the terminal enzyme of the mitochondrial respiratory chain [288]. Furthermore, the

glucose transporters GLUT1 and GLUT3 have been reported to be upregulated in response to TGF-β signaling [286] and paralleled by the expression of EMT markers like E-cadherin and vimentin [289]. TGF-β may also promote glycolysis through the upregulation of the 6-phosphofructo-2-kinase/fructose-2,6-biphosphatase 3 (PFKFB3) enzyme, which accelerates a rate-limiting step of glycolysis [286, 290, 291]. The increased glycolytic rate produced under TGF-β signaling leads to an increased extracellular release of lactate [292]. Lactate itself, that is known to promote SNAIL1 and EMT through TGF-β signaling [293], reinforces this cycle [294]. TGF-β also promotes a metabolic shift in cancer-associated fibroblasts (CAFs). Guido et al. showed that TGF-β-activated CAFs promoted oxidative stress through stimulation of catabolic pathways [62]. Daoxiang Zhang et al. also demonstrated that TGF-β1-activated CAFs exhibit a down-regulation of isocitrate dehydrogenase 3α (IDH3α) that causes the transition from oxidative phosphorylation to aerobic glycolysis. IDH3α influences the α-KG to fumarate ratio triggering a PHD inhibition, that in turn promotes HIF-1α protein stabilization and thus supports the transcription of various genes coding for glycolytic enzymes [295].

Although the above studies associate TGF-β with a glycolytic preference, TGF-β has been also reported to increase oxygen consumption and ATP generation together with EMT induction [296]. Furthermore, TGF-β was shown to be upregulated when the levels of fatty acids (FA) are above average in tumors. Nath et al. reported that elevated levels of free FA (FFA) could indeed promote TGF-β signaling and TGF-β-dependent EMT in hepatocellular carcinoma [297]. They also demonstrated that palmitate-treated HepG2 and Hep3B cells showed profound transcriptomic alterations with, among the top 20 genes to be upregulated, specific EMT genes (*eg. CDH2*) and *TGFB2* [297]. In this study, the authors reported that expression levels of CD36, one of the main fatty acid transporters at the plasma membrane, were positively correlated with TGF-β abundance ; of note further

investigations are still needed to address the contribution of other fatty acid transporters such as fatty acid-binding proteins (FABPs) and fatty acid transport proteins (FATPs) [298].

Other lipids such as oxysterols and sphingolipids have also been reported to be linked to TGFβ-induced EMT. Oxysterols (oxygenated derivatives of cholesterol) and hydroxy alkenals (molecules produced by lipid peroxidation) are reported to stimulate the expression and synthesis of TGF-β1 in non-cancer cells [299, 300] and colon cancer cells [301]. The relationship between sphingolipids and EMT is more complex since sphingosine-1-phosphate (S1P) was shown to stimulate an autocrine production of TGF-β1 in A549 lung cancer cells [302] whereas sphingomyelin synthases (SMS) were reported to block TGF-β-induced EMT. SMS1 inhibition of EMT was reported to be due to repression of TGFβR1 which leads to decreased Smad2 phosphorylation [303].

Altogether those reports indicate that different metabolic transitions can be either caused by or led to TGF-β signaling activation. However, the observed metabolic changes may vary and are greatly dependent on the cell type and tumor environment.

SCOPE AND AIMS

Cancer progression is strongly influenced by the physico-chemical properties of the tumor microenvironment. While the contribution of hypoxia to tumor biology has been largely documented in the last decades, tumor acidosis has only recently emerged from a merely collateral effect of the exacerbated glycolytic tumor metabolism to a driving force supporting disease development. In order to address how chronic acidosis may shape (metabolic) phenotypes in cancer cells, we exposed a variety of cell lines, originating from different human tumor types (*e.g.* cervix, pharynx and colon) to acidic conditions (pH 6.5) for at least 4 weeks until cancer cells recovered and grew again. In cell culture, pH disturbances are inevitable because of lack of continuous wash out of metabolic wastes. In order to prevent pH differences on the culture medium we use a combination of HEPES (pKa = 7.3 at 37 °C) [304] and PIPES (pKa = 6.7 at 37 °C) [304] buffers.

Previous work in the lab has identified a shift from glycolysis towards glutamine utilization in cancer cells chronically exposed to an acidic pH (pH 6.5), thereby limiting the rate of H^+ generation [34]. Whether fatty acid metabolism was also altered in response to ambient acidosis, was unknown at the beginning of this thesis. More generally, while acid-induced activation of proteases facilitating migration of cancer cells was abundantly documented, the relation between metabolic preferences under acidic pH and local/metastatic invasiveness was largely unexplored when we initiated this work. Investigators in our lab had however consistently observed a phenotypic change in acid-adapted cancer cells including a more mesenchymal, elongated shape and the presence of inclusions that could possibly represent lipid droplets. Altogether, the above data led us to the main question we aimed to address in this thesis: could metabolism, in

particular fatty acid metabolism, occupy a central and possibly driving position in the so-called epithelial-to-mesenchymal transition (EMT) and increased invasiveness potential associated with tumor acidosis.

Specific aims:

- To unravel the metabolic paths used by acidic cells to replace glycolysis as the main source of oxidative fuel [see Results, chapter 1]
- To identify the link between acidosis, preferred fatty acid metabolism and epithelial-mesenchymal transition (EMT), and from there, to propose new therapeutic strategies to target invasive and metastatic cancer cells [see Results, chapter 2]
- The identification of TGF-β2 at the interface between acidosis, metabolism and EMT led us to further search for the mechanism of preferential activation of TGF-β2 (vs. other TGF-β isoforms) [see Results, chapter 3].

RESULTS

1. Acidosis Drives the Reprogramming of Fatty Acid Metabolism in Cancer Cells

Cyril Corbet, Adan Pinto, Ruben Martherus, **Joao Pedro Santiago de Jesus**, Florence Polet and Olivier Feron

This study was reported in Cell Metabolism in 2016. Here below, I only report and discuss the part of the work I was involved in.

Cell Metabolism
Article

Acidosis Drives the Reprogramming of Fatty Acid Metabolism in Cancer Cells through Changes in Mitochondrial and Histone Acetylation

Cyril Corbet,[1] Adán Pinto,[1] Ruben Martherus,[1] João Pedro Santiago de Jesus,[1] Florence Polet,[1] and Olivier Feron[1,*]
[1]Pole of Pharmacology and Therapeutics (FATH), Institut de Recherche Expérimentale et Clinique (IREC), UCLouvain, 53 Avenue Mounier B1.53.09, 1200 Brussels, Belgium
*Correspondence: olivier.feron@uclouvain.be
http://dx.doi.org/10.1016/j.cmet.2016.07.003

Cell Metabolism *24*, 311–323, August 9, 2016

1.1 Summary

Bioenergetic preferences of cancer cells foster tumor acidosis that in turn leads to dramatic reduction in glycolysis and glucose-derived acetyl-coenzyme A (acetyl-CoA). Here, we show that the main source of this critical two-carbon intermediate becomes fatty acid (FA) oxidation in acidic pH-adapted cancer cells. FA-derived acetyl-CoA fuels the tricarboxylic acid (TCA) cycle and supports tumor cell respiration under acidosis. Also, while oxidative metabolism of glutamine supports the canonical TCA cycle in acidic conditions, reductive carboxylation of glutamine-derived α-ketoglutarate sustains FA synthesis. Concomitance of FA oxidation and synthesis is enabled upon sirtuin-mediated histone deacetylation and consecutive downregulation of acetyl-CoA carboxylase ACC2 making mitochondrial fatty acyl-CoA degradation compatible with cytosolic lipogenesis. Perturbations of these regulatory processes lead to tumor growth inhibitory effects further identifying FA metabolism as a critical determinant of tumor cell proliferation under acidosis.

1.2 Introduction

Rewiring of cellular metabolism is crucial for sustaining the increased growth and proliferation of tumor cells. Acetyl-coenzyme A (acetyl-CoA) occupies a critical position within tumor metabolic processes as a biosynthetic intermediate but also as a key determinant of protein acetylation [305] . While acetyl-CoA mostly derives from pyruvate or fatty acid oxidation in the mitochondria [306] acetyl-CoA may also be directly generated in the tumor cell cytosol under certain circumstances [307]. Tumor cells may indeed produce acetyl-CoA from reductive carboxylation of glutamine-derived α-ketoglutarate when they are exposed to

hypoxia, in the presence of mitochondrial defects [308] or upon glycolysis inhibition [309]. Tumor cells can also use acetate to produce cytosolic acetyl-CoA, via the reaction catalyzed by the acyl-CoA synthetase short-chain family, member 2 (ACSS2) [310], especially in hypoxic conditions [311, 312].

Acidosis, like hypoxia, is nowadays considered as a hallmark of most human tumors [313-315]. Tumor metabolic peculiarities, such as the exacerbated glycolytic metabolism and CO_2 hydratation, directly account for the acidification of the tumor microenvironment. Acidosis in turn contributes to the genetic instability of tumor cells [316] and profoundly alters their transcriptomic profile [317], leading to phenotypes that are particularly suited for survival and growth in an acidic environment. Our group and others have documented that acidosis leads to a net reduction in the use of glucose by tumor cells [34, 318], thereby suppressing glucose oxidation as a source of acetyl-CoA. In the present study, we provide evidence that instead of glucose, fatty acids (FA), and glutamine to a lesser extent, contribute to acetyl-CoA generation under chronic acidosis. In particular, we identified how FA oxidation (FAO) and FA synthesis (FAS) could co-exist in acidosis-adapted cancer cells through mechanisms orchestrated by concomitant non-enzymatic hyperacetylation of mitochondrial proteins and histone deacetylation, the former limiting complex I activity and the latter repressing the expression of acetyl-CoA carboxylase ACC2. This study further provides evidence that the therapeutic targeting of key players of the fatty acid metabolism driven by the acidic tumor microenvironment may have detrimental effects on tumor growth.

1.3 Results

Fatty acid oxidation is responsible for mitochondrial protein acetylation increase in acidic pH-adapted tumor cells

Previous data from our group demonstrated that HIF-1α and HIF-2α were differentially acetylated under acidosis [34] led them to examine the influence of chronic acidic pH on the full acetylome pattern of tumor cells. The AcetylScan technology (Cell Signaling Technology) was used to identify and quantify global differences in acetylation between parental and pH 6.5-adapted SiHa tumor cells. 9,750 redundant peptide assignments containing acetylated lysines were identified. Among the 4,799 acetyl-lysine sites used for quantification, 773 acetylated lysines from 529 non-redundant proteins had a cut-off greater than 2.5-fold and were considered for analysis. Clustering of (de-)acetylated proteins according to their intracellular location revealed that most of them were located in cytoplasm, nucleus, and mitochondrion with 277, 331, and 201 acetyl-sites identified, respectively. In the cytoplasmic and nuclear compartments of acidic pH-adapted cells, about 60% of the identified acetyl-lysine sites were found to be hypoacetylated (versus parental cells). By contrast, a dramatic increase in the extent of acetylated proteins was observed in the mitochondria of SiHa/6.5 tumor cells, with more than 95% of the AcetylScan-identified proteins found to be hyperacetylated. This was confirmed in immunoblotting experiments using mitochondrial extracts from SiHa as well as FaDu and HCT- 116 cancer cells (Figure 16a). The mitochondrial protein hyperacetylation in acidic pH-adapted cells was not associated with change in the expression of either GCN5L1, the only acetyltrans-ferase described as mitochondrion specific [319], or mitochondrial sirtuin deacylases SIRT3 (Fig. 16a), SIRT4, and SIRT5 (data not shown). Interestingly, while

cytosolic acetyl-CoA abundance was similar in parental and acidic pH-adapted cells (data not shown), the level of acetyl-CoA was significantly higher in the mitochondria of acidic pH-adapted cells (Fig. 16b). Contribution of fatty acid oxidation (FAO) to mitochondrial protein acetylation in acidosis-adapted cells was confirmed after silencing CPT1A and the long-chain-fatty-acid-CoA ligase 1 (ACSL1) enzyme with specific siRNA (Fig. 16c). Moreover, we showed that the increase in mitochondrial acetyl-CoA abundance in acidic pH-adapted cells was blunted by etomoxir treatment (Fig. 16d), 2-DG had no effect, and CB-839 treatment exhibited an intermediate inhibitory action. By contrast, in parental cells, mitochondrial acetyl-CoA pool was strongly decreased by 2-DG treatment, while CB-839 and etomoxir had either no effect or a slight inhibitory effect, respectively.

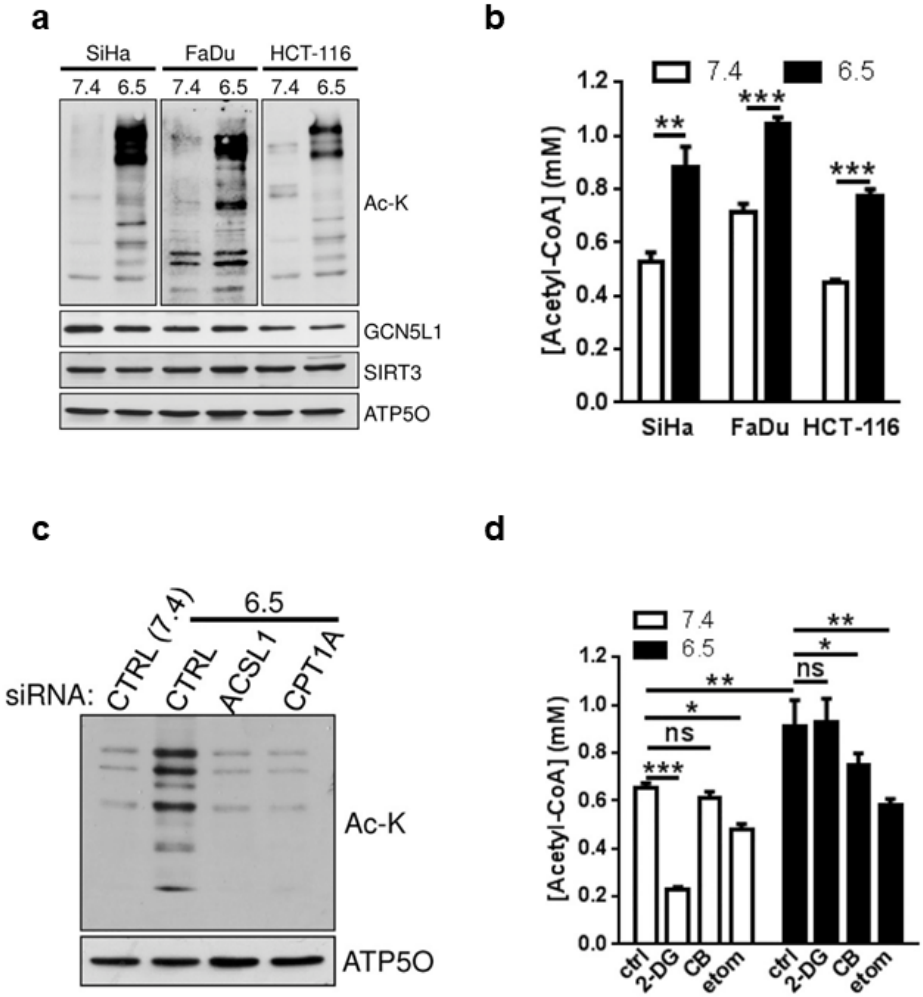

Figure 16: Fatty acid oxidation is responsible for mitochondrial protein acetylation increase in acidic pH-adapted tumor cells. (**a**) Representative immunoblotting for acetylated proteins, GCN5L1, and SIRT3 in isolated mitochondria extracts of parental and acidic pH-adapted tumor cells. ATP5O was used as a loading control. (**b**) Acetyl-CoA levels in isolated mitochondria extracts of parental and acidic pH-adapted tumor cells. (**c**) Representative immunoblotting for acetylated proteins in isolated mitochondria extracts from parental and acidic pH-adapted SiHa cells transfected with ACSL1- or CPT1A-targeting siRNA. (**d**) Acetyl-CoA concentration in isolated mitochondria extracts of parental and acidic pH-adapted SiHa cells treated for 24 hr with 10 mM 2-DG, 20 nM CB-839, or 30 mM etomoxir. (**b and d**) data are represented as mean ± SEM $p < 0.05$; $^{**}p < 0.01$; $^{***}p < 0.001$; ns, not significant.

FA oxidation is upregulated in acidic pH-adapted tumor cells and its inhibition leads to growth inhibitory effect *in vitro*.

Altogether, the data presented in the figure 16 highlighted the contribution of fatty acid oxidation (FAO) to the pool of acetyl-CoA involved in mitochondrial protein acetylation in tumor cells adapted to chronic acidosis. As acetyl-CoA is also an energetic fuel for the TCA cycle and associated oxidative phosphorylation, we investigated the role of FAO in mitochondrial respiration. We started by incubating tumor cells with [U-^{14}C] palmitate for 10 min, we documented that fatty acid uptake was increased in acidic pH-adapted cells (Fig. 17a). We further prove that acidic pH-adapted tumor cells were more prone to use the exogenous palmitate as a metabolic substrate to fuel mitochondrial respiration, as illustrated by a strong increase in both the oxygen consumption rate (OCR) (Fig. 17b) and the mitochondrial membrane potential (MMP), used to reflect the activity of the electron transport chain (Fig. 17c). The higher sensitivity of acidic pH-adapted cells for modalities targeting FAO was confirmed with the pharmacological CPT1 inhibitor etomoxir in acidic pH-adapted cells (Fig. 17d).

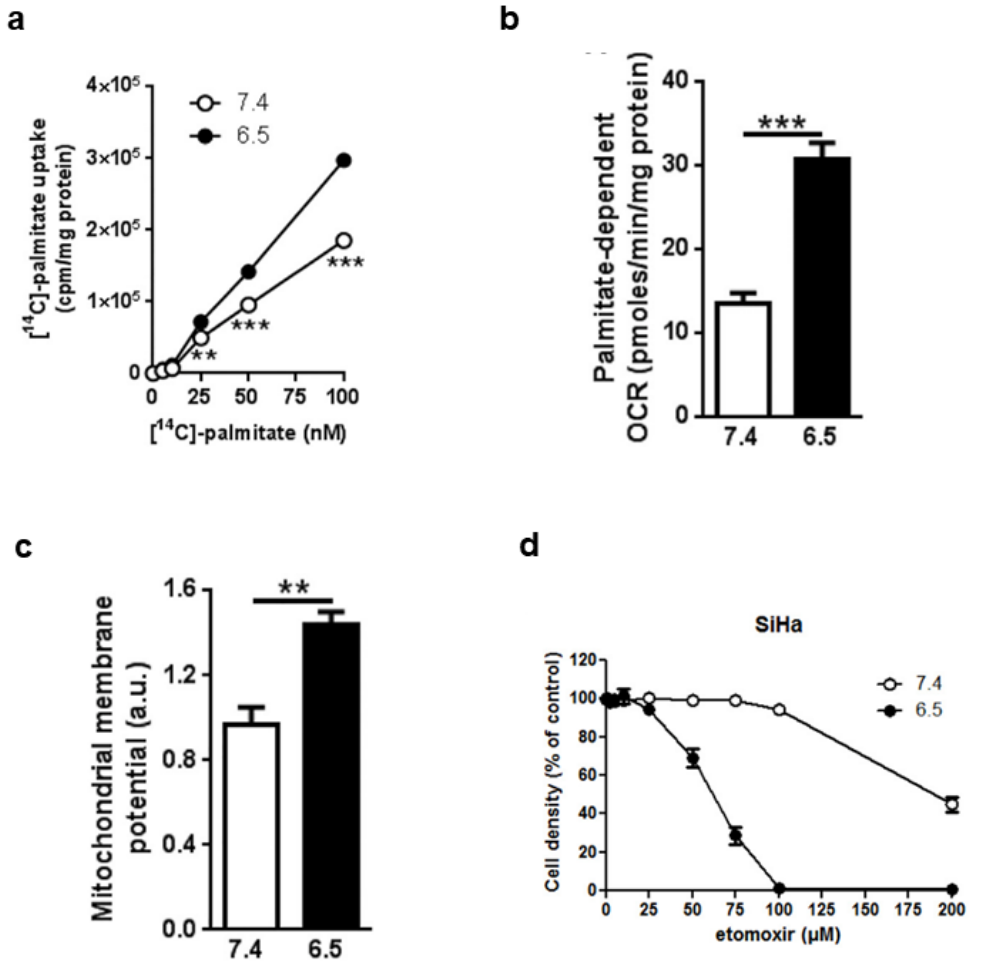

Figure 17: FA oxidation is upregulated in acidic pH-adapted tumor cells and its inhibition leads to growth inhibitory effect in vitro. (**a**) [U-^{14}C] palmitate 10 min uptake measured in parental and acidic pH-adapted SiHa cells. (**b and c**) Palmitate-dependent OCR (**b**) and mitochondrial membrane potential (**c**) in parental and acidic pH-adapted SiHa cells. (**d**) SiHa cell growth (72 hr) after etomoxir treatment. (**a, b and c**) data are represented as mean ± SEM **p < 0.01; ***p < 0.001.

Reductive carboxylation is the primary route of glutamine to lipids under chronic acidosis.

Since FAO was found to contribute (instead of glucose) to the main source of two-carbon acetyl-CoA in acidic pH-adapted cells, we reasoned that glutamine could provide the four-carbon molecule oxaloacetate to generate citrate and thereby support lipogenesis. We recently documented that proliferating tumor cells, when chronically exposed to acidic conditions, increased glutamine metabolism, in particular through IDH1-dependent reductive carboxylation of α-ketoglutarate (αKG) [34]. To evaluate the contribution of glutamine to FA synthesis in our different experimental conditions, we measured total amounts of citrate and αKG and found that total citrate levels, but not αKG, were significantly decreased in acidic pH-adapted cells (Figure 18a), accounting for a strong increase in the αKG to citrate ratio (Figure 18b) previously described as a major determinant of the reductive glutamine metabolism [320].

We next determined the extent to which reductive glutamine metabolism contributed to lipogenesis. Both parental and acidic pH-adapted cells produced fatty acids de novo (although to a lower extent for the adapted cells), as indicated by incorporation of $^{3}H_2O$ into lipids (Fig. 18c). Cells were then cultured with ^{14}C-labeled lipogenic substrates to examine carbon preferences for lipogenesis (Fig. 18d). Lipids derived from acidic pH-adapted cells were enriched in radioactivity from [5-^{14}C]glutamine, whereas [U-^{14}C]glucose only contributed for 25%–50% of the ^{14}C radioactive signal detected in parental cells (Fig. 18d), indicating a switch in the nature of the nutrients supplying lipogenesis.

We also documented that the phosphorylated (activated) state of ACLY was increased by 2-fold in acidic pH-adapted cells; expression of total ACLY and fatty acid synthase (FASN) was not altered (data not shown).

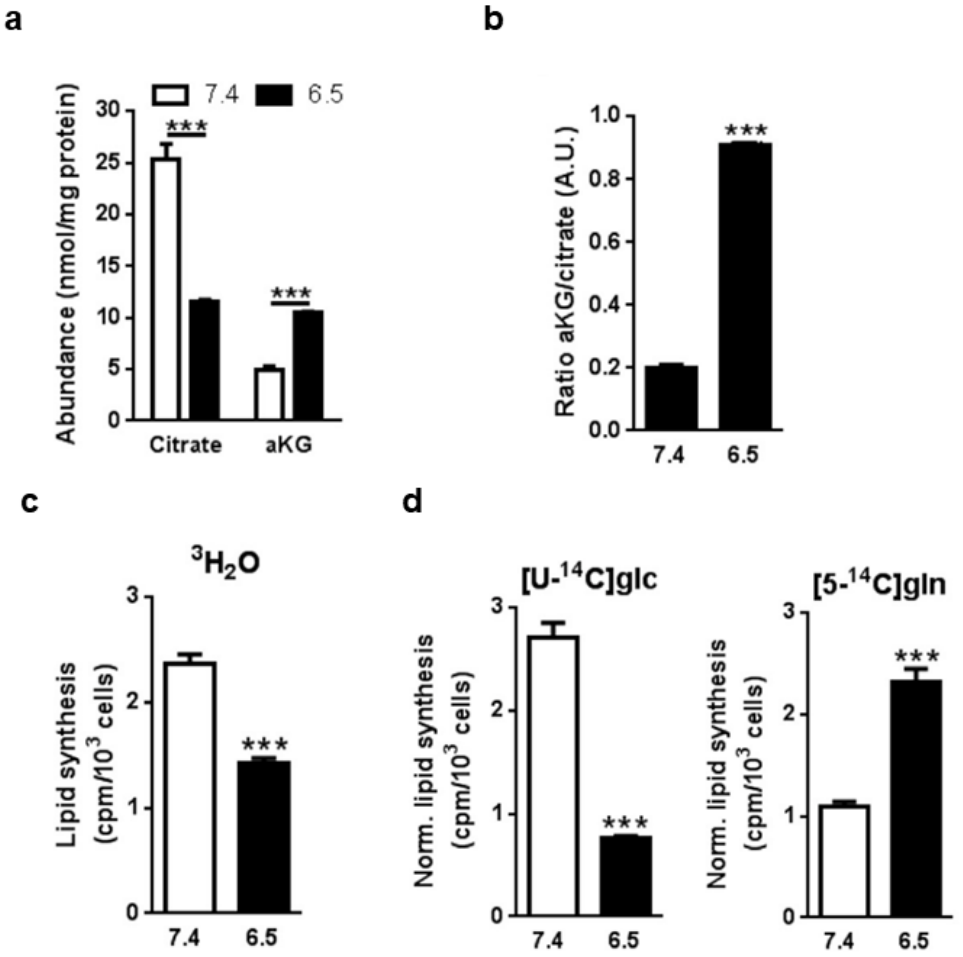

Figure 18: Reductive carboxylation is the primary route of glutamine to lipids under chronic acidosis. (**a and b**) Absolute intracellular abundance of citrate and alpha-ketoglutarate (**a**) and calculated alpha-ketoglutarate to citrate ratio (**b**) in parental and acidic pH-adapted SiHa cells. (**c and d**) Absolute rate (**c**) and specific contribution of ^{14}C-tracers (**d**) for lipid synthesis in parental and acidic pH-adapted SiHa cells. (**a-d**) data are represented as mean ± SEM ***$p < 0.001$.

Reduction in ACC2 functional expression allows for simultaneous FAO and FAS in acidic pH-adapted tumor cells.

Fatty acid synthesis (FAS) and oxidation (FAO) are two mutually exclusive pathways in healthy tissues largely through the regulatory effects of malonyl-CoA, which is involved in FA elongation but also negatively regulates FAO by inhibiting CPT1 [321]. We thus evaluated in acidic pH-adapted cells the status of acetyl-CoA carboxylases ACC1 and ACC2, the two enzymes that generate malonyl-CoA (encoded by ACACA and ACACB genes, respectively). Immunoblotting and qPCR experiments cell lines from distinct origin tissues (*i.e*. cervix, pharynx, and colon) for ACC1 and ACC2 revealed that ACACA mRNA abundance and ACC1 protein expression were not altered in parental and acidic pH-adapted tumor cells (Fig. 19a), whereas ACC2 protein expression was significantly decreased in acidic pH-adapted cells (Fig. 19a and 19b). Downregulation of ACC2 gene transcript (*ACACB*) was also found in those cells (Fig. 19c).

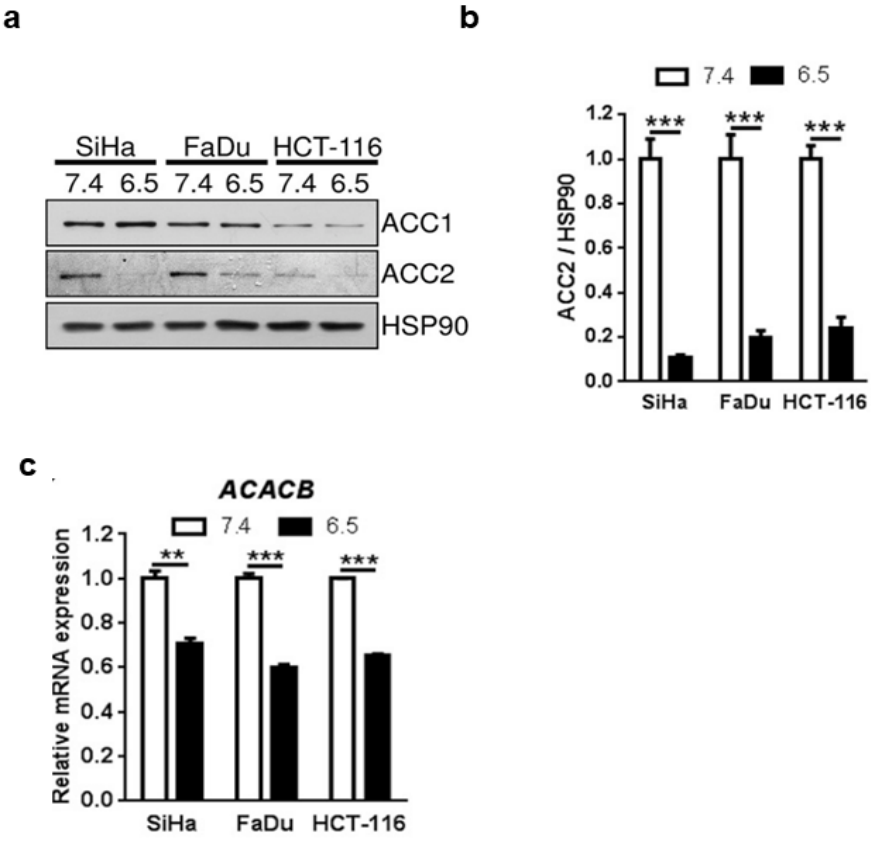

Figure 19: Downregulation of *ACACB* mRNA allows for simultaneous FAS and FAO in Acidic pH-Adapted Tumor Cells. (**a and b**) Representative immunoblotting (**a**) and quantification (**b**) for ACC1 and ACC2 expression in parental and acidic pH-adapted tumor cells. (**c**) Relative mRNA expression for *ACACB* in parental and acidic pH-adapted tumor cells. (**b and c**) data are represented as mean ± SEM **p < 0.01; ***p < 0.001.

Targeting the Fatty Acid Metabolism (FAO or FAS) in acidosis-adapted cancer cells leads to growth inhibitory effects *in vivo*.

Finally, to explore the *in vivo* relevance of targeting fatty acid metabolism, we evaluated the effects of targeting both FAO with etomoxir and FAS with the glutaminase inhibitor BPTES on the growth of SiHa/6.5 and HT-29/6.5 xenografts in mice. We found that daily administration of 40 mg/kg etomoxir rapidly reduced the growth of tumors arising from acidic pH-adapted cells, while the effect of this compound was significantly delayed in tumors arising from parental cells (Fig. 20a). The daily treatment with BPTES (10 mg/kg) exclusively impaired acidosis-adapted cell tumor growth (Fig.20a), and more importantly, the combined targeting of fatty acid and glutamine metabolism only showed additive inhibitory effects on the acidosis-adapted cell tumor growth (Fig. 20a).

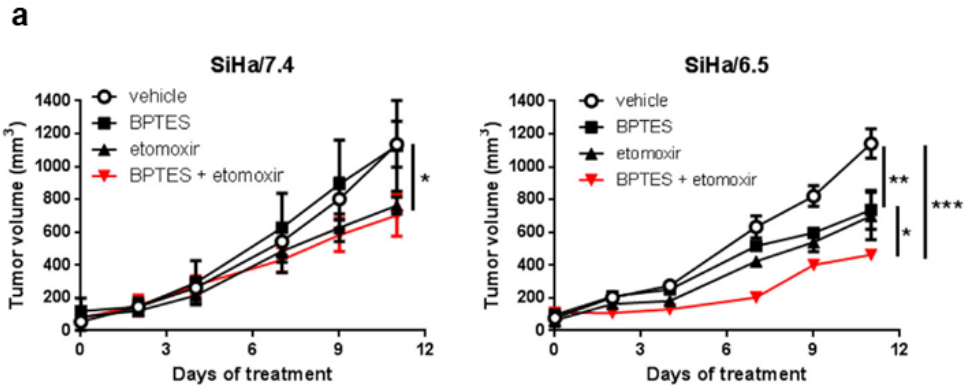

Figure 20: Inhibition of fatty acid metabolism delays tumor growth of acidic cells *in vivo*. (**a**) Tumor growth of SiHa/7.4 and SiHa/6.5 xenografts in nude mice treated daily or not with BPTES (10 mg/kg), etomoxir (40 mg/kg) alone, or in combination. (**a**) data are represented as mean ± SEM $p < 0.05$; **$p < 0.01$; ***$p < 0.001$; ns, not significant.

1.4 Discussion

The main findings of this study are that fatty acid metabolism in tumor cells is profoundly reprogrammed in response to acidosis and that associated changes in the acetylome tune this metabolic rewiring. We found indeed that FAO and FAS could occur concomitantly, with exogenous FA uptake fueling the TCA cycle with acetyl-CoA and glutamine metabolism actively supporting citrate production and lipogenesis. This apparent juxtaposition of mitochondrial FA catabolism and cytosolic FA synthesis is rendered possible through the downregulation of ACC2, a mitochondrion-anchored enzyme that normally prevents the degradation of neo-synthesized FA in healthy tissues. These observations point the pathways fueling the different acetyl-CoA pools as key determinants of tumor cell adaptation to acidic conditions and thereby provide a new rationale for the use of drugs interfering with FA metabolism to treat cancer [322]. Acetyl-CoA can then contribute to different processes in acidosis-adapted cancer cells. While we could demonstrate its important contribution to acetylation reactions, this component may be also a vital building block for the endogenous biosynthesis of fatty acids [323] and cholesterol [324].

Our data underline that although acidosis develops in the tumor microenvironment as a consequence of the metabolic requirements of proliferating cells, acidosis may in turn influence the tumor cell phenotype. We showed that these changes in metabolic preferences are profound since cancer cells chronically exposed to an acidic pH almost completely abandon glycolysis in favor of FAO as a source of mitochondrial acetyl-CoA that feeds into the TCA cycle and produces reducing equivalents for oxidative phosphorylation. Both aerobic and anaerobic glycolytic pathways contribute for a large part to protons that accumulate in the

extracellular tumor compartment. The group previously documented that the dramatic reduction in glucose metabolism under acidic pH could be interpreted as an auto-adaptation of tumor cells that cannot handle more protons in their extracellular environment [307]. In the current study, we now report that a net increase in FAO offers cancer cells the possibility to survive and proliferate in areas exhibiting a pH incompatible with further acidification. Interestingly, we found that while an increase in fatty acid uptake supports FAO, fatty acid synthesis is occurring at the same time in acidic pH-adapted cancer cells. We used labeled glutamine to document that reductive glutamine metabolism contributed to FA synthesis in cancer cells under acidosis, a pathway maintained through a mass action effect related to the increased α-KG/citrate ratio (Figure 18b) as previously proposed by Fendt et al. [320]. This is reminiscent of observations in tumor cells with defective mitochondria or under hypoxic conditions where reductive carboxylation of glutamine-derived a-ketoglutarate (α-KG) was reported to supply citrate for de novo lipogenesis [21, 23, 308]. However, in these studies, a role for FA as a source of mitochondrial acetyl-CoA was not identified, suggesting that under acidosis, stimulated FAO also required the maintenance of the canonical TCA cycle fueled by glutamine. The observed biosynthetic rewiring under acidosis is thus at odds with those studies reporting enhanced reductive carboxylation of glutamine when either electron transport chain (ETC) or TCA cycle function is altered by hypoxia or mutations. The acidosis-governed metabolic changes are actually in adequation with the anaplerotic needs of tumor cells proliferating independently of glucose, in particular to supply oxaloacetate to be combined with FAO-derived acetyl-CoA [309].

The compartmentation of FAO in mitochondria and FAS in the cytosol may offer a first biological basis to account for the concomitant occurrence of these two apparent opposite pathways. Still, in healthy tissues, the risk of a futile cycle within

cells degrading de novo synthesized FA is prevented by the capacity of malonyl-CoA produced by ACC enzymes to block CPT1 and thereby to impede the transport of fatty acyl-CoA into mitochondria for oxidation. Here, we showed that the mitochondrial ACC2 isoform [325] is downregulated in acidic pH- adapted cells preventing this negative feed-back loop. The only ACC isoform expressed in tumor cells under acidosis is thus ACC1, which, as in lipogenic tissues, generates malonyl-CoA as a substrate for FA synthesis. The critical role of ACC2 extinction under acidosis was documented in experiments where the re-expression of recombinant ACC2 in acidic pH-adapted cancer cells dose-dependently inhibits the capacity of tumor cells to handle exogenous FA and blocks cell growth (data not shown).

Our study provides insights in the acetylation-dependent regulation of specific actors of the metabolism of acidic pH-adapted cancer cells. Indeed, mitochondrial proteins were hyperacetylated because of the strong increase in the acetyl-CoA pool derived from stimulated FAO. More generally, we showed that fatty acyl-CoA formation and mitochondrial uptake though ACSL1 and CPT1, respectively, represent targets particularly suited to inhibit FAO-sup- porting anaplerotic processes under acidic conditions. Our data also point toward the glutamine metabolism as a target to limit FAS. Proliferating cancer cells are known to depend upon de novo FA synthesis, while most noncancer cells primarily take up lipids from circulation [326, 327]. Our study indicates that under acidosis, FAS is not supported by glucose metabolism but is mainly dependent on glutamine, making glutaminase inhibitors very attractive targets to perturb lipogenesis. Additive effects of etomoxir inhibiting CPT1 and BPTES blocking glutaminase GLS1 were observed in tumor-bearing mice. These in vivo experiments are, however, likely to underestimate the efficacy of these combo treatments since tumors were obtained from injection of in vitro acidosis-adapted cells to mice. This procedure is likely to transiently relieve the selective pressure of acidosis on the preferred expression of

key metabolic regulators until the growing tumors themselves develop local acidosis. In conclusion, this study supports a model wherein under acidosis, mitochondria of tumor cells are particularly active, importing glutamine and FA instead of glucose-derived pyruvate to produce energy and anabolic intermediates. How can these observations be reconciled with the well-established increased glycolytic pathway in many tumors? First, replacement of glucose by FA to produce acetyl-CoA and increased dependence on glutamine (through both reductive and oxidative pathways) are likely to be proportional to the extent of local acidosis. Second, tumor acidosis, like tumor hypoxia, is not a stable parameter in tumors but fluctuates with time or, in other words, may influence specific tumor areas at a given time. Correction of acidosis through the removal of excess protons (that saturate bicarbonate buffer) requires functional tumor vessels. As for the determinants of cycling hypoxia [328, 329], angiogenesis providing new blood vessels and variations in vessel hemodynamics (i.e., perturbations of tumor perfusion because of chaotic neovasculature) may thus account for an intermittent exposure of tumor areas to acidosis. Through the identification of major determinants of the specific behavior of tumor cells proliferating in (despite) the tumor acidic environment, our study opens new perspectives for the development of strategies to interfere with tumor FA metabolism in order to avoid the emergence of resistance from this acidic compartment.

1.5 Methods

Cell culture

Human cervix SiHa (#HTB-35), pharynx FaDu (#HTB-43) and colorectal HCT-116 (#CCL-247) and HT-29 (#HTB-38) cancer cell. Cells were stored according to the

supplier's instructions and used within 6 months after resuscitation of frozen aliquots. All cell lines were maintained in DMEM supplemented with 10% heat-inactivated FBS, 10 mM D-glucose, 2 mM L-glutamine and 25 mM of both PIPES and HEPES before adjusting pH to 7.4 or 6.5; regular sampling of cell culture media (directly from the CO_2 incubator) validated the maintenance of the neutral or acidic pH along the experiments. Acidic pH-adapted tumor cells were established as previously described [34]. All cell lines were tested for mycoplasma contamination with the MycoAlert™ Mycoplasma Detection kit (#LT07-318; Lonza) before being used.

Mitochondrial Isolation

Mitochondria were isolated from cells using a mitochondria isolation kit from Thermo Scientific. All steps were performed at 4°C. Cells were suspended in isolation buffer from the kit supplemented with protease inhibitor cocktail (Sigma-Aldrich), phosphatase inhibitor cocktail (Roche Applied Science), and deacetylase inhibitors (10 mM nicotinamide [NAM], 10 mM trichostatin A [TSA], 10 mM sodium butyrate). After the different isolation steps, mitochondria pellet was suspended in resuspension buffer (220 mM mannitol, 70 mM sucrose, 5 mM HEPES-KOH [pH 7.2], 1 mM EGTA, and 0.1% fatty acid-free BSA). Protein concentration was determined with the BCA method.

Metabolic Profiling

For tracer studies, custom, phenol red-free DMEM was formulated with 10% dialyzed FBS, 2 mM ^{13}C-labeled glutamine, and other components unlabeled. Cultures were washed with PBS before adding tracer media for 24–72 hours unless otherwise specified. Glucose and lactate concentrations were measured using enzymatic assays (CMA Microdialysis AB) and a CMA 600 analyzer (Aurora Borealis).

Oxygen-consumption rate (OCR) was measured using the Seahorse XF96 plate reader.

Radioactive Tracing of Mitochondrial Acetylation and Lipid Synthesis

For mitochondrial acetylation tracing, cells were cultured for 24 hr in complete medium supplemented with 10 mCi [U-^{14}C] tracers. Mitochondria were isolated and diluted in immunoprecipitation (IP) buffer (50 mM Tris/HCl [pH 7.4], 1% Triton X-100, 150 mM NaCl, 0.5 mM EDTA, 10 mM NAM, 10 mM TSA, 10 mM sodium butyrate, and protease inhibitors) to obtain 500 mg protein input for each IP. These fractions were then incubated with anti-acetylated lysine antibody (#9441 Cell Signaling Technology) and Dynabeads protein G beads (overnight, 4ºC) and eluted in 0.1 M glycine (pH 2.5), before neutralization with Tris-HCl (pH 8.0). For radioisotope lipid synthesis assays, cells were cultured for 18 hr in complete medium supplemented with $^{3}H_2O$ (21 vol. %) or ^{14}C tracers (10 mCi). Lipids were then extracted with a chloroform-free extraction kit (Cell Biolabs) according to manufacturer's instructions. Radioactivity was analyzed by scintillation counting (PerkinElmer Topcount). In the ^{14}C experiments, raw counts per 10^3 cells were normalized to the absolute rate of fatty acid synthesis established using $^{3}H_2O$.

In Vivo Experiments

All the experiments involving mice received the approval of the university ethic committee (approval ID 2012/UCL/MD005) and were carried out according to national animal care regulations. 7-week-old female NMRI nude mice were purchased from Elevage Janvier, and 2.10^6 parental tumor cells (pH 7.4) or pH 6.5-adapted tumor cells were injected subcutaneously in the left and right flanks, respectively. When tumors reached a mean diameter of 5 mm, BPTES (10 mg/kg) or etomoxir (40 mg/kg), alone or in combination, were injected intraperitoneally daily.

Statistical Analysis

Results are expressed as mean ± SEM of at least three independent experi- ments. Two-tailed unpaired Student's t test and one-way or two-way ANOVA tests (Bonferroni's post hoc test) were used where appropriate.

2. TGFβ2-induced formation of lipid droplets supports acidosis-driven EMT and the metastatic spreading of cancer cells

Cyril Corbet[1,4,*], Estelle Bastien[1,4], **Joao Pedro Santiago de Jesus**[1,4], Emeline Dierge[1], Ruben Martherus[1], Catherine Vander Linden[1], Bastien Doix[1], Charline Degavre[1], Céline Guilbaud[1], Laurenne Petit[1], Carine Michiels[2], Chantal Dessy[1], Yvan Larondelle[3] and Olivier Feron[1,*]

[1]Pole of Pharmacology and Therapeutics (FATH), Institut de Recherche Expérimentale et Clinique (IREC), UCLouvain, 57 Avenue Hippocrate B1.57.01, B-1200 Brussels, Belgium

[2]Laboratory of Cellular and Molecular Biology (URBC), Namur Research Institute for Life sciences (NARILIS), University of Namur, 61 rue de Bruxelles, B-5000 Namur, Belgium

[3]Louvain Institute of Biomolecular Science and Technology (LIBST), UCLouvain, Croix du Sud 2/L7.05.01, B-1348 Louvain-la-Neuve, Belgium.

[4]These authors contributed equally.

This study was published in *Nature Communications* in January 2020. I share the first authorship with two other members of the lab. I will mention my personal contribution to this work at the end of each Figure legend in the Results section.

nature COMMUNICATIONS

ARTICLE

https://doi.org/10.1038/s41467-019-14262-3 OPEN

TGFβ2-induced formation of lipid droplets supports acidosis-driven EMT and the metastatic spreading of cancer cells

Cyril Corbet[1,4*], Estelle Bastien[1,4], Joao Pedro Santiago de Jesus[1,4], Emeline Dierge[1], Ruben Martherus[1], Catherine Vander Linden[1], Bastien Doix[1], Charline Degavre[1], Céline Guilbaud[1], Laurenne Petit[1], Carine Michiels[2], Chantal Dessy[1], Yvan Larondelle[3] & Olivier Feron[1*]

NATURE COMMUNICATIONS | (2020)11:454 | https://doi.org/10.1038/s41467-019-14262-3 | www.nature.com/naturecommunications

2.1 Summary

Acidosis, a common characteristic of the tumor microenvironment, is associated with alterations in metabolic preferences of cancer cells and progression of the disease. Here we identify TGF-β2 isoform at the interface between these observations. We document that acidic pH promotes autocrine TGF-β2 signaling which in turn favors the formation of lipid droplets (LD) that represent energy stores readily available to support anoikis resistance and cancer cell invasiveness. We find that, in cancer cells of various origins, acidosis-induced TGF-β2 activation promotes both partial epithelial-to-mesenchymal transition (EMT) and fatty acid metabolism, the latter supporting Smad2 acetylation. We show that upon TGF-β2 stimulation, PKC-zeta-mediated translocation of CD36 facilitates the uptake of fatty acids that are either stored as triglycerides in LD through DGAT1 or oxidized to generate ATP to fulfill immediate cellular needs. We also address how, by preventing fatty acid mobilization from LD, distant metastatic spreading may be inhibited.

2.2 Introduction

Acidosis, like hypoxia, is a hallmark of the tumor microenvironment (TME) [330-335]. It largely arises from the conjunction of the exacerbated metabolism of cancer cells (and cancer-associated cells) with a spatio-temporal disorganization of the tumor vasculature which limits the access to O_2 and prevents the rapid elimination of waste products including protons (H^+) and CO_2 [336]. The most common source of H^+ is the one associated with lactate production from glucose

metabolism as observed under hypoxia but also in the presence of O_2 (the so-called Warburg effect) [337]. Hydration of CO_2 molecules generated upon decarboxylation of metabolic intermediates also leads to the production of H^+ together with bicarbonate anions [338, 339].

Importantly, we and others have recently provided evidence that tumor acidosis could in turn influence the metabolism of cancer cells [34, 77, 340-343]. We have for instance reported that glutamine metabolism is preferred to glucose metabolism when cancer cells are maintained at pH 6.5, thereby limiting the rate of H^+ generation from glycolysis [34]. We also documented that fatty acid (FA) metabolism is profoundly altered in response to ambient acidosis with FA oxidation (FAO) acting as a main source of acetyl-CoA to support TCA cycle [343]. Moreover, acidosis-mediated metabolic rewiring is closely associated with sirtuin-mediated deacetylation of hypoxia-inducible factors HIF-1α and HIF-2α as well as histones H3 and H4 in the nucleus, leading to the differential expression of several metabolism-related enzymes (*e.g*. downregulation of the acetyl-CoA carboxylase ACC2 that allows FA synthesis to occur from glutamine concomitantly to oxidation of exogenous FA) [34, 343]. In addition, acidosis can abolish hypoxia-induced gene reprogramming, in particular by inhibiting HIF-1α protein stabilization [344, 345]. Altogether, these data indicate that acidosis, on its own, may strongly influence cancer cell metabolic phenotype.

Tumor progression is well known to be driven by an acidic extracellular pH through both evasion from immunosurveillance and an increased invasive potential [330]. The link between acidosis-related metabolism and a deficiency in immune cell response was previously elicited by documenting how accumulation of H^+ and lactate in the TME strikingly decreased the production of cytokines by several immune cell populations, including T cells, NK cells and monocytes [102, 346]. By

contrast, while acid-induced activation of proteases facilitating migration of cancer cells is abundantly documented [347-349], the relation between metabolic preferences under acidic pH and local/metastatic invasiveness only begins to be explored [350, 351]. The link between the ability of cancer cells to generate metastases and their bioenergetics is however increasingly documented [352-358]. New insights on the interplay between acidosis-driven metabolic preferences and a potential invasive behavior are therefore of particular need.

Here we identified lipid droplets (LD) as a common denominator to acidosis-adapted cancer cells issued from different tissues and a critical driver of their increased invasiveness (*vs.* native cells maintained at neutral pH). A transcriptomic study comparing both cell populations led us to identify TGF-β2 as a transcript consistently upregulated in the different acid-adapted cancer cells. We expanded on this finding to document how lipid metabolism rewiring is associated with partial epithelial-to-mesenchymal transition (EMT). In particular, we documented how autocrine TGF-β2 signaling favors the formation of lipid droplets (LD) that may further act as energy stores to support anoikis resistance, local invasiveness and distant metastatic spreading.

2.3 Results

Acidosis-adapted cancer cells accumulate lipid droplets in a CD36- and DGAT1-dependent manner

The stimulated FA metabolism reported in acidosis-adapted cancer cells [343] led us to identify intracellular vacuole-like structures detected by electron microscopy in these cells as being lipid droplets (LD; positive for BODIPY 493/503 and Oil Red O staining) (Fig. 21a-c); a consistent increase in the cellular area covered by LD was observed in pH 6.5-adapted cancer cells (named 6.5/cancer cells here below) *vs.* native cells maintained at pH 7.4 or 7.4/cells (Fig. 21d and Suppl. Fig. 1a); 6.5/cancer cells (obtained after 4-6 weeks of culture at pH 6.5) were maintained at pH 6.5 for the rest of this study. LD accumulation could not be attributed to cell arrest as reported in other situations [359] since in our experimental setup, contrary to acutely acid-exposed cancer cells, acidosis-adapted cancer cells keep proliferating although to a smaller extent than native cells (Suppl. Fig. 1b-d). Of note, this result slightly differs from a previous report from our lab where similar growth rate had been observed [34]. Changes in our cell culture conditions over time, in particular lower frequency of culture medium changing and/or larger cell dilution during passaging, could account for these apparent lesser growth capacities of acidosis-adapted cell populations. A lipidomic analysis confirmed a net increase in neutral lipids in 6.5/cancer cells (Fig. 21e and Suppl. Fig. 1e), mainly represented by a gain in saturated and monounsaturated FA but not cholesteryl esters (CE) (Fig. 21f-g, Suppl. Fig. 1f-g, and Suppl. Table 1); in comparison, the pools of phospholipids were not altered in the different cell populations (Suppl. Fig. 1h).

We next searched to identify actors directly involved in the accumulation of neutral lipids in acidosis-adapted cancer cells. We first examined the expression

of perilipins (PLIN), a family of proteins that associate with LD surface and enzymes involved in the synthesis of neutral lipids. We found that, among major members of the PLIN family, PLIN2 mRNA and protein expression was consistently increased in each of the tested 6.5/cancer cells while other PLIN isoforms remained unaltered (Fig. 21h and Suppl. Fig. 1i-k). We further documented that in acidosis-adapted cancer cells, *PLIN2* silencing using four siRNA duplexes designed to target distinct gene sites (Dharmacon) significantly reduced LD accumulation (Fig. 21i). We then evaluated a series of pharmacological inhibitors or blocking antibodies targeting major proteins that mediate triglyceride (TG) and CE synthesis (Fig. 21j). It should be noted that in our hands, acidosis-adapted cancer cells were particularly resistant to plasmid or viral transduction and/or died during the selection procedure, further supporting the use of pharmacological inhibitors (or siRNA) instead of stable gene silencing approaches. We found that A922500, a diacylglycerol acyltransferase DGAT1 inhibitor, largely inhibited LD reformation contrary to PF-06424439, a DGAT2 inhibitor (Fig. 21k). Inhibitors of HMG-CoA reductase (simvastatin) and ACAT (avasimibe), as well as the use of lipoprotein-deficient serum, failed to influence LD formation (Suppl. Fig. 1l), in agreement with the lack of differences in the extent of CE between native and acidosis-adapted cancer cells (Fig. 21g and Suppl. Fig. 1g). The glutaminase inhibitor BPTES that we showed to block lipid synthesis in acidosis-adapted cancer cells [343] also failed to change the extent of LD in these cells (Suppl. Fig. 1m). On the contrary, we could document that LD formation was only observed in the presence of (lipid-containing) full serum but not charcoal-delipidated serum (Fig. 21l); addition of exogenous FA to the latter restored LD biogenesis (Fig. 21l and Suppl. Fig. 1n). Finally, we identified CD36 as a main entry path for exogenous FA, since the use of specific blocking antibodies (JC63.1 and FA6-152) prevented LD formation (Fig. 21m) as well as the uptake of a fluorescent palmitate analog (BODIPY-conjugated C_{16}) in acidosis-adapted cancer cells (Suppl.

Fig. 1o). Altogether these data indicate that chronic acidosis induces LD formation in cancer cells, with CD36 and DGAT1 as key players to mediate LD biogenesis through the uptake of exogenous FA and triglyceride synthesis, respectively.

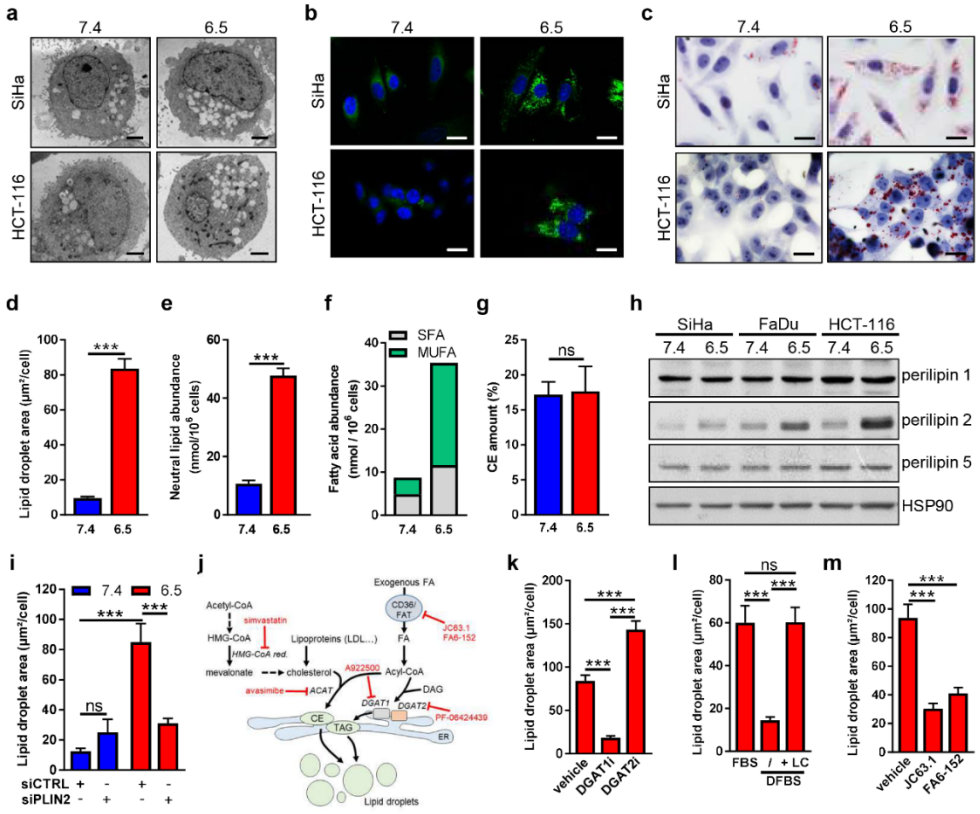

Figure 21: Acidosis-adapted cancer cells exhibit accumulation of lipid droplets in a CD36- and DGAT1-dependent manner. (**a**) Representative electron microscopy pictures depicting lipid droplet (LD) accumulation in acidosis-adapted SiHa and HCT-116 cancer cells. Scale bar: 2 µm. (**b-c**) Representative pictures of BODIPY 493/503 (**b**) and ORO-stained (**c**) LD in the same native and acidosis-adapted cancer cells. Scale bar: 20 µm. (**d**) Quantification of ORO-stained LD area in native and acidosis-adapted SiHa cells. (**e-g**) Abundance of the total pool of neutral lipids (**e**), SFA and MUFA in the neutral lipid fraction (**f**), and cholesteryl esters (**g**) in native and acidosis-adapted SiHa cells. (**h**) Representative immunoblotting for perilipins 1, 2 and 5 in native and acidosis-adapted cancer cells. (**i**) LD content in native and acidosis-adapted SiHa following transfection of PLIN2-targeting (or control) siRNA for 72h. (**j**) Scheme depicting the pathways leading to neutral lipid accumulation and lipid droplet biogenesis; specific inhibitors are indicated in red. (**k-m**) LD content in native and acidosis-adapted SiHa cells following treatment with 15 µM A922500 (DGAT1i) or 10 µM PF-06424439 (DGAT2i) for 24h (**k**), incubation in a medium supplemented with lipid-containing serum (FBS) or with charcoal-delipidated serum (DFBS) in presence or absence of an exogenous lipid concentrate (LC) for

24h (**l**) or treatment with two distinct CD36 blocking antibodies for 24h (**m**). Data are represented as mean ± SEM of three independent experiments (with ≥6 technical replicates). Significance was determined by Student's *t*-test (**d, e, g**), by one-way ANOVA (**k-m**) or two-way ANOVA (**i**) with Bonferroni multiple-comparison analysis. ***p<0.001; ns, not significant. I directly contributed to the panels a b, c, d, i, k, l and m.

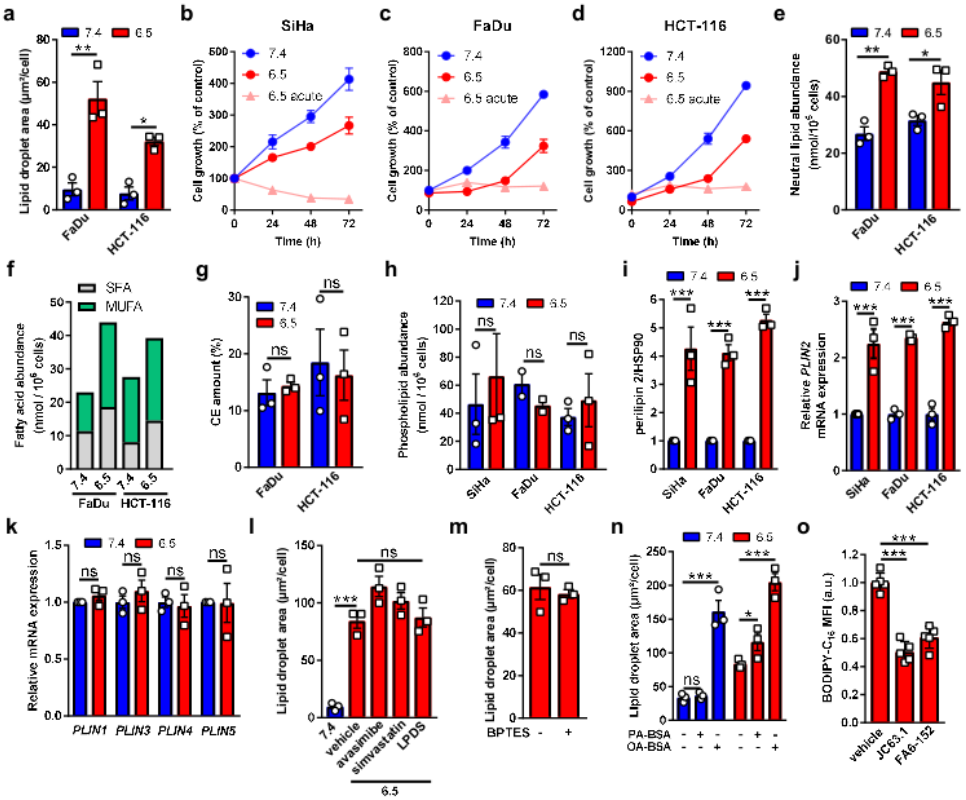

Supplementary Figure 1: Acidosis-adapted cancer cells exhibit accumulation of lipid droplets in a CD36- and DGAT1-dependent manner. (**a**) LD area in native and acidosis-adapted cancer cells. (b-d) Time courses of the growth of native, chronically and acutely pH6.5-exposed SiHa (b), FaDu (c), and HCT-116 (d) cancer cells. (e) Neutral lipid abundance in native and acidosis-adapted cancer cells. (f-g) Abundance of SFA and MUFA (f) and cholesteryl esters (g) in the neutral lipid fraction of native and acidosis-adapted cancer cells. (h) Phospholipid abundance in native and acidosis-adapted cancer cells. (i-j) quantification of protein expression (i) and mRNA expression (j) for PLIN2 in native and acidosis-adapted cancer cells. (k) mRNA expression for other PLIN genes in native and acidosis-adapted SiHa cells. (l) LD content in native and acidosis-adapted SiHa cells following treatment with 5 µM avasimibe, 1 µM simvastatin or upon incubation in a medium containing lipoprotein-deficient serum (LPDS). (m) LD content in forskolin-treated acidosis-adapted SiHa cells incubated for 24h in a full medium with or without 20 µM BPTES. (n) LD content in native and acidosis-adapted SiHa cancer cells following treatment with 100 µM BSA-conjugated palmitate (PA-BSA) or oleate (OA-BSA) for 24h. (o) Quantification for BODIPY FL C16 uptake in acidosis-adapted SiHa cells after incubation with the indicated CD36 blocking antibodies. Data are represented as mean ± SEM of three independent

experiments (with ≥6 technical replicates). Significance was determined by Student's t-test (m), one-way ANOVA (l, o), or two-way ANOVA (a, e, g-k, n) with Bonferroni multiple-comparison analysis. *p<0.05; **p<0.01; ***p<0.001; ns, not significant. Source data are provided as a Source Data file. I directly contributed to the panels a, i, j, l, and o.

Supplementary Table 1. Fatty acid abundance of the neutral lipid fraction in native SiHa cells treated or not for 6h with 4 ng/ml TGF-β2. Data indicated in the table are mean values of 2 biological replicates.

Saturated fatty acids (nmol/ 10^6 cells)		
	SiHa	
Fatty acid	CTRL	+ TGF-β2
C12:0	0.00	0.00
C14:0	0.30	0.07
C16:0	1.86	7.84
C18:0	1.24	5.65
C20:0	0.00	0.00
C22:0	0.00	0.00
C24:0	0.00	0.00
Total	3.40	13.56

Monounsaturated fatty acids (nmol/ 10^6 cells)		
	SiHa	
Fatty acid	CTRL	+ TGF-β2
C14:1cis9	0.00	0.00
C16:1cis9	0.10	0.57
C18:1cis9	1.10	2.30
C18:1cis11	0.31	0.63
C20:1c11	0.00	0.00
C22:1c13	0.00	0.00
C24:1c15	0.00	0.00
Total	1.51	3.50
TOTAL	4.91	17.05

FA mobilization from LD supports survival and invasiveness of acidosis-adapted cancer cells.

We then investigated the role of LD in acidosis-adapted cancer cells. First, since acidosis-adapted cancer cells take up large amounts of exogenous FA, we reasoned that storage into LD could prevent lipotoxicity. To examine this hypothesis, cells were treated with oleic acid (OA), a potent inducer of TG synthesis that becomes toxic for cells incapable of handling excess neutral lipids [360]. Consistent with a reduced capacity of FA storage into LD, OA exposure preferentially led to growth inhibition in PLIN2-silenced acidosis-adapted cells (Fig. 22a and Suppl. Fig. 2a). OA also induced ER stress as detected by BiP expression, an effect mimicked by DGAT1 inhibition and exacerbated when interventions were combined (Suppl. Fig. 21b). Another potential role for LD is to act as energy stores for cancer cells when facing fuel deprivation. We therefore pre-challenged 6.5/cancer cells with the adenylate cyclase activator forskolin to force lipolysis and acutely remove LD from 6.5/cancer cells (Suppl. Fig. 2c). This led us to document that LD deprivation accelerated cell death in 6.5/cancer cells cultured in a low serum-containing medium (Fig. 22b). Instead of removing LD from acidosis-adapted cancer cells, we next inhibited FA release from LD by blocking the activity of adipose triglyceride lipase (ATGL) with atglistatin and found that this treatment similarly accelerated cell death in 6.5/cancer cells cultured in a low serum-containing medium. (Fig. 22c and Suppl. Fig. 2d). We next found that the gain in survival of 6.5/cancer cells was lost under hypoxic conditions (Fig. 22d and Suppl. Fig. 2e), suggesting that oxidation of FA released from LD is needed to support cell survival. Finally, we examined whether LD, by providing an internal source of energy, could help resist to anoikis (*i.e.* anchorage-dependent cell death). A net effect on the survival of matrix-detached 6.5/cancer cells (*i.e.* viable cell suspension) was

observed *vs.* 7.4/cancer cells when adhesion was restricted by using low-attachment plate (Fig. 22e, left panel denoted as “static”) or fully prevented by applying dynamic force (*i.e*. slight plate shaking during the assay) (Fig. 22e, right panel denoted as “dynamic”). Strikingly, in these experiments, the presence of exogenous FA in the extracellular medium could not rescue non-anchored 7.4/cancer cells and LD deprivation significantly reduced the observed 6.5/cell survival gain (Fig. 22f). Because anoikis resistance is a major component of the invasive and metastatic potential of cancer cells, we next examined the invasiveness of acidosis-adapted cancer cells using modified (Matrigel-coated) Boyden chambers. We found that 6.5/cancer cells exhibited a higher invasion potential than corresponding native cancer cells (Fig. 22g). Importantly, this was largely independent of the environmental pH since similar results were obtained by using pH 6.5-adapted cancer cells in a pH 7.4-buffered medium during the time of the invasion assay (Suppl. Fig. 2f), supporting a profound phenotypic alteration (instead of an acute acid-mediated activation of migratory processes). We next addressed the possible roles of LD in the invasive potential of acidosis-adapted cancer cells. We found that upon LD deprivation, either by forskolin or DGAT1 inhibitor treatment (before the assay), 6.5/SiHa cancer cells exhibited a reduced invasiveness in modified Boyden chambers (Fig. 22h-i); similar results were obtained using HCT-116 cancer cells (Suppl. Fig. 21g-h). In 6.5/cancer cells, DGAT2 inhibition failed to inhibit invasion (Suppl. Fig. 2i-j). To more directly prove that fatty acid mobilization from LD accounted for the increased invasive potential of 6.5/cancer cells, we inhibited ATGL with atglistatin and documented a similar reduction in invasiveness (Fig. 22j); this experiment was carried out in the presence of serum further confirming that exogenous FA could not rescue the invasive capacity of lipase-inhibited 6.5/cancer cells. Finally, to address the fate of the increased FA release from LD in invading 6.5/cancer cells, we used inhibitors of

mitochondrial uptake of fatty acyl-CoA (etomoxir) (Fig. 22k and Suppl. Fig. 2k) and of ATP generation (oligomycin (ATP synthase inhibitor) and carbonyl cyanide m-chlorophenylhydrazone or CCCP (OXPHOS uncoupler)) (Fig. 22l and Suppl. Fig. 2l). These three different inhibitors dramatically reduced the invasive potential of 6.5/cancer cells. Altogether, these results confirm the direct contribution of LD (and FA mobilization therefrom) to anoikis resistance and increased invasiveness of acid-exposed cancer cells.

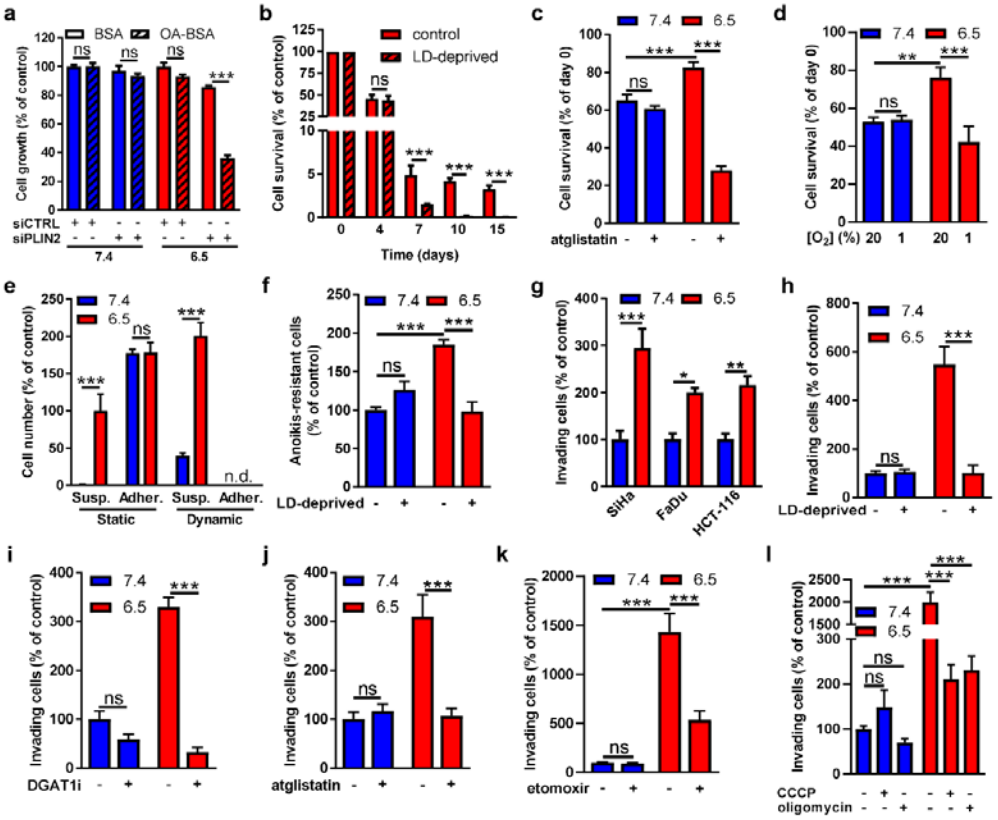

Figure 22: Lipid droplets support the survival and invasiveness of acidosis-adapted cancer cells. (**a**) Cell growth extent for native and acidosis-adapted SiHa cells following transfection of PLIN2-targeting (or control) siRNA and treatment with 50 µM BSA-conjugated oleic acid (OA) for 72h. (**b**) Survival capacity of LD-deprived acidosis-adapted SiHa cells, at different timings, in low serum-containing medium. (**c-e**) Survival capacity of native and acidosis-adapted SiHa cells for 3 days in low serum-containing medium following treatment with 10 µM atglistatin (**c**), in a dialyzed serum-containing medium without glucose nor glutamine under normoxic (20% O_2) or hypoxic (1% O_2) conditions (**d**) or incubation on low-attachment plates, without (static) or with slight shaking (dynamic) (**e**); are depicted the number of cells either adherent or in suspension (*i.e.* anoikis resistant); n.d., not detectable. (**f**) Extent of anoikis-resistant cells as determined in Figure 2e (*i.e.* cells in suspension) in LD-deprived native and acidosis-adapted SiHa cells. (**g**) Invasion capacity of native and acidosis-adapted tumor cells in Matrigel-coated Boyden chambers for 24h. (**h-l**) Invasion capacity of native and acidosis-adapted SiHa cells in the presence of serum (i.e. an exogenous FA source) upon LD deprivation (obtained by 24h treatment with 10 µM forskolin) (**h**), 15 µM A922500 (DGAT1i) (**i**), 10

µM atglistatin (**j**), 30 µM etomoxir (**k**) or 100 µM CCCP and 1 µg/ml oligomycin (**l**). Data are represented as mean ± SEM of three independent experiments (with ≥6 technical replicates). Significance was determined by two-way ANOVA (**a-l**) with Bonferroni multiple-comparison analysis. *p<0.05; **p<0.01; ***p<0.001; ns, not significant. I directly contributed to the panels a, b, c, e, f, g, h, I, j, k, and l.

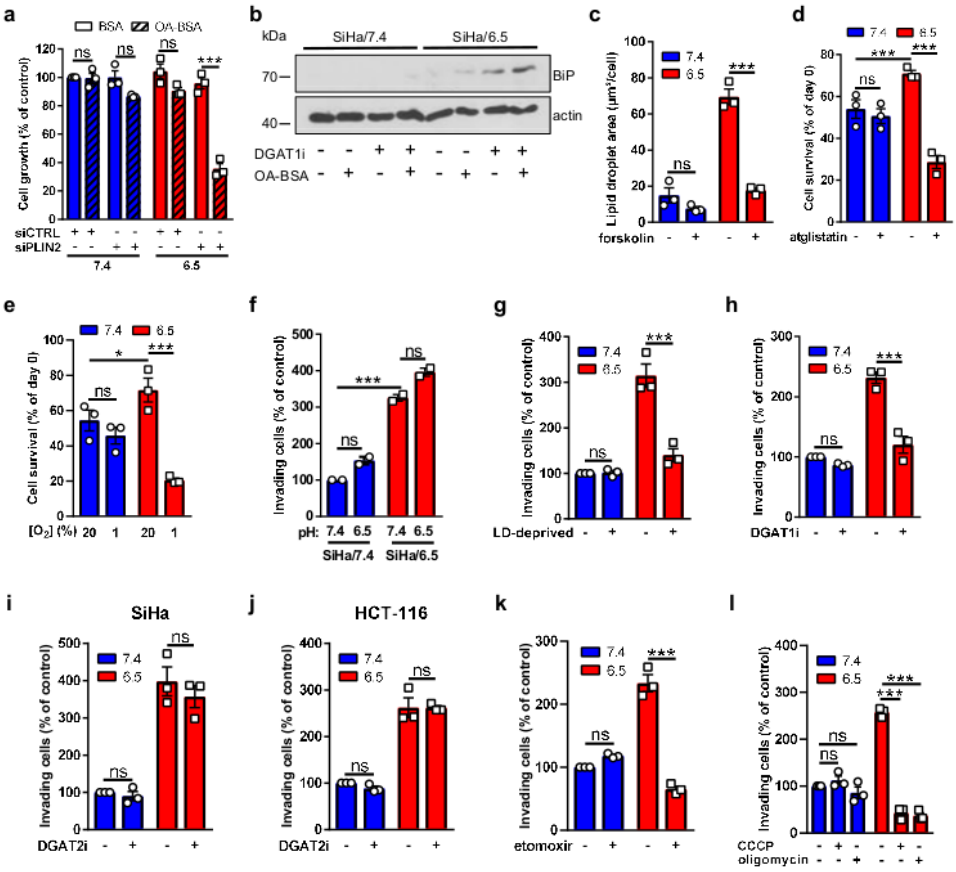

Supplementary Figure 2: Lipid droplets support the survival and invasiveness of acidosis-adapted cancer cells. (**a**) Cell growth extent for native and acidosis-adapted HCT-116 cells following transfection of control or PLIN2-targeting siRNA sequences and treatment with 50 µM BSA-conjugated oleic acid (OA) for 72h. (**b**) Representative immunoblotting for BiP (ER stress marker) in native and acidosis-adapted SiHa cells following treatment with 15 µM A922500 (DGAT1i) and/or 50 µM BSA-conjugated oleic acid (OA) for 48h. (**c**) LD content in native and acidosis-adapted HCT-116 cells following treatment with 10 µM forskolin for 24h. (**d-e**) Survival capacity of native and acidosis-adapted HCT-116 cells for 3 days in 0.1% serum-containing medium following treatment with 10 µM atglistatin (**d**) or in a dialyzed serum-containing medium without glucose nor glutamine under normoxic (20% O_2) or hypoxic (1% O_2) conditions (**e**). (**f**) Invasion capacity of native and acidosis-adapted SiHa cells placed at the indicated pH during the assay. (**g-h**) Invasion capacity of native and acidosis-adapted HCT-116 cells following treatment for 24h with 10 µM forskolin (**g**) or with 15 µM A922500 (DGAT1i) (**h**). (**i-j**) Invasion capacity of native and acidosis-adapted SiHa cells (i) and HCT-116

(**j**) following treatment for 24h with 10 µM PF-06424439 (DGAT2i). (**k-l**) Invasion capacity of native and acidosis-adapted HCT-116 cells following treatment with 30 µM etomoxir (**k**) or 100 µM CCCP and 1 µg/ml oligomycin (**l**). Data are represented as mean ± SEM of three independent experiments (with ≥6 technical replicates). Significance was determined by two-way ANOVA (a, c-l) with Bonferroni multiple-comparison analysis. *p<0.05; ***p<0.001; ns, not significant. I directly contributed to the panels c, d, f, g, h, I, j, k and i.

Autocrine TGF-β2 signaling supports invasiveness and LD formation in acidosis-adapted cancer cells.

To evaluate how chronic adaptation to acidosis may support the above LD-dependent invasive phenotype, we collected mRNA from 6.5/cell populations for a full transcriptome analysis (*vs* corresponding 7.4/cells). This led us to identify a list of 349 genes upregulated in each 6.5/cell line while 306 transcripts were significantly downregulated in the same three cell types (FDR< 0.01 and FPKM > 0.5) (Suppl. Fig. 2a). Interestingly, in the short list of the 20 genes the most upregulated in each of the three screened 6.5/cancer cells, we found *TGFB2* that encodes TGF-β2, which belongs to the family of transforming growth factors often associated with cancer cell invasiveness and the epithelial-mesenchymal transition (EMT) [361], and *FST* (follistatin), a gene under the control of TGF-β2 [362] (Fig. 23a). A net increase in TGF-β2 mRNA transcript was confirmed by qPCR in various acidosis-adapted cancer cells (Fig. 23b). ELISA confirmed a significant increase of active TGF-β2 protein levels in acidosis-adapted cancer cell extracts (Fig. 23c) and corresponding extracellular media (Suppl. Fig. 3b). Of note, in the same conditions, active TGF-β1 protein levels remained unchanged (Suppl. Fig. 3c-d). Increases in TGF-β2 mRNA and protein could be recapitulated by 12-24h exposure of native cancer cells to acidic pH 6.5 (Fig. 23d and Suppl. Fig. 3e) and further evidence of the activation of TGF-β2 signaling pathway in acidosis-adapted cancer cells was obtained by documenting an increase in the extent of phospho-Smad2/3 (Fig. 23e and Suppl. Fig. 3f). Our search for the mechanism driving the preferential increase in TGF-β2 activity under acidosis then led us to document an autocrine TGF-β2-induced TGF-β2 transcription loop (Fig. 23f and Suppl. Fig. 3g) and more importantly, the upregulation of thrombospondin-1 (TSP-1), a critical actor of TGF-β2 maturation (Fig. 23g). Contrary to other TGF-β isoforms that contain a RGD motif

in their latency-associated peptide to promote integrin-dependent activation, TGF-β2 activation requires TSP-1 to facilitate maturation in its active form [363]. To further prove a role of TSP-1, we showed that TSP-1 silencing reduced the extent of mature (active) TGF-β2 (Fig. 23h) and associated phospho-Smad signaling (Suppl. Fig. 3h).

A role for TGF-β2 in supporting the invasive potential of 6.5/cancer cells was next evaluated using Trabedersen, a specific TGF-β2-targeting antisense oligonucleotide currently evaluated in clinical trials [364-366], and SB431542, a selective TGF-βRI inhibitor. We first documented that Trabedersen reduced TGF-β2 mRNA and protein expression (Suppl. Fig. 3i-j) and that both inhibitors prevented Smad2/3 phosphorylation (Fig. 23i and Suppl. Fig. 3k-l). Importantly, inhibition of TGF-β2 signaling led to a significant reduction in the invasion of acidosis-adapted cancer cells through Matrigel (Fig. 23j and Suppl. Fig. 3m) and prevented LD formation in 6.5/cancer cells (Fig. 23k), an effect paralleled by a reduction in the amounts of neutral lipids (Suppl. Fig. 3n). Of note, addition of recombinant TGF-β2 reversed the effects of Trabedersen on LD formation (Fig 23l).

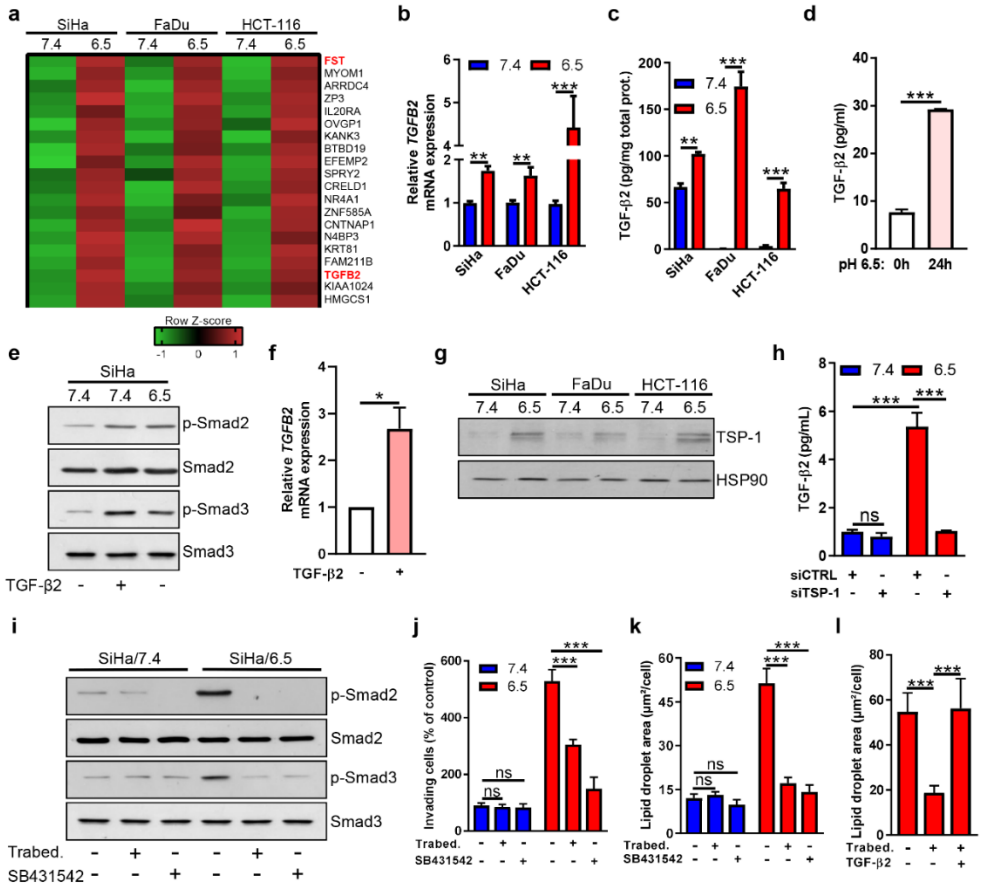

Figure 23: TGF-β2 supports invasiveness and LD formation in acidosis-adapted cancer cells. (**a**) Heat map representation of the top 20 genes upregulated in the indicated acidosis-adapted cancer cells. (**b**) mRNA expression for *TGFB2* in native and acidosis-adapted tumor cells. (**c-d**) Levels of active form of TGF-β2 in crude extracts (membrane-bound) from native and acidosis-adapted tumor cells (**c**) or in conditioned media (secreted) from native SiHa cells exposed to acidic pH 6.5 for 24h (**d**). (**e**) Representative immunoblotting for phosphorylated and total forms of Smad2 (Ser465/467) and Smad3 (Ser423/425) in native and acidosis-adapted SiHa cells (with or without treatment with 4 ng/ml TGF-β2 for 6 hours). (**f**) mRNA expression for *TGFB2* in native SiHa cells following treatment with 4 ng/ml TGF-β2 for 24h. (**g**) Representative immunoblotting for TSP-1 in native and acidosis-adapted tumor cells. (**h**) Levels of active form of TGF-β2 in conditioned media from native and acidosis-adapted SiHa cells following transfection of TSP-1-targeting (or control) siRNA for 72h. **(i-k**) Representative immunoblotting for phosphorylated and total forms of Smad3 (Ser423/425) (**i**), invasion capacity in Matrigel-coated Boyden chambers for 24h (**j**) and LD content (**k**) for native and acidosis-adapted SiHa

cells following treatment with 10 µM TGF-β2-specific antisense oligonucleotide Trabedersen for 7 days or 2 µM TGFβRI inhibitor SB431542 for 24h. (**l**) LD content in acidosis-adapted SiHa following treatment with 10 µM TGFβ2-specific antisense oligonucleotide Trabedersen for 7 days in absence or presence of 4 ng/ml TGF-β2 for 24h. Data are represented as mean ± SEM of three independent experiments (with ≥6 technical replicates). Significance was determined by Student's *t*-test (**d, f**), one-way ANOVA (**l**) or two-way ANOVA (**b-c, h, j-k**) with Bonferroni multiple-comparison analysis. *p<0.05; **p<0.01; ***p<0.001; ns, not significant. I directly contributed to the panels d, e, g, h, I, j, k, and l.

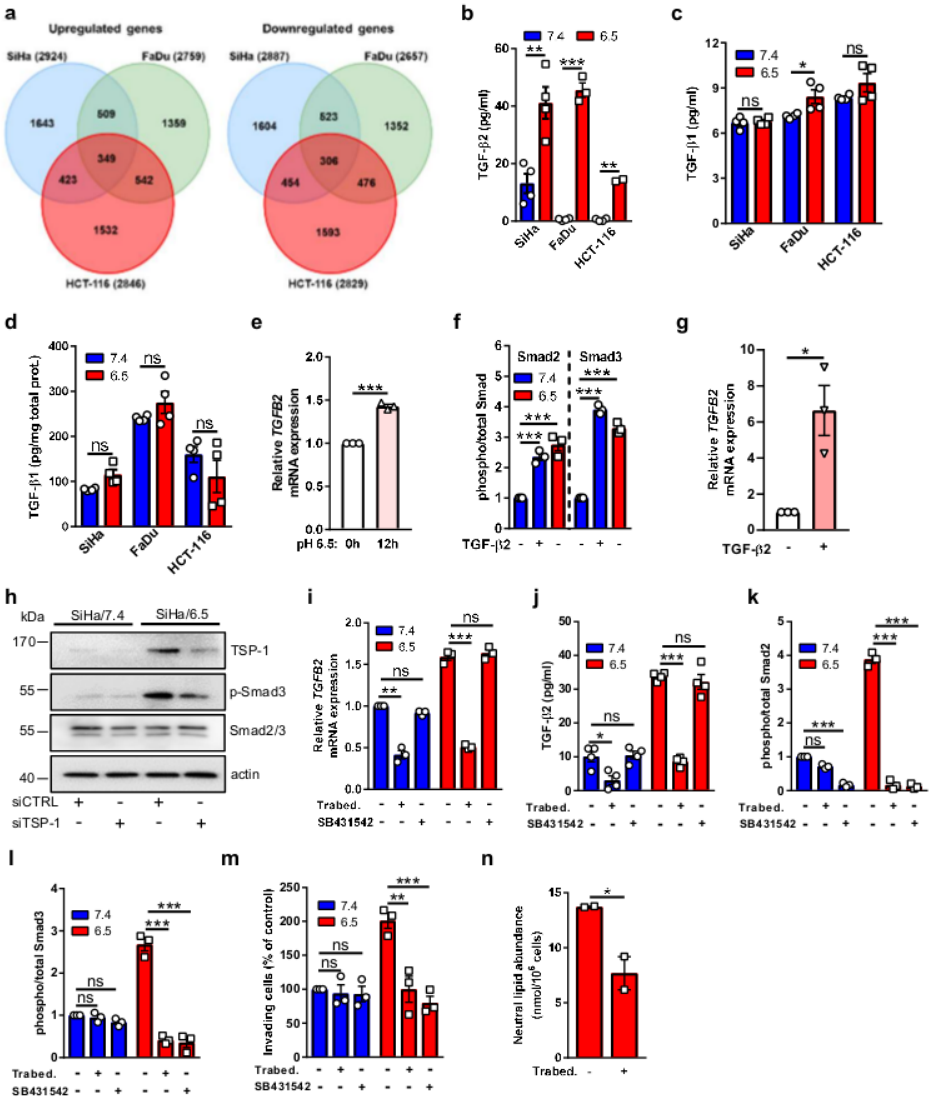

Supplementary Figure 3: Acidosis promotes a TGF-β2/TGF-βRI autocrine signaling pathway in cancer cells. (**a**) Venn diagrams showing overlap of up- and downregulated genes in pH 6.5-adapted SiHa, FaDu and HCT-116 cancer cell lines. Only the genes with a false discovery rate (FDR) < 0.01 and FPKM (fragments per kilobase of exon per million mapped reads) > 0.5 were considered for analysis. (**b**) Levels of active form of TGF-β2 in conditioned media (secreted) from native and acidosis-adapted tumor cells. (**c-d**) Levels of active form of TGF-β1 in conditioned media (secreted) (c) and in crude lysates (membrane-bound) (**d**) from native and acidosis-adapted tumor cells. (**e**) mRNA expression for

TGFB2 in native SiHa cells exposed to acidic pH 6.5 for 12h. (**f**) Quantification of Smad2 (Ser465/467) and Smad3 (Ser423/425) phosphorylation levels in native and acidosis-adapted SiHa cells (with or without treatment with 4 ng/ml TGF-β2 for 6 hours). (**g**) mRNA expression for *TGFB2* in native SiHa cells following treatment with 4 ng/ml TGF-β2 for 24h. (**h**) Representative immunoblotting for phosphorylated and total forms of Smad3 (Ser423/425) and TSP-1 in native and acidosis-adapted SiHa cells following transfection of TSP1-targeting (or control) siRNA for 72h. (**i-l**) mRNA expression for *TGFB2* (**i**), levels of active form of TGF-β2 in conditioned media (secreted) (j), quantification of Smad2 (**k**) and Smad3 (**l**) phosphorylation levels in native and acidosis-adapted SiHa cells following treatment with 10 μM TGFβ2-specific antisense oligonucleotide Trabedersen for 7 days or 2 μM TGF-βRI inhibitor SB431542 for 24h. (**m**) Invasion capacity for native and acidosis-adapted HCT-116 cells following treatment as above. (**n**) Neutral lipid abundance in acidosis-adapted SiHa cells following treatment with 10 μM Trabedersen for 7 days. Data are represented as mean ± SEM of three independent experiments (with ≥6 technical replicates). Significance was determined by Student's t-test (e, g, n), or two-way ANOVA (b-d, f, i-m) with Bonferroni multiple-comparison analysis. *p<0.05; **p<0.01; ***p<0.001; ns, not significant. I directly contributed to the panels b, f, h, i, and m.

TGF-β2 promotes FA uptake and TG accumulation together with increase in CD36 and DGAT1 expression in acidosis-adapted cancer cells.

We next focused on the causal link between TGF-β2-induced LD formation and the increased invasive potential of acidosis-adapted cancer cells. To address this question, we first examined how TGF-β2 could drive the formation of LD under acidosis. For this purpose, a lipidomic analysis was carried out to identify potential changes in the FA profile of cancer cells exposed to TGF-β2. We found a net increase in the extent of neutral lipids including saturated and monounsaturated FA in response to TGF-β2 stimulation for 6 hours (Fig. 24a-b and Suppl. Table 2) while the pools of phospholipids and free FA were not altered (Fig. 24a). Oil Red O staining confirmed that exposure of native 7.4/cancer cells to TGF-β2 also led to a rapid accumulation of LD (Fig. 24c and Suppl. Fig. 4a); similar results were obtained when BODIPY 493/503 or Nile Red were used to stain LD (not shown). To identify the source of FA involved in LD formation, we next used ^{14}C-labelled palmitate and showed that the uptake of palmitate by native cancer cells was stimulated upon TGF-β2 treatment (Fig. 24d) and that TGF-β2 silencing in 6.5/cancer cells could prevent palmitate influx, the latter effect being abrogated by the addition of exogenous TGF-β2 (Fig. 24e).

We next aimed to examine whether CD36, DGAT1 and PLIN2 that we had identified as key actors of FA accumulation in LD under acidosis were regulated by TGF-β2. While no change in total CD36 protein expression could be detected by immunoblotting (Suppl. Fig. 4b), using a method based on surface protein biotinylation, we found an increase in the expression of CD36 at the plasma membrane in pH 6.5-adapted cancer cells as well as in native cancer cells exposed to TGF-β2 (Fig. 24f). Blockade of TGF-β2 signaling reduced plasma membrane-

associated CD36 expression (Fig. 24g) and using a fluorescent palmitate analog (BODIPY-conjugated C_{16}), we confirmed the increased capacity of FA uptake by TGFβ2-stimulated native cancer cells (Suppl. Fig. 22c). Different pathways are known to regulate CD36 translocation, namely AMPK [367], SIRT1 [368] and PKC-ζ [369]. Since activation of the two former ones represses TGF-β signaling [370, 371], we focused on PKC-ζ which has already been reported to mediate TGF-β signaling [369]. Inhibition of CD36 translocation (in response to either acidic pH or direct TGF-β2 exposure) was observed in the presence of a PKC-ζ pseudo-substrate inhibitor (Fig. 24h, Figs 24i-j for quantification, Suppl. Fig. 4d-f). Of note, although SIRT1 activity was previously shown to be stimulated under acidosis [34], SIRT1 inhibitor EX-527 failed to show any change in the extent of CD36 translocation (Suppl. Fig. 4g).

We also documented a significant upregulation of DGAT1 mRNA and protein expression in pH6.5-adapted cancer cells (Fig. 24k-l and Suppl. Fig. 4h) that was completely prevented upon TGF-β2 silencing or TGF-βRI blockade (Fig. 24m and Suppl. Fig. 4i-j); DGAT2 expression was not altered in response to Trabedersen or SB431542 (Suppl. Fig. 22k). Interestingly, the PKC-ζ pseudo-substrate inhibitor (that prevented CD36 translocation) also blocked DGAT1 upregulation in 6.5/cancer cells (Fig. 24n and Suppl. Fig. 4l) and in TGF-β2-treated cancer cells (Suppl. Fig. 4l-m), suggesting that CD36 cell surface expression could be the primary event leading to subsequent upregulation of genes involved in FA handling. To support this hypothesis, we treated 6.5/cancer cells with GW6471, an antagonist of PPARα (a major FA-activated transcription factor regulating FA metabolism) and showed that the expression of DGAT1 but also that of mitochondrial fatty acyl-CoA transporter CPT1 were decreased (Fig. 24o). Furthermore, GW6471 treatment induced the inhibition of 6.5/cancer cell growth but did not alter 7.4/cell proliferation further

supporting a major role of FA-induced PPARα activity under acidic conditions (Suppl. Fig. 4n-o). Finally, expression of PLIN2 that we found to be upregulated in acidosis-adapted cancer cells (see Fig. 24h) was inhibited upon TGF-β2 silencing (Fig. 24p). Of note, in a study directly comparing gene expression in healthy and cancerous colorectal tissues, PLIN2 expression (but neither PLIN1, nor PLIN3) strongly correlated with TGF-β2 expression (Fig. 24q); a similar co-expression pattern between TGF-β2 and PLIN2 was also found in human clear cell renal cell carcinoma samples (Suppl. Fig. 4p).

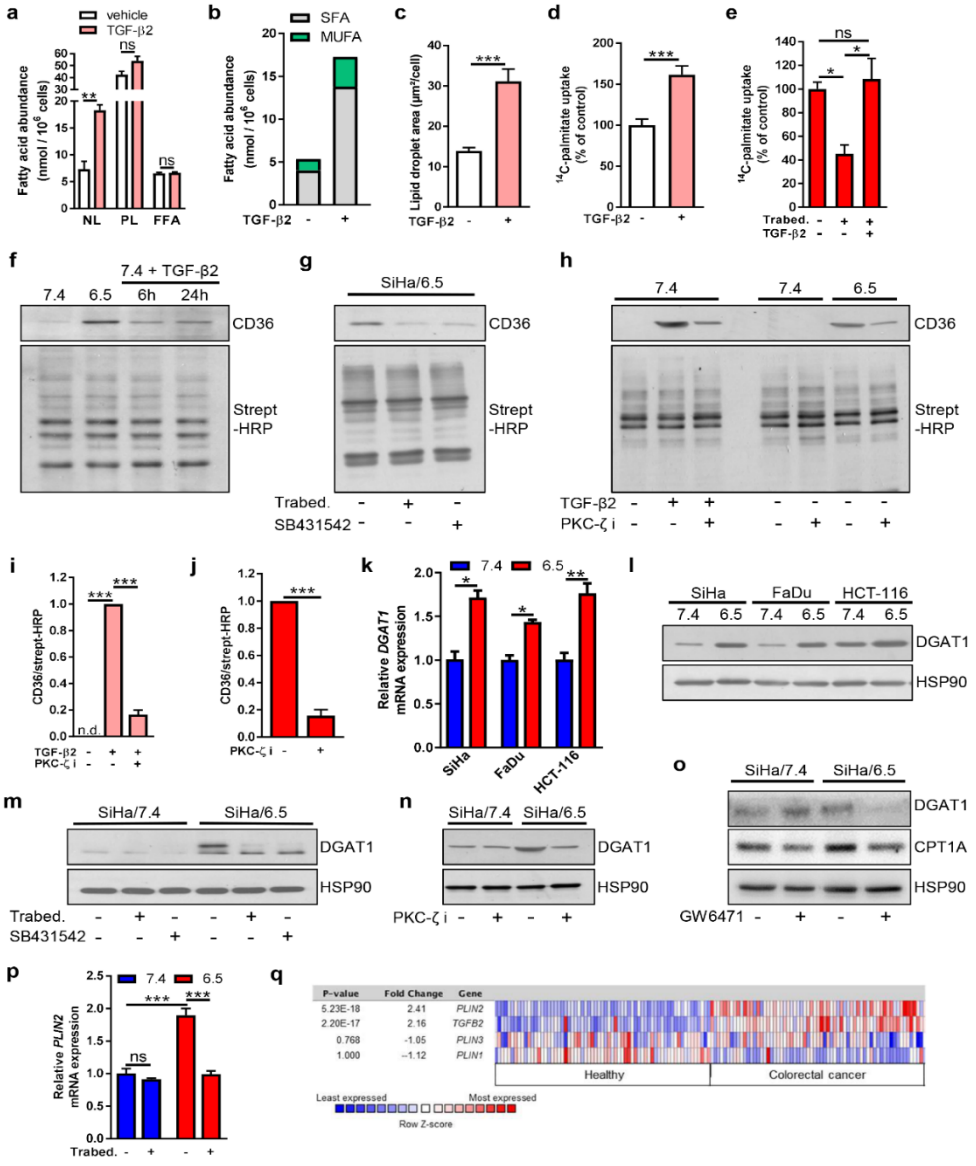

Figure 24: TGF-β2 promotes FA uptake and TG accumulation into LD in a CD36- and DGAT1-dependent manner. (**a-c)** Abundance of neutral lipids (NL), phospholipids (PL) and free fatty acids (FFA) (**a**), abundance of saturated and monounsaturated fatty acids (SFA and MUFA, respectively) in the neutral lipid fraction (**b**), and LD content (**c**) in native SiHa cells after treatment with 4 ng/ml TGF-β2 for 6h. (**d-e**) ^{14}C-palmitate uptake for 10 min in SiHa cells after treatment with 4 ng/ml TGF-β2 for 6h (**d**) and in acidosis-adapted SiHa cells following treatment with 10 µM Trabedersen for 7 days in

absence or presence of 4 ng/ml TGF-β2 for 24h (**e**). (**f-h**) Representative immunoblotting for cell surface-localized CD36 and total biotinylated proteins in native and acidosis-adapted SiHa cells following treatment with 4 ng/ml TGF-β2 for 6h and 24h (**f**), following treatment with 10 µM Trabedersen for 7 days or 2 µM SB431542 for 24h (**g**) or with 4 ng/ml TGF-β2 and 10 µM PKC-ζ pseudo-substrate inhibitor for 24h (**h**). (**i-j**) Quantification of surface-localized CD36 in native and acidosis-adapted SiHa cells treated as indicated in (**h**). (**k-l)** mRNA (**k**) and protein expression of DGAT1 (**l**) in native and acidosis-adapted tumor cells. (**m-o**) Representative immunoblotting for DGAT1 in native and acidosis-adapted SiHa cells following treatment with 10 µM Trabedersen for 7 days or 2 µM SB431542 for 24h (**m**), with 10 µM PKC-ζ pseudo-substrate inhibitor for 24h (**n**) or with 10 µM GW6471 for 48h (**o**). (**p**) mRNA expression of *PLIN2* in native and acidosis-adapted SiHa cells following treatment with 10 µM TGFβ2-specific antisense oligonucleotide Trabedersen for 7 days. (**q**) Co-expression analysis of *TGFB2*, *PLIN1*, *PLIN2* and *PLIN3* genes in human healthy volunteers and colorectal cancer patient samples. Data are represented as mean ± SEM of three independent experiments (with ≥6 technical replicates). Significance was determined by Student's *t*-test (**c-d, j**), by one-way ANOVA (**e, i**) or two-way ANOVA (**a, k, p**) with Bonferroni multiple-comparison analysis. *p<0.05; **p<0.01; ***p<0.001; ns, not significant. I directly contributed to the panels c and i.

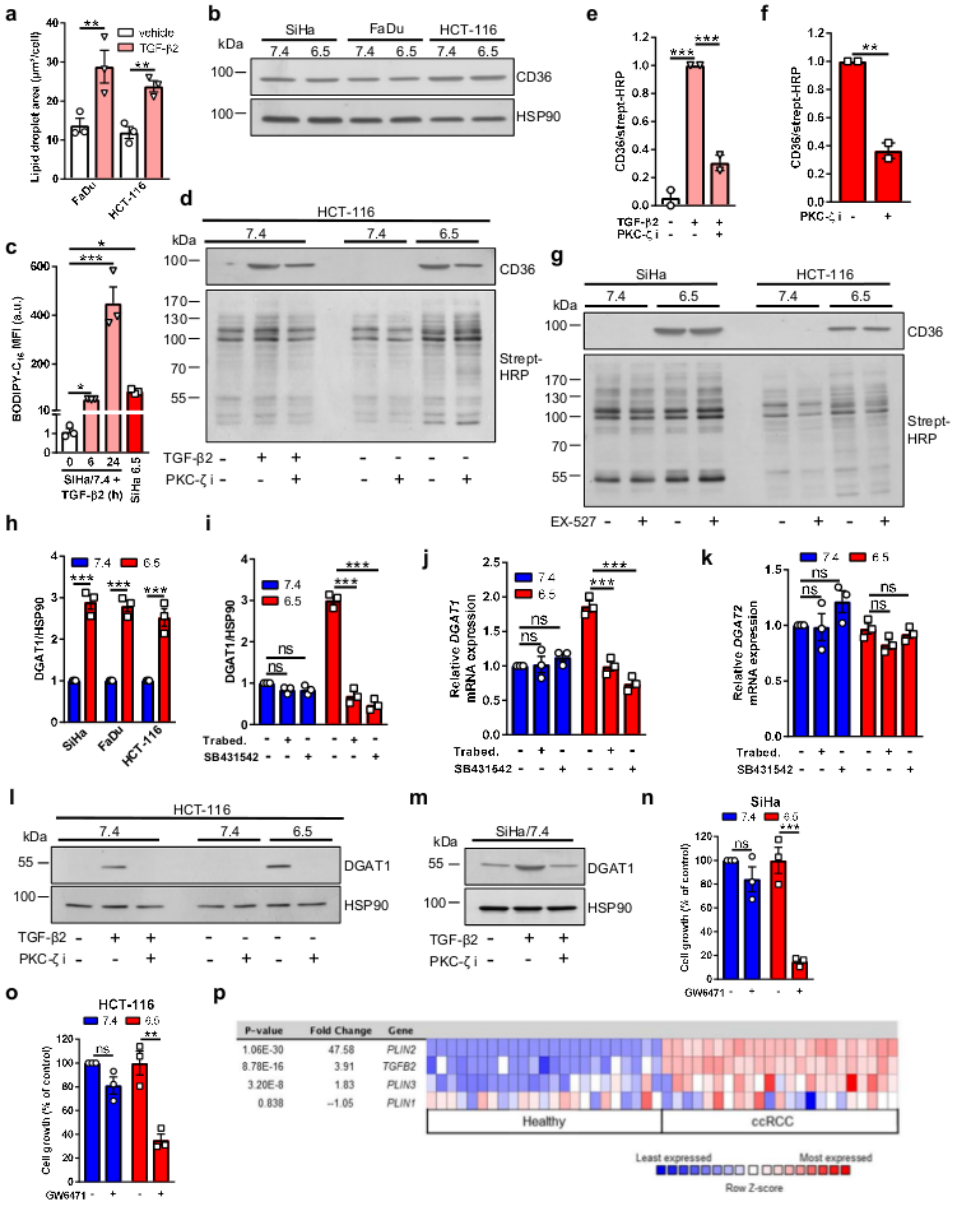

Supplementary Figure 4: TGF-β2 promotes FA uptake and TG accumulation into LD in a CD36 and DGAT1-dependent manner. (a) LD area in native FaDu and HCT-116 cells after treatment with 4 ng/ml TGF-β2 for 6h. (**b**) Representative immunoblotting for total CD36 in native and acidosis-adapted tumor cells. (**c**) Quantification for BODIPY FL C16 uptake in native and acidosis-adapted SiHa cells after treatment with 4 ng/ml TGF-β2 for 6h or 24h. (**d-f**) Representative immunoblotting (**d**) and

quantification (**e-f**) for cell surface-localized CD36 and total biotinylated proteins in native and acidosis-adapted HCT-116 cells following treatment with 4 ng/ml TGF-β2 and 10 µM PKC-ζ pseudo-substrate inhibitor for 24h. (**g**) Representative immunoblotting for cell surface-localized CD36 and total biotinylated proteins in native and acidosis-adapted tumor cells following treatment with 1 µM EX-527 (SIRT1 inhibitor) for 24h. (**h**) Quantification of DGAT1 protein levels in native and acidosis-adapted tumor cells. (**i-k**) Quantification of DGAT1 protein levels (**i**), mRNA expression for DGAT1 (**j**) and DGAT2 (**k**) in native and acidosis-adapted SiHa cells following treatment with 10 µM TGFβ2-specific antisense oligonucleotide Trabedersen for 7 days or 2 µM TGF-βRI inhibitor SB431542 for 24h. (**l-m**) Representative immunoblotting for DGAT1 in native and acidosis-adapted HCT-116 (**l**) or SiHa cells (**m**) following treatment with 4 ng/ml TGF-β2 and 10 µM PKC-ζ pseudo-substrate inhibitor for 24h. (**n-o**) Cell growth of native and acidosis-adapted SiHa (**n**) and HCT-116 cells (**o**) following treatment with 10 µM GW6471 (PPARα inhibitor) for 72h. (**p**) Co-expression analysis of TGFB2, PLIN1, PLIN2 and PLIN3 genes in human healthy and renal cancer (clear cell renal cell carcinoma; ccRCC) patient samples. Data are represented as mean ± SEM of three independent experiments (with ≥6 technical replicates). Significance was determined by Student's t-test (f), one-way ANOVA (c, e), or two-way ANOVA (a, h-k, n-o) with Bonferroni multiple-comparison analysis. *p<0.05; **p<0.01; ***p<0.001; ns, not significant. I directly contributed to the panels a, c and h.

Supplementary Table 2. Fatty acid abundance of the neutral lipid fraction in native and acidosis-adapted cancer cells. Data indicated in the table are mean values of 2 to 4 biological replicates.

Saturated fatty acids (nmol/ 10^6 cells)								
	SiHa		FaDu		HCT-116		HT-29	
Fatty acid	7.4	6.5	7.4	6.5	7.4	6.5	7.4	6.5
C12:0	0.00	0.10	0.43	0.49	0.13	0.16	0.09	0.12
C14:0	0.30	1.85	2.53	3.35	1.92	1.91	2.35	2.37
C16:0	2.97	7.52	6.52	12.28	5.04	10.88	11.28	16.39
C18:0	1.57	2.04	1.79	2.37	0.99	1.39	3.39	5.31
C20:0	0.00	0.07	0.02	0.00	0.00	0.08	0.18	0.34
C22:0	0.00	0.00	0.00	0.00	0.00	0.00	0.00	0.00
C24:0	0.00	0.02	0.11	0.13	0.00	0.12	0.15	0.27
Total	**4.84**	**11.61**	**11.41**	**18.62**	**8.08**	**14.54**	**17.45**	**24.79**
Monounsaturated fatty acids (nmol/ 10^6 cells)								
	SiHa		FaDu		HCT-116		HT-29	
Fatty acid	7.4	6.5	7.4	6.5	7.4	6.5	7.4	6.5
C14:1cis9	0.00	0.00	0.00	0.00	0.00	0.00	0.30	0.18
C16:1cis9	0.61	3.81	1.77	2.33	7.05	4.99	7.99	6.88
C18:1cis9	2.16	11.80	5.65	13.76	9.60	11.67	16.11	25.55
C18:1cis11	1.01	7.10	3.52	7.11	2.07	6.95	1.51	2.47
C20:1c11	0.07	0.58	0.30	1.23	0.52	0.70	0.14	0.39
C22:1c13	0.03	0.21	0.13	0.33	0.08	0.18	0.06	0.13
C24:1c15	0.00	0.24	0.20	0.53	0.14	0.17	0.01	0.07
Total	**3.87**	**23.74**	**11.57**	**25.28**	**19.47**	**24.66**	**26.13**	**35.67**
TOTAL	**8.71**	**35.35**	**22.98**	**43.90**	**27.55**	**39.20**	**43.58**	**60.46**

EMT in acidosis-adapted cancer cells is under the control of TGF-β2-stimulated fatty acid metabolism.

We next examined whether LD biogenesis, as driven by TGF-β2, represents a pre-requisite to support invasiveness of acidosis-adapted cancer cells. Since TGF-β2 is known to promote cancer cell invasiveness by inducing EMT, we first aimed to identify molecular markers of this phenotypic transition in 6.5/cancer cells. We actually showed that in SiHa cancer cells, chronic acidosis inversely influenced the expression of E-cadherin and vimentin, two critical markers of the epithelial and mesenchymal status, respectively (Fig. 25a). This led us to further explore a variety of EMT markers in different pairs of native and acidosis-adapted cancer cells. Although not all the EMT markers were similarly altered, partial EMT was confirmed in each cancer cell type, with an increase in several mesenchymal traits including N-cadherin (*CDH2*), Snail (*SNAIL1*), Slug (*SNAIL2*), ZEB1 and vimentin, and/or a reduction in ZO-1 and E-cadherin (*CDH1*) as documented by mRNA quantification (Fig. 25b and Suppl. Fig. 5a-b) and protein immunodetection (Fig. 25c and Suppl. Fig. 5c-d). Of note, exposure of 7.4/cancer cells to TGF-β2 recapitulated the EMT signature observed in 6.5/cancer cells (Suppl. Fig. 5e). More importantly, the use of Trabedersen and SB431542 allowed us to confirm that TGF-β2 supports the mesenchymal shift observed in 6.5/cancer cells. Both treatments actually reverted the upregulation of the mesenchymal markers *SNAIL1* (Fig. 25d), *ZEB1* (Fig. 25e) as well as N-cadherin and vimentin (Fig. 25f and Suppl. Fig. 5f-g) in acidosis-adapted cancer cells. To further prove the role of TGF-β2 in EMT under acidic conditions, we silenced Smad2/3 (Suppl. Fig. 5h-i) and confirmed a dramatic reduction in *SNAIL1* and *ZEB1* in 6.5/cancer cells (Fig. 25g-h and Suppl. Fig. 5j).

In an attempt to establish a link between EMT and LD accumulation, both being promoted by acidosis-driven TGF-β2 signaling, we could document that silencing ZEB1 blocked EMT in 6.5/cancer cells (Suppl. Fig. 5k) but also reduced the formation of LD under acidosis (Fig. 25i and Suppl. Fig. 5l). We also hypothesized that the other way around, an increase in FA oxidation and associated acetyl-CoA pool could account for Smad2 acetylation, a PTM known to augment its transcriptional activity [372] and to support EMT [373]. Using Seahorse respirometry, we first showed that exogenous FA significantly contributed to oxygen consumption rate (OCR) in native cancer cells exposed to TGF-β2 as well as in 6.5/cancer cells (*vs*. 7.4/cancer cells) (Fig. 25j and Suppl. Fig. 5m), an effect largely inhibited upon TGF-β2 silencing or TGF-βRI pharmacological blockade (Fig. 25k and Suppl. Fig. 5n). Stimulated FA oxidation was confirmed by a net increase in the cellular pool of acetyl-CoA in 6.5/cancer cells (Fig. 25l) and associated Smad2 acetylation (Fig. 25m and Suppl. Fig. 5o). Importantly, inhibition of either FA uptake by CD36 blocking antibodies or FA mitochondrial metabolism by CPT1 inhibitor etomoxir significantly reduced Smad2 acetylation in 6.5/cancer cells (Fig. 25n). Interestingly, when using non-tumorigenic MCF-10A mammary epithelial cells (instead of cancer cell lines), we failed to document LD accumulation in response to acidosis (Suppl. Fig. 5p) as well as increase in TGF-β2 activity (Suppl. Fig. 5q) and changes in EMT markers (Suppl. Fig. 5r), thereby indicating that the stimulation of the TGF-β2/LD axis in response to acidosis is largely cancer cell-specific.

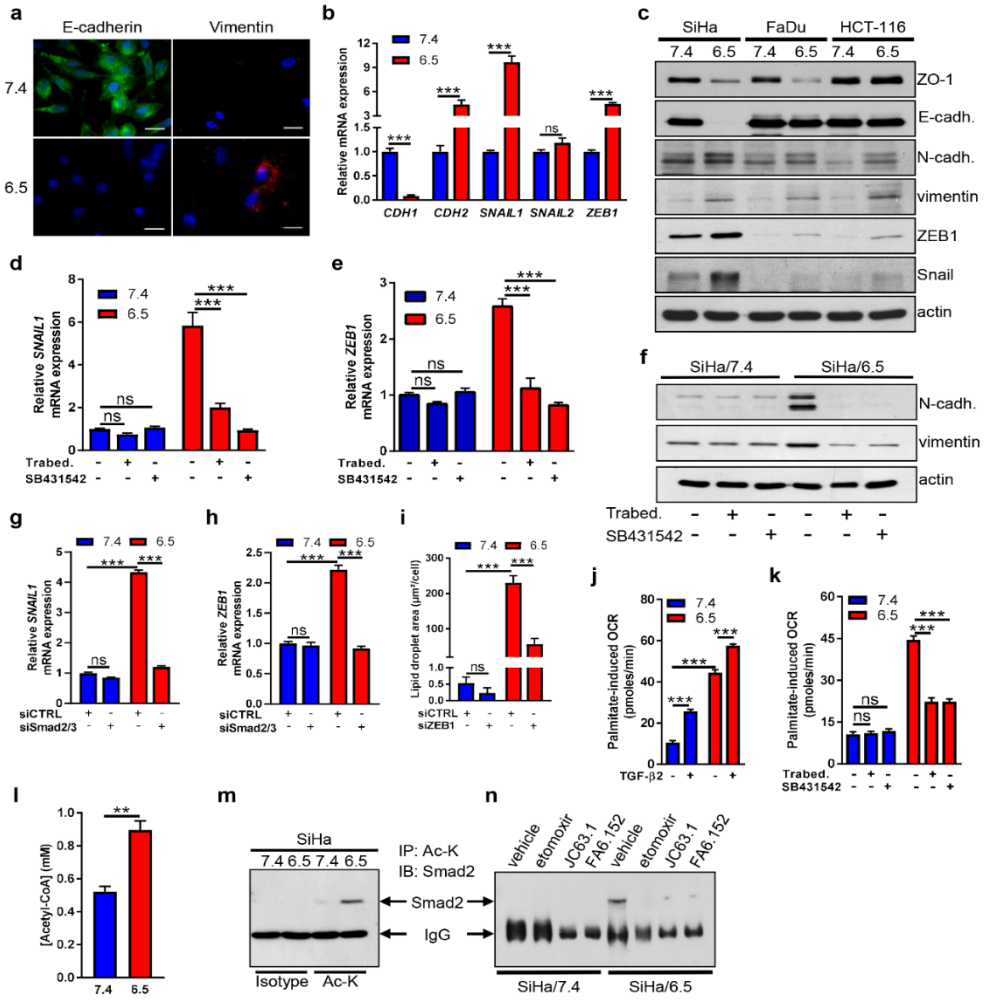

Figure 25: EMT in acidosis-adapted cancer cells is driven by TGF-β2 and further enhanced by FAO-dependent Smad2 acetylation. (**a**) Representative immunofluorescence pictures for EMT-related protein markers in native and acidosis-adapted SiHa cells. Scale bar: 20 µm. (**b**) mRNA expression for epithelial (*CDH1*) and mesenchymal (*CDH2*, *SNAIL1*, *SNAIL2* and *ZEB1*) genes in native and acidosis-adapted SiHa cells. (**c**) Representative immunoblotting for some epithelial (ZO-1 and E-cadherin) and mesenchymal (N-cadherin, vimentin, ZEB1, Snail) protein markers in native and acidosis-adapted cancer cell lines. (**d-e**) mRNA expression for *SNAIL1* (**d**) and *ZEB1* (**e**) in native and acidosis-adapted SiHa cells following treatment with 10 µM Trabedersen for 7 days or 2 µM SB431542 for 24h. (**f**) Representative immunoblotting for mesenchymal protein markers in native and acidosis-adapted

SiHa cells following treatment as above. (**g-h**) mRNA expression for *SNAIL1* (**g**) and *ZEB1* (**h**) in native and acidosis-adapted SiHa cells following transfection of Smad2/3-targeting (or control) siRNA for 72h. (**i**) LD content in native and acidosis-adapted SiHa cells following transfection with ZEB1-targeting (or control) siRNA for 72h. (**j-k**) Palmitate-dependent oxygen consumption rate (OCR) in native and acidosis-adapted SiHa cells after treatment with 4 ng/ml TGF-β2 for 6h (**j**) or following treatment with 10 μM Trabedersen for 7 days or 2 μM SB431542 for 24h (**k**). (**l**) Levels of cellular acetyl-CoA in native and acidosis-adapted SiHa cells. (**m-n**) Representative immunoblotting for acetylated Smad2 in native and acidosis-adapted cancer cells (with or without treatment with 4 ng/ml TGF-β2 for 6 hours) (**m**) and following treatments with 30 μM etomoxir (CPT1 inhibitor), 2 μg/ml JC63.1 or 1 μg/ml FA6-152 (anti-CD36 blocking antibodies) for 24h (**n**). Data are represented as mean ± SEM of three independent experiments (with ≥6 technical replicates). Significance was determined by Student's *t*-test (**l**) or two-way ANOVA (**b, d, e, g-k**) with Bonferroni multiple-comparison analysis. **p<0.01; ***p<0.001; ns, not significant. I directly contributed to the panels a, c and f.

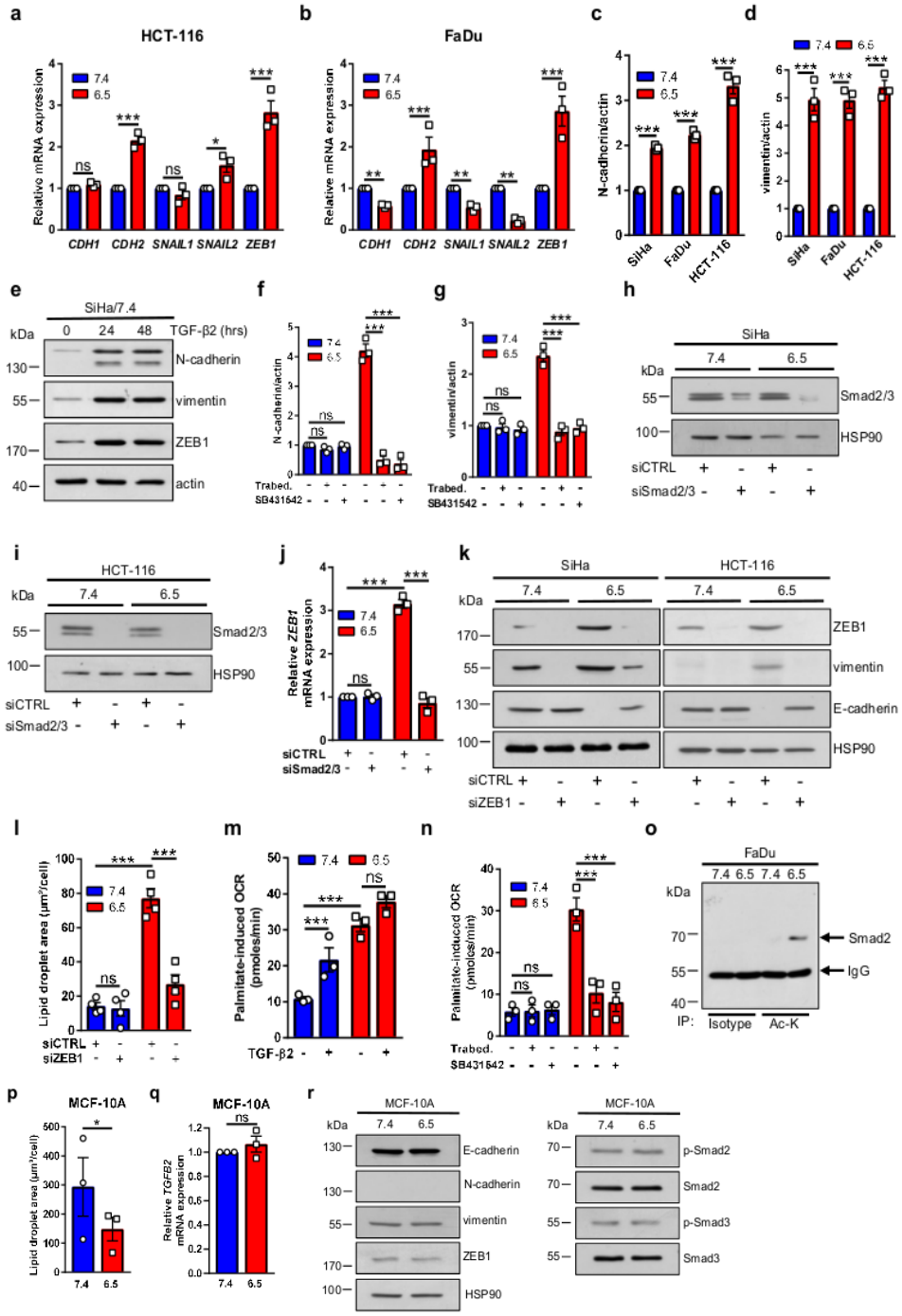
a
HCT-116
Relative mRNA expression
7.4
6.5
CDH1
CDH2
SNAIL1
SNAIL2
ZEB1
b
FaDu
c
N-cadherin/actin
SiHa
FaDu
HCT-116
d
vimentin/actin
e
SiHa/7.4
kDa
0
24
48
TGF-β2 (hrs)
N-cadherin
vimentin
ZEB1
actin
f
g
Trabed.
SB431542
h
SiHa
Smad2/3
HSP90
siCTRL
siSmad2/3
i
HCT-116
j
Relative ZEB1 mRNA expression
k
SiHa
HCT-116
ZEB1
vimentin
E-cadherin
HSP90
siZEB1
l
Lipid droplet area (μm²/cell)
m
Palmitate-induced OCR (pmoles/min)
TGF-β2
n
o
FaDu
Smad2
IgG
IP:
Isotype
Ac-K
p
MCF-10A
q
Relative TGFB2 mRNA expression
r
E-cadherin
N-cadherin
vimentin
ZEB1
HSP90
p-Smad2
Smad2
p-Smad3
Smad3

Supplementary Figure 5: EMT in acidosis-adapted cancer cells is driven by TGF-β2 and further enhanced by FAO-dependent Smad2 acetylation. (**a-b**) mRNA expression for some epithelial (CDH1) and mesenchymal (CDH2, SNAIL1, SNAIL2 and ZEB1) genes in native and acidosis-adapted HCT-116 (**a**) and FaDu cells (**b**). (**c-d**) Quantification of N-cadherin (**c**) and vimentin (**d**) protein levels in native and acidosis-adapted tumor cells. (**e**) Representative immunoblotting for EMT-related protein markers in native SiHa cells following treatment with 4 ng/ml TGF-β2 for 24 and 48 hours. (**f-g**) Quantification of N-cadherin (**f**) and vimentin (**g**) protein levels in native and acidosis-adapted SiHa cells following treatment with 10 µM Trabedersen for 7 days or 2 µM SB431542 for 24h. (**h-j**) Representative immunoblotting for Smad2/3 in native and acidosis-adapted SiHa (**h**) and HCT-116 cells (**i**) and mRNA expression for ZEB1 in native and acidosis-adapted HCT-116 cells (**j**) following transfection of Smad2/3-targeting (or control) siRNA for 72h. (k-l) Representative immunoblotting for EMT-related protein markers in native and acidosis-adapted tumor cells (k) and LD content in native and acidosis-adapted HCT-116 cells (**l**) following transfection with ZEB1-targeting (or control) siRNA for 72h. (**m-n**) Palmitate-dependent oxygen consumption rate in native and acidosis-adapted HCT-116 cells after treatment with 4 ng/ml TGF-β2 for 6h (**m**) or following treatment with 10 µM Trabedersen for 7 days or 2 µM SB431542 for 24h (**n**). (**o**) Representative immunoblotting for acetylated Smad2 in native and acidosis-adapted FaDu cancer cells. (**p-r**) LD content (**p**), mRNA expression for TGFB2 (**q**) and representative immunoblotting for EMT-related protein markers, phosphorylated and total forms of Smad2 (Ser465/467) and Smad3 (Ser423/425) (**r**) in non-tumorigenic MCF-10A mammary epithelial cells acutely exposed to acidic pH 6.5 for 48h (vs pH 7.4). Data are represented as mean ± SEM of three independent experiments (with ≥6 technical replicates). Significance was determined by Student's t-test (p-q), two-way ANOVA (a-d, f-g, j, l-n) with Bonferroni multiple-comparison analysis.*p<0.05; **p<0.01; ***p<0.001; ns, not significant. I directly contributed to the panels c, d, e, f and g.

Preventing LD accumulation reduces the growth of acidic tumor spheroids and the metastatic take of acidosis-adapted cancer cells in mice.

We finally aimed to document that LD accumulation could occur spontaneously in response to ambient acidosis developing in 3D spheroids (*i.e.* instead of extracellular acidic pH imposed by buffered medium) and could be targeted to reduce metastatic burden *in vivo*. For 3D tumor spheroid experiments, we used HT-29, a colorectal cancer cell line more prone to form spheroids than the other cell lines used above. We first confirmed that after adaptation to pH 6.5 (Suppl. Fig. 6a), HT-29 cancer cells accumulated neutral lipids within lipid droplets (Suppl. Fig. 6b-f) and exhibited a higher invasiveness potential (Suppl. Fig. 6g) together with an increased TGF-β2 (but not TGF-β1) signaling (Suppl. Fig. 6h-n). We showed that acidic pH spontaneously developed with growth in 3D HT-29 spheroids by using an Alexa568-conjugated pHLIP peptide as a pH sensor (Fig. 26a-b). Interestingly, pHLIP-positive acidic areas significantly overlapped with accumulation of neutral lipids as detected using BODIPY 493/503 staining (Fig. 26c-d) while Ki67 staining revealed that acidic areas were less proliferative than the rim of 3D spheroids (Fig. 26e). To establish a direct link between LD accumulation and TGF-β2 signaling in this 3D model, we exposed spheroids to TGF-βRI blocker SB431542 and observed a dramatic reduction in BODIPY-stained LD (Fig. 26f-g) together with a growth inhibitory effect (Fig. 26h); the latter was only detectable when spheroids reached a size compatible with spontaneous acidosis development (*i.e*. between 5 and 10 days; see Figs. 25b and 25h). Interestingly, we confirmed in sections of primary HT-29 tumors that LD-positive area (stained with ORO) could be identified in acidic tumor regions labelled using Alexa568-conjugated pHLIP peptide (Suppl. Fig. 6o). Of note, although LD could also be identified at the interface

between hypoxic and necrotic tumor areas, acidic LD-rich tumor regions did not overlap with tumor hypoxic area (as stained with pimonidazole) (Suppl. Fig. 6o).

We finally examined whether acidic adaptation was associated with a more aggressive phenotype *in vivo* and importantly whether therapeutic interventions could be derived from the observation of LD generation as part of the EMT phenotype induced by acidosis. For this purpose, we utilised a model of i.v. injection of HT-29 cancer cells to make sure to track the fate of cells whose phenotype resulted from acidosis adaptation and more particularly to evaluate their increased anoikis resistance (see above) when exposed to the bloodstream. We first documented that when compared with corresponding native cells, i.v. injection of acidosis-adapted HT-29 cancer cells led to a more extensive metastatic take in the lungs (Fig. 26i-j).

Then, to prove that LD contributed to a higher metastatic burden, we treated mice with etomoxir to prevent FA oxidation to occur in 6.5/HT-29 cancer cells upon i.v. injection. Lung metastatic burden was dramatically reduced in etomoxir-treated mice (Fig. 26k-l). Similar results were obtained with 6.5/FaDu and 6.5/HCT-116 cell lines with a reduced mouse survival following i.v. injection (Fig. 26m-n). With the latter, we could also generate LD-deprived 6.5/cancer cells as detailed in Suppl. Fig. 2d and document that the extent of metastases was significantly reduced (*vs.* LD-containing 6.5/cancer cells) (Fig. 26o-p).

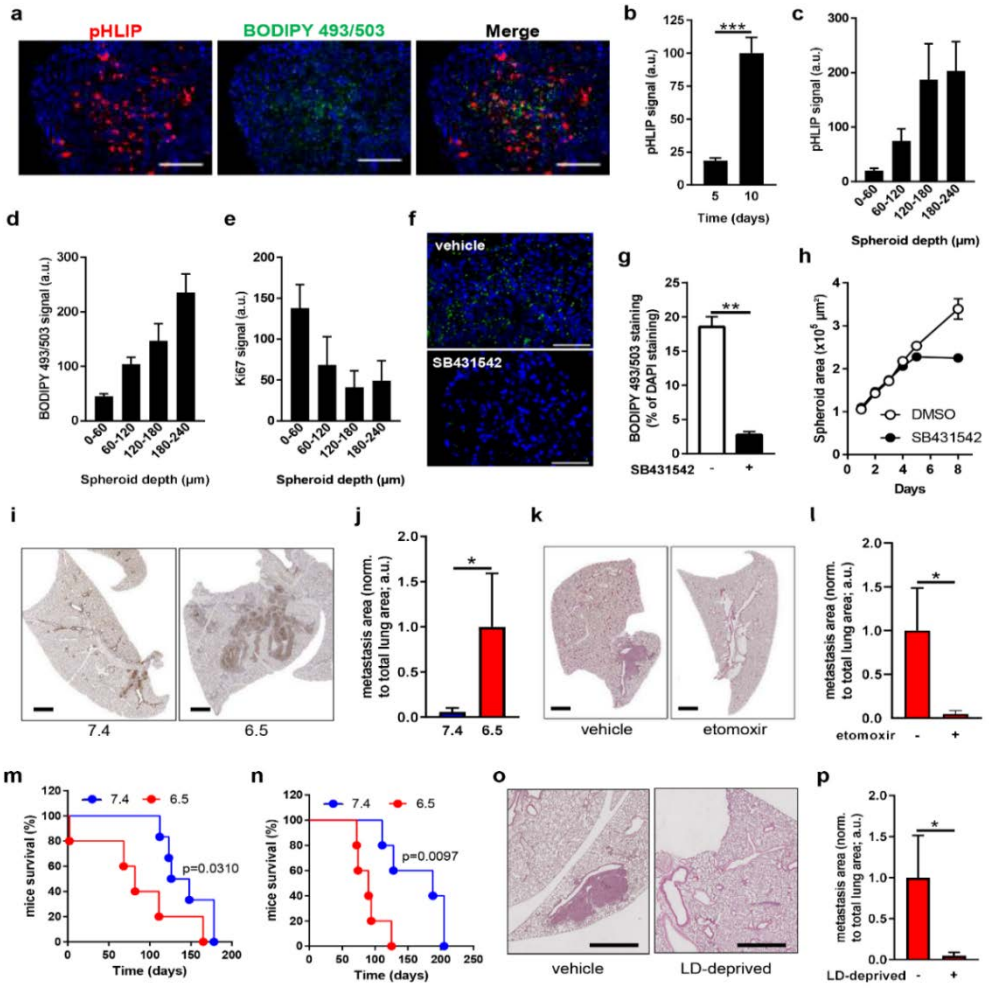

Figure 26: TGF-β2-driven LD formation spontaneously occurs under acidic conditions and fosters *in vivo* cancer cell invasiveness. (**a**) Representative immunofluorescent pictures of Alexa Fluor 568-conjugated pHLIP and BODIPY 493/503 staining in 10-day-old HT-29 spheroids. Scale bar: 100 µm. (**b**) Time-course accumulation of pHLIP during HT-29 spheroid growth. (**c-e**) Distribution (from the periphery to the core of the spheroids) of pHLIP (**c**), BODIPY 493/503 (**d**) and Ki67 (**e**) staining. (**f-g**) Representative immunofluorescent pictures (**f**) and quantification (**g**) of BODIPY 493/503 staining in 10-day-old HT-29 spheroids treated or not with 20 µM TGF-βRI inhibitor SB431542. (**h**) Time course of the growth inhibitory effects of 20 µM SB431542 on 3D tumor spheroid growth. (**i-j**) Representative immunohistochemical pictures (**i**) and quantification (**j**) of GFP- or mCherry-positive lung metastases in mice 5 weeks after i.v. injection of GFP-expressing native and mCherry-expressing acidosis-adapted HT-29 cancer cells (n=5-8 mice per group). Scale bar: 1 mm. (**k-l**) Representative H&E staining (**k**) and

quantification of metastasis area (**l**) in lungs from mice 5 weeks after i.v. injection of acidosis-adapted HT-29 cells and i.p. treatment with 40 mg/kg etomoxir (n=6-7 mice per group). Scale bar: 1 mm. (**m-n**) Kaplan-Meier curves depicting mouse survival after i.v. injection of native and acidosis-adapted FaDu (**m**) and HCT-116 (**n**) cancer cells. (**o-p**) Representative H&E staining (**o**) and quantification of metastasis area (**p**) in lungs from mice 5 weeks after i.v. injection of lipid droplet-deprived (forskolin-treated; or not) acidosis-adapted HCT-116 cells (n=5 mice per group). Scale bar: 250 µm. Data are represented as mean ± SEM of three independent experiments (with ≥6 technical replicates). Significance was determined by Student's *t*-test (**b**, **g**, **j, l, p**). *p<0.05; **p<0.01; ***p<0.001.

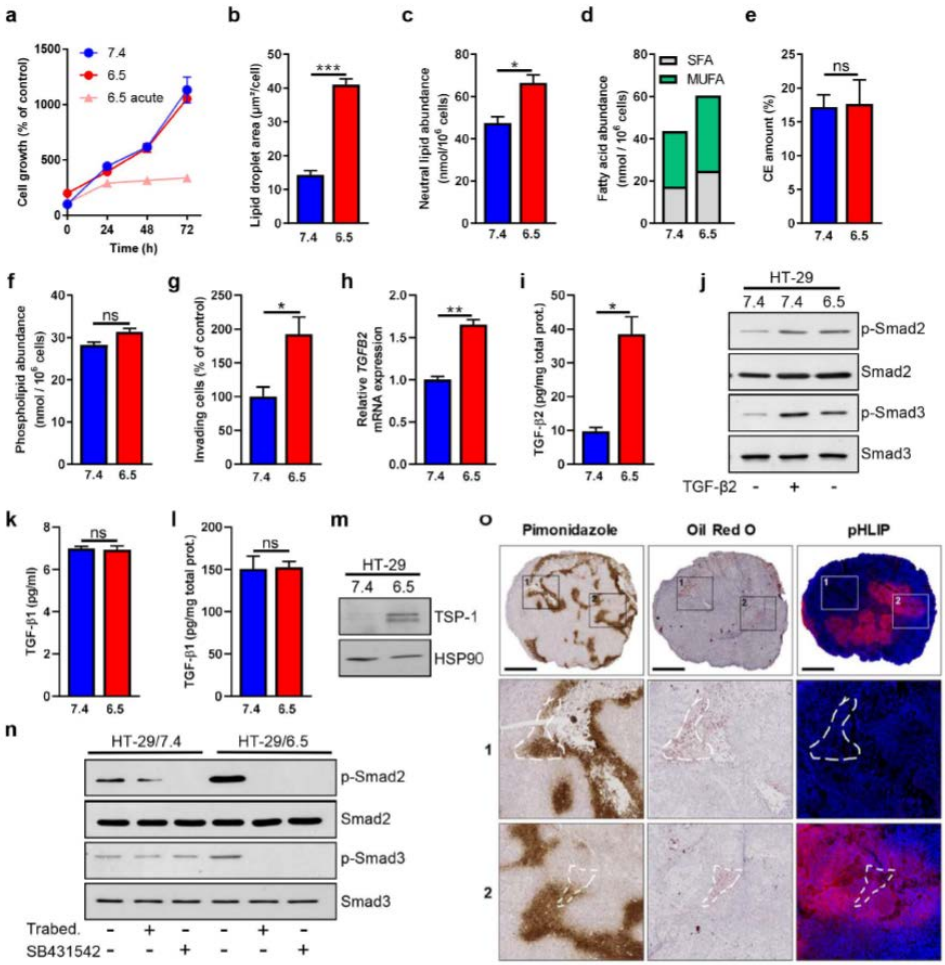

Supplementary Figure 6: EMT in acidosis-adapted cancer cells is driven by TGF-β2 and further enhanced by FAO-dependent Smad2 acetylation. (**a**) Time courses of the growth of native, chronically and acutely pH6.5-exposed HT-29 cancer cells. (**b-c**) LD content (**b**) and neutral lipid abundance (**c**) in native and acidosis-adapted HT-29 cells. (d-e) Abundance of SFA and MUFA (**d**) and cholesteryl esters (**e**) in the neutral lipid fraction of native and acidosis adapted HT-29 cells. (f) Phospholipid abundance in native and acidosis-adapted HT-29 cells. (**g**) Invasion capacity of native and acidosis-adapted HT-29 cells. (**h-i**) mRNA expression (**h**) and levels of active form of TGF-β2 in crude lysates (membrane-bound) (**i**) from native and acidosis-adapted HT-29 cells. (**j**) Representative immunoblotting for phosphorylated and total forms of Smad2 (Ser465/467) and Smad3 (Ser423/425) in native and acidosis-adapted HT-29 cells (with or without treatment with 4 ng/ml TGF-β2 for 6

hours). (**k-l**) Levels of active form of TGF-β1 in conditioned media (secreted) (**k**) and in crude lysates (membrane-bound) (l) from native and acidosis-adapted HT-29 cells. (**m**) Representative immunoblotting for TSP-1 in native and acidosis-adapted HT-29 cells. (**n**) Representative immunoblotting for phosphorylated and total forms of Smad2 (Ser465/467) and Smad3 (Ser423/425) in native and acidosis-adapted HT-29 cells following treatment with 10 µM TGFβ2-specific antisense oligonucleotide Trabedersen for 7 days or 2 µM TGF-βRI inhibitor SB431542 for 24h. (**o**) Representative immunohistochemical and immunofluorescent pictures of hypoxic, LD-rich or acidic areas (using pimonidazole, Oil Red O and pHLIP markers, respectively) in subcutaneous HT-29 tumors. I directly contributed to the panels b, g, and m.

2.4 Discussion

EMT is a debated concept in oncology mostly because it is not uniformly detected in every metastatic cancer and its contribution to the invasion-metastasis cascade remains influenced and thus confused by the mutation load of primary tumor cells, in particular for the final step of host tissue colonization [374]. Also, contrary to EMT occurring during embryonic development, mesenchymal transition is generally not fully executed in cancer cells. Partial (or incomplete) EMT is actually thought to facilitate the necessary reversion to an epithelial phenotype in order to resume proliferation at the metastatic sites [375, 376]. This plasticity may account for part of the misperception about the absolute requirement of EMT for cancer progression but also brings an interesting perspective on the role of the microenvironment of primary tumors [377, 378]. One may indeed speculate that TME peculiarities trigger the phenotypic shift required to increase cell motility and initiate invasion but are *de facto* unable to maintain it when cells have left the primary site, thereby facilitating the reverse transitioning when facing a new "physiological" distant environment. Here, we identified the formation of lipid

droplets in response to tumor acidosis as a major actor of the shift towards a transitory mesenchymal-like, invasive cancer cell phenotype.

Our study pinpoints TGF-β2 as the main driver of the lipid-based metabolic rewiring fostered by tumor acidosis and required to support the energy needs of invading cancer cells. While several studies have identified a role of lipids in EMT [287, 379-381], our study tackles this issue by integrating the TME concept (i.e. tumor acidosis). We previously reported how cancer cells chronically exposed to an acidic pH progressively abandon glycolysis in favor of FAO [343]. Now, we show that this acidosis-guided metabolic preference is dependent on TGF-β2 and further complemented by the formation of LD acting as energy stores that are used to support anoikis resistance and invasiveness. Moreover, we provide evidence that stimulation of FA uptake and oxidation directly supports TGFβ2-induced EMT by increasing the acetyl-CoA pool which in turn promotes the acetylation of Smad2, a PTM associated with an increased activity of this transcription factor [372]. These findings underly a major difference with hypoxia, another TME hallmark also known to promote LD formation [382]. Indeed, the lack of O_2 prevents β-oxidation to occur from LD-released FA under hypoxia and as previously documented by Bensaad and colleagues[382], tumor reoxygenation is required for invasive cancer cells to exploit internal FA stores. The specificity of acidosis is that cancer cells may accumulate FA within LD to reduce lipotoxicity but with the concomitant transition towards the mesenchymal phenotype they may also directly take advantage of these internal FA stores to generate energy for efficient metastatic spreading.

Expressions of both CD36 and DGAT1, the main entry path for FA in the cytosol and the final actor of their accumulation as neutral lipids respectively, are regulated by TGF-β2, either produced by acidosis-adapted cancer cells or upon exogenous addition of the growth factor on native cancer cells. We identified the

upregulation of TSP-1 in response to extracellular acidosis as a critical actor of integrin-independent TGF-β2 activation. TGF-β2 indeed lacks an integrin-binding RGD sequence in its latency-associated peptide and instead requires TSP-1 to be converted in its mature form [363]. Increase in the active form of TGF-β2 was detected in acidosis-adapted cancer cells derived from various tissues and TGF-β2 upregulation was reproduced in native cancer cells acutely exposed to an acidic pH (Fig. 23a-c). We further documented a positive feedback loop wherein TGF-β2 transcription is stimulated by TGF-β2 itself, thereby reinforcing TGF-β2 signaling under acidosis. Remarkably, this mode of autocrine, isoform-specific TGF-β2 activation in cancer cells differs from that described in models where a reactive stroma leads to TGF-β secretion [383-385] or where excess free FA uptake itself promotes TGF-β signaling to initiate EMT [381]. In our study, we provide evidence that addition of exogenous TGF-β2 on native cancer cells led to both neutral lipid accumulation and LD formation and that inhibition of TGF-β2 signaling in 3D spheroids undergoing spontaneous acidification dramatically prevented LD accumulation (Fig. 26f-h). Of note, TGF-β1 was reported to shift cell metabolism from FA synthesis to enhanced oxidative phosphorylation [380]. Whether, in the latter study, FA uptake was increased leading to LD formation was however not addressed. Although, based on the well-known shared signal transduction pathways induced by the three TGF-β forms, we cannot exclude this possibility, TGF-β2 was in our study the only TGF-β isoform induced in response to ambient acidosis. Thus, collectively, our results allow to propose a model wherein acidosis, by promoting autocrine TSP-1-dependent TGF-β2 activation, triggers signaling pathways driving the shift towards a mesenchymal-like invasive phenotype from one hand, and supporting fatty acid uptake, oxidation but also storage in LD from the other hand. Each arm reinforces each other since FA oxidation favors Smad2 acetylation/activity and thereby supports EMT while the *bona fide* EMT

transcription factor ZEB1 is necessary for LD formation; ZEB-1-driven TGF-β2 expression [386] may actually account for the capacity of TGF-β2 to promote its own gene expression.

Importantly, we documented the druggability of this intrinsic alteration of the cancer cell phenotype with SB431542, a potent and specific inhibitor of TGF-β superfamily type 1 receptor, and AP12009/Trabedersen, a FDA- and EMEA-approved orphan anticancer drug, active as a TGF-β2-specific antisense oligodeoxynucleotide. While TGF-β2 was identified as an attractive target to block oncogenesis resulting from stem cell renewal [387] and encouraging survival results have been reported with Trabedersen in gliomas [364] and pancreatic cancers [365, 366], inhibitors of TGF-β2 signaling may actually represent a therapeutic strategy with a broader potential of reducing metastatic burden. Potential therapeutic targets may also be derived from the observation that LD represent a non-dispensable source of fuels to support anoikis resistance, thereby increasing the survival of cancer cells in the bloodstream and thus facilitating metastatic take. We showed for instance that preventing LD formation in cancer cells facing an acidic pH with a DGAT1 inhibitor represents an achievable goal to limit invasion, offering a rationale for the repurposing of such drugs currently under clinical evaluation for the treatment of type 2 diabetes and obesity [388]. We also found that mouse survival was significantly reduced after injection of acidosis-adapted cancer cells (*vs.* native cancer cells) and that pre-treatment to remove LD from pH 6.5-adapted cancer cells or acute treatment to prevent the oxidation of FA released from these LD considerably reduced their capacity to form metastases. Together with our data on the supportive role of LD in anoikis resistance and local cancer cell invasion, these findings also offer a rationale for the development of drugs inhibiting the mobilization of FA (*e.g*. atglistatin) to reduce metastatic spreading by preventing the use by cancer cells of the energy stored in preformed LD; the blockade of

triglyceride lipase is all the more relevant as it can also interfere with (tumor-induced) release of FA from adipocytes to fuel cancer cell LD [389]. Finally, our observation of a functional CD36 upregulation in response to TGF-β2 is reminiscent of the reported role of CD36 in metastasis-initiating CD44-positive cells in human oral carcinoma [390]. Although CD36-expressing cells in the above study could not be related to EMT, we provide evidence that neutralizing anti-CD36 antibodies, used by these authors to impair metastasis, could also prevent LD formation in acidosis-adapted cancer cells, making this strategy particularly suited to prevent TGF-β2-driven tumor progression.

In conclusion, the identification of an autocrine TGF-β2-LD axis led us to expand on the driving role of acidosis on metabolic adaptation in cancer cells but importantly to identify new prophylactic and therapeutic perspectives to reduce metastatic burden and thereby extend cancer patient survival.

2.5 Methods

Cell culture

Human cervix SiHa (#HTB-35), pharynx FaDu (#HTB-43) and colorectal HCT-116 (#CCL-247) and HT-29 (#HTB-38) cancer cell lines and the normal human breast epithelial cell line MCF-10A (#CRL-10317) were purchased from ATCC. Cells were stored according to the supplier's instructions and used within 6 months after resuscitation of frozen aliquots. All cell lines were maintained in DMEM supplemented with 10% heat-inactivated FBS, 10 mM D-glucose, 2 mM L-glutamine and 25 mM of both PIPES and HEPES before adjusting pH to 7.4 or 6.5. Acidic pH-adapted tumor cells were established as previously described [34, 343]. All cell lines

were tested for mycoplasma contamination with the MycoAlert™ Mycoplasma Detection kit (#LT07-318; Lonza) before being used. GFP-expressing native and mCherry-expressing acidosis-adapted HT-29 cancer cells were established by infection with eGFP Lentifect™ (#LPP-EGFR-LV105-205; GeneCopoeia) and mCherry Lentifect™ (#LPP-MCHR-LV105-025; GeneCopoeia) purified lentiviral particles according to manufacturer's instructions.

Cell treatment and transfection

Cell treatment was performed in a full culture medium with 4 ng/ml recombinant human TGF-β2 (#ab84070; Abcam), 1 µM EX-527 (E7034; Sigma-Aldrich), 10 µM GW6471 (#4618; Tocris), 2 µM SB431542 (#1614; Tocris Bioscience), 10 µM Trabedersen (Eurogentec), 10 µM PKC-ζ pseudo-substrate inhibitor (sc-397537; Santa Cruz Biotechnology), 2 µg/ml JC63.1 (ab23680; Abcam), or 1 µg/ml FA6-152 (ab17044; Abcam) anti-CD36 blocking antibodies at different timings, as indicated in the figure legends. To study lipid droplet biogenesis, cells were first treated with 10 µM forskolin (#F3917; Sigma-Aldrich) for 24h in a medium supplemented with 10% charcoal-stripped FBS (#F6765; Sigma-Aldrich) to induce lipolysis. After extensive washing, cells were then incubated for 24h with either a medium supplemented with 10% charcoal-stripped FBS in absence or presence of a chemically-defined lipid concentrate (#11905031; Thermo Fisher Scientific) or with a medium supplemented with 10% lipoprotein-deficient FBS (#S5394; Sigma-Aldrich). A medium supplemented with 10% normal FBS (#F7524; Sigma-Aldrich) was also used for cell treatment with 15 µM A922500 (#A1737), 10 µM atglistatin (#SML1075), 5 µM avasimibe (#PZ0190), 20 µM BPTES, 10 µM PF-06424439 (#PZ0233) and 1 µM simvastatin (#S6196). All inhibitors were from Sigma-Aldrich, except BPTES that was synthesized and purified in our lab, as previously described [34]. For cell growth assays, oleic acid (#10-1801; Larodan) was conjugated to BSA

and added at 50 µM in culture medium for 72h. In some conditions, cells were maintained at 37°C in normoxic conditions (20% O_2, 5% CO_2) or exposed to hypoxia (1% O_2, 5% CO_2) in an Invivo2 300 hypoxia chamber (Ruskinn). Cell growth was assessed by using the PrestoBlue® cell viability reagent (#A13262; Thermo Fisher Scientific) according to manufacturer's instructions. Cell transfection with a non-targeting pool of 4 siRNA sequences (D-001810-10-05) or a pool of 4 siRNA sequences targeting either human *PLIN2* (#L-019204-01), human *SMAD2* (#L-003561-00), human *SMAD3* (#L-020067-00), human *TSP-1* (*THBS1)* (L-019743-00) or human *ZEB1* gene (L-006564-01), all from Dharmacon, was carried out with Lipofectamine™ RNAiMAX transfection reagent (#13778150; Thermo Fisher Scientific), according to manufacturer's instructions.

Gene expression analysis in patient samples

Comparison of expression patterns for *TGFB2*, *PLIN1*, *PLIN2* and *PLIN3* genes was performed in colorectal and renal datasets using ONCOMINE data-mining platform (https://www.oncomine.org). Sixty-five rectal adenocarcinomas and their paired normal rectal mucosa samples [391] as well as 32 clear cell renal cell carcinoma and 23 normal kidney samples [392] were analyzed for gene expression. Log2 median-centered intensity was used to show the (over)expression of selected genes in tumor samples vs normal samples. Of note, colors used in the chart are z-score normalized to depict relative values within rows. They cannot be used to compare values between rows.

RNA sequencing data analysis

Total RNA was extracted using the Maxwell RSC SimplyRNA tissue kit (#AS1340; Promega) according to manufacturer's instructions including a DNAse treatment. RNA quantity and quality were evaluated with a Nanodrop 1000 spectrophotometer (Thermo Fisher Scientific) and RNA 6000 nano chips on a

Bioanalyzer 2100 system (Agilent), respectively. RNA sequencing (RNA-Seq) analysis was performed by the VIB Nucleomics Core (Leuven, Belgium). Briefly, samples (biological triplicates) were prepared with the TruSeq RNA Library Prep Kit v2 (#RS-122-2001; Illumina) from 2 µg RNA and sequencing was performed using the NextSeq 500 High Output Kit V2 (75 cycles; Illumina) with single end reads all according to manufacturer's recommendations.

Quality filtering was performed using FastX toolkit 0.0.13 (http://hannonlab.cshl.edu/fastx_toolkit/index.html) and ShortRead 1.16.3. Low quality ends with <Q20 were trimmed and reads shorter than 35 bases after trimming were discarded. Further adapter trimming was performed using Cutadapt 1.7.1. Adapters were trimmed only at the end with at least 10 bases overlap and 90% match. Poly-A reads (more than 90% of the bases equal A), low quality reads (more than 50% of the bases <Q25) and artifact reads (all but 3 bases in the read equal one base type) were all discarded. Reads matching Illumina PhiX sequencing controls were removed following alignment using Bowtie 2.2.4. Sequences were mapped to the human reference genome (GRCh37.73) with TopHat V2.0.13 (https://ccb.jhu.edu/software/tophat/index.shtml) with parameters set; library-type-firststrand, min-intron-length 50, max-intron length 500000, no-coverage-search, no-mixed, read-realign-edit-dist 3. Using SAMtools 1.1, reads that were non-primary mappings or had mapping qualities of 20 or lower were removed from the alignment. Reads overlapping with gene features were identified using FeatureCounts 1.4.6 with parameters set at –Q 0 –s 2 –t exon –g gene_id. Reads that could be attributed to more than one target or not be attributed to any gene were omitted. Gene-segments for which all samples had less than 1 count per million reads, were removed (44602). To correct for GC-content, full quantile normalization was applied on bins of GC-content with the EDASeq Bioconductor package. Correction for library size and RNA composition was performed using full

quantile normalization with the EDASeq package. For generating the heatmap, relative gene expression Z-scores were subjected to unsupervised clustering using Cluster 3.0 (http://bonsai.hgc.jp/~mdehoon/software/cluster/) by single linkage uncentered correlation clustering of both genes and samples at default settings. The heatmap of obtained cluster data was generated using GraphPad Prism 7 software. Acidosis-regulated genes were classified, according to their cellular function, by KEGG pathway term analysis using DAVID v6.8 software (http://david.abcc.ncifcrf.gov/).

Oil Red O staining

Cells grown on coverslips were fixed with 4% (wt/vol) paraformaldehyde (PFA) for 10 min before staining with 3 mg/ml Oil Red O solution in 60% (vol/vol) isopropanol for 20 min. After nuclear counterstain with hematoxylin, bright-field images were acquired at 63x magnification using an AxioImager.z1-ApoTome1 (Zeiss) and lipid droplet area per cell was evaluated with Fiji software.

Acetyl-CoA measurements

Acetyl-CoA concentration in cellular extracts was determined by using the PicoProbe Acetyl-CoA assay kit from Abcam, according to manufacturer's instructions.

RNA extraction and RT-qPCR

Samples were collected from an equal number of intact cells in TRI Reagent® (#TR118; Molecular Research Center). RNA was recovered after separation in 1-bromo-3-chloropropane and precipitation with isopropanol, washed with ethanol (70%), resuspended in RNAse-free water, and then quantified by spectrophotometry (Nanodrop 1000, Thermo Fisher Scientific). After reverse transcription on 500 ng of total RNA with the RevertAid Reverse-Transcriptase,

oligo-dT and random hexamers (Thermo Fisher Scientific), quantitative PCR amplification was performed on a ViiA™ 7 real-time PCR system (Applied Biosystems) using Takyon Low Rox SYBR® MasterMix dTTP Blue (#UF-LSMT-B0701; Eurogentec). Relative gene expression was calculated using the ddCt method, with *GTF2B* as reference gene. Gene-specific primers used in this study are listed in Table S3.

Supplementary Table 3. Sequences of gene-specific primers for qRT-PCR used in this study.

Gene name	Forward primer (5' – 3')	Reverse primer (5' – 3')
CDH1	TCACCACTGGGCTGGACCGA	TACAGCCTCCCACGCTGGGG
CDH2	CGAGCCGCCTGCGCTGCCAC	CGCTGCTCTCCGCTCCCCGC
DGAT1	CAACTACCGTGGCATCCTG	TTCTCCAGAAATAACCGGGC
DGAT2	CTGCACTGATTGCTGGCTCATCG	GAAAGTAGCGCCACACAGCCCAG
GTF2B	ACTACAGAGCCGGTGATATGAT	GTTGCTTTGTCATTGCTGAAAGT
PLIN1	CTCTCGATACACCGTGCAGA	TGGTCCTCATGATCCTCCTC
PLIN2	CTGCTCACGAGCTGCATCATC	TGTGAGATGGCAGAGAACGGT
PLIN3	GCTGGACAAGTTGGAGGAGA	CCGACACCTTAGACGACACA
PLIN4	TGCTGCAGAATGAGTTGGAG	GACCCAGGTCACCTAAACGA
PLIN5	AGCTTCCCTTTCTCCAGCAACCTT	AGTGATCCACCAGCTCCTCTGATT
SNAIL1	AATCCAGAGTTTACCTTCCAGCA	TCCCAGATGAGCATTGGCAG
SNAIL2	GAACTGGACACACATACAGTGAT	ACAGTGATGGGGCTGTATGC
TGFB2	TGTCCCTGCTGCACTTTTGTA	GGTGCCATCAATACCTGCAAATC
TGFBR1	GGCCAAATATCCCAAACAGA	TGATGCCTTCCTGTTGACTG
ZEB1	GCCCAAACTGCAAGAAACGC	GTCGCCCATTCACAGGTATCA

Immunocytochemistry

Cells grown on coverslips were fixed with 4% PFA for 10 min. After blocking with 5% BSA for 1h, cells were incubated overnight at 4°C with anti-E-cadherin and anti-vimentin antibodies (#14472 and #5741, respectively; Cell Signaling Technology). Cells were then incubated with Alexa Fluor 488- and 568-conjugated anti-rabbit secondary antibodies (#A11034 and #A11036, respectively; Thermo Fisher Scientific) for 1h and nuclei were counterstained with DAPI. For neutral lipid staining, PFA-fixed cells were incubated with 0.5 µg/ml BODIPY 493/503 (#D3922; Thermo Fisher Scientific) for 30 min at room temperature. Slides were prepared with a fluorescence mounting medium (Dako) and staining was visualized with a Zeiss Imager 1.0 Apotome microscope.

ELISA anti-TGFβ1/2

Active human TGF-β1 and TGF-β2 protein levels were assessed by using dedicated ELISA detection kits (#DB100B and #DB250, respectively; R&D Systems) following the manufacturer's instructions with some modifications. Indeed, samples (conditioned media or cell lysates) were not activated by acid treatment; this modified protocol allowed us to determine the levels of "naturally" active TGF-β, without the fraction of latent TGF-β being "artificially" activated to an immunoreactive form with the acid treatment.

Western blot analysis

Protein samples were denatured for 5 min at 95°C with Laemmli sample buffer containing 10% 2-mercaptoethanol. Samples (20 µg per well) were then loaded onto 8 to 15% acrylamide/bis-acrylamide gels and SDS-PAGE was carried out as previously described [34]. Nitrocellulose membranes were blocked with 5% BSA for 1h at RT. Primary antibodies against BiP (#3177), CPT1A (#12252), E-cadherin

(#3195), N-cadherin (#13116), phospho-Smad2 (#3108); phospho-Smad3 (#9520), Smad2 (#5339), Smad3 (#9523), Smad2/3 (#8685), Snail (#3879), vimentin (#5741), ZEB1 (#3396), and ZO-1 (#8193), all from Cell Signaling Technology, were applied at 1:1,000 in 5% BSA overnight at 4°C. Anti-actin (#A5441; Sigma-Aldrich; 1:1,000), anti-CD36 (#100011; Cayman Chemical Company; 1:1,000), anti-DGAT1 (#ab54037; Abcam; 1:1,000), anti-HSP90 (#610419; BD Biosciences; 1:2,000), anti-perilipin 1 (#ab3526; Abcam; 1:1,000), anti-perilipin 2 (ab78920; Abcam; 1:1,000), anti-perilipin 5 (#PA1-46215; Thermo Fisher Scientific; 1:1,000), HRP-conjugated streptavidin (#SA10001; Thermo Fisher Scientific; 1:25,000) and anti-TSP1 (ab85762; Abcam; 1:1,000) antibodies were also applied in 5% BSA overnight at 4°C. In some experiments, cell lysates (1 mg) were first pre-cleared with 5 µg rabbit IgG (#02-6102; Thermo Fisher Scientific) and 30 µl Dynabeads Protein G (#10003D; Thermo Fisher Scientific) for 1h, at 4°C on an end-to-end roller, and then incubated with 5 µg anti-acetylated lysine (#9441; Cell Signaling Technology) or rabbit IgG (overnight, 4°C). Immunoprecipitated proteins were pulled down after incubation with 30 µl Dynabeads Protein G (2h, 4°C) and then eluted with 60 µl Laemmli 2X.

Palmitate uptake assays

Palmitate uptake in native and acidosis-adapted SiHa cells was assessed by two different assays. In the first assay, cancer cells were incubated for 10 min at 37°C in culture medium containing 50 nM ^{14}Cpalmitate (#NEC534050UC; PerkinElmer). Radioactivity was determined in a microplate counter (PerkinElmer Topcount) and raw counts were normalized with the protein content in each well. In the second assay, the culture medium was removed and the cells were washed with PBS before being incubated with 0.2 µM BODIPY™ FL C_{16} (#D3821; Thermo Fisher Scientific) for 15 min at RT. Cells were washed three times with ice-cold PBS and fixed with 4% PFA for 30 min at RT. To determine FA uptake, cells were analyzed by flow

cytometry using the FL1-FITC channel (BD FACSCanto™ II; BD Biosciences). Data were analyzed with the FlowJo v10 software.

Oxygen consumption rate measurements

Oxidation of exogenous fatty acids, by native and acidic pH-adapted cells, was assessed by treating the cells with 50 µM BSA-conjugated palmitate in a substrate-limited medium. Oxygen-consumption rate (OCR) was measured using the Seahorse XF96 plate reader (Agilent Technologies). Palmitate-induced OCR was evaluated by calculating the difference of OCR values before and after palmitate addition in each experimental condition.

3D spheroid models

Spheroids were prepared and processed as previously described [393]. Briefly, HT-29 cells (1,500 cells/well) were seeded in Ultra-Low Attachment 96-well plates (Corning) in DMEM supplemented with 10% heat-inactivated FBS, 10 mM D-glucose and 2 mM L-glutamine. For immunohistochemical studies, spheroids were incubated for 24h with 2 µM Alexa Fluor 568-conjugated pH-low insertion peptide variant 3 (pHLIP V3; NH_2-ACDDQNPWRAYLDLLFPTDTLLLDLLW-COOH; [394]) to label acidic regions. Spheroids were then washed twice in PBS, fixed in 4% PFA, harvested and embedded in OCT. Frozen sections (5 µm) were stained with either BODIPY™ 493/503 (#D3922; Thermo Fisher Scientific) or anti-Ki67 antibody (#556003, BD Biosciences). Sections were incubated with Alexa Fluor 568-conjugated anti-mouse secondary antibodies (#A11031; Thermo Fisher Scientific), and nuclei were counterstained with DAPI. Slides were prepared with fluorescence mounting medium (Dako), and staining was visualized with a Zeiss Imager 1.0 Apotome microscope. All spheroid samples from a same experiment were imaged by using the same gain and exposure settings.

In vivo mouse experiments

All experiments involving mouse xenograft and experimental metastasis models received the approval of the ethic committee from the Université Catholique de Louvain (approval ID 2016/UCL/MD018) and were carried out according to national care regulations. All experiments were performed with 7-week-old female Rj:NMRI-*Foxn1*$^{nu/nu}$ mice from Janvier Labs. Before injection, tumor cells (unlabeled, GFP- or mCherry-expressing) were washed twice with PBS, resuspended in 0.9% NaCl (1.10^6 cells or 2.10^6/100 µl for i.v. or s.c. injection, respectively) and then injected into the tail vein or the right flank of the animals. In some experiments, mice were treated i.p. with 40 mg/kg etomoxir (Tocris) for 6 days, including one day before cell injection. Long-term mouse survival was then evaluated or the number of metastases was determined 5 weeks post-injection using hematoxylin/eosin (H&E) staining or immunohistochemistry with anti-GFP (#NB600-308; Novus Biologicals) or anti-mCherry (ab167453; Abcam) antibodies on sections from embedded lung samples (nine to eleven sections were evaluated per lung). Pimonidazole (60 mg/kg) and pHLIP-AF568 (40 µM) were injected i.v. 24h or 6h before tumor resection, respectively and staining on tumor sections (pimonidazole, pHLIP, Oil Red O) was carried out on acetone-fixed samples as previously described [393]. Images were acquired by using a slide scanner (SCN400; Leica) and analyzed with Author 2017.2 software (Visiopharm®).

Cell-surface protein biotinylation

Biotinylation of cell-surface proteins was performed as previously described [395] with minor modifications. Briefly, subconfluent cells were rinsed twice with ice-cold biotinylation buffer (PBS, 1 mM $CaCl_2$, 0.5 mM $MgCl_2$), and then incubated (30 min, 4°C) with 1 mg/ml EZ-Link™ Sulfo-NHS-SS-biotin (#21331; Thermo Fisher Scientific) to label membrane proteins. After quenching of free biotin with 0.1 M glycine (30

min, 4°C) two washes with ice-cold biotinylation buffer, cells were lysed for protein extraction. Biotinylated proteins were then isolated by immobilization on a streptavidin agarose resin (#20347; Thermo Fisher Scientific) for 2h at 4°C. Beads were washed three times (lysis buffer, 4°C) and eluted in Laemmli sample buffer containing 10% 2-mercaptoethanol (5 min, 95°C).

Invasion assays

Invasion assays were performed in 12-well Transwell microchambers (Corning) with 8 µm pore-sized membranes, coated with growth factor-reduced Matrigel (#356231; Corning). Cells ($1x10^5$/well for SiHa and FaDu; $2x10^5$/well for HCT-116 and HT-29) were seeded, in the upper chamber of the transwells, in 0.1% FBS-containing medium, in presence or not of the treatments. In some conditions (as described in figure legends), BSA-conjugated oleate and palmitate (25 µM of each; #10-1801 and #10-1600, respectively; Larodan), 15 µM A922500, 10 µM atglistatin or 30 µM etomoxir were added in the upper chamber for the time of the invasion assay (24h). Otherwise, cancer cells were pre-incubated with 100 µM CCCP or 1 µg/ml oligomycin for 30 min before starting the assay. All inhibitors were purchased from Sigma-Aldrich. A medium containing 10% FBS was added in the lower chamber and the cells were allowed to invade for 24h at 37°C. The transwell membranes were then fixed with ice-cold methanol and stained with DAPI. Cells that had not invaded through the chamber were removed with a cotton swab. Invading cells were imaged by fluorescence microscopy with the Axiovert 100 (CarlZeiss) (excitation filter G365 and emission filter Band Pass 445/50), and four fields were independently counted from each invasion chamber.

Anoikis resistance assays

Anoikis resistance was determined by incubating cancer cells on low attachment, hydrophobic 100 mm-plates (#82.1472.001, Sarstedt) either in a static or dynamic

mode, the latter being obtained by slight shaking of the plate within the incubator. Cells under suspension after 24h incubation were collected by centrifugation and adherent cells were detached with trypsin (# 25300-054, Life Technologies) for cell counting (Cellometer, Auto T4 Bioscience).

Lipidomic analysis

Lipids were extracted from subconfluent cells following the Folch method with subsequent modifications. Briefly, cells were suspended in PBS and lipids were extracted with chloroform:methanol (1:2, v/v) (VWR Chemicals). Samples were then dried under a stream of nitrogen at 30°C and resuspended in chloroform. Dosage of cholesterol esters was carried out using the Amplex™ Red Cholesterol Assay kit (#A12216; Thermo Fisher Scientific) according to manufacturer's instructions. Gas chromatography (GC) analysis of fatty acid methyl esters (FAME) was also performed after lipid extraction. Tridecanoic acid, 1,2-dipentadecanoyl-sn-glycero-3-phosphatidylcholin and triheptadecanoin (Larodan) were used as internal standards for free fatty acids, phospholipids and triglycerides quantification, respectively. Solid phase extraction was performed on Bond Elut aminopropyl-modified cartridges to successively retrieve the neutral lipid fraction (triglycerides, diglycerides, monoglycerides and cholesteryl esters), the free fatty acid fraction, and the phospholipid fraction. Extracted fatty acids were converted into FAME via methylation under alkaline conditions (KOH 0.1 M in methanol, at 70°C for 1 hour) and then under acidic conditions (HCl 1.2 M in methanol, at 70°C for 20 min). FAME were then separated by GC with a GC Trace 1310 (Thermo Fisher Scientific) equipped with a RT2560 capillary colum (100 m x 0.25 mm internal diameter; 0.2 µm film thickness; Restek), an "on-column" automatic injector (CTC Analytics AG) and a flame ionization detector kept at a constant temperature of 255°C. The system used hydrogen as the carrier gas at an operating pressure of 200

kPa. The GC temperature program was as follows: an initial temperature of 80°C which progressively increased to 175°C (for 25 min) at 25°C/min, then to 200°C (for 20 min) at 10°C/min, then to 220°C (for 5 min) at 10°C/min, and finally to 235°C (for 15 min) at 10°C/min. Each peak was identified by comparison of retention times with those for pure methyl ester standards (Larodan and Nu-Check Prep). Data processing was operated by using the ChromQuest 5.0 software (Thermo Fisher Scientific). Results are expressed in nmol FA per million of cells after data normalization with the background values, the percentage of recovery and the starting cell number.

Electron microscopy

For transmission electron microscopy (TEM), subconfluent cells were fixed for 2 h at 4°C in 2.5% (w/v) glutaraldehyde (Agar Scientific) in 0.1 M cacodylate buffer (pH 7.4). Cells were washed with cacodylate buffer and subsequently post-fixed in 1% (v/w) osmium tetroxide (Merck). Samples were dehydrated by successive passages in increasing concentrated ethanol baths (30%, 50%, 70%, 85% and 100%). After embedding in epon resin LX 112 (Ladd Research Industries), ultra-thin sections of cell-covered filters were prepared using an 8800 ultrotome III (LKB). TEM analysis was then performed at 80 keV (FEI Tecnai 10, Philips) using TEM grids (Agar Scientific) covered with non-porous formvar.

Statistical analysis

Statistical analyses were performed using GraphPad Prism 7. Two-tailed unpaired Student t-test, one-way or two-way ANOVA tests (Bonferroni's post-hoc test) were used where appropriate. For all statistical analyses, the expected variance was similar between the groups that were compared, and significance was accepted at the 95% confidence level (*$p < 0.05$, **$p < 0.01$, ***$p < 0.001$).

Data availability

The data supporting the findings of this study are available within the article and the associated Supplementary Information. The accession number for the RNA sequencing data reported in this paper is GEO: GSE116035 and can be accessed via the following link https://www.ncbi.nlm.nih.gov/geo/query/acc.cgi?acc=GSE116035. Any further information about resources and reagents should be directed to, and will be fulfilled by the corresponding authors upon reasonable request.

3. Thrombospondin 1 and CD36 translocation support acidosis-induced activation of TGF-β2 and associated increase in cancer cell migration.

Joao Pedro Santiago de Jesus, Estelle Bastien, Cyril Corbet and Olivier Feron

Pole of Pharmacology and Therapeutics (FATH), Institut de Recherche Expérimentale et Clinique (IREC), UCLouvain, 57 Avenue Hippocrate B1.57.01, B-1200 Brussels, Belgium

3.1 Summary

TGF-β-signaling regulates different cellular processes – including invasion and metastasis in the later stages of cancer. Under acidosis, elevated levels of TGF-β2 support partial epithelial-to-mesenchymal transition (EMT) and promote the accumulation of fatty acids in lipid droplets (LD). However, it is not clear how acidosis-adapted cancer cells activate TGF-β2 since contrary to latent TGF-β1 and β3, TGF-β2 does not exhibit a RGD motif allowing activation through $\alpha_v\beta$ integrins. Thrombospondin 1 (TSP-1) can however bind to latent TGF-β2 complex and through a non-proteolytic mechanism gives rise to biologically active TGF-β2 form.

We found that TSP-1 was upregulated in acidosis-adapted cancer cells and directly contributed to increased TGF-β2 signaling. Interestingly, we could also document that CD36 (a previously identified actor of LD formation) acts as an "anchor" for the TSP-1/TGF-β2 complex, leading to the polarization of the TGF-β2 release in filopodia of invading cancer cells. Finally, we provided evidence for the compartmentation of TGF-β-receptors and CD36 within lipid rafts and for the TSP-1-dependent degradation of RhoA in acid-adapted cancer cells. Altogether, these data support an exquisite polarization of TGF-β2 signaling under acidosis that supports local cytoskeleton rearrangement to support cancer cell migration.

3.2 Introduction

During the early phases of tumor development, TGF-β signaling acts as a tumor suppressor. It is required for maintenance of genomic stability, induction of replicative senescence, and suppression of telomerase activity [121, 132, 396].

However, in later phases, tumor cells overproduce TGF-β whose autocrine and paracrine actions switch into a tumor promoter stimulating tumor stimulating, among other processes, cell invasiveness and metastasis [116, 133].

Acidosis, a hallmark of the tumor microenvironment (TME), progressively develops in tumors in response of the exacerbated metabolism of cancer cells and because of a poorly efficient tumor vasculature that prevents the rapid elimination of waste products including protons (H^+) and CO_2 [1, 33, 397]. From the comparison of the transcriptomes of native and acidic pH-adapted cancer cells, we recently identified TGF-β2 among the top 20 of the most upregulated genes under acidosis [398]. We further documented how the increase in TGF-β2 favors the formation of lipid droplets (LD) and promotes EMT, the latter taking advantage of mobilization of fatty acids from LD to support the energy needs associated with anoikis resistance, local invasiveness and distant metastatic spreading.

The upregulation of TGF-β2 mRNA however does not allow to understand how TGF-β2 signaling occurs since TGF-β is generated as a latent precursor that requires the disruption of the interaction with an inhibitory peptide to give rise to the active cytokine [117, 118]. Activation of secreted latent TGF-β is actually a highly regulated event [399], making this process crucial for downstream signaling [400]. There are three different TGF-β isoforms – TGF-β1, TGF-β2 and TGF-β3 – that have similar properties *in vitro*, but distinct effects *in vivo* [209]. All isoforms can be activated by extreme pH, heat and denaturating agents like SDS and urea [209, 210]. There are different latent TGF-β activators including integrin αVβ6 and thrombospondin-1 (TSP-1) [118]. However, only LAP/TGF-β1 and LAP/TGF-β3 contain RGD sequences (Arg-Gly-Asp) that act as a recognition motif for the integrins [399] [117]. LAP/TGF-β2 is thus largely dependent on TSP-1 to be activated [401] [402].

TSP-1 differs from the other TSP molecules (TSP-2, 3, 4 and 5) because it contains a tetrapeptide (KRFK) [403] that associates with LSLK peptide of latent TGF-β [117, 404, 405]. The TSP-1/TGF-β complex is able to bind with CD36 at the cell surface [406]. The CLESH domain within CD36 actually binds to a specific sequence present in the Type 1 domain of TSP-1 [407]. The formation of the TGF-β/TSP-1/CD36 muticomplex is actually key to disrupt the non-covalent interactions between LAP and TGF-β, and thereby lead to activation of the cytokine. This mechanism is thus yet more critical for RGD-deficient TGF-β2 isoform. Also, it has the potential to initiate a feedforward loop since activated TGF-β2 can in turn promote TGF-β2 mRNA [398, 408, 409]. Interestingly, we previously reported that under acidosis CD36 was translocated into the membrane of cancer cells where it participates to the uptake of fatty acids [398]. This led us to explore the role played by TSP-1 together with CD36 in the autocrine TGF-β2 signaling and to evaluate whether this could offer new therapeutic perspectives to block the invasive potential of acid-adapted cancer cells.

3.3 Results and Discussion

Acidosis leads to a net increase in TSP-1 expression in cancer cells.

Our search for the mechanism of preferential activation of TGF-β2 under acidosis led us to examine potential changes in the expression of TSP-1, a glycoprotein known to mediate activation of latent TGF-β. We found a dramatic upregulation of active TGF-β2 in pH 6.5-adapted SiHa and HCT-116 cancer cells (named 6.5/cancer cells here below) vs. parental cancer cells maintained at pH 7.4 (or 7.4/cancer cells) (Fig. 27 a-b). We next confirmed an increased in surface expression of TSP-1 in acid-adapted cancer cells by immunocytochemistry performed on non-permeabilized cancer cells (Fig. 27c). We also evaluated whether a short-term exposure to an acidic medium could lead to a similar change in TSP-1 expression. We found that TSP-1 expression was significantly increased in SiHa cells as soon as 24h post-exposure to pH 6.5 and further increased in the next 24 hours (Fig. 27d).

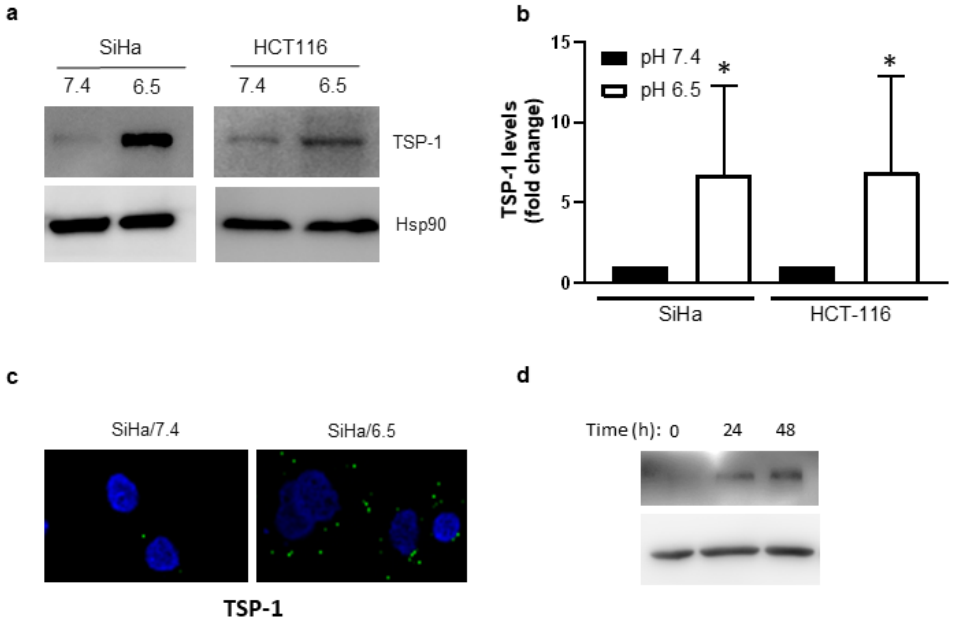

Figure 27: Acidosis promotes TSP-1 upregulation (a) Representative immunoblotting of protein thrombospondin-1 for native and acidosis-adapted SiHa and HCT-116 cancer cells and **(b)** quantification (data are represented as mean ± SEM of four independent biological experiments; *P<0.05, n=3). (**c**) Representative immunofluorescence pictures of thrombospondin-1. **(d)** Representative immunoblotting of TSP-1 in native SiHa cells exposed to acidic medium (pH 6.5) during the indicated period of time. These experiments were repeated twice with similar results.

Acidosis promotes TSP-1-mediated activation of TGF-β2 signaling in cancer cells.

We next examined whether TGF-β2 activation was directly dependent on TSP-1 in our experimental conditions. We found that TSP-1 silencing led to a dramatic reduction in the P-Smad signaling (Fig. 28a) as well as in the extent of secreted TGF-β2 (Fig. 28b). Since TGF- β2 is a critical actor of EMT, we also examined the effects of TSP-1 silencing on the expression of well-known markers of the mesenchymal phenotype. We found that the expression of both N-cadherin and vimentin was reduced upon TSP1-silencing (Fig. 28c). Moreover, using public data sets for cervix and colon cancers (corresponding to the origin of SiHa and HCT-116 cancer cells used in this study), we could identify significant correlation between the expression of TGF-β2 and TSP1 (Fig. 28d).

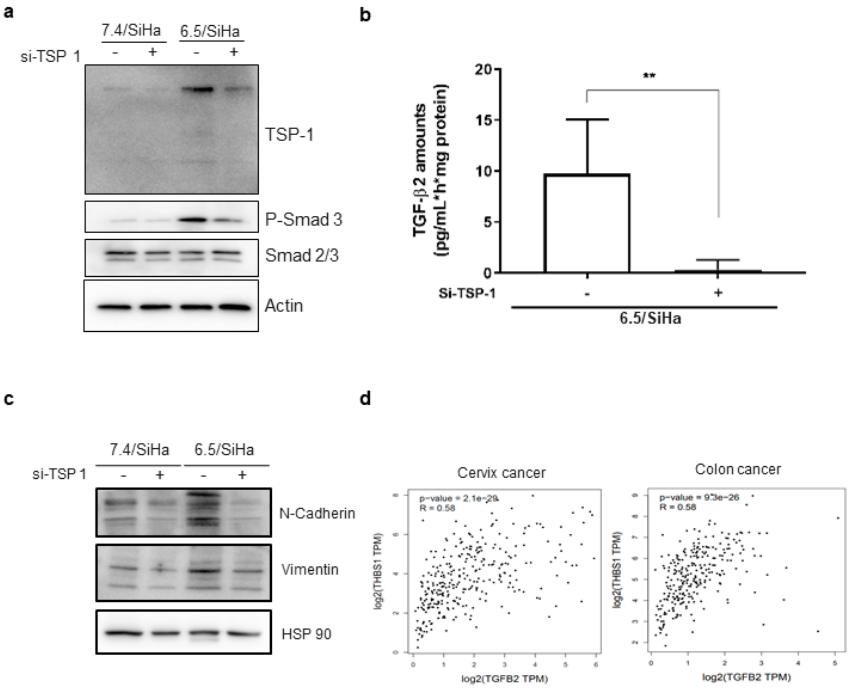

Figure 28: Acidosis-induced partial EMT and migration are reversed upon TSP-1 knock-down(a) Representative immunoblotting for TSP-1, phosphorylated Smad3 (Ser423/425) and total forms Smad2/3 from native and acidosis-adapted SiHa cells after transfection with control or TSP-1-targeting siRNA. **(b)** Levels of active form of TGF-β2 in conditioned media (secreted) from native and acidosis-adapted SiHa cells after transfection with control or TSP-1-targeting siRNA (**P<0.01, n=3). **(c)** Representative immunoblotting for N-cadherin and Vimentin from native and acidosis-adapted SiHa cells after transfection with control or TSP-1-targeting siRNA. **(d)** Correlation between *THBS1* and *TGFB2* genes in cervix and colon cancer patient samples (data extracted from GEPIA data-mining platform).

TSP-1/LAP interaction is required to support TGF-β2 signaling and cancer cell migration under acidosis.

We next explored the different protein-protein interactions potentially involved in the acid-driven TSP-1-mediated activation of TGF-β2, starting with the binding of the latent complex to TSP-1 through its central repeat type 1. In particular, the KRFK sequence within TSP-1 has been proposed to mediate the close interaction with the LSKL sequence in LAP [402, 410] (Fig. 29a). We therefore used a LSKL peptide to interfere with the binding of TSP-1 to LAP and found that it completely prevented the production of active TGF-β2 in 6.5/SiHa cancer cells while the control scramble SLLK peptide failed to do so (Fig. 29b). Inhibition of phospho-Smad signaling was also observed upon the addition of LSKL peptide but not SLLK peptide (Fig. 29c-d). We next aimed to document the functional role of TSP-1 in TGF-β2 signaling under acidosis. We found that LSKL peptide (but not control SLLK peptide) could abrogate the increased migratory capacity of 6.5/SiHa cancer cells (vs. parental cancer cells) (Fig. 29e). Although 6.5/HCT116 cancer cells showed a lesser migratory capacity than 6.5/SiHa cancer cells, we found a similar inhibition of the migrating potential upon exposure to LSKL peptide (Fig. 29f). Although it does not completely eliminate it, low FBS percentage (0.1%) limits the proliferation of cells during the migration process.

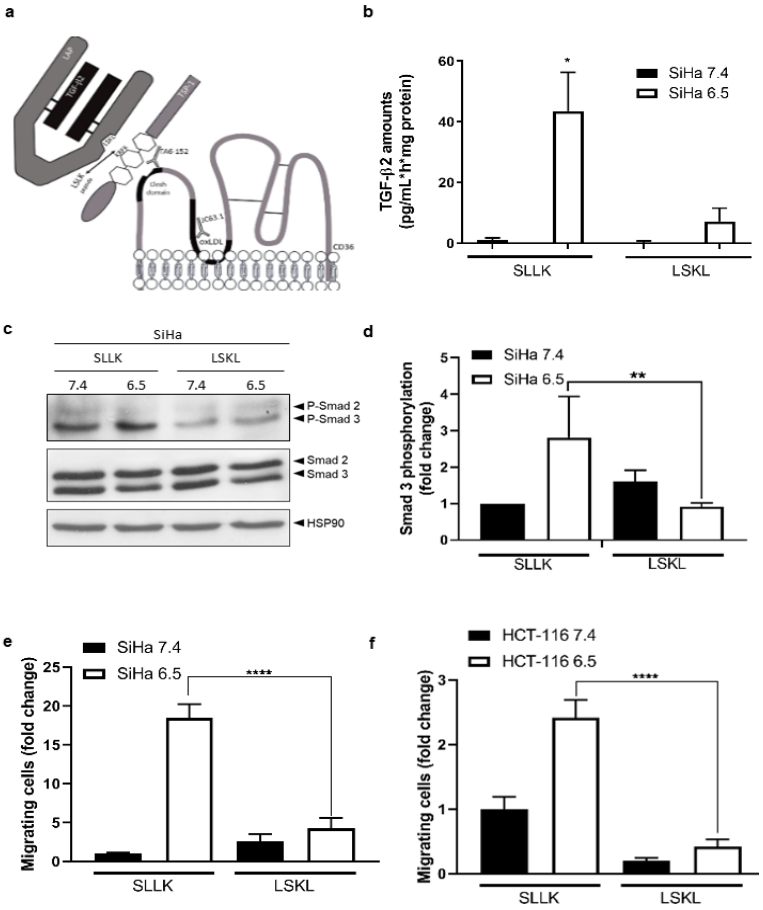

Figure 29: TSP-1 activates TGF-β2 and TGF-β2/TGF-βRI signaling pathway. **(a)** Schematic representation of the interactions between TSP-1 and both LAP-TGF-β2 and CD36. The sequence KRFK present on type 1 central repeat of TSP-1 (represented with hexagon) can connect with LAP through LSKL sequence [402, 410]. This binding can be inhibited by LSLK peptide (vs. SLLK used as a control peptide). The clesh domain of CD36 can bind to motif CSVTCG [407] present on TSP-1 type 1 central repeat. FA6-152 and JC.163 are functionally neutralizing anti-CD36 antibodies targeting the clesh domain and the oxLDL binding site, respectively [411, 412]. **(b)** Levels of active form of TGF-β2 in conditioned media (secreted) from native and acidosis-adapted SiHa cells upon treatment with SLLK or LSKL petides for 4 hours (*P<0.05, n=3). **(c)** Representative immunoblotting for phosphorylated and total forms of Smad 2 (Ser465/467) and Smad 3 (Ser423/425) from native and acidosis-adapted SiHa cells upon treatment with SLLK or LSKL peptides and **(d)** quantification (**P<0.01, n=3). **(e-f)** Migration potential of native and acidosis-adapted SiHa (**e**) and HCT-116 **(f)** cells upon treatment with SLLK or LSKL peptides (****P<0.001, n=3).

TSP-1/CD36 interaction supports the increase in the migratory potential of acid-adapted cancer cells.

In another series of experiments, we explored the potential role of CD36 in the above process of TGF-β2 activation. CD36 is indeed a membrane receptor for TSP-1 [407, 413, 414] and we have recently documented that acidosis was associated with an increase in fatty acid uptake (giving rise to intracellular lipid droplets) through CD36. The sequence YRVRFLAKENVTQDAEDNC present in the clesh domain of CD36 was reported to bind TSP-1 central repeat type 1 (ie, a sequence different from that involved in the interaction with TGF-β2,)[407] (see Fig. 29a). We first performed co-immunoprecipitation experiments using anti-TSP1 antibodies and confirmed the presence of an increased amount of CD36 in the TSP1 precipitates (Figs. 30a-b). Using PLA technology, we could similarly document the preferential co-localization of CD36 and TSP-1 in acid-adapted cancer cells (Fig. 30c-d). To further explore the functional role of CD36/TSP-1 interaction in acid-adapted cancer cells, we took advantage of an antibody directed against the clesh domain of CD36 (ie, FA6-152 clone) [411]. We first showed that this antibody could prevent the interaction between TSP-1 and CD36 as revealed by the net reduction in PLA signal (Figs. 30c-d). We next evaluated whether preventing TSP-1 interaction with CD36 could prevent the increased migratory capacity of acid-adapted cancer cells. Using the anti-CD36 clesh domain blocking antibody, we found a dramatic reduction in the invasive capacity of acid-adapted SiHa and HCT116 cancer cells. The failure of another antibody directed against the oxidized low-density lipoprotein (oxLDL) site within CD36 (ie, JC63.1 clone) to block cell migration allowed us to exclude that an indirect effect on fatty acid metabolism could account for the observed effects [411, 415] (Figs. 30e-f).

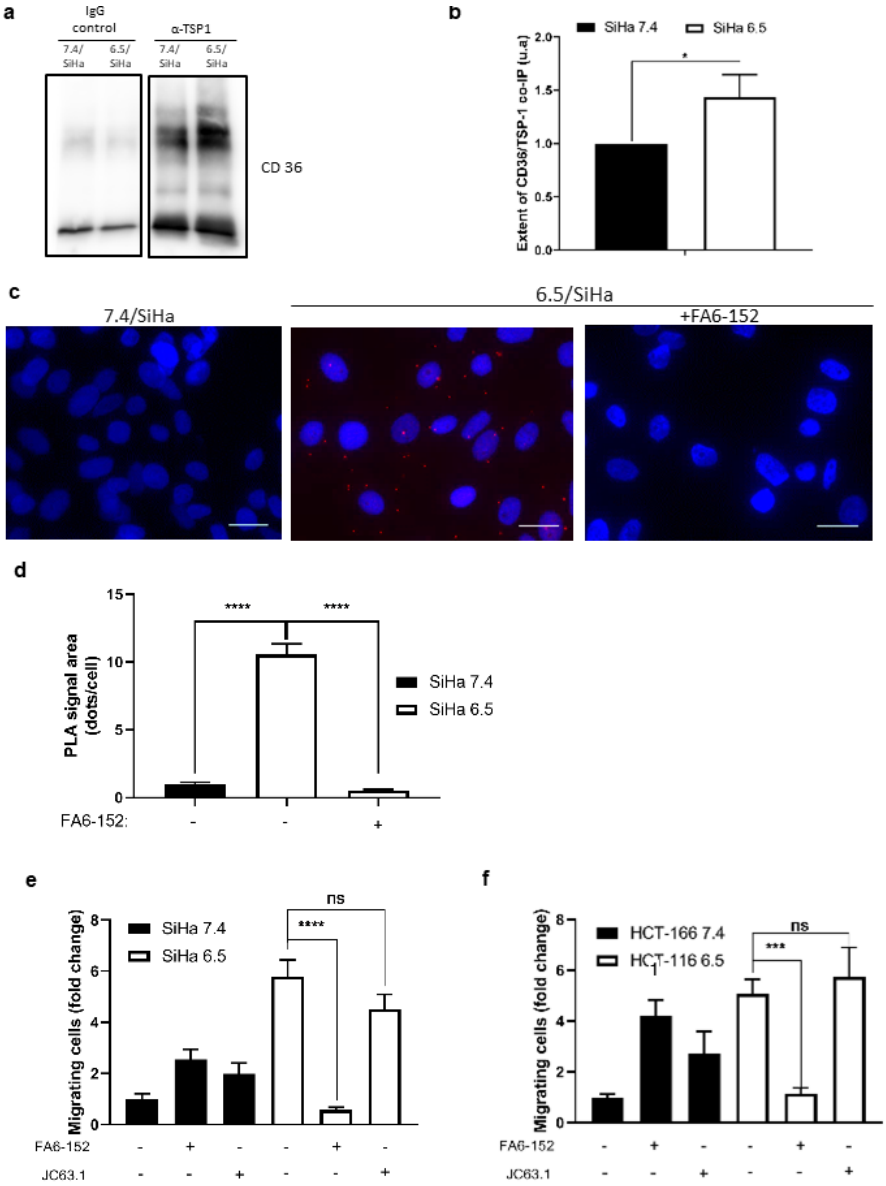

Figure 30: CD36 interaction with TSP-1 in the membrane of acidosis adapted cells is responsible for acidosis-adapted cell migration. (a) Representative CD36 immunoblotting of TSP-1 immunoprecipitates (*vs.* control IgG IP) from native and acidosis-adapted SiHa cells and **(b)** quantification ($p<0.05$, n=3). **(c)** Representative pictures of proximity ligation assay (in red) using CD36 and TSP-1 antibodies in native and acidosis-adapted SiHa cells upon exposure to FA6-152 antibody and **(d)** quantification (****P<0.001, n=3). **(e-f)** Migration potential of native and acidosis-adapted cells SiHa (**e**) and HCT-116 (f) cancer cells upon exposure toe either FA6-152 or JC63.1 antibodies (***P<0.005, ****P<0.001, ns = non-significatnt; n=3).

Lipid raft compartmentation of CD36 and TGF-βR1 supports the migration of cancer cells under acidosis.

The above experiments indicated a preferential activation of TGF-β2 by TSP-1 immobilized on CD36, itself preferentially expressed at the cell surface of acid-adapted cancer cells. In parallel, the analysis of the location of CD36 at the cell surface led us to document the polarization of CD36 distribution, including within lamellipodia and filopodia (Fig. 31a). Confocal microscopy also revealed a specific enrichment within filopodia in close contact with F-actin structures (Fig. 31b). This led us to postulate that CD36, besides its role in FA uptake to fuel oxidative metabolism of 6.5/cancer cells, could actually act as a scaffold to promote the release of activated TGF-β2 at the forefront of migrating acid-adapted cancer cells. This, however, would require TGF-β receptors to be also located in the same membrane microdomains in order to support the cell migrating machinery. Using immunostainings, we could validate this hypothesis by documenting the proximity of CD36 and TGF-β receptor I (TGF-βRI) in acid-adapted SiHa cancer cells (Fig. 31c), in particular within filopodia. Previous reports about the lipid raft compartmentation of TGF-βRI [127, 416] led us to explore whether these microdomains played a role in the co-localization with CD36. The use of nystatin confirmed that lipid raft disruption significantly altered the compartmentation of both proteins (Fig. 31c), a process reversed by the addition of exogenous cholesterol to restore lipid raft integrity (Fig. 31c). Importantly, the role of lipid rafts to support acid-adapted cancer cell migration was confirmed using nystatin. Together with a global alteration of cell morphology leading to more rounded 6.5/cancer cells (compare panels 2 and 3 in Fig. 31c), nystatin treatment prevented 6.5/Siha and 6.5/HCT116 cancer cell migration, a process again largely reversed by cholesterol re-supplementation (Figs. 31 d-e).

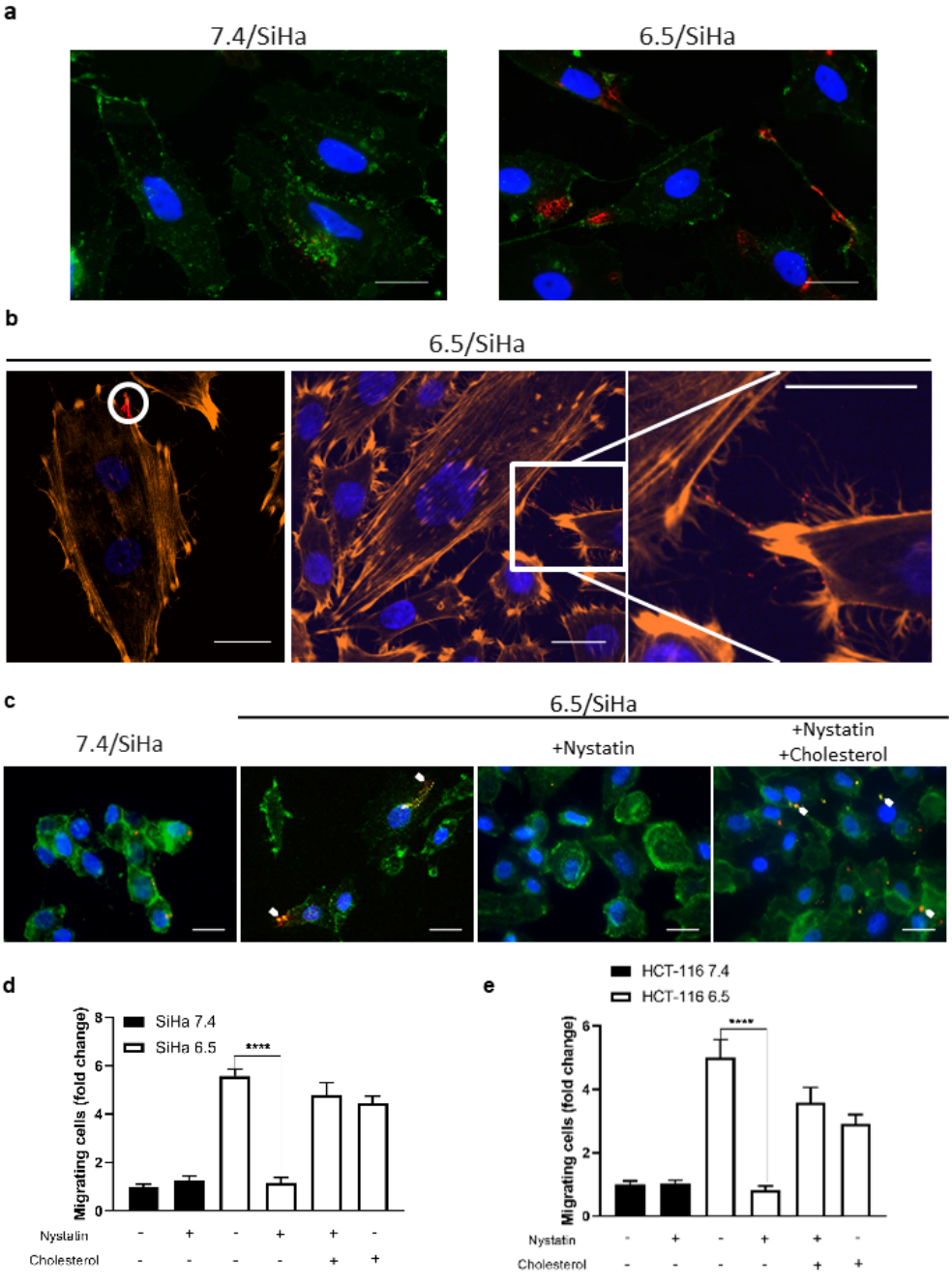
a
7.4/SiHa
6.5/SiHa
b
6.5/SiHa
c
7.4/SiHa
6.5/SiHa
+Nystatin
+Nystatin
+Cholesterol
d
SiHa 7.4
SiHa 6.5
****
Migrating cells (fold change)
0
2
4
6
8
Nystatin
Cholesterol
e
HCT-116 7.4
HCT-116 6.5
****
Migrating cells (fold change)
0
2
4
6
Nystatin
Cholesterol

Figure 31: CD36 co-localizes with TGF-β receptor in lamellipodias of acidosis-adapted cells. (a) Representative immunofluorescence images of native and acidosis-adapted SiHa cells stained for CD36 (red) and WGA (green), cell nuclei appear in blue. Scale bar: 20 µm. **(b)** Representative confocal images of CD36 (red), phalloidin (orange) and cell nuclei (blue). Scale bar: 20 µm. **(c)** Representative immunofluorescence images of parental and acidosis-adapted SiHa cells upon treatment with nystatin (or not) with or without cholesterol. Red and white stainings correspond to CD36 and TGF-β receptors, respectively (white arrows indicate co-localization); cells are also stained with WGA (green) and nuclei appear in blue. Scale bar: 20 µm. **(d-e)** Migration potential of native and acidosis-adapted SiHa **(d)** and HCT-116 **(e)** cancer cells upon treatment with nystatin (or not) with or without cholesterol (****P<0.001).

Actin cytoskeletal remodeling in acid-adapted cancer cells.

TGF-β/TGF-βRI signaling has been reported to promote EMT through cell cytoskeletal rearrangement [417], in particular through Smurf-regulated RhoA ubiquitination and degradation. In a pilot study, we could document that 6.5/cells (SiHa and HCT-116) have a higher amount of RhoA when compared to parental cells, and upon TSP-1 silencing, RhoA levels further increased due to a loss of RhoA degradation capacity (Fig. 32a). This preliminary result emphasizes the role of the CD36/TSP1/TGF-β2 axis in the local degradation of RhoA, which is required for dynamic actin cytoskeletal remodeling. Premiminary data using phalloidin to stain F-actin also suggest that CD36 blocking antibody can prevent actin rearrangement in 6.5/cancer cells (Fig. 32b).

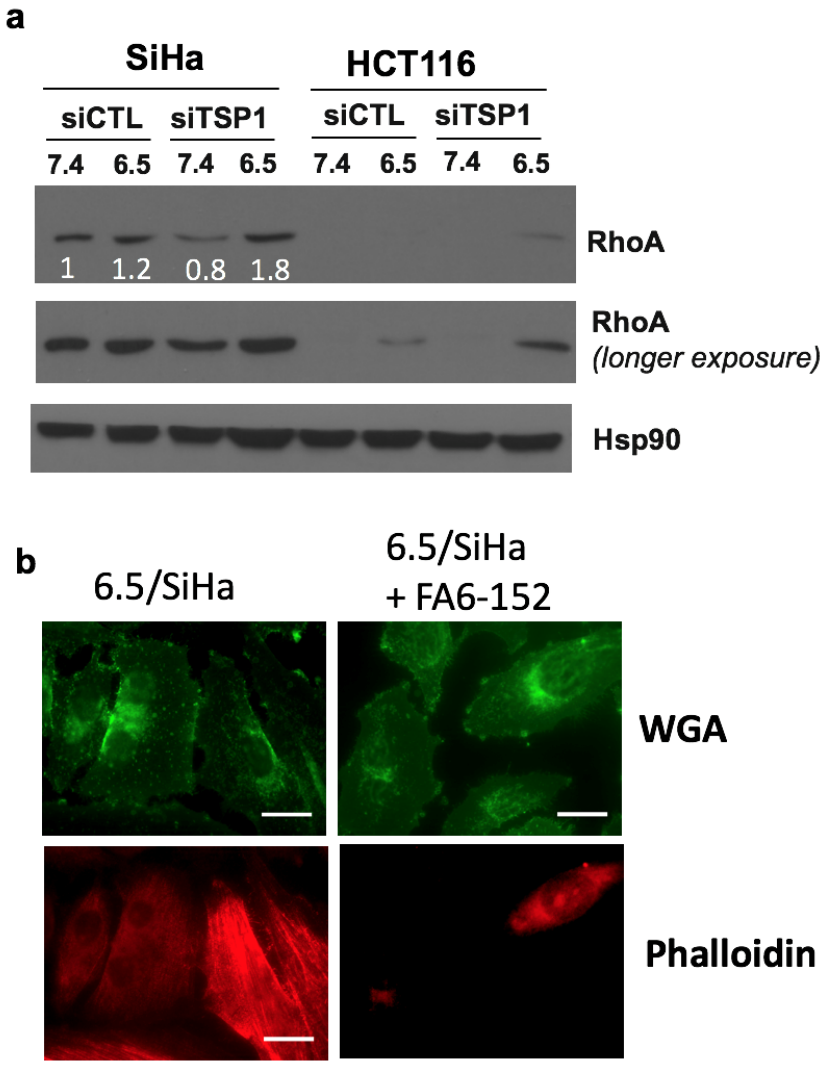

Figure 32: Actin cytoskeletal remodeling in acid-adapted cancer cells. (a) Representative immunoblotting of RhoA and HSP90 in native and acidosis-adapted SiHa and HCT116 cells after transfection of control or TSP-1-targeting siRNA; relative quantification is indicated for SiHa cell conditions. Of note, a longer film exposure is also presented to better reveal RhoA signal in HCT116 cells. **(b)** Representative immunofluorescence images of parental and acidosis-adapted SiHa cells with or without treatment with anti-CD36 antibody FA6-152. Red color corresponds phalloidin; cells are also stained with WGA (green) and nuclei appear in blue. These experiments were repeated twice with similar results.

3.4 Conclusions

The two main findings of this study are the identification of two critical events induced by acidosis that support the capacity of TGF-β2 to promote cancer cell invasiveness. First, we have identified the upregulation of TSP-1 under acidic conditions and showed how the promoted interaction of TSP-1 with latent TGF-β2 contributed to the activation of the cytokine. Second, we have documented how the polarization of CD36 expression in specific locations within the plasma membrane (ie. filopodia) could favor TGF-β2 autocrine signaling.

We found that importantly the exquisite compartmentation of the different actors, namely CD36, TSP-1, TGF-β2 and its receptor, was particularly relevant to induce the cytoskeleton rearrangement associated with cell migration.

These data further support the concept of a feed-forward loop promoted by acidosis. We have indeed previously reported how TGF-β2 could promote both the expression of TGF-β2 itself and the translocation of CD36 at the plasma membrane in a PKCζ-dependent manner [398]. Whether fatty acids themselves influence the role of scaffold played by CD36 warrants further studies. Nevertheless, the capacity of CD36 to promote the activation of TGF-β2 makes therefore the loop particularly suited to support a strong EMT process as long as the cancer cell remains in the acidic environment. Interestingly, it has been reported that TGF-β-mediated RhoA proteasomal degradation was achieved by phosphorylation of PAR-6 [143] through the recruitment of PKCζ [144, 145]. The implication of this atypical PKC appears therefore key to support activation of the whole process of compartmentation of the TGF-β2 production and associated cytoskeleton rearrangement [144-146] needed to facilitate cell motility and support EMT [276].

3.5 Methods

Cell culture

The human cell lines SiHa (#HTB-35), FaDu (#HTB-43), HCT-116 (#CCL-247) and HT-29 (#HTB-38) were purchased from ATCC. Cells were stored according to the supplier's instructions and used within 6 months after resuscitation of frozen aliquots. All cell lines were maintained in DMEM supplemented with 10% heat-inactivated FBS, 10 mM D-glucose, 2 mM L-glutamine and 25 mM of both PIPES and HEPES before adjusting pH to 7.4 or 6.5. Acidic pH-adapted tumor cells were established as previously described [34, 343]. All cell lines were tested for mycoplasma contamination with the MycoAlert™ Mycoplasma Detection kit (#LT07-318; Lonza) before being used.

Cell treatment and transfection

Cell treatment was performed in a full culture medium with 4 ng/ml recombinant human TGF-β2 (#ab84070; Abcam), 10 µM LSLK (#as-60877) and 10 µM SSLK (#as-60875) peptides, 2 µg/ml JC63.1 (ab23680; Abcam), or 1 µg/ml FA6-152 (ab17044; Abcam) anti-CD36 blocking antibodies, 25 µg/ml nystatin (N6261, Sigma) and 50 µg/ml Cholesterol (C8667, Sigma) at different timings as indicated in the figure legends. Cell transfection with non-targeting control or human TSP1-targeting siRNA sequences (pool of 4 siRNA sequences; #SO-2688721G; Dharmacon) was carried out with Lipofectamine™ RNAiMAX transfection reagent (#13778150; Thermo Fisher Scientific), according to manufacturer's instructions.

Immunocytochemistry

Cells grown on coverslips were fixed with 0.5% PFA for 5 min. After blocking with 5% BSA for 1h, cells were incubated overnight at 4°C with anti-CD36, anti-TSP1, anti-TGFBR1 or phalloidin-FITC antibodies (#ab23680, #ab85762, #ab31013 and P5282 respectively). Cells were then incubated with Alexa Fluor 488- and/or 568-conjugated and/or 647-conjugated secondary antibodies (#A11034, #A11036 and #A21236 respectively; Thermo Fisher Scientific) for 1h. In some experiments cell membrane were stained with WGA Alexa Fluor® 488 conjugate (W11261, Invitrogen) for 20min. The nuclei were counterstained with DAPI. Slides were prepared with a fluorescence mounting medium (Dako) and staining was visualized with a Zeiss Imager 1.0 Apotome microscope or Zeiss Spinning disk confocal microscope.

ELISA anti-TGFβ2

Active human TGF-β2 protein levels were assessed by using dedicated ELISA detection kits (#DB100B and #DB250, respectively; R&D Systems) following the manufacturer's instructions with some modifications. Indeed, samples (conditioned media or cell lysates) were not activated by acid treatment; this modified protocol allowed us to determine the levels of "naturally" active TGF-β, without the fraction of latent TGF-β being "artificially" activated to an immunoreactive form with the acid treatment.

Western blot analysis

Protein samples were denatured for 5 min at 95°C with Laemmli sample buffer containing 10% 2-mercaptoethanol. Samples (20 µg per well) were then loaded onto 8 to 15% acrylamide/bis-acrylamide gels and SDS-PAGE. Nitrocellulose

membranes were blocked with 5% BSA for 1h at RT. Primary antibodies against E-cadherin (#3195; cell signaling; 1:1000), N-cadherin (#13116; cell signaling; 1:1000), Smad2/3 (#D7G7; cell signaling; 1:1000); phospho-Smad2/3 (#D27F4; cell signaling; 1:1000) phospho-Smad3 (#9520; cell signaling; 1:1000), Snail (#3879; cell signaling; 1:1000), vimentin (#5741; cell signaling; 1:1000), Anti-β-actin (#A5441; Sigma-Aldrich; 1:1000), anti-CD36 (#100011; Cayman Chemical Company; 1:1,000), anti-RhoA (#ab54835; abcam; 1:1000), and anti-HSP90 (#610419; BD Biosciences; 1:2,000), were applied at 1:1,000 in 5% BSA overnight at 4°C. In some experiments, cell lysates (1 mg) were first pre-cleared with 5 µg rabbit IgG (#02-6102; Thermo Fisher Scientific) and 30 µl Dynabeads Protein G (#10003D; Thermo Fisher Scientific) for 1h, at 4°C on an end-to-end roller, and then incubated with 5 µg anti-acetylated lysine (#9441; Cell Signaling Technology) or rabbit IgG (overnight, 4°C). Immunoprecipitated proteins were pulled down after incubation with 30 µl Dynabeads Protein G (2h, 4°C) and then eluted with 60 µl Laemmli 2X.

Proximity ligation assay

Proximity ligation assay was done according with the kit Duolink PLA Technology from Sigma (#DUO92101). Cells grown on coverslips were fixed with 0.5% PFA for 5 min and then blocked with the kit blocking solution for 30min in a humidity chamber at 37°C. Primary antibodies were then added, TSP-1 overnight and CD36 for 2H at room temperature. Then, PLA probes were added for 1H at 37°C follow by 30min with Ligation mix (ligation stock and ligase diluted in high purity water). The signal is then amplified by an amplification mix (amplification stock together with polymerase diluted in high purity water) incubated for 1hour and 45min at 37°C. Nuclei were counterstained with DAPI. Slides were prepared with a fluorescence

mounting medium (Dako) and staining was visualized with a Zeiss Imager 1.0 Apotome microscope.

Migration assay

In this assay, we use a transmembrane/Boyden Chamber with 8 µm pore-sized membrane coated with 1% growth factor-reduced Matrigel (#356231; Corning). Cells are seeded on one side of the membrane with 0.1% FBS-containing medium, in presence or not of the treatments. A medium containing 10% FBS was added in the lower chamber and the cells were incubated for 4 hours at 37°C. After an incubation period, the membrane is fixed with ice-cold methanol and stained with DAPI. Cells that had not invaded through the chamber were removed. The number of cells which have migrated through the pores to the underside of the membrane are counted microscopically with the Axiovert 100 (CarlZeiss) (excitation filter G365 and emission filter Band Pass 445/50), and four fields were independently counted from each invasion chamber.

Immunoprecipitation

Lysates containing 1mg of protein were precleared by adding 100 ml of Dynabeads Protein G (#10009D, thermos fisher) for 1 h at 4 °C. The supernatant was incubated at 4°C for 2 hours in the presence of 5µg anti-TSP-1 antibody (ab85762, abcam) or rabbit immunoglobulin (X0903, DAKO). 100µl of Dynabeads Protein G were added overnight at 4°C. Beads were washed three times with lysis buffer and resuspended in Laemmli 2x (5 min, 95°C).

Data mining

Data from patients with cervical cancer, colon adenocarcinoma or the healthy counterparts were analyzed for survival curves and correlation of expression between TGFB2 and THBS1 genes [418]. This was performed using GEPIA data-mining platform (http://gepia.cancer-pku.cn/). For the survival curve, 292 and 270 cervical and colon adenocarcinoma (respectively) cancer patients were analyzed.

GENERAL DISCUSSION

1. Novelty and significance

The pH in solid tumors becomes more acidic as the tumor grows and this acidic environment, in turn, promotes the selection of more aggressive cancer cells. Our work is based on these two premises and identified a major metabolic rewiring of cancer cells as the link between extracellular acidosis and increased invasiveness.

In the first part of this thesis, we indeed document that cancer cells exposed to acidosis exhibit a dysregulated fatty acid metabolism with the coexistence of FA oxidation with glutamine-fueled FA synthesis (figure 33). At first glance, to imagine FAO and FAS occurring at the same time in a single cell may look like a futile cycle but the pressure put on cells by acidosis forced them to adopt the concomitance of these apparently paradoxical metabolic paths.

Proliferating cancer cells are known to depend upon de novo FA synthesis to support the needs to build up lipid membranes. We showed that acid-exposed cancer cells exploit the reductive glutamine metabolism to form FA. At the same time, proliferating cancer cells also need energy to support cell division. Here, while other cells could use glucose- or lactate fueled-TCA cycle and OXPHOS, we found that under acidosis, cancer cells prefer to use FAO. This is made possible through the downregulation of the mitochondrion-anchored ACC2 enzyme which thereby reduces the abundance of malonyl-CoA. In healthy cells, malonyl-CoA acts as an inhibitor of the mitochondrial FA transporter CPT1 (to avoid a futile cycle in cells performing FAS). Other investigators in the lab documented that under acidosis, histone deacetylation leads to ACC2 downregulation, thereby allowing cancer cells

to bypass the inhibitory mechanism and thus allowing FAO and FAS to occur in the same cell. Together with FAO becoming the main source of energy in acid-adapted cancer cells, glucose metabolism is abrogated to minimize the prejudicial accumulation of protons that results from high glycolytic turnover.

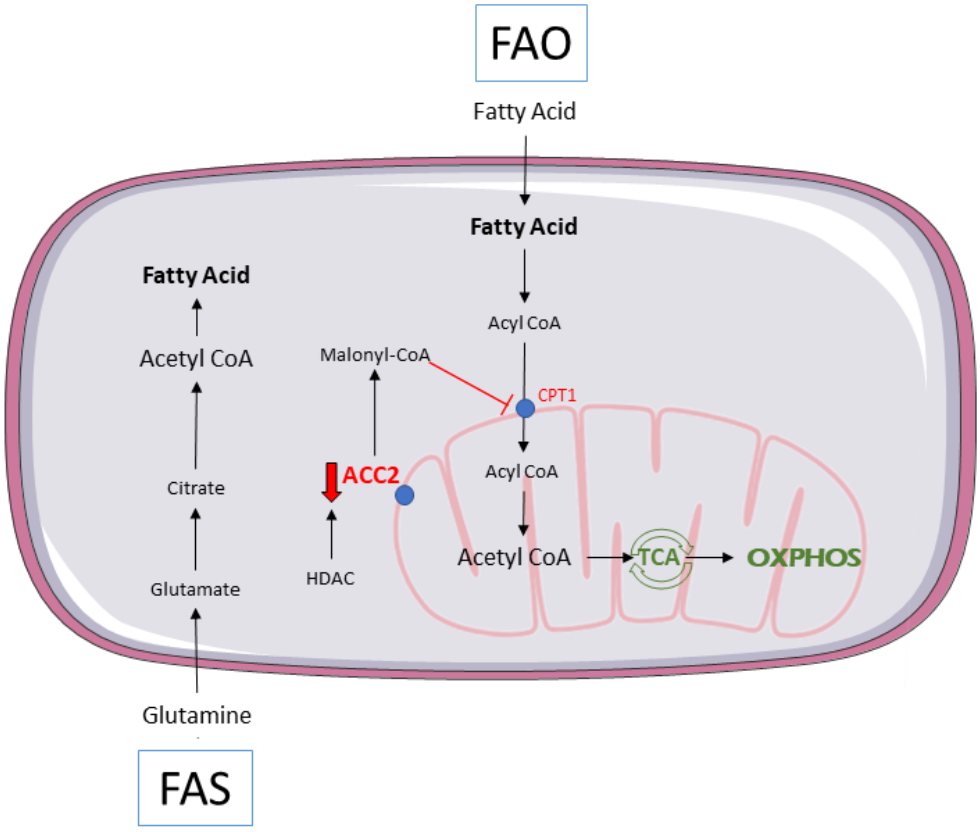

Figure 33 – The acidosis adapted cancer cell model (part 1 out of 4). Acidosis adapted cancer cells show a dependency on fatty acid metabolism

The metabolism of acidosis adapted cancer cells is to a great extend based on fatty acids. FAS plays a big role in replenish the acetyl CoA needed as building block, and FAO is required for energy fueling. The two are allowed to proceed at the same time due to the low levels of malonyl-CoA. The latter is affected by the downregulation of ACC2 which is caused by histone deacetylation.

In the second part of the thesis, we identified TGF-β2 as a major trigger of the increased invasive potential of cancer cells under acidosis and importantly established a direct link between this cytokine and the lipid metabolism rewiring that we had identified. This study was inspired by the observation of the elongated, mesenchymal-like morphology of acid-adapted cancer cells, together with the presence of large vesicles inside in their cytosol. The identification of these vesicles as being lipid droplets led us to document their supportive functions in survival, anoikis resistance and invasiveness. Through these features, LD account for a large part of the metastatic potential of acidosis-adapted cancer cells and thus making them an attractive therapeutic target to reduce metastasis formation. Although we have clearly documented how LD support the above biological processes, the rationale for their formation is still unknown. Still, we may propose that the dramatic shift from glucose to fatty acid metabolism drives an excessive uptake of free fatty acids and since those may be toxic at high concentrations, they are concentrated and thus masked within lipid bodies. The mechanisms underlying FA-induced lipotoxicity remain inconclusive, however, it is accepted that reactive oxygen species and endoplasmic reticulum stress are the major pathways involved. Palmitate was indeed reported to induce multiple signals like apoptosis, autophagy, and endoplasmic reticulum stress [419]. Also, FA accumulation in cancer cells may prevent lipid peroxidation and associated cell damages to occur as previously reported in drosophilas. Lipid droplets were reported as essential to protect drosophila from PUFA peroxidation [420].

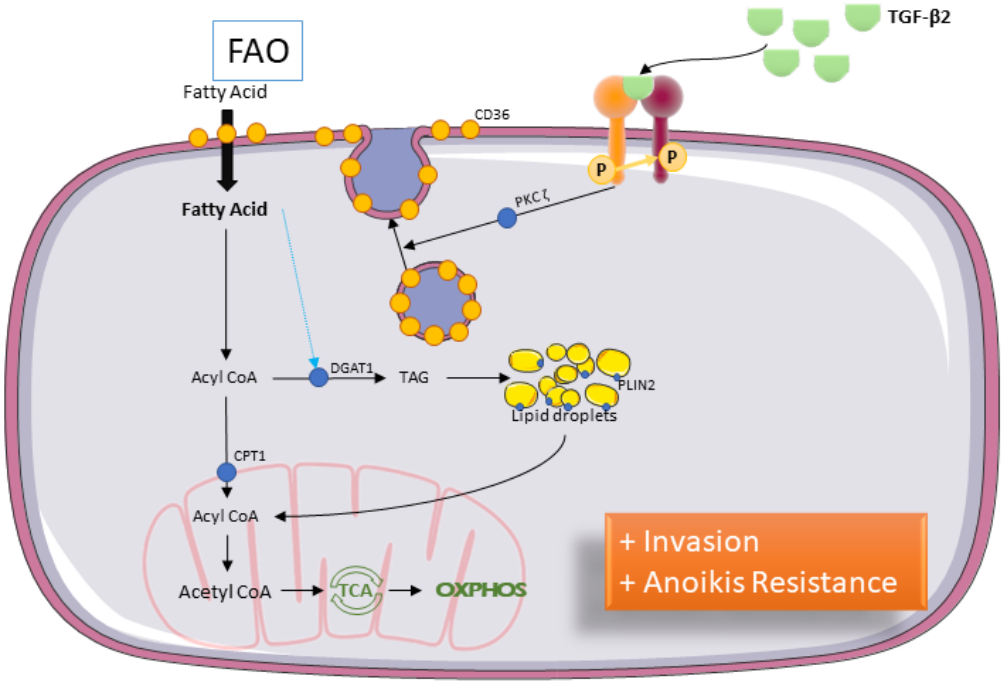

Figure 34 – The acidosis adapted cancer cell model (part 2 out of 4). Acidosis adapted cancer cells store fatty acids in lipid droplets.

Activation of the TGF-β receptors by TGF-β2 leads to translocation of CD36 to the cell membrane, in a process mediated by PKCζ. The high level of membrane CD36 leads to a large internalization of FFA. The pressure created by the high quantities of FFA forces the upregulation of DGAT-1 in order to produce TAG that can be stored in LD. These LD are reach in Plin2, which allows their stabilization. The LD can be used as fuel upon needed and were described to guarantee invasion capacity and anoikis resistance.

Importantly, we demonstrated that TGF-β2 was greatly accountable for LD formation in acid-adapted cancer cells by promoting the translocation of CD36 (that facilitates the uptake of FA) and the upregulation of DGAT-1 (that support the last step of triglyceride synthesis) and PLIN2 (a major coat protein that stabilizes LD formation).

While the link between TGF-β2 and lipid metabolism was a major finding, the connection with EMT was more obvious. Still, although TGF-β has indeed been extensively reported as an EMT promoter, our work brought a series of new insights

on the role of this cytokine in supporting the mesenchymal transition associated with acid-adapted cancer cells.

First, we showed that the TGF-β2 isoform but not the more classically studied TGF-β1 isoform was involved in acid-adapted cancer cells. We documented that thrombospondin was directly helping with the maturation of TGF-β2, which contrary to TGF-β1 and TGF-β3 does not contain a RGD sequence. The lack of a RGD motif does not allow the recognition and activation by integrins αVβ6. This limits the activation methods available for TGF-β2, making TSP-1-dependent activation even more vital. It should also be emphasized that the autocrine TGF-β2 signaling is reinforced by the capacity of the cytokine to induce its own expression. We found indeed that TGF-β2-dependent expression of ZEB1 led to an increase in the TGF-β2 mRNA expression in acidosis-adapted cancer cells.

Second, we showed that the modulation of lipid metabolism by TGF-β2 directly reinforced the downstream signal transduction as well as the biological consequences associated with the EMT. We indeed showed that Smad2 was acetylated in acid-adapted cancer cells as a direct consequence of the increased extent of FAO in these cells. Acetylation of Smad is known to occur in the Smad2 lysine residues (Lys19, Lys20, and Lys39) and perhaps Smad3 [421]. The acetylation contributes to the nuclear accumulation of the two proteins by diminishing the rate of nuclear exportation [421]. Also, we showed that upon LD deprivation, cancer cells were less prone to invasion than normally their mesenchymal phenotype would entitle them. In other words, the two axes, namely the mesenchymal shift and the rewiring of FA metabolism are needed to make the cells more invasive and prone to form metastases.

Finally, by making TGF-β2 as a switch exquisitely dependent on the acidic condition, it offers an explanation of how MET, the reverse process of EMT, can be initiated. When present in a non-acidic microenvironment, cells lose the *stimulus* (TGF-β2) to perform EMT, allowing them to transition back to a more epithelial phenotype. This capacity brings plasticity to the new mesenchymal cells that can easily do the inverse transition – MET – and proliferate to form a new tumor.

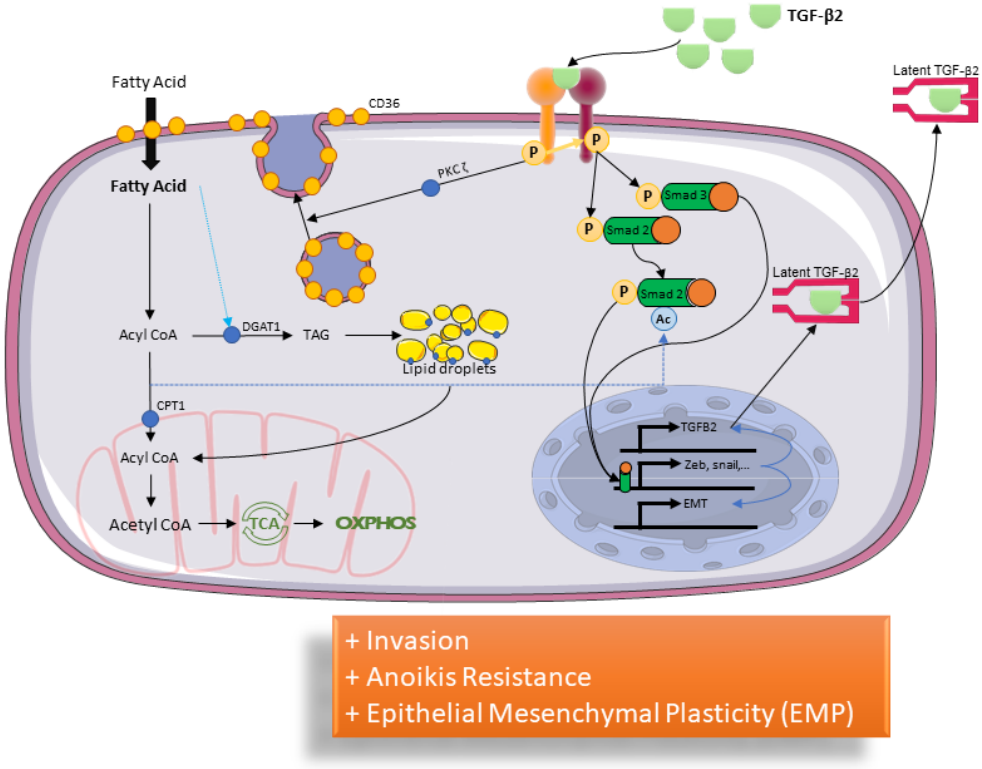

Figure 35 – The acidosis adapted cancer cell model (part 3 out of 4). TGF-β-mediated EMT improves the metastatic aggressiveness of acidosis adapted cells

Activation of the TGF-β receptors by TGF-β2 leads to R-Smad activation (phosphorylation of Smad 2 and 3). Smad 2 is further acetylated by the excess of acetyl CoA that is present in the cell, this enhances the nuclear localization of this protein. P-Smad 2 and 3 connect with Smad 4 (co-smad) and enter in the nucleus where they can transcribe a series of genes. Between the genes promoted, there are transcription factors for EMT (ZEB, Snail, …), these will not only allow an EMT transition but also the production of latent TGF-β2. Ultimately, acidosis adapted cancer cells gain EMP that allows them to be more metastatic aggressive.

In the last part of this thesis, we further dissected the process of thrombospondin-induced activation of TGF-β2 and identified an unique compartmentation of different actors supporting cancer cell invasiveness within lipid rafts. The previous knowledge of CD36 being able to bind TSP1 and our observation that the expression of both was increased under acidosis, led us to hypothesize that this could reinforce the capacity of acid-exposed cancer cells to activate TGF-β2. In the course of this study, we realized that CD36 expression was polarized at the plasma membrane in filopodias suggesting that besides an increased capacity to generate TGF-β2, the location of this production could have a functional role. This hypothesis is further supported by evidence that CD36 is specifically located within lipid rafts together with TGF-β receptors. Altogether this set of data led us to propose the model depicted in Figure 35. Although further investigations are needed, our work may be directly related to a previous publication in Science where TGF-β drives the polarized and rapid proteasomal degradation of RhoA to support the motility of cancer cells. The role of TSP1 at the interface between CD36 and TGF-β2 therefore appears critical to generate the cytokine at the vicinity of its receptor located in lipid rafts (together with CD36). As a first evidence of this role, we showed that silencing TSP-1 restored the expression of RhoA, thereby abrogating the increased invasive potential of acid-adapted cancer cells.

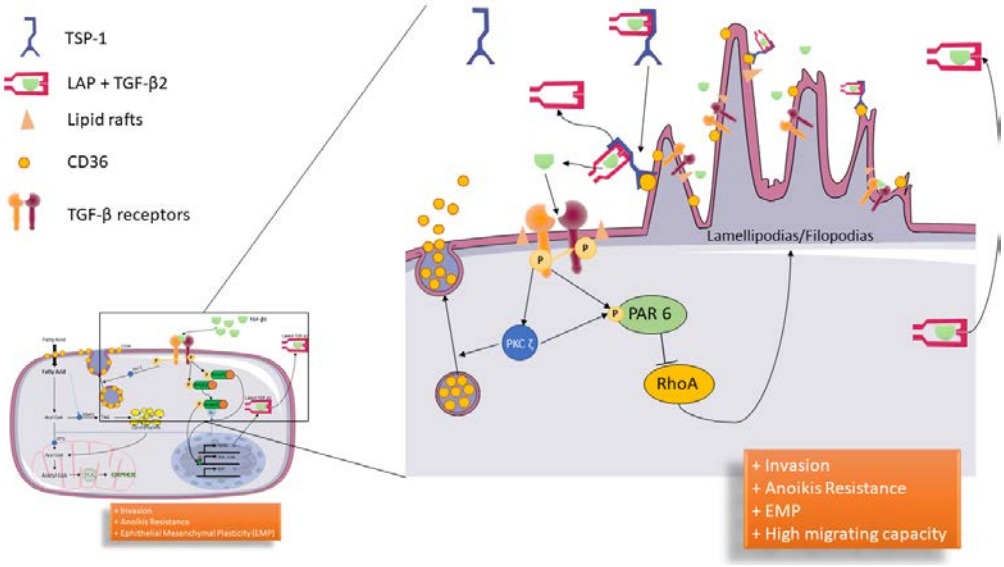

Figure 36 – The acidosis exposed cancer cell model (part 4 out of 4). TSP-1-dependent TGF-β activation in the filopodia of acidosis adapted cancer cells.

Lipid rafts allow the co-localization of TGF-β receptors and CD36. TSP-1, connects with LAP-TGF-β2, and uses CD36 to activate the cytokine. The proximity to a TGF-β receptor allows it to be activated locally. TGF-β signaling causes PAR6 phosphorylation that in turns inhibits RhoA. This is an important process for the formation of filopodia. Finally, this gives a high migratory capacity to the acidosis adapted cancer cells.

2. Therapeutic implications

The final goal of cancer studies should be to find the best therapeutic strategy for a certain tumor situation and hence aid the patients in need of treatment. With that in mind, we will focus this part of the discussion in what can be the best clinical strategy to tackle tumor acidosis-dependent aggressivity. Different approaches to interfere with tumor pH have been already tested in vitro and even in vivo. There are two major ways to directly target tumor acidosis: (i) globally increase the pH of the tumor and (ii) targeting and inhibiting membrane proton transporters to disrupt pH control.

For centuries, chemists know that an acid can be neutralized with a basic buffer. Therefore, an obvious therapeutic approach to interfere with tumor acidosis has been to directly interfere with tumor pH. One of the most used buffers is bicarbonate (HCO_3^-), normally administrated orally in conjugation with sodium ($NaHCO_3$). In mouse experiments, bicarbonate by neutralizing tumor pH has been shown to improve immunotherapy [422] and inhibit spontaneous metastases [423], without affecting the systemic pH (according to 3D mathematical models the pH in the blood remains unchanged with $NaHCO_3$ concentrations that can impact tumor growth [424]). However, in humans, it is well known that bicarbonate ingestion has some risks and is for instance associated with hypokalaemia and QT interval prolongation [1].

For several years drugs targeting lactate membrane transporters and acid efflux proteins have been synthesized. Both small molecules and antibodies have the final goal of dysregulating pH control within acidosis-exposed cancer cells, leading them to their demise. This therapeutic strategy is present at various stages of clinical trials and its appropriately resumed in the review from Dario Neri and Claudiu T. Supuran [425]. However, the less specific targeting of acidosis can cause off-target harm. pH-controlling enzymes have multiple isoforms, some not connected to malignant tumors, making difficult to target only the desired isoform from a chemical viewpoint. Also, targeting proteins involved in crucial physiological processes can cause disturbances in healthy cells. For example, a drug targeting NHE1 was stopped in Phase III of clinical trials because it could cause strokes [425].

Although more work is ongoing to identify drugs able to selectively target tumor acidosis while sparing pH homeostasis in healthy tissues, our work suggests that targeting the consequences of acidosis may offer the specificity needed to impact cancer progression without inducing major toxic events for the patients. We

have indeed documented how the lipid metabolic reprogramming introduced vulnerabilities in acid-adapted cancer cells. Hence, drugs targeting FAO and LD formation were shown to have a high impact on the survival and/or invasive potential of acid-exposed cells. We identified etomoxir and CD36 blocking antibodies to inhibit FA transport at the mitochondria and the plasma membrane respectively, as relevant strategies to inhibit cancer cell growth and invasion. Similar results were obtained with DGAT inhibitors as well as atglistatin through the inhibition of FA storage in LD and FA mobilization from LD, respectively. Our work can also be correlated to changes observed after antiangiogenic treatment, during which intensified glycolysis and lactate production is observed [426], causing an acidic microenvironment. Sounni et al. observed that during the treatment withdrawal (*i.e.* a more oxygenated tumor) there was a metabolic shift towards lipid metabolism and TCA activity [427]. It was also detected an increased abundance of lipid droplets (stabilized by PLIN) in the tumors [427]. These observations indicate that a treatment applied to acidic tumors could also be effective for tumors previously treated with antiangiogenic drugs. Targeting TGF-β2 could also represent an attractive strategy, in particular by expanding the use of Trabedersen, an anti-TGF-β2 oligonucleotide, the clinical use of it being currently restricted to glioma where low doses of Trabedersen were more beneficial than chemotherapy [428, 429]. Although based on our results, such TGF-β2 mRNA repressors, TGF-β2 ligand traps, neutralizing anti-TGF-β2 antibodies may offer some advantages when compared with blockers of TGF-β receptor II or Smad inhibitors, further investigation is warranted to proceed with strategies aiming to disrupt TGF-β2 signaling. As emphasized in the Introduction, TGF-β may indeed exert both tumor suppressive and tumorigenic roles. More insights will very likely arise from the ongoing clinical trials exploring strategies to tackle TGF-β signaling;

out of the thirty-two anti-TGF-β signaling drugs described today, thirteen of them were in a clinical trial in 2014 [430].

Of note, since the tumorigenic effects of TGF-β signaling are "generally" obtained when the levels of TGF-β signaling are above the normal physiological levels, an attractive strategy could be to restore "normal" levels of TGF-β. Our identification of TSP-1 as the driver of TGF-β2 activation under acidic conditions suggests that blocking the role of TSP-1 in TGF-β2 maturation could be of interest.

Besides developing new drugs to target tumor acidosis or the phenotypical consequences of it, there is also an imperious need to have a biomarker of acidic pH to determine which cancers will be the more prone to be treated with these strategies. While hypoxic zones in experimental tumors can be easily detected by CA IX staining [52, 431], reductive compounds such as pimonidazole [432] or even HIF-1a labeling [431], detection of acidic tumor area is still in its infancy. Yet, some molecules, including the pH-low insertion peptides (pHLIP) have shown some potential to act as a specific acidic marker. The pHLIP consists of a water-soluble membrane that can be inserted across a cellular membrane in response to a lower extracellular pH in contrast with a normal physiologic pH [433, 434]. This gives pHLIP the capacity of identifying cells in the presence of an extracellular acidosis and therefore, it has been normally associated with imaging proteins (e.g. tracers) in order to detect tissue acidity or metastatic lesions. Of note, pHLIP can also be conjugated with drugs that target specific pathways in acidic exposed cells. Designed peptides like pHLIP are just one example of acidosis-specific drug delivery system that also includes nanogels [435], polymersomes [436], and micelles [437]. These drug delivery systems can be modified to only be responsive in acidic environments. For example, MPEG-b-PNLG nanogels are stable at pH 7.4, but the contact with acidic environments leads them to rapidly release their content [438].

3. Future directions

In this thesis, we explored extensively the phenotype of acidosis-adapted cancer cells from the metabolic adaptation till the increased metastatic potential. Our work has also opened various perspectives, a few of them are briefly mentioned here below.

Discovering the TSP-1 regulator

We identified TSP-1 as the major regulator of the TGF-β2 levels, but nothing is still known for what causes the TSP-1 to increase. This process appears to happen in early acidosis, since acute acidic exposure can quickly promote the translation of this protein (fig. 27). HIF-2α is known to upregulate TSP-1 levels [439, 440]. Since it has been identified as a key regulator of metabolic adaptation in acidosis-adapted cancer cells [307], we considered it as a potential candidate for TSP-1 regulation in our experimental setup. However HIF2α silencing had no impact in TPS-1 levels (data not shown). Lactate is also described to upregulate TSP-1 [441]. Although it would make sense *in vivo* in a context of acidosis, it cannot explain our *in vitro* changes. There is a possible reinforcement, but not initiating event, through TGF-β signaling since SMAD3 is known to bind to the *THBS1* gene promoter and promote its transcription [442]. AP-1 (activator protein-1), CREB (cAMP response element binding protein) and NF-κB (nuclear factor-κB) are major transcription factors for which consensus binding sites are present in the *THBS1* gene promoter [443]. Among them NF-κB is attractive since it can be activated through acid-sensing anion channel ASIC1 [444] and was recently proven to induce TSP-1 transcription [445]. More work is need to test this hypothesis in our acid-adapted cancer cell models.

Further describing the goal of lipid uptake

We have demonstrated that acidosis-adapted cancer cells can uptake a large amount of fatty acids that are mostly stored in lipid droplets. Furthermore, we did a lipidomic analysis (supplement table 1) that illustrates the entry of mostly saturated and monounsaturated FA. Nonetheless, it would be interesting to follow the fate of specific fatty acids that are uptaken by the cells.

Further understand the process of lamellipodia and filopodia formation

Lamellipodias and filopodias are extremely important for the migration capacity, and therefore, the invasive capacity of the cells. The presence of CD36 and TGF-β2 in these structures is quite intriguing. TGF-β-dependent RhoA inhibition is a well-described process. However, it might not be the only cause for the observation of atypic CD36 localization. The role of CD36 in facilitating FA uptake in specific (polarized) cellular locations cannot be completely ruled out. Although lamellipodias and filopodias are narrow structures that render the presence of mitochondria to burn locally captured FA (confirmed in our hands by the failure to detect them by immunostaining), the local increase in fatty acid bioavailability could sub serve other functions. Very recent work has revealed the release of a large quantities of cholesterol-rich particles during migrating movement involving lamellipodias and filopodias [446]. It is possible that CD36 has a role on replacing the cholesterol and other specific lipids in order to keep with projections and retractions done by filopodia and lamellipodia filaments. It would be interesting to investigate whether our finding of CD36/TSP1/TGF-β receptor co-localization can somehow be further associated with discovery.

REFERENCES

1. Corbet, C. and O. Feron, *Tumour acidosis: From the passenger to the driver's seat.* Nature Reviews Cancer, 2017. **17**(10): p. 577-593.
2. "The History of Cancer". American Cancer Society. 2009.
3. Weinberg, D.H.a.R.A., *The Hallmarks of Cancer.* Cell, 2000. **100**: p. 57–70.
4. Foulds, L., *The Experimental Study of Tumor Progression: A Review.* Cancer Research, 1954. **14**(5): p. 327-339.
5. Hanahan, D. and R.A. Weinberg, *Hallmarks of cancer: the next generation.* Cell, 2011. **144**(5): p. 646-74.
6. Balkwill, F.R., M. Capasso, and T. Hagemann, *The tumor microenvironment at a glance.* J Cell Sci, 2012. **125**(Pt 23): p. 5591-6.
7. Bardos, J.I. and M. Ashcroft, *Hypoxia-inducible factor-1 and oncogenic signalling.* Bioessays, 2004. **26**(3): p. 262-9.
8. Bondurant, M.C. and M.J. Koury, *Anemia induces accumulation of erythropoietin mRNA in the kidney and liver.* Molecular and cellular biology, 1986. **6**(7): p. 2731-2733.
9. Caro, J., et al., *Renal biogenesis of erythropoietin*, in *Molecular and Cellular Aspects of Erythropoietin and Erythropoiesis*. 1987, Springer. p. 329-336.
10. Semenza, G.L. and G.L. Wang, *A nuclear factor induced by hypoxia via de novo protein synthesis binds to the human erythropoietin gene enhancer at a site required for transcriptional activation.* Molecular and cellular biology, 1992. **12**(12): p. 5447-5454.
11. Wang, G.L., et al., *Hypoxia-inducible factor 1 is a basic-helix-loop-helix-PAS heterodimer regulated by cellular O2 tension.* Proceedings of the national academy of sciences, 1995. **92**(12): p. 5510-5514.
12. Wang, G.L. and G.L. Semenza, *Purification and characterization of hypoxia-inducible factor 1.* Journal of Biological Chemistry, 1995. **270**(3): p. 1230-1237.

13. Semenza, G.L., *Regulation of cancer cell metabolism by hypoxia-inducible factor 1.* Semin Cancer Biol, 2009. **19**(1): p. 12-6.

14. Ke, Q. and M. Costa, *Hypoxia-inducible factor-1 (HIF-1).* Mol Pharmacol, 2006. **70**(5): p. 1469-80.

15. Lee, J.-W., et al., *Hypoxia-inducible factor (HIF-1) α: its protein stability and biological functions.* 2004. **36**(1): p. 1-12.

16. Iervolino, A., et al., *Bcl-2 overexpression in human melanoma cells increases angiogenesis through VEGF mRNA stabilization and HIF-1-mediated transcriptional activity.* FASEB J, 2002. **16**(11): p. 1453-5.

17. Komatsu, D.E. and M. Hadjiargyrou, *Activation of the transcription factor HIF-1 and its target genes, VEGF, HO-1, iNOS, during fracture repair.* Bone, 2004. **34**(4): p. 680-8.

18. Chen, C., et al., *Regulation of glut1 mRNA by hypoxia-inducible factor-1. Interaction between H-ras and hypoxia.* J Biol Chem, 2001. **276**(12): p. 9519-25.

19. Kim, J.W., et al., *HIF-1-mediated expression of pyruvate dehydrogenase kinase: A metabolic switch required for cellular adaptation to hypoxia.* Cell Metabolism, 2006. **3**(3): p. 177-185.

20. Semenza, G.L. *Regulation of cancer cell metabolism by hypoxia-inducible factor 1*. in *Seminars in cancer biology*. 2009. Elsevier.

21. Metallo, C.M., et al., *Reductive glutamine metabolism by IDH1 mediates lipogenesis under hypoxia.* Nature, 2012. **481**(7381): p. 380.

22. Gameiro, P.A., et al., *In vivo HIF-mediated reductive carboxylation is regulated by citrate levels and sensitizes VHL-deficient cells to glutamine deprivation.* Cell metabolism, 2013. **17**(3): p. 372-385.

23. Wise, D.R., et al., *Hypoxia promotes isocitrate dehydrogenase-dependent carboxylation of α-ketoglutarate to citrate to support cell growth and viability.* Proceedings of the National Academy of Sciences, 2011. **108**(49): p. 19611-19616.

24. Corbet, C. and O. Feron, *Metabolic and mind shifts: from glucose to glutamine and acetate addictions in cancer.* Current Opinion in Clinical Nutrition & Metabolic Care, 2015. **18**(4): p. 346-353.

25. Sun, R.C. and N.C. Denko, *Hypoxic regulation of glutamine metabolism through HIF1 and SIAH2 supports lipid synthesis that is necessary for tumor growth.* Cell metabolism, 2014. **19**(2): p. 285-292.

26. Zhang, H., et al., *Mitochondrial autophagy is an HIF-1-dependent adaptive metabolic response to hypoxia.* Journal of Biological Chemistry, 2008. **283**(16): p. 10892-10903.

27. Ashby, B.S., *pH studies in human malignant tumours.* The Lancet, 1966: p. 312-315.

28. Helmlinger, G., et al., *Interstitial pH and pO2 gradients in solid tumors in vivo: high-resolution measurements reveal a lack of correlation.* Nat Med, 1997. **3**(2): p. 177-82.

29. Kallinowski, F. and P. Vaupel, *Ph distributions in spontaneous and isotransplanted rat tumours.* British Journal of Cancer, 1988. **58**(3): p. 314-321.

30. Schornack, P.A. and R.J. Gillies, *Contributions of Cell Metabolism and H+ Diffusion to the Acidic pH of Tumors.* Neoplasia, 2003. **5**(2): p. 135-145.

31. Busco, G., et al., *NHE1 promotes invadopodial ECM proteolysis through acidification of the peri-invadopodial space.* FASEB J, 2010. **24**(10): p. 3903-15.

32. Gillies, R.J., et al., *MRI of the tumor microenvironment.* J Magn Reson Imaging, 2002. **16**(4): p. 430-50.

33. Webb, B.a., et al., *Dysregulated pH: A perfect storm for cancer progression.* Nature Reviews Cancer, 2011. **11**(9): p. 671-677.

34. Corbet, C., et al., *The SIRT1/HIF2alpha axis drives reductive glutamine metabolism under chronic acidosis and alters tumor response to therapy.* Cancer Res, 2014. **74**(19): p. 5507-19.

35. Pouysségur, J., et al., *A specific mutation abolishing Na+/H+ antiport activity in hamster fibroblasts precludes growth at neutral and acidic pH.*

Proceedings of the National Academy of Sciences, 1984. **81**(15): p. 4833-4837.

36. L'allemain, G., S. Paris, and J. Pouysségur, *Growth factor action and intracellular pH regulation in fibroblasts. Evidence for a major role of the Na+/H+ antiport.* Journal of Biological Chemistry, 1984. **259**(9): p. 5809-5815.

37. Pedersen, S.F., *The Na+/H+ exchanger NHE1 in stress-induced signal transduction: implications for cell proliferation and cell death.* Pflugers Arch, 2006. **452**(3): p. 249-59.

38. Steffan, J.J., et al., *Na+/H+ exchangers and RhoA regulate acidic extracellular pH-induced lysosome trafficking in prostate cancer cells.* Traffic, 2009. **10**(6): p. 737-53.

39. Bourguignon, L.Y., et al., *CD44 interaction with Na+-H+ exchanger (NHE1) creates acidic microenvironments leading to hyaluronidase-2 and cathepsin B activation and breast tumor cell invasion.* Journal of Biological Chemistry, 2004. **279**(26): p. 26991-27007.

40. Frantz, C., et al., *Positive feedback between Cdc42 activity and H+efflux by the Na-H exchanger NHE1 for polarity of migrating cells.* The Journal of Cell Biology, 2007. **179**(3): p. 403-410.

41. Paradiso, A., et al., *The Na+–H+ exchanger-1 induces cytoskeletal changes involving reciprocal RhoA and Rac1 signaling, resulting in motility and invasion in MDA-MB-435 cells.* Breast Cancer Research, 2004. **6**(6): p. R616.

42. Gorbatenko, A., et al., *Regulation of the Na+, HCO3-cotransporter NBCn1 (SLC4A7) by a constitutively active ErbB2 receptor in MCF-7 breast cancer cells*. 2013, Federation of American Societies for Experimental Biology.

43. Saroussi, S. and N. Nelson, *Vacuolar H+-ATPase—an enzyme for all seasons.* Pflügers Archiv-European Journal of Physiology, 2009. **457**(3): p. 581-587.

44. Chi, S.L. and S.V. Pizzo, *Angiostatin is directly cytotoxic to tumor cells at low extracellular pH: a mechanism dependent on cell surface–associated ATP synthase.* Cancer research, 2006. **66**(2): p. 875-882.

45. Das, B., et al., *A novel ligand in lymphocyte-mediated cytotoxicity: expression of the beta subunit of H+ transporting ATP synthase on the surface of tumor cell lines.* Journal of Experimental Medicine, 1994. **180**(1): p. 273-281.

46. Zhao, Y., et al., *Proteomic analysis of integral plasma membrane proteins.* Analytical chemistry, 2004. **76**(7): p. 1817-1823.

47. Petersen, C., et al., *MCT1 and MCT4 expression and lactate flux activity increase during white and brown adipogenesis and impact adipocyte metabolism.* Scientific reports, 2017. **7**(1): p. 1-13.

48. Kong, S.C., et al., *Monocarboxylate transporters MCT1 and MCT4 regulate migration and invasion of pancreatic ductal adenocarcinoma cells.* Pancreas, 2016. **45**(7): p. 1036-1047.

49. Monti, S.M., C.T. Supuran, and G. De Simone, *Anticancer carbonic anhydrase inhibitors: a patent review (2008–2013).* Expert opinion on therapeutic patents, 2013. **23**(6): p. 737-749.

50. Supuran, C.T., *Carbonic anhydrases: novel therapeutic applications for inhibitors and activators.* Nature reviews Drug discovery, 2008. **7**(2): p. 168.

51. M Monti, S., C. T Supuran, and G. De Simone, *Carbonic anhydrase IX as a target for designing novel anticancer drugs.* Current medicinal chemistry, 2012. **19**(6): p. 821-830.

52. Sedlakova, O., et al., *Carbonic anhydrase IX, a hypoxia-induced catalytic component of the pH regulating machinery in tumors.* Frontiers in Physiology, 2014. **4**(400).

53. Chiche, J., et al., *Hypoxia-inducible carbonic anhydrase IX and XII promote tumor cell growth by counteracting acidosis through the regulation of the intracellular pH.* Cancer research, 2009. **69**(1): p. 358-368.

54. Gorbatenko, A., et al., *Regulation and roles of bicarbonate transport in cancer.* Frontiers in physiology, 2014. **5**: p. 130.

55. Lee, S., et al., *Disrupting Na+, HCO 3−-cotransporter NBCn1 (Slc4a7) delays murine breast cancer development.* Oncogene, 2016. **35**(16): p. 2112-2122.

56. Song, L.-J., et al., *Gastrin inhibits a novel, pathological colon cancer signaling pathway involving EGR1, AE2, and P-ERK.* Journal of molecular medicine, 2012. **90**(6): p. 707-718.

57. Shen, W.-W., et al., *Expression of anion exchanger 1 sequestrates p16 in the cytoplasm in gastric and colonic adenocarcinoma.* Neoplasia (New York, NY), 2007. **9**(10): p. 812.

58. Erra Diaz, F., E. Dantas, and J. Geffner, *Unravelling the Interplay between Extracellular Acidosis and Immune Cells.* Mediators Inflamm, 2018. **2018**: p. 1218297.

59. Warburg, O., *On the origin of cancer cells.* Science, 1956. **123**(3191): p. 309-314.

60. Racker, E., *Bioenergetics and the problem of tumor growth: an understanding of the mechanism of the generation and control of biological energy may shed light on the problem of tumor growth.* American scientist, 1972. **60**(1): p. 56-63.

61. Hiraki, Y., O. Rosen, and M. Birnbaum, *Growth factors rapidly induce expression of the glucose transporter gene.* Journal of Biological Chemistry, 1988. **263**(27): p. 13655-13662.

62. Guido, C., et al., *Metabolic reprogramming of cancer-associated fibroblasts by TGF-β drives tumor growth: connecting TGF-β signaling with "Warburg-like" cancer metabolism and L-lactate production.* Cell cycle, 2012. **11**(16): p. 3019-3035.

63. Mekhail, K., et al., *HIF activation by pH-dependent nucleolar sequestration of VHL.* Nat Cell Biol, 2004. **6**(7): p. 642-7.

64. Filatova, A., et al., *Acidosis Acts through HSP90 in a PHD/VHL-Independent Manner to Promote HIF Function and Stem Cell Maintenance in Glioma.* Cancer Res, 2016. **76**(19): p. 5845-5856.

65. Gordan, J.D., et al., *HIF-2alpha promotes hypoxic cell proliferation by enhancing c-myc transcriptional activity.* Cancer Cell, 2007. **11**(4): p. 335-47.

66. Damaghi, M., J.W. Wojtkowiak, and R.J. Gillies, *pH sensing and regulation in cancer.* Front Physiol, 2013. **4**: p. 370.

67. Gupta, S.C., et al., *Regulation of breast tumorigenesis through acid sensors.* Oncogene, 2016. **35**(31): p. 4102-11.

68. https://www.proteinatlas.org/ENSG00000110881-ASIC1/pathology

69. Sin, W.C., et al., *G protein-coupled receptors GPR4 and TDAG8 are oncogenic and overexpressed in human cancers.* Oncogene, 2004. **23**(37): p. 6299-303.

70. Wyder, L., et al., *Reduced pathological angiogenesis and tumor growth in mice lacking GPR4, a proton sensing receptor.* Angiogenesis, 2011. **14**(4): p. 533-544.

71. Marie-Gabrielle Ludwig, M.V., Danilo Guerini, and C.E.J. Jurg A. Gasser, Uwe Junker, Hans Hofstetter,Romain M. Wolf & Klaus Seuwen, *Proton-sensing G-protein-coupled receptors.* Nature, 2003. **425**(6953).

72. Yu, M., et al., *Increased proton-sensing receptor GPR4 signalling promotes colorectal cancer progression by activating the hippo pathway.* EBioMedicine, 2019. **48**: p. 264-276.

73. Ishii, S., Y. Kihara, and T. Shimizu, *Identification of T cell death-associated gene 8 (TDAG8) as a novel acid sensing G-protein-coupled receptor.* J Biol Chem, 2005. **280**(10): p. 9083-7.

74. Heuser, J., *Changes in lysosome shape and distribution correlated with changes in cytoplasmic pH.* J Cell Biol, 1989. **108**(3): p. 855-64.

75. Kristine Glunde, S.E.G., Meiyappan Solaiyappan, Arvind P. Pathak, Yoshitaka Ichikawaz, and a.Z.M. Bhujwalla, *Extracellular Acidification Alters Lysosomal Trafficking in Human Breast Cancer Cells.* Neoplasia 2003. **5**.

76. Damaghi, M., et al., *Chronic acidosis in the tumour microenvironment selects for overexpression of LAMP2 in the plasma membrane.* Nature communications, 2015. **6**: p. 8752-8752.

77. Wojtkowiak, J.W., et al., *Chronic autophagy is a cellular adaptation to tumor acidic pH microenvironments.* Cancer Res, 2012. **72**(16): p. 3938-47.

78. Marino, M.L., et al., *Autophagy is a protective mechanism for human melanoma cells under acidic stress.* J Biol Chem, 2012. **287**(36): p. 30664-76.

79. Ma, Z., et al., *BNIP3 induces apoptosis and protective autophagy under hypoxia in esophageal squamous cell carcinoma cell lines: BNIP3 regulates cell death.* Dis Esophagus, 2017. **30**(9): p. 1-8.

80. Ji, K., et al., *Acidosis and proteolysis in the tumor microenvironment.* Cancer and Metastasis Reviews, 2019. **38**(1-2): p. 103-112.

81. Rohl, J., et al., *Invasion by activated macrophages requires delivery of nascent membrane-type-1 matrix metalloproteinase through late endosomes/lysosomes to the cell surface.* Traffic, 2019. **20**(9): p. 661-673.

82. Jurij Rozhin, M.S., Grace Ziegler, and Bonnie F. Sloane, *Pericellular pH Affects Distribution and Secretion of Cathepsin B in Malignant Cells.* CANCER RESEARCH, 1994. **54**: p. 6517-6525.

83. Husain, Z., et al., *Tumor-derived lactate modifies antitumor immune response: effect on myeloid-derived suppressor cells and NK cells.* J Immunol, 2013. **191**(3): p. 1486-95.

84. Mohamed, M.M. and B.F. Sloane, *Cysteine cathepsins: multifunctional enzymes in cancer.* Nat Rev Cancer, 2006. **6**(10): p. 764-75.

85. Koblinski, J.E., M. Ahram, and B.F. Sloane, *Unraveling the role of proteases in cancer.* Clinica chimica acta, 2000. **291**(2): p. 113-135.

86. Linda L. Johnson‡§, A.G.P., Adam R. Johnsoni, Jeffrey A. Janowiczi,, D.F.O. Chiu-Fai Mani, Claude F. Purchase II¶, Andrew D. White¶,, and a.D.J. Hupe, *A Rationalization of the Acidic pH Dependence for Stromelysin-1 (Matrix Metalloproteinase-3) Catalysis and Inhibition.* THE JOURNAL OF BIOLOGICAL CHEMISTRY, 2000. **275**.

87. Kato, Y., et al., *Acidic extracellular pH induces matrix metalloproteinase-9 expression in mouse metastatic melanoma cells through the phospholipase D-mitogen-activated protein kinase signaling.* J Biol Chem, 2005. **280**(12): p. 10938-44.

88. Pope, B.J., et al., *Solution structure of human cofilin: actin binding, pH sensitivity, and relationship to actin-depolymerizing factor.* J Biol Chem, 2004. **279**(6): p. 4840-8.

89. Glendon D. McLachlan, S.M.C., Mark E. Girvin, and Steven C. Almon, *Acid-Induced Equilibrium Folding Intermediate of Human Platelet Profilin.* Biochemistry, 2007. **46**: p. 6931-6943.

90. J. Srivastava*, G.B., S. Groscurth†, A. R. Gingras‡, B. T. Goult‡, D. R. Critchley‡, M. J. S. Kelly†, M. P. Jacobson†, and a.D.L. Barber, *Structural model and functional significance of pH-dependent talin–actin binding for focal adhesion remodeling.* PNAS, 2008. **105**.

91. Marie-Egyptienne, D.T., I. Lohse, and R.P. Hill, *Cancer stem cells, the epithelial to mesenchymal transition (EMT) and radioresistance: potential role of hypoxia.* Cancer Lett, 2013. **341**(1): p. 63-72.

92. Joseph, J.P., et al., *Hypoxia induced EMT: A review on the mechanism of tumor progression and metastasis in OSCC.* Oral Oncol, 2018. **80**: p. 23-32.

93. Jiang, J., Y.L. Tang, and X.H. Liang, *EMT: a new vision of hypoxia promoting cancer progression.* Cancer Biol Ther, 2011. **11**(8): p. 714-23.

94. Atsuko Suzuki, et al., *Acidic extracellular pH promotes epithelial mesenchymal transition in Lewis lung carcinoma model.* Cancer Cell International, 2014.

95. Riemann, A., et al., *Extracellular Acidosis Modulates the Expression of Epithelial-Mesenchymal Transition (EMT) Markers and Adhesion of Epithelial and Tumor Cells.* Neoplasia, 2019. **21**(5): p. 450-458.

96. Robertson-Tessi, M., et al., *Impact of Metabolic Heterogeneity on Tumor Growth, Invasion, and Treatment Outcomes.* Cancer Research, 2015. **75**(8): p. 1567-1579.

97. Gatenby, R.A., et al., *Acid-Mediated Tumor Invasion: a Multidisciplinary Study.* Cancer Research, 2006. **66**(10): p. 5216-5223.

98. Robey, I.F., et al., *Bicarbonate increases tumor pH and inhibits spontaneous metastases.* Cancer Res, 2009. **69**(6): p. 2260-8.

99. Chouaib, S., et al., *Hypoxic stress: obstacles and opportunities for innovative immunotherapy of cancer.* Oncogene, 2017. **36**(4): p. 439-445.

100. Dietl, K., et al., *Lactic acid and acidification inhibit TNF secretion and glycolysis of human monocytes.* The Journal of Immunology, 2010. **184**(3): p. 1200-1209.

101. Fischer, K., et al., *Inhibitory effect of tumor cell–derived lactic acid on human T cells.* Blood, 2007. **109**(9): p. 3812-3819.

102. Brand, A., et al., *LDHA-Associated Lactic Acid Production Blunts Tumor Immunosurveillance by T and NK Cells.* Cell Metab, 2016. **24**(5): p. 657-671.

103. Potzl, J., et al., *Reversal of tumor acidosis by systemic buffering reactivates NK cells to express IFN-gamma and induces NK cell-dependent lymphoma control without other immunotherapies.* Int J Cancer, 2017. **140**(9): p. 2125-2133.

104. Gottfried, E., et al., *Tumor-derived lactic acid modulates dendritic cell activation and antigen expression.* Blood, 2006. **107**(5): p. 2013-21.

105. Chen, Y., et al., *Cellular Metabolic Regulation in the Differentiation and Function of Regulatory T Cells.* Cells, 2019. **8**(2).

106. Damgaci, S., et al., *Hypoxia and acidosis: immune suppressors and therapeutic targets.* Immunology, 2018. **154**(3): p. 354-362.

107. Calcinotto, A., et al., *Modulation of microenvironment acidity reverses anergy in human and murine tumor-infiltrating T lymphocytes.* Cancer Res, 2012. **72**(11): p. 2746-56.

108. Hiskias G. Keizer, H.J., *Increased Cytosolic pH in Multidrug-Resistant Human Lung Tumor Cells: Effect of Verapamil.* Journal of the National Cancer Institute, 1989. **81**.

109. Tadashi MURAKAMI1, Izumi SHIBUYA3, Tomoko ISE1, Zhe-Sheng CHEN4, Shin-ichi AKIYAMA4, Masayuki NAKAGAWA5, Hiroto IZUMI1, Toshitaka NAKAMURA2, Ken-ichi MATSUO6, Yuji YAMADA6 and Kimitoshi KOHNO, *ELEVATED EXPRESSION OF VACUOLAR PROTON PUMP GENES AND CELLULAR PH IN CISPLATIN RESISTANCE.* Int. J. Cancer, 2001. **93**: p. 869 – 874.

110. SANFORD SIMON, DEBORSHI RoY, and A.M. SCHINDLER, *Intracellular pH and the control of multidrug resistance.* Cell Biology, 1994. **91**: p. 1128-1132.

111. Wojtkowiak, J.W., et al., *Drug resistance and cellular adaptation to tumor acidic pH microenvironment.* Mol Pharm, 2011. **8**(6): p. 2032-8.

112. Zahia OUAR*, M.B., Caroline VIGNES†, Marc PAULAIS‡, Claudine PRINGEL§, Jocelyne FLEURY§, FrancToise CLUZEAUD*, and R.L.a.A. VANDEWALLE, *Inhibitors of vacuolar Hu-ATPase impair the preferential accumulation of daunomycin in lysosomes and reverse the resistance to anthracyclines in drug-resistant renal epithelial cells.* Biochem. J., 2003. **370**: p. 185–193.

113. Parks, S.K. and J. Pouyssegur, *The Na+/HCO3−Co-Transporter SLC4A4 Plays a Role in Growth and Migration of Colon and Breast Cancer Cells.* Journal of Cellular Physiology, 2015. **230**(8): p. 1954-1963.

114. Yen, K., et al., *Cancer-associated IDH mutations: biomarker and therapeutic opportunities.* Oncogene, 2010. **29**(49): p. 6409-6417.

115. Morikawa, M., R. Derynck, and K. Miyazono, *TGF- β and the TGF-β family: Context-dependent roles in cell and tissue physiology.* Cold Spring Harbor Perspectives in Biology, 2016. **8**(5).

116. Elliott, R.L. and G.C. Blobe, *Role of transforming growth factor beta in human cancer.* Journal of Clinical Oncology, 2005. **23**(9): p. 2078-2093.

117. Annes, J.P., J.S. Munger, and D.B. Rifkin, *Making sense of latent TGFbeta activation.* Journal of cell science, 2003. **116**(Pt 2): p. 217-24.

118. Lawrence, D.a., *Latent-TGF-beta: an overview.* Molecular and cellular biochemistry, 2001. **219**(1-2): p. 163-70.

119. Robertson, I.B., et al., *Latent TGF-β-binding proteins.* Matrix Biology, 2015. **47**: p. 44-53.

120. Massagué, J., *TGFβ signalling in context.* Nature Reviews Molecular Cell Biology, 2012. **13**(10): p. 616-630.

121. Pardali, K. and A. Moustakas, *Actions of TGF-β as tumor suppressor and pro-metastatic factor in human cancer.* Biochimica et Biophysica Acta - Reviews on Cancer, 2007. **1775**(1): p. 21-62.

122. Chen, Y.-G., *Endocytic regulation of TGF-β signaling.* Cell research, 2009. **19**(1): p. 58.

123. Le Roy, C. and J.L. Wrana, *Clathrin-and non-clathrin-mediated endocytic regulation of cell signalling.* Nature reviews Molecular cell biology, 2005. **6**(2): p. 112.

124. Zhao, B., et al., *PICK1 promotes caveolin-dependent degradation of TGF-β type I receptor.* Cell research, 2012. **22**(10): p. 1467.

125. Huang, F. and Y.-G. Chen, *Regulation of TGF-β receptor activity.* Cell & bioscience, 2012. **2**(1): p. 9.

126. Shi, Y. and J. Massagué, *Mechanisms of TGF-β Signaling from Cell Membrane to the Nucleus.* Cell, 2003. **113**(6): p. 685-700.

127. Huang, F. and Y.G. Chen, *Regulation of TGF-beta receptor activity.* Cell Biosci, 2012. **2**: p. 9.

128. Di Guglielmo, G.M., et al., *Distinct endocytic pathways regulate TGF-β receptor signalling and turnover.* Nature cell biology, 2003. **5**(5): p. 410.

129. Anders, R.A., et al., *Distinct endocytic responses of heteromeric and homomeric transforming growth factor β receptors.* Molecular biology of the cell, 1997. **8**(11): p. 2133-2143.

130. Bascom, C.C., et al., *Complex regulation of transforming growth factor beta 1, beta 2, and beta 3 mRNA expression in mouse fibroblasts and keratinocytes by transforming growth factors beta 1 and beta 2.* Molecular and Cellular Biology, 2015. **9**(12): p. 5508-5515.

131. Colak, S. and P. ten Dijke, *Targeting TGF-β Signaling in Cancer.* Trends in Cancer, 2017. **3**(1): p. 56-71.

132. Derynck, R., R.J. Akhurst, and A. Balmain, *TGF-beta signaling in tumor suppression and cancer progression.* Nat Genet, 2001. **29**(2): p. 117-29.

133. Massagué, J., *TGFβ in Cancer.* Cell, 2008. **134**(2): p. 215-230.

134. Derynck, R., R.J. Akhurst, and A. Balmain, *TGF-β signaling in tumor suppression and cancer progression.* Nature Genetics, 2001. **29**(2): p. 117-129.

135. Xi, Q., et al., *A poised chromatin platform for TGF-beta access to master regulators.* Cell, 2011. **147**(7): p. 1511-24.

136. Schmierer, B. and C.S. Hill, *Kinetic analysis of Smad nucleocytoplasmic shuttling reveals a mechanism for transforming growth factor beta-dependent nuclear accumulation of Smads.* Mol Cell Biol, 2005. **25**(22): p. 9845-58.

137. Feng, X.H., Zhang, Y., Wu, R.Y. & Derynck, R., *The tumor suppressor Smad4/DPC4 and transcriptional adaptor CBP/p300 are coactivators for Smad3 in TGF-b-induced transcriptional activation.* GENES & DEVELOPMENT, 1998(12): p. 2153–2163.

138. Xing Shen, P.P.-c.H., *Nicole T. Liberati, Michael B. Datto, Joshua P. Frederick, and Xiao-Fan Wang, *TGF-b–induced Phosphorylation of Smad3 Regulates*

Its Interaction with Coactivator p300/CREB-binding

Protein. Molecular Biology of the Cell, 1998. **9**: p. 3309–3319.

139. Yan, X., Z. Liu, and Y. Chen, *Regulation of TGF-beta signaling by Smad7.* Acta Biochim Biophys Sin (Shanghai), 2009. **41**(4): p. 263-72.

140. Peter Kavsak, R.K.R., S.B. Carrie G. Causing, Haitao Zhu,, and a.J.L.W. Gerald H. Thomsen, *Smad7 Binds to Smurf2 to Form an E3 Ubiquitin Ligase that Targets the TGFb Receptor for Degradation.* Mol Biol Cell, 2000. **6**: p. 1365–1375.

141. Ebisawa, T., et al., *Smurf1 interacts with transforming growth factor-beta type I receptor through Smad7 and induces receptor degradation.* J Biol Chem, 2001. **276**(16): p. 12477-80.

142. Takeshi Imamura, M.T., Ayako Nishihara,, J.-i.H. Eiichi Oeda, Masahiro Kawabata, and K. Miyazono, *Smad6 inhibits signalling by the TGF-b superfamily.* Nature, 1997. **389**.

143. Gunaratne, a., B.L. Thai, and G.M. Di Guglielmo, *Atypical Protein Kinase C Phosphorylates Par6 and Facilitates Transforming Growth Factor -Induced Epithelial-to-Mesenchymal Transition.* Molecular and Cellular Biology, 2013. **33**(5): p. 874-886.

144. Mu, Y., et al., *TGFβ-induced phosphorylation of Par6 promotes migration and invasion in prostate cancer cells.* British Journal of Cancer, 2015. **112**(7): p. 1223-1231.

145. Ozdamar, B., et al., *Regulation of the polarity protein Par6 by TGFβ receptors controls epithelial cell plasticity.* Science, 2005. **307**(5715): p. 1603-1609.

146. Viloria-Petit, A.M., et al., *A role for the TGFβ-Par6 polarity pathway in breast cancer progression.* Proceedings of the National Academy of Sciences of the United States of America, 2009. **106**(33): p. 14028-14033.

147. Frolik, C.A., et al., *Purification and initial characterization of a type beta transforming growth factor from human placenta.* Proceedings of the National Academy of Sciences, 1983. **80**(12): p. 3676-3680.

148. C. SANDHU, J.G., N. BHATTACHARYA, J. DAKSIS, C.-H. PAN, P. YASWEN, J. KOH, J. M. SLINGERLAND, AND M. R. STAMPFER, *Transforming Growth Factor b Stabilizes p15INK4B Protein, Increases p15INK4B-cdk4 Complexes, and Inhibits Cyclin D1-cdk4 Association in Human Mammary Epithelial Cells.* MOLECULAR AND CELLULAR BIOLOGY, 1997. **17**(5).

149. Feng, X.H., X. Lin, and R. Derynck, *Smad2, Smad3 and Smad4 cooperate with Sp1 to induce p15Ink4B transcription in response to TGF-β.* The EMBO journal, 2000. **19**(19): p. 5178-5193.

150. Mulder, K.M. and S.L. Morris, *Activation of p21ras by transforming growth factor beta in epithelial cells.* Journal of Biological Chemistry, 1992. **267**(8): p. 5029-5031.

151. Datto, M.B., et al., *Transforming growth factor beta induces the cyclin-dependent kinase inhibitor p21 through a p53-independent mechanism.* Proceedings of the National Academy of Sciences, 1995. **92**(12): p. 5545-5549.

152. Polyak, K., et al., *p27Kip1, a cyclin-Cdk inhibitor, links transforming growth factor-beta and contact inhibition to cell cycle arrest.* Genes & development, 1994. **8**(1): p. 9-22.

153. Wen-Sheng, W., *ERK signaling pathway is involved in p15 INK4b/p16 INK4a expression and HepG2 growth inhibition triggered by TPA and Saikosaponin a.* Oncogene, 2003. **22**(7): p. 955.

154. Hu, P.P.-c., et al., *The MEK pathway is required for stimulation of p21WAF1/CIP1 by transforming growth factor-β.* Journal of Biological Chemistry, 1999. **274**(50): p. 35381-35387.

155. Pardali, K., et al., *Smad pathway-specific transcriptional regulation of the cell cycle inhibitor p21WAF1/Cip1.* Journal of cellular physiology, 2005. **204**(1): p. 260-272.

156. Ijichi, H., et al., *Smad4-independent regulation of p21/WAF1 by transforming growth factor-β.* Oncogene, 2004. **23**(5): p. 1043.

157. Scandura, J.M., et al., *Transforming growth factor β-induced cell cycle arrest of human hematopoietic cells requires p57KIP2 up-regulation.* Proceedings of the National Academy of Sciences, 2004. **101**(42): p. 15231-15236.

158. Ewen, M.E., et al., *p53-dependent repression of CDK4 translation in TGF-beta-induced G1 cell-cycle arrest.* Genes & development, 1995. **9**(2): p. 204-217.

159. Miller, S.J., et al., *p53 Binds Selectively to the 5′ Untranslated Region ofcdk4, an RNA Element Necessary and Sufficient for Transforming Growth Factor β-and p53-Mediated Translational Inhibition of cdk4.* Molecular and cellular biology, 2000. **20**(22): p. 8420-8431.

160. Frederick, J.P., et al., *Transforming growth factor β-mediated transcriptional repression of c-myc is dependent on direct binding of Smad3 to a novel repressive Smad binding element.* Molecular and cellular biology, 2004. **24**(6): p. 2546-2559.

161. Baldwin, R.L., H. Tran, and B.Y. Karlan, *Loss of c-myc repression coincides with ovarian cancer resistance to transforming growth factor β growth arrest independent of transforming growth factor β/Smad signaling.* Cancer research, 2003. **63**(6): p. 1413-1419.

162. Iavarone, A. and J. Massagué, *E2F and histone deacetylase mediate transforming growth factor β repression of cdc25A during keratinocyte cell cycle arrest.* Molecular and Cellular Biology, 1999. **19**(1): p. 916-922.

163. Massagué, J., *TGFβ signalling in context.* Nature reviews Molecular cell biology, 2012. **13**(10): p. 616.

164. Schuster, N. and K. Krieglstein, *Mechanisms of TGF-β-mediated apoptosis.* Cell and tissue research, 2002. **307**(1): p. 1-14.

165. Shin, I., et al., *Transforming growth factor β enhances epithelial cell survival via Akt-dependent regulation of FKHRL1.* Molecular biology of the cell, 2001. **12**(11): p. 3328-3339.

166. Chalaux, E., et al., *A zinc-finger transcription factor induced by TGF-β promotes apoptotic cell death in epithelial Mv1Lu cells.* FEBS letters, 1999. **457**(3): p. 478-482.

167. Yoo, J., et al., *Transforming growth factor-β-induced apoptosis is mediated by Smad-dependent expression of GADD45b through p38 activation.* Journal of biological chemistry, 2003. **278**(44): p. 43001-43007.

168. Takekawa, M., et al., *Smad-dependent GADD45β expression mediates delayed activation of p38 MAP kinase by TGF-β.* The EMBO journal, 2002. **21**(23): p. 6473-6482.

169. Jang, C.-W., et al., *TGF-β induces apoptosis through Smad-mediated expression of DAP-kinase.* Nature cell biology, 2002. **4**(1): p. 51.

170. Sorrentino, A., et al., *The type I TGF-β receptor engages TRAF6 to activate TAK1 in a receptor kinase-independent manner.* Nature cell biology, 2008. **10**(10): p. 1199.

171. Valderrama-Carvajal, H., et al., *Activin/TGF-β induce apoptosis through Smad-dependent expression of the lipid phosphatase SHIP.* Nature cell biology, 2002. **4**(12): p. 963.

172. Myeroff, L.L., et al., *A transforming growth factor β receptor type II gene mutation common in colon and gastric but rare in endometrial cancers with microsatellite instability.* Cancer research, 1995. **55**(23): p. 5545-5547.

173. Parsons, R., et al., *Microsatellite instability and mutations of the transforming growth factor β type II receptor gene in colorectal cancer.* Cancer research, 1995. **55**(23): p. 5548-5550.

174. Kim, W., et al., *Microsatellite instability (MSI) in non-small cell lung cancer (NSCLC) is highly associated with transforming growth factor-beta type II receptor (TGF-beta RII) frameshift mutation.* Anticancer research, 2000. **20**(3A): p. 1499-1502.

175. Izumoto, S., et al., *Microsatellite instability and mutated type II transforming growth factor-β receptor gene in gliomas.* Cancer letters, 1997. **112**(2): p. 251-256.

176. Levy, L. and C.S. Hill, *Alterations in components of the TGF-β superfamily signaling pathways in human cancer.* Cytokine and Growth Factor Reviews, 2006. **17**(1-2): p. 41-58.

177. Chen, T., et al., *Transforming growth factor-β receptor type I gene is frequently mutated in ovarian carcinomas.* Cancer research, 2001. **61**(12): p. 4679-4682.

178. Chen, T., et al., *Transforming growth factor β type I receptor kinase mutant associated with metastatic breast cancer.* Cancer research, 1998. **58**(21): p. 4805-4810.

179. Goggins, M., et al., *Genetic alterations of the transforming growth factor β receptor genes in pancreatic and biliary adenocarcinomas.* Cancer research, 1998. **58**(23): p. 5329-5332.

180. Schiemann, W.P., et al., *A deletion in the gene for transforming growth factor β type I receptor abolishes growth regulation by transforming growth factor β in a cutaneous T-cell lymphoma.* Blood, 1999. **94**(8): p. 2854-2861.

181. Kim, S.-J., et al., *Molecular mechanisms of inactivation of TGF-β receptors during carcinogenesis.* Cytokine & growth factor reviews, 2000. **11**(1-2): p. 159-168.

182. Hahn, S.A., et al., *DPC4, a candidate tumor suppressor gene at human chromosome 18q21. 1.* Science, 1996. **271**(5247): p. 350-353.

183. Miyaki, M. and T. Kuroki, *Role of Smad4 (DPC4) inactivation in human cancer.* Biochemical and biophysical research communications, 2003. **306**(4): p. 799-804.

184. Maliekal, T.T., et al., *Loss of expression, and mutations of Smad 2 and Smad 4 in human cervical cancer.* Oncogene, 2003. **22**(31): p. 4889.

185. Takagi, Y., et al., *Somatic alterations of the SMAD-2 gene in human colorectal cancers.* British journal of cancer, 1998. **78**(9): p. 1152.

186. Han, S.-U., et al., *Loss of the Smad3 expression increases susceptibility to tumorigenicity in human gastric cancer.* Oncogene, 2004. **23**(7): p. 1333.

187. Zhu, Y., et al., *Smad3 mutant mice develop metastatic colorectal cancer.* Cell, 1998. **94**(6): p. 703-714.

188. Boulay, J.L., et al., *Combined copy status of 18q21 genes in colorectal cancer shows frequent retention of SMAD7.* Genes, Chromosomes and Cancer, 2001. **31**(3): p. 240-247.

189. Kretzschmar, M., et al., *A mechanism of repression of TGFβ/Smad signaling by oncogenic Ras.* Genes & development, 1999. **13**(7): p. 804-816.

190. De Caestecker, M.P., et al., *Smad2 transduces common signals from receptor serine–threonine and tyrosine kinases.* Genes & development, 1998. **12**(11): p. 1587-1592.

191. Lehmann, K., et al., *Raf induces TGFβ production while blocking its apoptotic but not invasive responses: a mechanism leading to increased malignancy in epithelial cells.* Genes & development, 2000. **14**(20): p. 2610-2622.

192. Sun, Y., et al., *SnoN and Ski protooncoproteins are rapidly degraded in response to transforming growth factor β signaling.* Proceedings of the National Academy of Sciences, 1999. **96**(22): p. 12442-12447.

193. Luo, K., et al., *The Ski oncoprotein interacts with the Smad proteins to repress TGFβ signaling.* Genes & development, 1999. **13**(17): p. 2196-2206.

194. Stroschein, S.L., et al., *Negative feedback regulation of TGF-β signaling by the SnoN oncoprotein.* Science, 1999. **286**(5440): p. 771-774.

195. Zhang, H., et al., *KLF8 involves in TGF-beta-induced EMT and promotes invasion and migration in gastric cancer cells.* Journal of cancer research and clinical oncology, 2013. **139**(6): p. 1033-1042.

196. Merzak, A., et al., *Control of human glioma cell growth, migration and invasion in vitro by transforming growth factor β 1.* British journal of cancer, 1994. **70**(2): p. 199.

197. Pang, M.F., et al., *TGF-β1-induced EMT promotes targeted migration of breast cancer cells through the lymphatic system by the activation of CCR7/CCL21-mediated chemotaxis.* Oncogene, 2016. **35**(6): p. 748-760.

198. Syed, V., *TGF- b Signaling in Cancer.* 2016. **1287**(January): p. 1279-1287.

199. Xie, F., et al., *TGF-β signaling in cancer metastasis.* Acta Biochimica et Biophysica Sinica, 2018. **50**(1): p. 121-132.

200. Shooner, C., et al., *TGF-beta expression during rat pregnancy and activity on decidual cell survival.* Reproductive biology and endocrinology, 2005. **3**(1): p. 20.

201. Thiolloy, S., et al., *An osteoblast-derived proteinase controls tumor cell survival via TGF-beta activation in the bone microenvironment.* PloS one, 2012. **7**(1): p. e29862.

202. Beck, C., H. Schreiber, and D.A. Rowley, *Role of TGF-β in immune-evasion of cancer.* Microscopy research and technique, 2001. **52**(4): p. 387-395.

203. Thomas, D.A. and J. Massagué, *TGF-β directly targets cytotoxic T cell functions during tumor evasion of immune surveillance.* Cancer cell, 2005. **8**(5): p. 369-380.

204. Joshi, A. and D. Cao, *TGF-beta signaling, tumor microenvironment and tumor progression: the butterfly effect.* Front Biosci, 2010. **15**(1): p. 180-194.

205. Stover, D.G., B. Bierie, and H.L. Moses, *A delicate balance: TGF-β and the tumor microenvironment.* Journal of cellular biochemistry, 2007. **101**(4): p. 851-861.

206. Derynck, R., et al., *Synthesis of messenger RNAs for transforming growth factors α and β and the epidermal growth factor receptor by human tumors.* Cancer research, 1987. **47**(3): p. 707-712.

207. Hasegawa, Y., et al., *Transforming growth factor-β1 level correlates with angiogenesis, tumor progression, and prognosis in patients with nonsmall cell lung carcinoma.* Cancer, 2001. **91**(5): p. 964-971.

208. Dalal, B., P. Keown, and A. Greenberg, *Immunocytochemical localization of secreted transforming growth factor-beta 1 to the advancing edges of primary tumors and to lymph node metastases of human mammary carcinoma.* The American journal of pathology, 1993. **143**(2): p. 381.

209. Munger, J.S., et al., *Latent transforming growth factor-β: Structural features and mechanisms of activation.* Kidney International, 1997. **51**(5): p. 1376-1382.

210. Khalil, N., *TGF-β: From latent to active.* Microbes and Infection, 1999. **1**(15): p. 1255-1263.

211. Lawrence, D.A., *Latent-TGF-β: an overview.* Molecular and cellular biochemistry, 2001. **219**(1-2): p. 163-170.

212. Taylor, A. W. (2008). Review of the activation of TGF- in immunity. Journal of Leukocyte Biology, 85(1), 29–33. https://doi.org/10.1189/jlb.0708415

213. Lyons, R.M., et al., *Mechanism of activation of latent recombinant transforming growth factor beta 1 by plasmin.* The Journal of cell biology, 1990. **110**(4): p. 1361-1367.

214. Andreasen, P.A., et al., *The urokinase-type plasminogen activator system in cancer metastasis: a review.* International journal of cancer, 1997. **72**(1): p. 1-22.

215. Li, M.O., et al., *Transforming growth factor-β regulation of immune responses.* Annu. Rev. Immunol., 2006. **24**: p. 99-146.

216. Torre-Amione, G., et al., *A highly immunogenic tumor transfected with a murine transforming growth factor type beta 1 cDNA escapes immune surveillance.* Proceedings of the National Academy of Sciences, 1990. **87**(4): p. 1486-1490.

217. Gorelik, L. and R.A. Flavell, *Abrogation of TGFβ signaling in T cells leads to spontaneous T cell differentiation and autoimmune disease.* Immunity, 2000. **12**(2): p. 171-181.

218. Becker, C., et al., *TGF-β suppresses tumor progression in colon cancer by inhibition of IL-6 trans-signaling.* Immunity, 2004. **21**(4): p. 491-501.

219. Kehrl, J.H., et al., *Production of transforming growth factor beta by human T lymphocytes and its potential role in the regulation of T cell growth.* Journal of Experimental Medicine, 1986. **163**(5): p. 1037-1050.

220. Bogdan, C., et al., *Contrasting mechanisms for suppression of macrophage cytokine release by transforming growth factor-beta and interleukin-10.* Journal of Biological Chemistry, 1992. **267**(32): p. 23301-23308.

221. Riedl, E., et al., *TGF-beta 1 promotes in vitro generation of dendritic cells by protecting progenitor cells from apoptosis.* The Journal of Immunology, 1997. **158**(4): p. 1591-1597.

222. Dong, Y., et al., *The Smad3 protein is involved in TGF-β inhibition of class II transactivator and class II MHC expression.* The Journal of Immunology, 2001. **167**(1): p. 311-319.

223. Arteaga, C.L., et al., *Anti-transforming growth factor (TGF)-beta antibodies inhibit breast cancer cell tumorigenicity and increase mouse spleen natural killer cell activity. Implications for a possible role of tumor cell/host TGF-beta interactions in human breast cancer progression.* The Journal of clinical investigation, 1993. **92**(6): p. 2569-2576.

224. Chen, J.-J., Y. Sun, and G.J. Nabel, *Regulation of the proinflammatory effects of Fas ligand (CD95L).* Science, 1998. **282**(5394): p. 1714-1717.

225. Nieto, M.A., et al., *Emt: 2016.* Cell, 2016. **166**(1): p. 21-45.

226. Williams, E.D., et al., *Controversies around epithelial–mesenchymal plasticity in cancer metastasis.* Nature Reviews Cancer, 2019. **19**(12): p. 716-732.

227. Tan, T.Z., et al., *Epithelial-mesenchymal transition spectrum quantification and its efficacy in deciphering survival and drug responses of cancer patients.* EMBO molecular medicine, 2014. **6**(10): p. 1279-1293.

228. Lamouille, S., J. Xu, and R. Derynck, *Molecular mechanisms of epithelial–mesenchymal transition.* Nature Reviews Molecular Cell Biology, 2014. **15**(3): p. 178-196.

229. Li, L. and W. Li, *Epithelial-mesenchymal transition in human cancer: Comprehensive reprogramming of metabolism, epigenetics, and differentiation.* Pharmacology and Therapeutics, 2015. **150**: p. 33-46.

230. Marcucci, F., G. Stassi, and R. De Maria, *Epithelial-mesenchymal transition: A new target in anticancer drug discovery.* Nature Reviews Drug Discovery, 2016. **15**(5): p. 311-325.

231. Polyak, K. and R.a. Weinberg, *Transitions between epithelial and mesenchymal states: acquisition of malignant and stem cell traits.* Nature reviews. Cancer, 2009. **9**(4): p. 265-73.

232. Khoo, B.L., et al., *Short-term expansion of breast circulating cancer cells predicts response to anti-cancer therapy.* Oncotarget, 2015. **6**(17): p. 15578.

233. May, C.D., et al., *Epithelial-mesenchymal transition and cancer stem cells: a dangerously dynamic duo in breast cancer progression.* Breast Cancer Research, 2011. **13**(1): p. 202.

234. Mitra, A., L. Mishra, and S. Li, *EMT, CTCs and CSCs in tumor relapse and drug-resistance.* Oncotarget, 2015. **6**(13): p. 10697-10711.

235. Scheel, C. and R.a. Weinberg, *Cancer stem cells and epithelial-mesenchymal transition: Concepts and molecular links.* Seminars in Cancer Biology, 2012. **22**(5-6): p. 396-403.

236. Wang, S.-S., et al., *Links between cancer stem cells and epithelial-mesenchymal transition.* OncoTargets and therapy, 2015. **8**: p. 2973-80.

237. Mani, S.A., et al., *The epithelial-mesenchymal transition generates cells with properties of stem cells.* Cell, 2008. **133**(4): p. 704-715.

238. Shipitsin, M., et al., *Molecular definition of breast tumor heterogeneity.* Cancer cell, 2007. **11**(3): p. 259-273.

239. Mercado-Pimentel, M.E. and R.B. Runyan, *Multiple transforming growth factor-β isoforms and receptors function during epithelial-mesenchymal*

cell transformation in the embryonic heart. Cells Tissues Organs, 2007. **185**(1-3): p. 146-156.

240. Nawshad, A., D. LaGamba, and E. Hay, *Transforming growth factor β (TGFβ) signalling in palatal growth, apoptosis and epithelial mesenchymal transformation (EMT).* Archives of oral biology, 2004. **49**(9): p. 675-689.

241. Schnaper, H.W., et al., *TGF-β signal transduction and mesangial cell fibrogenesis.* American Journal of Physiology-Renal Physiology, 2003. **284**(2): p. F243-F252.

242. Oft, M., et al., *TGF-beta1 and Ha-Ras collaborate in modulating the phenotypic plasticity and invasiveness of epithelial tumor cells.* Genes & development, 1996. **10**(19): p. 2462-2477.

243. Miettinen, P.J., et al., *TGF-beta induced transdifferentiation of mammary epithelial cells to mesenchymal cells: involvement of type I receptors.* The Journal of cell biology, 1994. **127**(6): p. 2021-2036.

244. Deckers, M., et al., *The tumor suppressor Smad4 is required for transforming growth factor β–induced epithelial to mesenchymal transition and bone metastasis of breast cancer cells.* Cancer research, 2006. **66**(4): p. 2202-2209.

245. Fuxe, J., T. Vincent, and A. Garcia de Herreros, *Transcriptional crosstalk between TGFβ and stem cell pathways in tumor cell invasion: role of EMT promoting Smad complexes.* Cell cycle, 2010. **9**(12): p. 2363-2374.

246. Piek, E., et al., *TGF-(beta) type I receptor/ALK-5 and Smad proteins mediate epithelial to mesenchymal transdifferentiation in NMuMG breast epithelial cells.* J cell Sci, 1999. **112**(24): p. 4557-4568.

247. Hoot, K.E., et al., *Keratinocyte-specific Smad2 ablation results in increased epithelial-mesenchymal transition during skin cancer formation and progression.* The Journal of clinical investigation, 2008. **118**(8): p. 2722-2732.

248. Morita, T., T. Mayanagi, and K. Sobue, *Dual roles of myocardin-related transcription factors in epithelial–mesenchymal transition via slug induction and actin remodeling.* The Journal of cell biology, 2007. **179**(5): p. 1027-1042.

249. Postigo, A.A., *Opposing functions of ZEB proteins in the regulation of the TGFβ/BMP signaling pathway.* The EMBO journal, 2003. **22**(10): p. 2443-2452.

250. Kang, Y., C.-R. Chen, and J. Massagué, *A self-enabling TGFβ response coupled to stress signaling: Smad engages stress response factor ATF3 for Id1 repression in epithelial cells.* Molecular cell, 2003. **11**(4): p. 915-926.

251. Lamouille, S. and R. Derynck, *Cell size and invasion in TGF-β–induced epithelial to mesenchymal transition is regulated by activation of the mTOR pathway.* The Journal of cell biology, 2007. **178**(3): p. 437-451.

252. Lamouille, S., et al., *TGF-β-induced activation of mTOR complex 2 drives epithelial–mesenchymal transition and cell invasion.* J Cell Sci, 2012. **125**(5): p. 1259-1273.

253. Bakin, A.V., et al., *Phosphatidylinositol 3-kinase function is required for transforming growth factor β-mediated epithelial to mesenchymal transition and cell migration.* Journal of Biological Chemistry, 2000. **275**(47): p. 36803-36810.

254. Yamashita, M., et al., *TRAF6 mediates Smad-independent activation of JNK and p38 by TGF-β.* Molecular cell, 2008. **31**(6): p. 918-924.

255. Alexander, N.R., et al., *N-cadherin gene expression in prostate carcinoma is modulated by integrin-dependent nuclear translocation of Twist1.* Cancer research, 2006. **66**(7): p. 3365-3369.

256. Shamir, E.R., et al., *Twist1-induced dissemination preserves epithelial identity and requires E-cadherin.* J Cell Biol, 2014. **204**(5): p. 839-856.

257. Hong, J., et al., *Phosphorylation of serine 68 of Twist1 by MAPKs stabilizes Twist1 protein and promotes breast cancer cell invasiveness.* Cancer research, 2011. **71**(11): p. 3980-3990.

258. Parvani, J.G., M.A. Taylor, and W.P. Schiemann, *Noncanonical TGF-β signaling during mammary tumorigenesis.* Journal of mammary gland biology and neoplasia, 2011. **16**(2): p. 127-146.

259. Xie, L., et al., *Activation of the Erk pathway is required for TGF-β1-induced EMT in vitro.* Neoplasia, 2004. **6**(5): p. 603-610.

260. Portella, G., et al., *Transforming growth factor beta is essential for spindle cell conversion of mouse skin carcinoma in vivo: implications for tumor invasion.* Cell growth & differentiation: the molecular biology journal of the American Association for Cancer Research, 1998. **9**(5): p. 393-404.

261. Oft, M., K.-H. Heider, and H. Beug, *TGFβ signaling is necessary for carcinoma cell invasiveness and metastasis.* Current Biology, 1998. **8**(23): p. 1243-1252.

262. Dong, L., et al., *Transforming growth factor-β and epithelial–mesenchymal transition are associated with pulmonary metastasis in adenoid cystic carcinoma.* Oral oncology, 2013. **49**(11): p. 1051-1058.

263. Xiao, H., et al., *Metformin is a novel suppressor for transforming growth factor (TGF)-β1.* Scientific reports, 2016. **6**: p. 28597.

264. Park, I.-H., et al., *Metformin Reduces TGF-β1–Induced Extracellular Matrix Production in Nasal Polyp–Derived Fibroblasts.* Otolaryngology--Head and Neck Surgery, 2014. **150**(1): p. 148-153.

265. Cufí, S., et al., *Metformin against TGFβ-induced epithelial-to-mesenchymal transition (EMT): from cancer stem cells to aging-associated fibrosis.* Cell cycle, 2010. **9**(22): p. 4461-4468.

266. Like, B. and J. Massague, *The antiproliferative effect of type beta transforming growth factor occurs at a level distal from receptors for growth-activating factors.* Journal of Biological Chemistry, 1986. **261**(29): p. 13426-13429.

267. Staršíchová, A., et al., *Dynamic monitoring of cellular remodeling induced by the transforming growth factor-β1.* Biological procedures online, 2009. **11**(1): p. 316.

268. Koyasu, S., et al., *Alteration in growth, cell morphology, and cytoskeletal structures of KB cells induced by epidermal growth factor and transforming growth factor-β.* Experimental cell research, 1988. **176**(1): p. 107-116.

269. Cox, D., et al., *Requirements for both Rac1 and Cdc42 in membrane ruffling and phagocytosis in leukocytes.* Journal of Experimental Medicine, 1997. **186**(9): p. 1487-1494.

270. Nobes, C. and A. Hall, *Rho, rac and cdc42 GTPases: regulators of actin structures, cell adhesion and motility*. 1995, Portland Press Limited.

271. Dawe, H.R., et al., *ADF/cofilin controls cell polarity during fibroblast migration.* Current biology, 2003. **13**(3): p. 252-257.

272. Bravo-Cordero, J.J., et al., *Functions of cofilin in cell locomotion and invasion.* Nature reviews Molecular cell biology, 2013. **14**(7): p. 405-415.

273. Park, J.S., et al., *The effect of matrix stiffness on the differentiation of mesenchymal stem cells in response to TGF-β.* Biomaterials, 2011. **32**(16): p. 3921-3930.

274. Masszi, A., et al., *Central role for Rho in TGF-β1-induced α-smooth muscle actin expression during epithelial-mesenchymal transition.* American Journal of Physiology-Renal Physiology, 2003. **284**(5): p. F911-F924.

275. Fukata, Y., K. Kaibuchi, and M. Amano, *Rho–Rho-kinase pathway in smooth muscle contraction and cytoskeletal reorganization of non-muscle cells.* Trends in pharmacological sciences, 2001. **22**(1): p. 32-39.

276. Hanna, S. and M. El-Sibai, *Signaling networks of Rho GTPases in cell motility.* Cellular Signalling, 2013. **25**(10): p. 1955-1961.

277. Iden, S. and J.G. Collard, *Crosstalk between small GTPases and polarity proteins in cell polarization.* Nature Reviews Molecular Cell Biology, 2008. **9**(11): p. 846-859.

278. Fidler, I.J., *The pathogenesis of cancer metastasis: the'seed and soil'hypothesis revisited.* Nature Reviews Cancer, 2003. **3**(6): p. 453.

279. Malanchi, I., et al., *Interactions between cancer stem cells and their niche govern metastatic colonization.* Nature, 2012. **481**(7379): p. 85.

280. Paget, S., *The distribution of secondary growths in cancer of the breast.* The Lancet, 1889. **133**(3421): p. 571-573.

281. Fidler, I.J., S.J. Kim, and R.R. Langley, *The role of the organ microenvironment in the biology and therapy of cancer metastasis.* Journal of cellular biochemistry, 2007. **101**(4): p. 927-936.

282. Nguyen, D.H., et al., *Radiation acts on the microenvironment to affect breast carcinogenesis by distinct mechanisms that decrease cancer latency and affect tumor type.* Cancer cell, 2011. **19**(5): p. 640-651.

283. Calon, A., et al., *Dependency of colorectal cancer on a TGF-β-driven program in stromal cells for metastasis initiation.* Cancer cell, 2012. **22**(5): p. 571-584.

284. Javelaud, D., et al., *Stable overexpression of Smad7 in human melanoma cells impairs bone metastasis.* Cancer Research, 2007. **67**(5): p. 2317-2324.

285. Kominsky, S.L., et al., *TGF-β Promotes the Establishment of Renal Cell Carcinoma Bone Metastasis.* Journal of Bone and Mineral Research, 2007. **22**(1): p. 37-44.

286. Hua, W., et al., *TGFβ-induced metabolic reprogramming during epithelial-to-mesenchymal transition in cancer.* Cellular and Molecular Life Sciences, 2019: p. 1-21.

287. Morandi, A., et al., *Targeting the Metabolic Reprogramming That Controls Epithelial-to-Mesenchymal Transition in Aggressive Tumors.* Front Oncol, 2017. **7**: p. 40.

288. Lee, S.Y., et al., *Dlx-2 is implicated in TGF-β-and Wnt-induced epithelial-mesenchymal, glycolytic switch, and mitochondrial repression by Snail activation.* International journal of oncology, 2015. **46**(4): p. 1768-1780.

289. Li, W., et al., *Increased 18F-FDG uptake and expression of Glut1 in the EMT transformed breast cancer cells induced by TGF-β.* Neoplasma, 2010. **57**(3): p. 234.

290. Rodríguez-García, A., et al., *TGF-β1 targets Smad, p38 MAPK, and PI 3K/Akt signaling pathways to induce PFKFB 3 gene expression and glycolysis in glioblastoma cells.* The FEBS journal, 2017. **284**(20): p. 3437-3454.

291. Yalcin, A., et al., *6-phosphofructo-2-kinase/fructose 2,6-bisphosphatase-3 is required for transforming growth factor β1-enhanced invasion of Panc1 cells in vitro.* Biochemical and Biophysical Research Communications, 2017. **484**(3): p. 687-693.

292. Liu, M., et al., *Epithelial-mesenchymal transition induction is associated with augmented glucose uptake and lactate production in pancreatic ductal adenocarcinoma.* Cancer & Metabolism, 2016. **4**(1): p. 19.

293. Fischer, K., et al., *Inhibitory effect of tumor cell–derived lactic acid on human T cells.* Blood, 2007. **109**(9): p. 3812-3819.

294. Baumann, F., et al., *Lactate promotes glioma migration by TGF-β2–dependent regulation of matrix metalloproteinase-2.* Neuro-Oncology, 2009. **11**(4): p. 368-380.

295. Zhang, D., et al., *Metabolic reprogramming of cancer-associated fibroblasts by IDH3α downregulation.* Cell reports, 2015. **10**(8): p. 1335-1348.

296. Jiang, L., et al., *Metabolic reprogramming during TGFβ1-induced epithelial-to-mesenchymal transition.* Oncogene, 2015. **34**(30): p. 3908-3916.

297. Nath, A., et al., *Elevated free fatty acid uptake via CD36 promotes epithelial-mesenchymal transition in hepatocellular carcinoma.* Scientific reports, 2015. **5**: p. 14752.

298. Schwenk, R.W., et al., *Fatty acid transport across the cell membrane: regulation by fatty acid transporters.* Prostaglandins, Leukotrienes and Essential Fatty Acids (PLEFA), 2010. **82**(4-6): p. 149-154.

299. Leonarduzzi, G., et al., *The lipid peroxidation end product 4-hydroxy-2, 3-nonenal up-regulates transforming growth factor beta1 expression in the macrophage lineage: a link between oxidative injury and fibrosclerosis.* The FASEB Journal, 1997. **11**(11): p. 851-857.

300. Biasi, F., et al., *Associated changes of lipid peroxidation and transforming growth factor β1 levels in human colon cancer during tumour progression.* Gut, 2002. **50**(3): p. 361-367.

301. Barcellos-Hoff, M. and T.A. Dix, *Redox-mediated activation of latent transforming growth factor-beta 1.* Molecular endocrinology, 1996. **10**(9): p. 1077-1083.

302. Milara, J., et al., *Sphingosine-1-phosphate is increased in patients with idiopathic pulmonary fibrosis and mediates epithelial to mesenchymal transition.* Thorax, 2012. **67**(2): p. 147-156.

303. Liu, S., et al., *Sphingomyelin synthase 1 regulates the epithelial-to-mesenchymal transition mediated by the TGF-β/Smad pathway in MDA-MB-231 cells.* Molecular medicine reports, 2019. **19**(2): p. 1159-1167.

304. Michl, J., K.C. Park, and P. Swietach, *Evidence-based guidelines for controlling pH in mammalian live-cell culture systems.* Communications biology, 2019. **2**(1): p. 1-12.

305. Choudhary, C., et al., *The growing landscape of lysine acetylation links metabolism and cell signalling.* Nature reviews Molecular cell biology, 2014. **15**(8): p. 536.

306. Pietrocola, F., et al., *Acetyl coenzyme A: a central metabolite and second messenger.* Cell metabolism, 2015. **21**(6): p. 805-821.

307. Corbet, C., et al., *The SIRT1/HIF2α axis drives reductive glutamine metabolism under chronic acidosis and alters tumor response to therapy.* Cancer research, 2014. **74**(19): p. 5507-5519.

308. Mullen, A.R., et al., *Reductive carboxylation supports growth in tumour cells with defective mitochondria.* Nature, 2012. **481**(7381): p. 385.

309. Yang, C., et al., *Glutamine oxidation maintains the TCA cycle and cell survival during impaired mitochondrial pyruvate transport.* Molecular cell, 2014. **56**(3): p. 414-424.

310. Mashimo, T., et al., *Acetate is a bioenergetic substrate for human glioblastoma and brain metastases.* Cell, 2014. **159**(7): p. 1603-1614.

311. Schug, Z.T., et al., *Acetyl-CoA synthetase 2 promotes acetate utilization and maintains cancer cell growth under metabolic stress.* Cancer cell, 2015. **27**(1): p. 57-71.

312. Kamphorst, J.J., et al., *Quantitative analysis of acetyl-CoA production in hypoxic cancer cells reveals substantial contribution from acetate.* Cancer & metabolism, 2014. **2**(1): p. 23.

313. Brahimi-Horn, M.C., G. Bellot, and J. Pouyssegur, *Hypoxia and energetic tumour metabolism.* Current opinion in genetics & development, 2011. **21**(1): p. 67-72.

314. Gatenby, R.A. and R.J. Gillies, *A microenvironmental model of carcinogenesis.* Nature Reviews Cancer, 2008. **8**(1): p. 56-61.

315. Hashim, A.I., et al., *Imaging pH and metastasis.* NMR in biomedicine, 2011. **24**(6): p. 582-591.

316. Morita, T., et al., *Clastogenicity of low pH to various cultured mammalian cells.* Mutation Research/Fundamental and Molecular Mechanisms of Mutagenesis, 1992. **268**(2): p. 297-305.

317. Chen, J.L.-Y., et al., *The genomic analysis of lactic acidosis and acidosis response in human cancers.* PLoS genetics, 2008. **4**(12).

318. LaMonte, G., et al., *Acidosis induces reprogramming of cellular metabolism to mitigate oxidative stress.* Cancer & metabolism, 2013. **1**(1): p. 23.

319. Scott, I., et al., *Identification of a molecular component of the mitochondrial acetyltransferase programme: a novel role for GCN5L1.* Biochemical Journal, 2012. **443**(3): p. 655-661.

320. Fendt, S.-M., et al., *Reductive glutamine metabolism is a function of the α-ketoglutarate to citrate ratio in cells.* Nature communications, 2013. **4**: p. 2236.

321. Foster, D.W., *Malonyl-CoA: the regulator of fatty acid synthesis and oxidation.* The Journal of clinical investigation, 2012. **122**(6): p. 1958-1959.

322. Currie, E., et al., *Cellular fatty acid metabolism and cancer.* Cell metabolism, 2013. **18**(2): p. 153-161.

323. Zaidi, N., J.V. Swinnen, and K. Smans, *ATP-citrate lyase: a key player in cancer metabolism.* Cancer research, 2012. **72**(15): p. 3709-3714.

324. Chang, T., C.C. Chang, and D. Cheng, *Acyl-coenzyme A: cholesterol acyltransferase.* Annual review of biochemistry, 1997. **66**(1): p. 613-638.

325. Abu-Elheiga, L., et al., *The subcellular localization of acetyl-CoA carboxylase 2.* Proceedings of the National Academy of Sciences, 2000. **97**(4): p. 1444-1449.

326. Harjes, U., J. Kalucka, and P. Carmeliet, *Targeting fatty acid metabolism in cancer and endothelial cells.* Critical reviews in oncology/hematology, 2016. **97**: p. 15-21.

327. Su, X. and N.A. Abumrad, *Cellular fatty acid uptake: a pathway under construction.* Trends in Endocrinology & Metabolism, 2009. **20**(2): p. 72-77.

328. Polet, F. and O. Feron, *Endothelial cell metabolism and tumour angiogenesis: glucose and glutamine as essential fuels and lactate as the driving force.* Journal of internal medicine, 2013. **273**(2): p. 156-165.

329. Boidot, R., et al., *A generic cycling hypoxia-derived prognostic gene signature: application to breast cancer profiling.* Oncotarget, 2014. **5**(16): p. 6947.

330. Corbet, C. and O. Feron, *Tumour acidosis: from the passenger to the driver's seat.* Nat Rev Cancer, 2017. **17**(10): p. 577-593.

331. Damaghi, M. and R. Gillies, *Phenotypic changes of acid-adapted cancer cells push them toward aggressiveness in their evolution in the tumor microenvironment.* Cell Cycle, 2017. **16**(19): p. 1739-1743.

332. Swietach, P., et al., *The chemistry, physiology and pathology of pH in cancer.* Philos Trans R Soc Lond B Biol Sci, 2014. **369**(1638): p. 20130099.

333. Webb, B.A., et al., *Dysregulated pH: a perfect storm for cancer progression.* Nat Rev Cancer, 2011. **11**(9): p. 671-7.

334. Parks, S.K., J. Chiche, and J. Pouyssegur, *Disrupting proton dynamics and energy metabolism for cancer therapy.* Nat Rev Cancer, 2013. **13**(9): p. 611-23.

335. Newell, K., et al., *Studies with glycolysis-deficient cells suggest that production of lactic acid is not the only cause of tumor acidity.* Proc Natl Acad Sci U S A, 1993. **90**(3): p. 1127-31.

336. Secomb, T.W., M.W. Dewhirst, and A.R. Pries, *Structural adaptation of normal and tumour vascular networks.* Basic Clin Pharmacol Toxicol, 2012. **110**(1): p. 63-9.

337. Chiche, J., M.C. Brahimi-Horn, and J. Pouyssegur, *Tumour hypoxia induces a metabolic shift causing acidosis: a common feature in cancer.* J Cell Mol Med, 2010. **14**(4): p. 771-94.

338. Svastova, E., et al., *Hypoxia activates the capacity of tumor-associated carbonic anhydrase IX to acidify extracellular pH.* FEBS Lett, 2004. **577**(3): p. 439-45.

339. Swietach, P., et al., *New insights into the physiological role of carbonic anhydrase IX in tumour pH regulation.* Oncogene, 2010. **29**(50): p. 6509-21.

340. Khacho, M., et al., *Acidosis overrides oxygen deprivation to maintain mitochondrial function and cell survival.* Nat Commun, 2014. **5**: p. 3550.

341. Nadtochiy, S.M., et al., *Acidic pH Is a Metabolic Switch for 2-Hydroxyglutarate Generation and Signaling.* J Biol Chem, 2016. **291**(38): p. 20188-97.

342. Kondo, A., et al., *Extracellular Acidic pH Activates the Sterol Regulatory Element-Binding Protein 2 to Promote Tumor Progression.* Cell Reports, 2017. **18**: p. 2228-42.

343. Corbet, C., et al., *Acidosis Drives the Reprogramming of Fatty Acid Metabolism in Cancer Cells through Changes in Mitochondrial and Histone Acetylation.* Cell Metab, 2016. **24**(2): p. 311-23.

344. Chen, J.L., et al., *The genomic analysis of lactic acidosis and acidosis response in human cancers.* PLoS Genet, 2008. **4**(12): p. e1000293.

345. Tang, X., et al., *Functional interaction between responses to lactic acidosis and hypoxia regulates genomic transcriptional outputs.* Cancer Res, 2012. **72**(2): p. 491-502.

346. Chang, C.H., et al., *Metabolic Competition in the Tumor Microenvironment Is a Driver of Cancer Progression.* Cell, 2015. **162**(6): p. 1229-41.

347. Estrella, V., et al., *Acidity generated by the tumor microenvironment drives local invasion.* Cancer Res, 2013. **73**(5): p. 1524-35.

348. Damaghi, M., et al., *Chronic acidosis in the tumour microenvironment selects for overexpression of LAMP2 in the plasma membrane.* Nat Commun, 2015. **6**: p. 8752.

349. Quail, D.F. and J.A. Joyce, *Microenvironmental regulation of tumor progression and metastasis.* Nat Med, 2013. **19**(11): p. 1423-37.

350. Lehuede, C., et al., *Metabolic Plasticity as a Determinant of Tumor Growth and Metastasis.* Cancer Res, 2016. **76**(18): p. 5201-8.

351. Peppicelli, S., F. Bianchini, and L. Calorini, *Extracellular acidity, a "reappreciated" trait of tumor environment driving malignancy: perspectives in diagnosis and therapy.* Cancer Metastasis Rev, 2014. **33**(2-3): p. 823-32.

352. Shaul, Y.D., et al., *Dihydropyrimidine accumulation is required for the epithelial-mesenchymal transition.* Cell, 2014. **158**(5): p. 1094-1109.

353. Dupuy, F., et al., *PDK1-Dependent Metabolic Reprogramming Dictates Metastatic Potential in Breast Cancer.* Cell Metab, 2015. **22**(4): p. 577-89.

354. Andrzejewski, S., et al., *PGC-1alpha Promotes Breast Cancer Metastasis and Confers Bioenergetic Flexibility against Metabolic Drugs.* Cell Metab, 2017. **26**(5): p. 778-787 e5.

355. Porporato, P.E., et al., *A mitochondrial switch promotes tumor metastasis.* Cell Rep, 2014. **8**(3): p. 754-66.

356. Luo, C., et al., *A PGC1alpha-mediated transcriptional axis suppresses melanoma metastasis.* Nature, 2016. **537**(7620): p. 422-426.

357. Torrano, V., et al., *The metabolic co-regulator PGC1alpha suppresses prostate cancer metastasis.* Nat Cell Biol, 2016. **18**(6): p. 645-656.

358. Schild, T., et al., *Unique Metabolic Adaptations Dictate Distal Organ-Specific Metastatic Colonization.* Cancer Cell, 2018. **33**(3): p. 347-354.

359. Delikatny, E.J., et al., *MR-visible lipids and the tumor microenvironment.* NMR Biomed, 2011. **24**(6): p. 592-611.

360. Listenberger, L.L., et al., *Triglyceride accumulation protects against fatty acid-induced lipotoxicity.* Proc Natl Acad Sci U S A, 2003. **100**(6): p. 3077-82.

361. Lamouille, S., J. Xu, and R. Derynck, *Molecular mechanisms of epithelial-mesenchymal transition.* Nat Rev Mol Cell Biol, 2014. **15**(3): p. 178-96.

362. Fitzgerald, A.M., et al., *The effects of transforming growth factor-beta2 on the expression of follistatin and activin A in normal and glaucomatous human trabecular meshwork cells and tissues.* Invest Ophthalmol Vis Sci, 2012. **53**(11): p. 7358-69.

363. Ribeiro, S.M., et al., *The activation sequence of thrombospondin-1 interacts with the latency-associated peptide to regulate activation of latent transforming growth factor-beta.* J Biol Chem, 1999. **274**(19): p. 13586-93.

364. Bogdahn, U., et al., *Targeted therapy for high-grade glioma with the TGF-beta2 inhibitor trabedersen: results of a randomized and controlled phase IIb study.* Neuro Oncol, 2011. **13**(1): p. 132-42.

365. Oettle, H., et al., *Final results of a phase I/II study in patients with pancreatic cancer, malignant melanoma, and colorectal carcinoma with trabedersen.* Journal of Clinical Oncology, 2012. **30**(15_suppl): p. 4034-4034.

366. Trieu, V.N., et al., *IL-8 as PD biomarker for TGF-b antisense (OT-101) therapy: Results of a phase II trial.* Journal of Clinical Oncology, 2017. **35**(15_suppl): p. e15742.

367. Glatz, J.F., J.J. Luiken, and A. Bonen, *Membrane fatty acid transporters as regulators of lipid metabolism: implications for metabolic disease.* Physiol Rev, 2010. **90**(1): p. 367-417.

368. Luiken, J.J., et al., *Permissive action of protein kinase C-zeta in insulin-induced CD36- and GLUT4 translocation in cardiac myocytes.* J Endocrinol, 2009. **201**(2): p. 199-209.

369. Xia, L., et al., *High glucose activates PKC-zeta and NADPH oxidase through autocrine TGF-beta1 signaling in mesangial cells.* Am J Physiol Renal Physiol, 2008. **295**(6): p. F1705-14.

370. Li, Z., et al., *SIRT1 inhibits TGF-beta-induced endothelial-mesenchymal transition in human endothelial cells with Smad4 deacetylation.* J Cell Physiol, 2018. **233**(11): p. 9007-9014.

371. Lin, H., et al., *AMPK Inhibits the Stimulatory Effects of TGF-beta on Smad2/3 Activity, Cell Migration, and Epithelial-to-Mesenchymal Transition.* Mol Pharmacol, 2015. **88**(6): p. 1062-71.

372. Tu, A.W. and K. Luo, *Acetylation of Smad2 by the co-activator p300 regulates activin and transforming growth factor beta response.* J Biol Chem, 2007. **282**(29): p. 21187-96.

373. Rios Garcia, M., et al., *Acetyl-CoA Carboxylase 1-Dependent Protein Acetylation Controls Breast Cancer Metastasis and Recurrence.* Cell Metab, 2017. **26**(6): p. 842-855 e5.

374. Ye, X. and R.A. Weinberg, *Epithelial-Mesenchymal Plasticity: A Central Regulator of Cancer Progression.* Trends Cell Biol, 2015. **25**(11): p. 675-86.

375. Chaffer, C.L., et al., *EMT, cell plasticity and metastasis.* Cancer Metastasis Rev, 2016. **35**(4): p. 645-654.

376. Aiello, N.M. and Y. Kang, *Context-dependent EMT programs in cancer metastasis.* J Exp Med, 2019. **216**(5): p. 1016-1026.

377. Gillies, R.J., et al., *Eco-evolutionary causes and consequences of temporal changes in intratumoural blood flow.* Nat Rev Cancer, 2018.

378. Chaffer, C.L. and R.A. Weinberg, *A perspective on cancer cell metastasis.* Science, 2011. **331**(6024): p. 1559-64.

379. Dalmau, N., et al., *Epithelial-to-mesenchymal transition involves triacylglycerol accumulation in DU145 prostate cancer cells.* Mol Biosyst, 2015. **11**(12): p. 3397-406.

380. Jiang, L., et al., *Metabolic reprogramming during TGFbeta1-induced epithelial-to-mesenchymal transition.* Oncogene, 2015. **34**(30): p. 3908-16.

381. Nath, A., et al., *Elevated free fatty acid uptake via CD36 promotes epithelial-mesenchymal transition in hepatocellular carcinoma.* Sci Rep, 2015. **5**: p. 14752.

382. Bensaad, K., et al., *Fatty acid uptake and lipid storage induced by HIF-1alpha contribute to cell growth and survival after hypoxia-reoxygenation.* Cell Rep, 2014. **9**(1): p. 349-365.

383. Calon, A., et al., *Dependency of colorectal cancer on a TGF-beta-driven program in stromal cells for metastasis initiation.* Cancer Cell, 2012. **22**(5): p. 571-84.

384. Peppicelli, S., et al., *Contribution of acidic melanoma cells undergoing epithelial-to-mesenchymal transition to aggressiveness of non-acidic melanoma cells.* Clin Exp Metastasis, 2014. **31**(4): p. 423-33.

385. Tang, Y.A., et al., *Hypoxic tumor microenvironment activates GLI2 via HIF-1alpha and TGF-beta2 to promote chemoresistance in colorectal cancer.* Proc Natl Acad Sci U S A, 2018. **115**(26): p. E5990-E5999.

386. Gregory, P.A., et al., *An autocrine TGF-beta/ZEB/miR-200 signaling network regulates establishment and maintenance of epithelial-mesenchymal transition.* Mol Biol Cell, 2011. **22**(10): p. 1686-98.

387. Penuelas, S., et al., *TGF-beta increases glioma-initiating cell self-renewal through the induction of LIF in human glioblastoma.* Cancer Cell, 2009. **15**(4): p. 315-27.

388. Birch, A.M., L.K. Buckett, and A.V. Turnbull, *DGAT1 inhibitors as anti-obesity and anti-diabetic agents.* Curr Opin Drug Discov Devel, 2010. **13**(4): p. 489-96.

389. Wang, Y.Y., et al., *Mammary adipocytes stimulate breast cancer invasion through metabolic remodeling of tumor cells.* JCI Insight, 2017. **2**(4): p. e87489.

390. Pascual, G., et al., *Targeting metastasis-initiating cells through the fatty acid receptor CD36.* Nature, 2017. **541**(7635): p. 41-45.

391. Gaedcke, J., et al., *Mutated KRAS results in overexpression of DUSP4, a MAP-kinase phosphatase, and SMYD3, a histone methyltransferase, in rectal carcinomas.* Genes Chromosomes Cancer, 2010. **49**(11): p. 1024-34.

392. Jones, J., et al., *Gene signatures of progression and metastasis in renal cell cancer.* Clin Cancer Res, 2005. **11**(16): p. 5730-9.

393. Corbet, C., et al., *Interruption of lactate uptake by inhibiting mitochondrial pyruvate transport unravels direct antitumor and radiosensitizing effects.* Nat Commun, 2018. **9**(1): p. 1208.

394. Weerakkody, D., et al., *Family of pH (low) insertion peptides for tumor targeting.* Proc Natl Acad Sci U S A, 2013. **110**(15): p. 5834-9.

395. Aubert, L., et al., *NGF-induced TrkA/CD44 association is involved in tumor aggressiveness and resistance to lestaurtinib.* Oncotarget, 2015. **6**(12): p. 9807-19.

396. Siegel, P.M. and J. Massagué, *Cytostatic and apoptotic actions of TGF-β in homeostasis and cancer.* Nature Reviews Cancer, 2003. **3**(11): p. 807-820.

397. Chiche, J., M.C. Brahimi-Horn, and J. Pouysségur, *Tumour hypoxia induces a metabolic shift causing acidosis: A common feature in cancer.* Journal of Cellular and Molecular Medicine, 2010. **14**(4): p. 771-794.

398. Corbet, C., et al., *TGFβ2-induced formation of lipid droplets supports acidosis-driven EMT and the metastatic spreading of cancer cells.* Nature Communications, 2020. **11**(1): p. 1-15.

399. Shi, M., et al., *Latent TGF-β structure and activation.* Nature, 2011. **474**(7351): p. 343-351.

400. Bouché, M., et al., *TGF-β autocrine loop regulates cell growth and myogenic differentiation in human rhabdomyosarcoma cells.* The FASEB Journal, 2018. **14**(9): p. 1147-1158.

401. Schultz-Cherry, S. and J.E. Murphy-Ullrich, *Thrombospondin causes activation of latent transforming growth factor-beta secreted by endothelial cells by a novel mechanism.* J Cell Biol, 1993. **122**(4): p. 923-32.

402. Crawford, S.E., et al., *Thrombospondin-1 is a major activator of TGF-β1 in vivo.* Cell, 1998. **93**(7): p. 1159-1170.

403. Stacey Schultz-Cherry, H.C., Deane F. Mosher, Tina M. Misenheimer, Henry C. Krutzsch, David D. Roberts and Joanne E. Murphy-Ullrich, *Regulation of Transforming Growth Factor-β Activation by Discrete Sequences of Thrombospondin 1.* The Journal of Biological Chemistry, 1995.

404. Murphy-Ullrich, J.E. and M. Poczatek, *Activation of latent TGF-β by thrombospondin-1: Mechanisms and physiology.* Cytokine and Growth Factor Reviews, 2000. **11**(1-2): p. 59-69.

405. Lu, A., et al., *Blockade of TSP1-Dependent TGF-* *Activity Reduces Renal Injury and Proteinuria in a Murine Model of Diabetic Nephropathy.* 2011. **178**(6): p. 2573-2586.

406. Kaur, B., et al., *Vasculostatin inhibits intracranial glioma growth and negatively regulates in vivo angiogenesis through a CD36-dependent mechanism.* Cancer Research, 2009. **69**(3): p. 1212-1220.

407. Asch, A.S., et al., *Thrombospondin sequence motif (CSVTCG) is responsible for CD36 binding.* Biochemical and Biophysical Research Communications, 1992. **182**(3): p. 1208-1217.

408. Abrigo, J., et al., *Apocynin inhibits the upregulation of TGF-β1 expression and ROS production induced by TGF-β in skeletal muscle cells.* Phytomedicine, 2015. **22**(10): p. 885-893.

409. Noma, T., et al., *Molecular cloning and structure of the human transforming growth factor-β2 gene promoter.* Growth Factors, 1991. **4**(4): p. 247-255.

410. Lawler, J., *Thrombospondin-1 as an endogenous inhibitor of angiogenesis and tumor growth.* J Cell Mol Med, 2002. **6**(1): p. 1-12.

411. Mwaikambo, B.R., et al., *Activation of CD36 inhibits and induces regression of inflammatory corneal neovascularization.* Investigative Ophthalmology and Visual Science, 2006. **47**(10): p. 4356-4364.

412. Sharif, O., et al., *The Scavenger Receptor CD36 Downmodulates the Early Inflammatory Response while Enhancing Bacterial Phagocytosis during Pneumococcal Pneumonia.* The Journal of Immunology, 2013. **190**(11): p. 5640-5648.

413. Neubauer, E.F., et al., *A diverse host thrombospondin-type-1 repeat protein repertoire promotes symbiont colonization during establishment of cnidarian-dinoflagellate symbiosis.* eLife, 2017. **6**: p. 1-26.

414. Receptor, C.S., et al., *Activation of Rat Alveolar Macrophage-Derived Latent Transforming Growth Factor -1 by Plasmin Requires Interaction*

with Thrombospondin-1 and its. The American Journal of Pathology, 1999. **155**(3): p. 841-851.

415. Pascual, G., et al., *Targeting metastasis-initiating cells through the fatty acid receptor CD36.* Nature, 2017. **541**(7635): p. 41-45.

416. Chen, C.L., S.H. Shuan, and S.H. Jung, *Cholesterol modulates cellular TGF-β responsiveness by altering TGF-β binding to TGF-β receptors.* Journal of Cellular Physiology, 2008. **215**(1): p. 223-233.

417. Hubchak, S.C., et al., *Cytoskeletal rearrangement and signal transduction in TGF-β1-stimulated mesangial cell collagen accumulation.* Journal of the American Society of Nephrology, 2003. **14**(8): p. 1969-1980.

418. Tang, Z., et al., *GEPIA: a web server for cancer and normal gene expression profiling and interactive analyses.* Nucleic Acids Res, 2017. **45**(W1): p. W98-W102.

419. Park, E.-J., et al., *Multiple pathways are involved in palmitic acid-induced toxicity.* Food and chemical toxicology, 2014. **67**: p. 26-34.

420. Bailey, Andrew P., et al., *Antioxidant Role for Lipid Droplets in a Stem Cell Niche of Drosophila.* Cell, 2015. **163**(2): p. 340-353.

421. Tu, A.W. and K. Luo, *Acetylation of Smad2 by the co-activator p300 regulates activin and transforming growth factor β response.* Journal of Biological Chemistry, 2007. **282**(29): p. 21187-21196.

422. Pilon-Thomas, S., et al., *Neutralization of tumor acidity improves antitumor responses to immunotherapy.* Cancer research, 2016. **76**(6): p. 1381-1390.

423. Robey, I.F., et al., *Bicarbonate increases tumor pH and inhibits spontaneous metastases.* Cancer research, 2009. **69**(6): p. 2260-2268.

424. Silva, A.S., et al., *The potential role of systemic buffers in reducing intratumoral extracellular pH and acid-mediated invasion.* Cancer research, 2009. **69**(6): p. 2677-2684.

425. Neri, D. and C.T. Supuran, *Interfering with pH regulation in tumours as a therapeutic strategy.* Nature reviews Drug discovery, 2011. **10**(10): p. 767.

426. Curtarello, M., et al., *Rewiring of Lipid Metabolism and Storage in Ovarian Cancer Cells after Anti-VEGF Therapy.* Cells, 2019. **8**(12): p. 1601.

427. Sounni, N.E., et al., *Blocking lipid synthesis overcomes tumor regrowth and metastasis after antiangiogenic therapy withdrawal.* Cell metabolism, 2014. **20**(2): p. 280-294.

428. Vallieres, L., *Trabedersen, a TGFbeta2-specific antisense oligonucleotide for the treatment of malignant gliomas and other tumors overexpressing TGFbeta2.* IDrugs, 2009. **12**(7): p. 445-453.

429. Bogdahn, U., et al., *Targeted therapy for high-grade glioma with the TGF-β2 inhibitor trabedersen: results of a randomized and controlled phase IIb study.* Neuro-oncology, 2010. **13**(1): p. 132-142.

430. Fabregat, I., et al., *TGF-beta signaling in cancer treatment.* Current pharmaceutical design, 2014. **20**(17): p. 2934-2947.

431. Rademakers, S.E., et al., *Metabolic markers in relation to hypoxia; staining patterns and colocalization of pimonidazole, HIF-1α, CAIX, LDH-5, GLUT-1, MCT1 and MCT4.* BMC cancer, 2011. **11**(1): p. 167.

432. Raleigh, J.A., et al., *Hypoxia and vascular endothelial growth factor expression in human squamous cell carcinomas using pimonidazole as a hypoxia marker.* Cancer research, 1998. **58**(17): p. 3765-3768.

433. Reshetnyak, Y.K., et al., *Energetics of peptide (pHLIP) binding to and folding across a lipid bilayer membrane.* Proceedings of the National Academy of Sciences, 2008. **105**(40): p. 15340-15345.

434. Yao, L., et al., *pHLIP®-mediated delivery of PEGylated liposomes to cancer cells.* Journal of controlled release, 2013. **167**(3): p. 228-237.

435. Du, J.Z., et al., *A tumor-acidity-activated charge-conversional nanogel as an intelligent vehicle for promoted tumoral-cell uptake and drug delivery.* Angewandte Chemie International Edition, 2010. **49**(21): p. 3621-3626.

436. Ahmed, F., et al., *Shrinkage of a rapidly growing tumor by drug-loaded polymersomes: pH-triggered release through copolymer degradation.* Molecular pharmaceutics, 2006. **3**(3): p. 340-350.

437. Bae, Y., et al., *Design of environment-sensitive supramolecular assemblies for intracellular drug delivery: Polymeric micelles that are responsive to intracellular pH change.* Angewandte Chemie International Edition, 2003. **42**(38): p. 4640-4643.

438. Li, Y., et al., *One-step preparation of pH-responsive polymeric nanogels as intelligent drug delivery systems for tumor therapy.* Biomacromolecules, 2018. **19**(6): p. 2062-2070.

439. Labrousse-Arias, D., et al., *HIF-2α-mediated induction of pulmonary thrombospondin-1 contributes to hypoxia-driven vascular remodelling and vasoconstriction.* Cardiovascular research, 2016. **109**(1): p. 115-130.

440. Zhao, C., *COMPUTATIONAL MODELS OF MICRORNA-MEDIATED AND HIF-COORDINATED SYNTHESIS OF VEGF AND TSP-1: INSIGHTS INTO NOVEL THERAPEUTIC STRATEGIES IN CANCER AND PERIPHERAL ARTERIAL DISEASE*. 2016, Johns Hopkins University.

441. Seliger, C., et al., *Lactate-modulated induction of THBS-1 activates transforming growth factor (TGF)-beta2 and migration of glioma cells in vitro.* PloS one, 2013. **8**(11).

442. Daubon, T., et al., *Deciphering the complex role of thrombospondin-1 in glioblastoma development.* Nature communications, 2019. **10**(1): p. 1-15.

443. Yang, Y.-L., et al., *Thrombospondin-1 mediates distal tubule hypertrophy induced by glycated albumin.* Biochemical Journal, 2004. **379**(1): p. 89-97.

444. Chen, B., et al., *ERK-mediated NF-κB activation through ASIC1 in response to acidosis.* Oncogenesis, 2016. **5**(12): p. e279.

445. Terrinoni, M., et al., *Proteomic analysis of cholera toxin adjuvant-stimulated human monocytes identifies Thrombospondin-1 and Integrin-β1 as strongly upregulated molecules involved in adjuvant activity.* Scientific reports, 2019. **9**(1): p. 1-13.

446. Hu, X., et al., *Release of cholesterol-rich particles from the macrophage plasma membrane during movement of filopodia and lamellipodia.* eLife, 2019. **8**.

ANEXES

Transcription factor	Downregulated expression during EMT	Upregulated expression during EMT	Regulatory signalling pathways	Refs
SNAIL1 and SNAIL2	E-cadherin, claudins, occludin, Crumbs3, PALS1, PATJ, cytokeratins, desmoplakin and plakophilin	Fibronectin, N-cadherin, collagen, MMP15, MMP2, MMP9, TWIST, ID1, ID2, ZEB1 and ZEB2	TGFβ–SMAD3, WNT–β-catenin, Notch, PI3K–AKT, NF-κB, EGF and FGF	11,45,59,60,61, 66,159,185
TWIST1	E-cadherin, claudins, occludin, desmoplakin and plakoglobin	Fibronectin, N-cadherin and α5 integrin	MAPK	11,45,67,68,72
ZEB1 and ZEB2	E-cadherin, ZO1, Crumbs3 and plakophilin	N-cadherin and MMPs	TGFβ–SMAD3, WNT–β-catenin and RAS–MAPK	11,45,73–75, 77,142, 143
FOXD3	Unknown	Unknown	β1 integrin and laminin	266
FOXC2	E-cadherin	Fibronectin, vimentin, N-cadherin and αSMA	TGFβ–SMAD3	267
FOXF1	E-cadherin, claudin1, occludin, desmoglein1β, desmoglein2, desmocollin2 and desmoplakin	Fibronectin and N-cadherin	Unknown	268
FOXQ1	E-cadherin	Fibronectin, N-cadherin and vimentin	Unknown	269
FOXO3A	E-cadherin	SNAIL1	AKT	270
FOXA1	E-cadherin	Fibronectin, vimentin and SNAIL1	TGFβ, HGF and AKT	271
FOXA2	E-cadherin and ZO1	Fibronectin, vimentin, N-cadherin, SNAIL1 and SNAIL2	TGFβ, HGF and AKT	271
Serpent, GATA4 and GATA6	E-cadherin, Crumbs and claudins	N-cadherin and MMP1	Unknown	81
HMGA2	E-cadherin	SNAIL1, SNAIL2 and TWIST	TGFβ–SMAD3	103
SOX9	Unknown	SNAIL2	BMPs and PKA	83
KLF8	E-cadherin	MMP9	Unknown	272
CBFA–KAP1	Unknown	FSP1	Unknown	273
ZNF703 (also known as Zeppo1 in mice)	E-cadherin	Vimentin, N-cadherin, SNAIL1 and cytokeratin	RHO-GTPase	274
PRX1	E-cadherin	Vimentin and laminin	BMP2 and TGFβ	275

From : Lamouille, S., Xu, J., & Derynck, R. (2014). Molecular mechanisms of epithelial–mesenchymal transition. Nature Reviews Molecular Cell Biology, 15(3), 178–196. https://doi.org/10.1038/nrm3758